Synthesis and Small Molecule Chemistry of the Niobaziridine-Hydride Functional Group

Joshua S. Figueroa

B.S. University of Delaware
2000

Submitted to the Department of Chemistry
In Partial Fulfillment of the Requirements
for the Degree of

DOCTOR OF PHILOSOPHY

at the

MASSACHUSETTS INSTITUTE OF TECHNOLOGY

June 2005

Signature of Author _____
Department of Chemistry
May 9th 2005

Certified by _____
Christopher C. Cummins
Thesis Supervisor

Accepted by _____
Robert W. Field
Chairman, Departmental Committee for Graduate Studies

This Doctoral Thesis has been examined by a Committee of the Department of Chemistry as follows:

Professor Richard R. Schrock _____
Frederick G. Keyes Professor of Chemistry
Chairman

Professor Christopher C. Cummins _____
Thesis Supervisor

Professor Joseph P. Sadighi _____

A LESSON IN FOCUS AND DISTRACTION

'WHEN YOU SEE ME ON THE REAL, FORMIN' LIKE
VOLTRON, REMEMBER? GOT DEEP LIKE A BABY SEAL'
– RAEKWON
36 CHAMBERS

For My Parents, The Kindest and Most Loving People I Know

Table of Contents

Synthesis and Small Molecule Chemistry of the Niobaziridine-Hydride Functional Group

Joshua S. Figueroa

Submitted to the Department of Chemistry
Massachusetts Institute of Technology
In Partial Fulfillment of the Requirements for the Degree of
Doctor of Philosophy in Chemistry
June 2005

Thesis Supervisor: Christopher C. Cummins

Title: Professor of Chemistry

ABSTRACTS

Chapter 1. Synthesis and Divergent Reactivity of the Niobaziridine-Hydride Functional Group

The synthesis, characterization and reactivity of the niobaziridine-hydride complex Nb(H)(η^2-*t*-Bu(H)C=NAr)(N[Np]Ar)$_2$ (**1a**-H; Np = neopentyl, Ar = 3,5-$Me_2C_6H_3$) is discussed. The niobaziridine-hydride functional group in complex **1a**-H serves as a protecting group for the reactive three-coordinate d^2 species, Nb(N[Np]Ar)$_3$ (**2a**), via reversible C-H activation of the β-H–containing N[Np]Ar ligand. At elevated temperatures, complex **1a**-H rapidly converts to the neopentylimido complex, Nb(NNp)(Ar)(N[Np]Ar)$_3$ (**3a**), which is the product of N[Np]Ar ligand C-N oxidative addition by putative three-coordinate **2a**. Although not observed directly, the evidence for the intermediacy of **2a** in N[Np]Ar ligand C-H and C-N activation processes has been obtained through isotopic labeling (H/D) studies. To further ascertain the propensity of **1a**-H to serve as a masked form of **2a**, its reactivity with small-molecule substrates was surveyed. Treatment of **1a**-H with nitrous oxide (N_2O) or triphenylphosphine oxide ($OPPh_3$), readily generated the oxo Nb(V) complex, ONb(N[Np]Ar)$_3$, thus establishing **1a**-H as a source of the potent two-electron reductant **2a**. Complex **1a**-H was also found to effect the two-electron reduction of a host of other inorganic substrates. However, when treated with certain unsaturated organic molecules, insertion into the Nb-H moiety of complex **1a**-H is observed in which the niobaziridine ring is left intact. Based on synthetic studies, a coordinatively induced, C-H bond reductive elimination mechanism is proposed for reactions between **1a**-H and small molecules.

This mechanistic proposal accounts for both the observed insertion and two-electron reduction behavior exhibited by niobaziridine-hydride **1a**-H. To extend the generality of niobaziridine-hydride functional group as a protecting group for three-coordinate $Nb(NR_2)_3$ species, the complexes $Nb(H)(\eta^2\text{-}Me_2C{=}NAr)(N[i\text{-}Pr]Ar)_2$ (**1b**-H) and $Nb(H)(\eta^2\text{-}Ad(H)C{=}NAr)(N[CH_2\text{-}Ad]Ar)_2$ (**1c**-H) were synthesized. The thermal behavior of niobaziridine-hydrides **1b**-H and **1c**-H is compared and contrasted to that of the *N*-neopentyl variant **1a**-H.

Chapter 2. Activation of Elemental Phosphorus: Synthesis of an Anionic Terminal Phosphide of Niobium

The niobaziridine-hydride complex $Nb(H)(\eta^2\text{-}t\text{-}Bu(H)C{=}NAr)(N[Np]Ar)_2$ (**1a**-H; Np = neopentyl, Ar = 3,5-$Me_2C_6H_3$) was found to react quantitatively with elemental phosphorus (P_4) to provide the bridging diphosphide complex $(\mu_2{:}\eta^2,\eta^2\text{–}P_2)[Nb(N[Np]Ar)_3]_2$ (μ-P_2)[**2a**]$_2$. Reductive cleavage of (μ-P_2)[**2a**]$_2$ with sodium amalgam afforded the sodium salt of the terminal niobium phosphide anion, $[PNb(N[Np]Ar)_3)]^-$ ([**2a**-P]$^-$), which is best formulated as containing a Nb–P triple bond. The phosphorus atom of [**2a**-P]$^-$ has proven to be nucleophilic and is readily functionalized upon addition of an electrophile. Treatment of [**2a**-P]$^-$ with trimethylstannyl chloride provided the terminal phosphinidene complex $Me_3SnP{=}Nb(N[Np]Ar)_3$ which contains a P-Sn single bond. However, treatment of [**2a**-P]$^-$ with $ClP(t\text{-}Bu)_2$ or $ClP(Ph)_2$ provided niobium-complexed η^2–phosphinophosphinidene complexes, which contain considerable P-P multiple bonding character. Thus, substantial electronic reorganization of the Nb≡P moiety in [**2a**-P]$^-$ is induced upon functionalization. The tendency for the Nb≡P unit in [**2a**-P]$^-$ to undergo electronic reorganization has been exploited, resulting in the synthesis of a complexed η^2–*P*,*P*–diphosphaorganoazide (PPNR) species, which eliminates a 'P_2' unit when heated. Furthermore, treatment of the phosphido anion [**2a**-P]$^-$ with divalent group 14 salts affords complexes of the formulation $(\mu_2{:}\eta^3,\eta^3\text{-}cyclo\text{–}EP_2)[Nb(N[Np]Ar)_3]_2$ (E = Ge, Sn, Pb). The bridging *cyclo*-EP_2 units in these complexes can be considered as neutral 2π-electron, three-membered rings isolobal to the cyclopropenium ion. The molecular and electronic structure of anion [**2a**-P]$^-$ and several of its derivatives are discussed.

Chapter 3. Isovalent Pnictogen for O(Cl) Exchange Mediated by Terminal Pnictide Anions of Niobium

Reported herein is a new, metathetical P for O(Cl) exchange mediated by an anionic niobium phosphide complex which furnished phosphaalkynes (RC≡P) from acyl chlorides (RC(O)Cl) under mild conditions. The niobaziridine hydride complex, $Nb(H)(t\text{-}Bu(H)C{=}NAr)(N[Np]Ar)_2$ (**1a**-H, Np = neopentyl, Ar = 3,5-$Me_2C_6H_3$), has been shown in chapter 2 to react with elemental phosphorus (P_4) affording the μ-diphosphide complex, $(\mu_2{:}\eta^2,\eta^2\text{–}P_2)[Nb(N[Np]Ar)_3]_2$ ((μ-P)[**2a**]$_2$), which can be subsequently reduced by sodium amalgam to the anionic, terminal phosphide complex, [Na][$PNb(N[Np]Ar)_3$] (Na[**2a**-P]). Treatment of Na[**2a**-P] with either pivaloyl (*t*-BuC(O)Cl) or 1-adamantoyl (1-AdC(O)Cl) chloride provides the thermally unstable, niobacycles, (*t*-BuC(O)P)$Nb(N[Np]Ar)_3$ (**2**-*t*-Bu) and (1-AdC(O)P)$Nb(N[Np]Ar)_2$ (**2**-1-Ad) which are intermediates along the pathway to ejection of the known phosphaalkynes *t*-BuC≡P (**3**-*t*-Bu) and 1-AdC≡P (**3**-1-Ad). Phosphaalkyne ejection from **2**-*t*-Bu and **2**-1-Ad proceeds with formation of the niobium(V) oxo complex $ONb(N[Np]Ar)_3$ (**2a**-O) as a stable byproduct.

Preliminary kinetic measurements for fragmentation of **2**-*t*-Bu to **3**-*t*-Bu and **2a**-O in C_6D_6 solution are consistent with a first order process. Separation of volatile **3**-*t*-Bu from **2a**-O after thermolysis has been readily achieved by vacuum transfer in yields of 90%. Pure **2a**-O is recovered after vacuum transfer and can be treated with 1.0 equivalent of triflic anhydride (Tf_2O, Tf = SO_2CF_3) to afford the bistriflate complex, $Nb(OTf)_2(N[Np]Ar)_3$ (**2a**-$(OTf)_2$), in high yield. Complex **2a**-$(OTf)_2$ provides direct access to **1a**-H upon reduction with magnesium anthracene, thus completing a cycle of element activation, small-molecule generation via metathetical P–atom transfer and deoxygenative recycling of the final niobium(V) oxo product. Extension of this metathetical P for O(Cl) exchange to the synthesis of novel phosphaalkynes is discussed. In addition, the analogous N for O(Cl) exchange reaction for the synthesis of organonitriles from the niobium nitrido anion, $[NNb(N[Np]Ar)_3]^-$ ([**2a**-N]$^-$) has been developed. Nitrido anion [**2a**-N]$^-$ is obtained in a heterodinuclear N_2 scission reaction which employs the molybdenum trisamide system as a reaction partner. Treatment of [**2a**-N]$^-$ with acyl chloride substrates rapidly furnishes organonitriles concomitant with the formation of niobium oxo **2a**-O. Deoxgenative recycling of **2a**-O to a niobium complex appropriate for heterodinuclear N_2 scission has been developed as well. Utilization of ^{15}N-labeled $^{15}N_2$ gas in this chemistry has afforded a series of ^{15}N-labeled organonitriles which have been characterized by solution ^{15}N NMR. While, no intermediate complexes are observed during the organonitrile formation process, synthetic and computational studies on model systems provide strong evidence for the intermediacy of niobacyclic species.

Biographical Note

Seven pound–seven ounce Joshua Salustiano Figueroa arrived on the scene in Los Angeles, California on April 6th 1978. Although surely temped to attack life solo, he nevertheless accepted Mary (Cookie) and José Antonio Figueroa as his loving parents. Approximately two years after his birth, Cookie (a Brooklyn native) succumbed to a terrible case of L.A. sickness (see Woody Allen's Annie Hall) and, with Joshua and José in tow, departed the L.A. suburb of Irvine for the neighborhood of Douglaston in Queens, New York. A new command post was set up by Cookie and Jose at 240-41 70th Avenue in close proximity to the East Queens Septic Facility and the Creedmore Institute for the mentally ill. During Joshua's formative years, both establishments would provide conduits for wonderment in the physical and, to put it mildly, not-so-tangible worlds.

It may seem merely consequential, but the return of Cookie and Jose to New York was an integral development in Joshua's life. At that time (ca. 1980), both the Figueroa and Rosenberg sub-clans had strong representation throughout the five boroughs. This exposed Joshua not only to many diverse microcosmic areas of the city at a young age, but more importantly, allowed for the development of strong family and cultural ties to both his Judeo-New York and Puerto Rican heritages. Not surprisingly, traversing the interface of two such distinct and highly ritualized cultures would profoundly influence Joshua's social and personal consciousness.

In 1983 Joshua enrolled in Public School 221 in order to commence a lifetime study in the arts of reading, writing and arithmetic. In the first grade he was united with his future legal counsel and best friend, Daniel J. Schiffer. After a brief jaunt at Public School 203 for the 1989 and 1990 academic seasons, Joshua attended Middle School 67 where he was introduced to spray paint and indelible markers as media for artistic expression. Around this time an infatuation with the wickedness of the night-time hours also developed. In September of 1993 amid the Great Public School Asbestos Crisis, Joshua entered the da Vinci Science Program of Benjamin N. Cardozo High School and fell in love with the principles of chemical science.

Joshua joined the ranks of the Fightin' Blue Hens of the University of Delaware in 1996 and pursued chemistry as an academic major. Late in his freshman year Joshua joined the research group of Professor Arnold L. Rheingold and quickly became enamored with the beauty and mystique of inorganic synthesis and X-ray crystallography. It was at Delaware were Joshua learned the crafts of courting female fine arts majors and coffee-shop kibitzing. He also became a critic of the hippy subculture.

Upon graduation in 2000 and with his passion for chemistry solidified, Joshua devoted himself to the intense and ascetic life required by an inorganic graduate student at the Massachusetts Institute of Technology. Joshua was fortunately accepted into the research group of Professor Christopher C. Cummins where he was able to lift the skirt of and gaze upon the forbidden parts of the goddess Niobe. Thanks to the opportunities presented by Professor Cummins, Joshua was also able to reach several personal goals in the area of small molecule activation during his stay at MIT. In the summer of 2005 Joshua will begin his postdoctoral studies in the Laboratory of Professor Gerard Parkin at Columbia University.

Joshua has several nicknames and is rarely referred to as Joshua. He has many interests, the most prominent of which include people, chemistry, art, baseball and making-up nonsensical words, in that order. Joshua is prone to irrational mood-swings, but fundamentally, is a pretty happy dude. He holds lots of beliefs, but none more important than family, friends and a strong work ethic are all you really need to get by.

List of Abbreviations Used in Text

Ad = Adamantyl

Anal. = combustion analysis (elemental)

Ar = 3,5-dimethylphenyl (3,5–$Me_2C_6H_3$)

Å = Angstrom (10^{-10} m)

a = unit cell axis a

anth = anthracene ($C_{14}H_{10}$)

atm = atmosphere

a.u. = atomic units

α = position one-atom removed, unit cell angle α

Bu = butyl

b = broad, unit cell axis b

β = position two-atoms removed, unit cell angle β

Cp = cyclopentadienyl ($C_5H_5^-$)

Cy = cyclohexyl (*cyclo*-C_6H_{11})

c = unit cell axis c

cal = calories

calcd. = calculated

cm^{-1} = wavenumber

°C = degrees Celsius

D = density

DFT = Density Functional Theory

DME = dimethoxyethane

d = doublet, days, deuterated

d^n = electron count n of transition metal d-orbital manifold

dia = diamagnetic

Δ = difference

δ = delta, chemical shift, NMR shift tensor

E = energy, main group atom

Et = ethyl

Et_2O = diethyl ether

e = electron

equiv = equivalents

eq. = equation

eV = electron volts (23.060 kcal/mol)

F = crystallographic structure factor (F_o, observed; F_c, calculated)

Fc = Ferrocene ($(C_5H_5)_2Fe$)

$F(000)$ = number of electrons in unit cell

fw = formula weight

GoF = Goodness of Fit

g = grams

γ = unit cell angle γ

H = enthalpy

HOMO = Highest Occupied Molecular Orbital

Hz = Herz (s^{-1}, cycles per second)

h = hours

IR = Infrared

i-Pr = *iso*-propyl ($CH(CH_3)_2$)

J = Joules

^nJ = n^{th} bond NMR coupling constant

K = degrees Kelvin

k = kilo (10^3)

L = liters

LAH = Lithium Aluminum Hydride

LUMO = Lowest Unoccupied Molecular Orbital

M = transition metal, molar (mol/L)

MDC-q = Multipole Derived Charge at the quadrupole level

Mag. Suscep. = magnetic susceptibility

Me = methyl

Mes = mesityl, 2,4,6-trimethylphenyl (2,4,6-$Me_3C_6H_2$)

Mes* = super mesityl, 2,4,6-tri(*tert*-butyl)phenyl (2,4,6-(*t*-Bu)$_3C_6H_2$)

MO = Molecular Orbital

m = multiplet, meters, mili- (10^{-3})

min = minutes

mol = moles

μ = absorption coefficient (crystallography), magnetic moment

NMR = nuclear magnetic resonance

Np = Neopentyl ($CH_2(C(CH_3)_3$)

n = nano (10^{-9})

n = normal, number

ν = radiative frequency

$\nu_{1/2}$ = line width at half height

ORTEP = Oak Ridge Thermal Ellipsoid Plot

OTf = triflate, trifluoromethylsulfonate ($[OSO_2CF_3]^-$)

o = *ortho* position

Ph = phenyl

Pr = propyl

p = *para* position

para = paramagnetic

ppm = parts per million

py = pyridine (NC_5H_5)

q = quartet

R = rotation operator (NMR), residual value (crystallography)

S = singlet electronic state

S = entropy, electronic spin

SOF = site occupancy factor

SOMO = Singly Occupied Molecular Orbital

s = singlet

sec = seconds

so = spin orbit

σ = sigma, NMR shielding tensor

Σ = sum

T = temperature, triplet electronic state

THF = tetrahydrofuran

TS = transition state

t = triplet, time

tol = toluene (*p*-MeC_6H_5 or C_7H_8)

t-Bu = *tertiary*-butyl (*tert*, $C(CH_3)_3$)

UV = Ultraviolet

V = unit cell volume

VT = variable temperature

vis = visible

w = weighted

x = number

Z = number of molecules in unit cell

Chapter 1. Synthesis and Divergent Reactivity of the Niobaziridine-Hydride Functional Group

Joshua S. Figueroa

Department of Chemistry, Room 6-332
Massachusetts Institute of Technology
Cambridge, Massachusetts

May 9th 2005

CONTENTS

List of Figures

List of Schemes

List of Tables

1 Introduction and History

1.1 Three-Coordinate Early Transition Metal Complexes

Sustained interest in the chemistry of trivalent, three-coordinate early transition metal complexes supported by hard, anionic ligands stems from their ability to effect reductive activation of small molecule substrates.[1] It is the specific combination of coordinative unsaturation, Lewis acidity and chemically active d-electrons inherent to these MX_3 systems which is responsible for endowing rich reactivity patterns. Most notably, the reductive potency of early metal MX_3 complexes has resulted in the complete scission of strong multiple bonds in di[2-5] and triatomic[6,7] molecules. However, these MX_3 complexes also readily mediate other important chemical transformations including, carbon-hydrogen[2,8-12] and carbon-heteroatom[13-17] bond activations, in addition to the coupling of unsaturated organic substrates.[18-21] Therefore not surprisingly, harnessing the chemistry of such reactive metal systems is of interest for applications ranging from organic synthesis to dinitrogen fixation.

The chemistry of trivalent, three-coordinate early transition metal complexes dates to the late 1960's with Bradley's pioneering studies on the trisamido chromium complex, $Cr(N(i\text{-}Pr)_2)_3$.[22-24] The monodentate coordination mode of the $N(i\text{-}Pr)_2$ ligand highlighted that a trigonal planar geometry was preferred by the Cr^{3+} center when subjected to a coordination number of three. This trisamido Cr complex was found to exist with a stable, high-spin, d^3 ground-state electronic configuration, in accord with simple ligand-field considerations. While the monomeric nature of $Cr(N(i\text{-}Pr)_2)_3$ is enforced in part by the complement of three sterically encumbering amido ligands, electronic stability arises from half-filled e'' (dxz and dyz) and a'_1 (dz^2) orbital sets for the d^3 Cr center in idealized D_{3h} symmetry (Figure 1, right). Half-filled orbitals in the trigonal ligand field are not required to provide a stable three-coordinate species, as neutral MX_3 complexes are known for all first row 3+ metal ions from Ti to Co.[18-27] Indeed, several first row MX_3 complexes containing large alkyl,[28,29] amide and alkoxide[30] ligands have been reported. For many, most notably Ti(III), electronic stability of the metal center is supplemented by dative interactions from the ligand framework.[31-33] Reactivity studies of these first row MX_3 complexes have shown them to readily form simple adducts with both Lewis basic and π-acidic ligands. Furthermore, three-coordinate complexes of Ti(III) and V(III) have demonstrated marked utility as one[18-20,31,32] and two[13,14,33,34] electron reductants, respectively. However, not until the synthesis of 2nd and 3rd row metal MX_3 complexes, was the dramatic small molecule activation chemistry available to this system clearly established.

The seminal work of Wolczanski[2,3] and Rothwell[8,10] in the mid-1980's demonstrated some of the remarkable chemistry available to early metal MX_3 complexes. Wolczanski's successful isolation of the trivalent tantalum tris-siloxide complex, $Ta(silox)_3$ (silox = $OSi(t\text{-}Bu)_3$), showed that TaX_3 species were capable of mediating a diverse array of organometallic transformations. For example, early reactivity studies of three-coordinate $Ta(silox)_3$, resulted in an unprecedented example of CO reductive scission under mild synthetic conditions.[2,3] Furthermore, both $Ta(silox)_3$ and Rothwell's *in situ* generated trisaryloxide Ta(III) variants were shown to readily induce the cleavage of strong C-H[10-12] and C-N[15] bonds. Accordingly, three-coordinate TaX_3 complexes have subsequently been utilized as arene hydrogenation and alkane dehydrogenation catalysts,[12] potent oxygen-atom abstraction reagents[35-37] and solution-phase

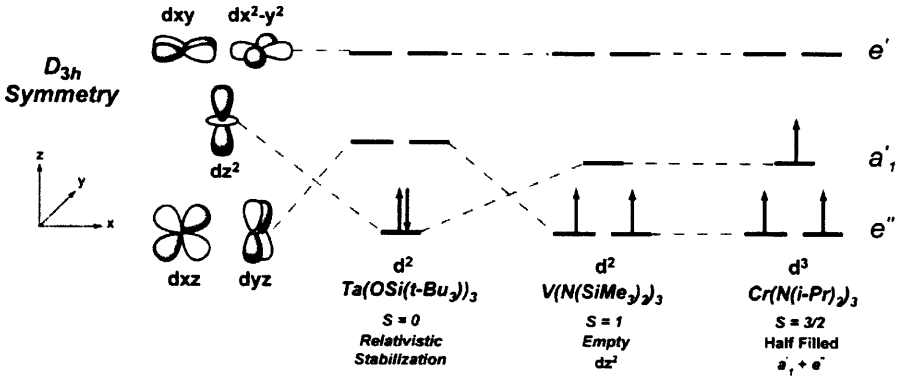

Figure 1. Qualitative molecular orbital splitting diagram for selected MX_3 complexes.

models for heterogeneous hydrodenitrogenation processes.[16-17] Three-coordinate Ta(silox)$_3$ exists as a diamagnetic, low-spin d^2 species, with the electron pair housed in a metal orbital of dz^2 parentage (Figure 1, left).[2] The reordering of the a'_1 and e'' orbital sets in the trigonal crystal field may be considered a manifestation of relativistic stabilization of dz^2 relative to dxz and dyz, which is important for 3rd row metals, but absent in those of the 1st row. However, despite d-electron spin-paring, the electropositive Ta center readily serves as a potent two-electron reductant.

The small molecule activation chemistry of three-coordinate group 6 complexes remained untapped until the synthesis of Mo(N[*t*-Bu]Ar)$_3$ (Ar = 3,5-$Me_2C_6H_3$ or C_6H_5) by our group in 1995.[4] Previous to that report, the d^3 Mo(III) fragment was known only in the triply-bound $X_3Mo{\equiv}MoX_3$ (X = NR_2, OR, alkyl) dimers extensively studied by Chisholm and Cotton.[38,39] The steric demand of the N[*t*-Bu]Ar ligand served to inhibit the dimerization of the d^3 Mo$(NR_2)_3$ fragment and accordingly, engendered the isolation of a monomeric three-coordinate complex. Like Cr(N(*i*-Pr)$_2$)$_3$[22-24] and Cr(N(SiMe$_3$)$_2$)$_3$,[40] pseudo-D_{3h}-symmetric Mo(N[*t*-Bu]Ar)$_3$ displays a stable high-spin, d^3 electronic configuration, with an a'_1 over e'' orbital splitting pattern as suggested by theoretical calculations. However, in contrast to d^3 Cr(N(*i*-Pr)$_2$)$_3$, Mo(N[*t*-Bu]Ar)$_3$ exhibits an extraordinary manifold of small molecule activation chemistry. Indeed, Mo(N[*t*-Bu]Ar)$_3$ was responsible for the first example of dinitrogen (N_2) reductive cleavage by a synthetic system under mild conditions.[4,5] Furthermore, Mo(N[*t*-Bu]Ar)$_3$ effected the first denitrogenation of N_2O,[6,7] rather than deoxygenation which is much more commonly observed. Despite, however, displaying behavior as a powerful three-electron reductant, Mo(N[*t*-Bu]Ar)$_3$ has proven to be exceedingly electrochemically versatile.

As depicted in Scheme 1, Mo(N[*t*-Bu]Ar)$_3$ is capable of activating a host of small molecule substrates by one, two and three electron reductive processes. The disparate reactivity profiles displayed between Mo(N[*t*-Bu]Ar)$_3$ and its trisamido Cr analogues arise mainly from intrinsic electronic differences between the metals themselves. Thus, the decreased electronegativity of Mo relative to Cr and the greater radial extension of the 4d vs. 3d orbitals are thought to render the d^3 Mo system more reactive than the corresponding Cr system. Further, the propensity of the three-coordinate Mo(III) to bind and activate N_2 is not mimicked for Cr. This observation has been proposed to result from the ability of Mo to undergo a facile spin-state change from the d^3 quartet (S = 3/2) ground state to the d^3 doublet (S = 1/2) excited state (Figure

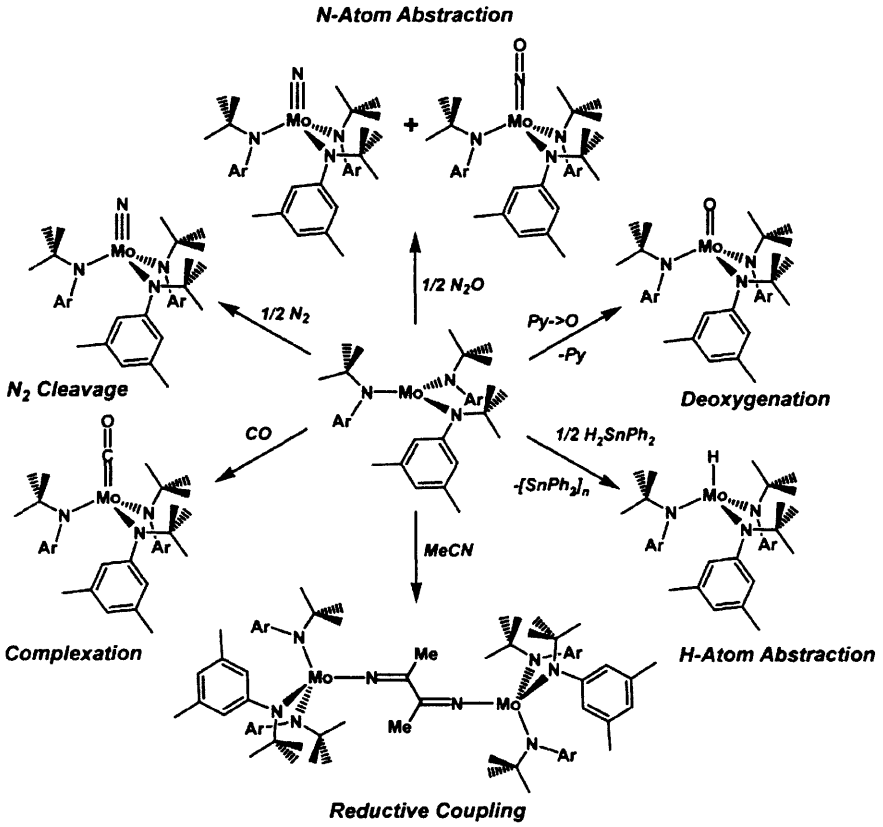

Scheme 1. Reaction pinwheel for three-coordinate Mo(N[*t*-Bu]Ar)$_3$.

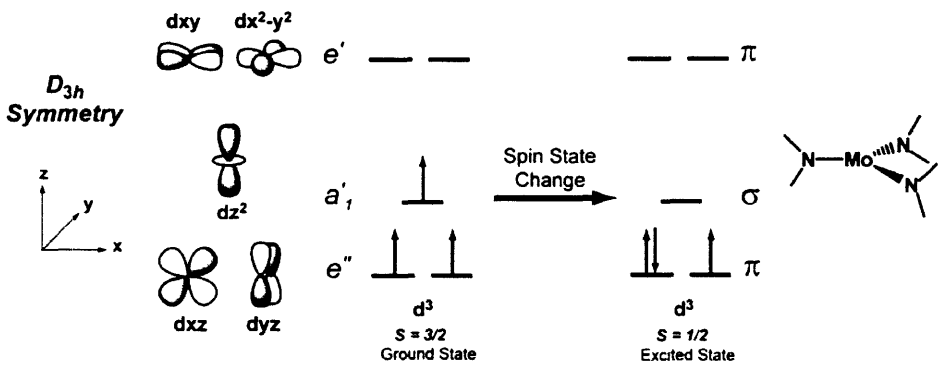

Figure 2. Qualitative molecular orbital splitting diagram for the ground and excited electronic states of three-coordinate Mo(N[*t*-Bu]Ar)$_3$.

2), while Cr is resistant to a similar spin-state change.[41] In other words, a smaller energy gap exists between the quartet and doublet spin states of three-coordinate Mo, relative to three-coordinate Cr. Consequently, the facile quartet to doublet conversion populates the π-symmetry orbital manifold (dxz and dyz) of Mo, which is an electron configuration known to favor the binding of dinitrogen. Indeed, Ta(silox)$_3$, with its d^2 electron pair housed in a σ-symmetry dz^2 orbital, has not been reported to bind N_2.

As stated above, several three-coordinate complexes of titanium and vanadium have been reported which exhibit marked reductive ability. For the former, Wolczanski's d^1 $Ti(silox)_3$ complex[18,19] and the d^1 $Ti(N[t\text{-}Bu]Ar)_3$ system reported by our group[20,31,32] have proven to be powerful one-electron, transition metal-based reductants. Each complex displays aggressive halogen-atom abstraction behavior and efficiently mediates the pinacol-type coupling of unsaturated organic substrates. Furthermore, $Ti(N[t\text{-}Bu]Ar)_3$ has also been employed in one-electron activation reactions of thermodynamically stable transition metal oxo and nitrido moieties.[31,32] Three-coordinate, vanadium(III) complexes have been prepared with alkyl,[28,29] aryl,[13,14] amido,[33,42] siloxide[36,37] and aryloxide[30] ancillary ligands. Most show a penchant for two-electron reduction chemistry, but are far less assertive for the reduction of strong bonds (*e.g.* C-H and C-N) than are three-coordinate TaX_3 complexes. Furthermore, three-coordinate V complexes show a marked tendency to bind σ-donor ligands such as THF,[13,14] pyridine[18] and phosphine oxides[36,37] without effecting their reduction. Such behavior is again in contrast to $Ta(silox)_3$, in which the filled dz^2 orbital repels σ-donor ligands. This dichotomy is rationalized by the fact that three-coordinate V complexes adopt a high-spin, triplet, d^2 electronic configuration (Scheme 1, center for $V(N(SiMe_3)_2)_3$), where an empty dz^2 orbital is available for substrate docking. Indeed three-coordinate vanadium complexes have been found to bind and activate N_2 by virtue of providing an empty σ-orbital for docking and filled π-symmetry orbitals for back-donation.[43,44]

While the varying reactivity of early metal MX_3 complexes of different periodic groups is dictated largely by d-electron count, it is clear that reactivity differences displayed by metals of the *same* group is a consequence of subtle electronic preferences. As exemplified by trisamido Cr vs. trisamido Mo complexes, each early metal offers potential patterns of reactivity inaccessible to its intragroup congeners. Therefore, in order to delineate the full range of chemistry available to MX_3 complexes, the imposition of three-coordination on all early metal 3+ ions has been of long standing interest. However, successful synthesis and isolation of three-coordinate complexes of some early metals has been a challenging endeavor. Indeed, niobium fits into this latter category[10,12,16,37] and the difficulty in obtaining an isolable three-coordinate NbX_3 complex tantalizingly points to the inherent high reactivity of such a system.

1.2 Mononuclear Niobium(III) Complexes Supported by Hard Oxygen Donor Ligands.

To date, genuine three-coordinate Nb(III) complexes are unknown. However, seminal studies by Rothwell demonstrated that d^2 Nb(III) trisaryloxide (OAr) species could be generated *in situ* by the reduction of the corresponding dichloro Nb(V) trisaryloxide complexes.[9-12] The existence of the putative d^2 $Nb(OAr)_3$ species was inferred from product analysis, which included examples of aryl and alkyl C-H activations of the aryloxide supporting ligands. These studies largely paralleled the *in situ* formation of $Ta(OAr)_3$ complexes by Rothwell,[8,10] where similar attacks on the ligand framework were observed. Thus the $Nb(OAr)_3$ fragment, though not isolable, showed the capability to serve as a powerful two-electron reductant. Subsequently, both the Nb and Ta trisaryloxide reaction systems were utilized for the catalytic hydrogenation of arenes and, interestingly, the Nb variant was found to be considerably more active than its Ta congener.[12] More recent reduction studies of a Nb(V) dihalide complex supported by a chelating trisaryloxide ligand by Kawaguchi and coworkers have resulted in the isolation of an N_2-derived niobium nitrido anion. Again, in this latter system, the intermediacy of a three-coordinate

$Nb(OAr)_3$ complex is implicated in the ensuing N_2 activation chemistry, but the exact mechanistic details are unclear.[45]

Wolczanski has provided two examples where the trivalent, three-coordinate niobium fragment is stabilized by coordination of a Lewis base.[15,16,37] Reduction of the dichloride complex, $Nb(Cl)_2(silox)_3$, in the presence of 4-picoline (4-pic) or in neat PMe_3 provided the Lewis base-stabilized complexes (η^2-*N,C*-4-pic)$Nb(silox)_3$ and $(Me_3P)Nb(silox)_3$, respectively (Scheme 2). In contrast to $V(silox)_3$ and $Ta(silox)_3$, the base-free $Nb(silox)_3$ is not amenable to isolation. Dissociation of either 4-pic or PMe_3 from the $Nb(silox)_3$ fragment leads rapidly and quantitatively to the C-H activated, cyclometallation product **A** (Scheme 2). It is noteworthy that the analogous cyclometallation of $Ta(silox)_3$ proceeds with a half-life of ca. 90 h at 25 °C,[2] further highlighting the high inherent reactivity of the NbX_3 fragment. In addition, $V(silox)_3$ has not been reported to undergo a similar ligand cyclometallation reaction.

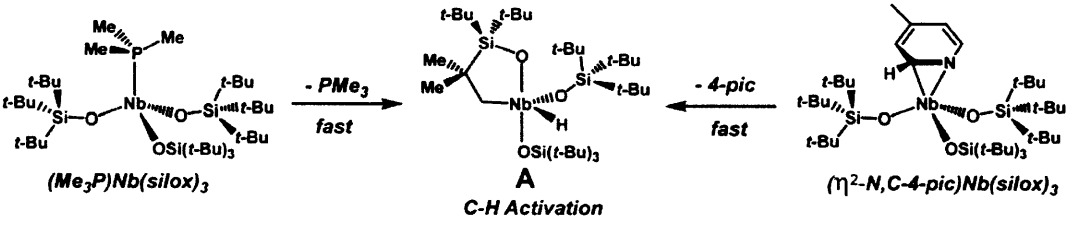

Scheme 2. Lewis base-stabilized variants of $Nb(silox)_3$ and subsequent cyclometallation.

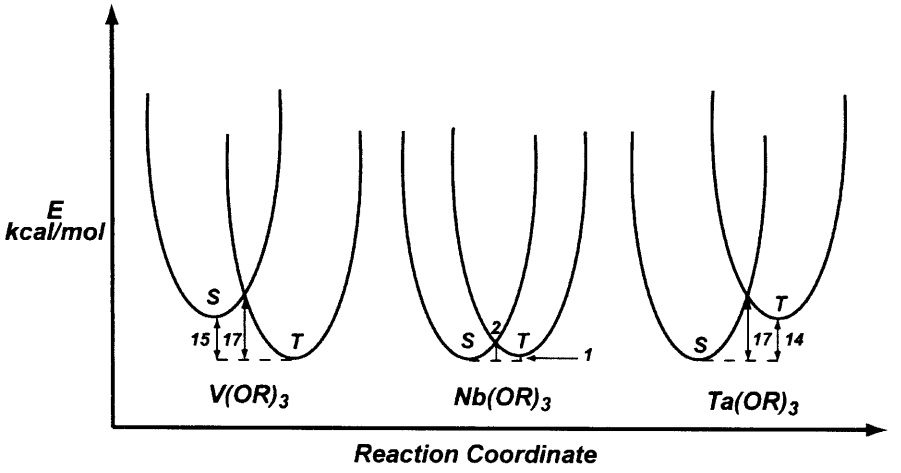

Figure 3. Potential energy surfaces for the singlet (S) and triplet (T) states of three-coordinate $M(OR)_3$ complexes (M = V, Nb, Ta). Adapted from reference 37.

An explanation for the observed kinetic instability of $Nb(OR)_3$ complexes as compared to its $V(OR)_3$ and $Ta(OR)_3$ congeners can be extracted from DFT calculations reported by Cundari and Wolczanski.[37] They have suggested that the disparate deoxygenation capabilities between these d^2 group 5 species arise from the preferred electronic configuration of the metal. In accord with experiment, the calculations reveal that the triplet ($S = 1$) d^2 ground state in formal D_{3h} symmetry is the preferred configuration for $V(OR)_3$. The corresponding singlet state is 15 kcal/mol higher in energy, and a sizable (17 kcal/mol) geometric reorganization barrier exists to the intersystem

crossing (i.e. triplet (T) → singlet (S), Figure 3). For $Ta(OR)_3$ the singlet ($S = 0$) d^2 configuration is the ground state and the corresponding triplet state lies 14 kcal/mol higher in energy (Scheme 5). The latter intersystem crossing must also overcome a 17 kcal/mol reorganization barrier to proceed. Thus the stability of $Ta(OR)_3$ can be considered as a result of a stable singlet ground state which can not readily achieve a triplet configuration. The same is true for $V(OR)_3$, where a difficult T→S conversion is responsible for stability.

A markedly different energetic situation exists for the d^2 electronic states of $Nb(OR)_3$. As shown in Scheme 5, the singlet ($S = 0$) d^2 configuration is calculated to be the ground state. However, the corresponding triplet ($S = 1$) state is only 1 kcal/mol higher in energy and the corresponding S→T intersystem crossing is only inhibited by 2 kcal/mol (Scheme 5). Furthermore, intersystem crossing between the S and T spin states is not accompanied by significant geometric reorganization. Therefore, the S and T states of d^2 $Nb(OR)_3$ can be considered as destabilized with respect to each other. If the singlet d^2 ground state is preferred by $Nb(OR)_3$, crossing to the triplet state is unavoidable due to the thermally accessible 2 kcal/mol barrier. Accordingly, the reverse T→S conversion is also readily accomplished. Thus the rapid ligand activation process as seen for base-free $Nb(silox)_3$, whether originating from the S or T d^2 state, provides irreversible access to a stable singlet state (e.g. a d^0 alkyl-hydride complex). In short, electronic stability is achieved by ligand activation. Conversely, coordination of PMe_3, as in $S = 1$ $(Me_3P)Nb(silox)_3$, stabilizes the triplet electronic configuration by providing a substantial energy gap between the a'_1 and e'' orbitals of free $Nb(silox)_3$.

Experimental evidence for facile singlet/triplet spin-state interconversions in Nb^{III} complexes has been reported by Fryzuk.[46] Variable temperature magnetic susceptibility measurements conducted on the trigonal bipyramidal, chloro Nb^{III} complex, $Nb(Cl)^{Cy}[P_2N_2]$ ($^{Cy}[P_2N_2]$ = $CyP(CH_2SiMe_2NSiMe_2CH_2)_2PCy$, Cy = cyclohexyl), indicated a steady rise in magnetic moment as temperature was lowered from 300 to 40 K. Such behavior is consistent with a facile spin-state crossover for Nb^{III} and is analogous to the classic temperature-dependent Fe^{II} high-spin/low-spin interconversion systems.[47,48] Notably, Fryzuk's results indicate a triplet ($S = 1$) ground-state for $Nb(Cl)^{Cy}[P_2N_2]$, at variance with the computational results for $Nb(OR)_3$, but reasonable given that trigonal bipyramidal $Nb(Cl)^{Cy}[P_2N_2]$ can be considered as a bisphosphine-adduct of three-coordinate NbX_3.

Further computational support for the role of spin-state changes in affecting the stability of NbX_3 can be gleaned from calculations performed by Morokuma on the molybdenum *tris*-amide system $Mo(NH_2)_3$.[41] As discussed above, the high-spin d^3 ($S = 3/2$) configuration is the calculated ground-state for $Mo(NH_2)_3$, but facile conversion to the doublet ($S = 1/2$) state was noted. Similar to the group-5 $M(OR)_3$ system, both $Cr(NH_2)_3$ and $W(NH_2)_3$, were suggested to adopt quartet and doublet ground-state configurations, respectively, and the barrier for intersystem crossings was considerably higher than that for $Mo(NH_2)_3$. Evidently, facile spin-state change is a hallmark of the 2nd row early transition metals and may partially account for the rich reactivity they display. However, while the three-coordinate, high-spin d^3 configuration of Mo is known to be stable, the instability of the corresponding d^2 Nb system configuration is particularly pronounced. Thus, as is the case for (η^2-*N,C*-4-pic)$Nb(silox)_3$ and $(Me_3P)Nb(silox)_3$, it stands to reason that an efficient stabilization system must be utilized in order to obtain a functional equivalent of NbX_3. While Lewis base-stabilized (η^2-*N,C*-4-pic)$Nb(silox)_3$ and

$(Me_3P)Nb(silox)_3$ indeed act as a source of $Nb(silox)_3$,[16,37] subsequent small molecule activation chemistry has been found to be somewhat impeded by the presence of liberated base in solution.[49] Needed is the development of a system which does not require the presence of an external stabilization agent for three-coordinate NbX_3.

1.3 The Pursuit of a Masked Three-Coordinate Niobium Trisamido Complex.

Whereas the encumbering anilido ligand, N[*t*-Bu]Ar, popularized by our group allowed for the isolation of three-coordinate Ti, V, Cr and Mo complexes, it did not engender the isolation of a corresponding $Nb(N[t\text{-}Bu]Ar)_3$ species. As shown by Fickes, reduction of the chloro Nb^{IV} complex, $ClNb(N[t\text{-}Bu]Ar)_3$,[50] with a host of alkali and alkaline earth reductants invariably led to the bridging bis-imido dimer, $[(\mu_2\text{-}NAr)Nb(N[t\text{-}Bu]Ar)_2]_2$ (Scheme 3).[51] Formation of $[(\mu_2\text{-}NAr)Nb(N[t\text{-}Bu]Ar)_2]_2$ is proposed to occur by a multi-step process in which the putative $[Nb(N[t\text{-}Bu]Ar)_3]$ formed upon reduction elicits the ejection of *tert*-butyl radical, concomitant with the formation of the Nb^{IV} imido species $[Nb(NAr)(N[t\text{-}Bu]Ar)_2]$. The latter is thought to rapidly dimerize with Nb-Nb bond formation to the observed dimeric product. Therefore, the N[*t*-Bu]Ar ligand was unable to stabilize a NbX_3 complex due to its susceptibility to *tert*-butyl radical ejection. However, these results additionally suggest that the NbX_3 system is capable of mediating one-electron reductive processes.

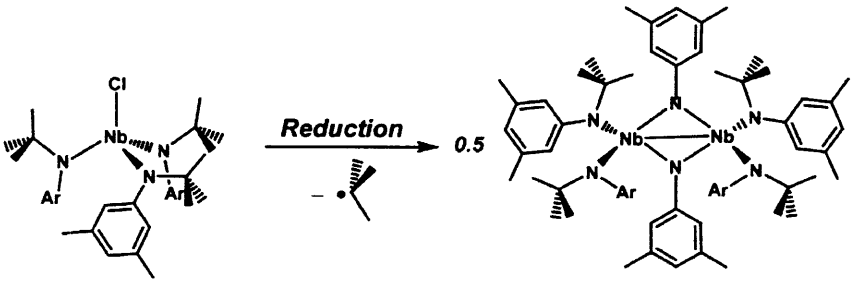

Scheme 3. Attempted preparation of $Nb(N[t\text{-}Bu]Ar)_3$ via reduction of $ClNb(N[t\text{-}Bu]Ar)_3$.

Gambarotta has also reported several examples of dramatic ligand degradation reactions in his attempts to prepare related low-valent Nb-amido complexes using the NPh_2,[52] NCy_2[53,54] and NPy_2[55] amido ligands (Cy = cyclohexyl, Py = pyridyl). Indeed, these ligands have been shown to be vulnerable to C-H and C-N reductive cleavages by presumed low valent Nb-amido species. Furthermore, implementation of the larger N[1-Ad]Ar and N[1-Nor]Ar ligands (Ad = adamantyl, Nor = norbornyl) by Gambarotta[53,56] and our group toward the synthesis of a $Nb(N[R]Ar)_3$ complex resulted in mixtures of products attributable to ligand degradation processes. Since $Nb(NR_2)_3$ species are conspicuously able to perform ligand degradation reactions, it was of interest to utilize this tendency as a means for stabilization of the $Nb(NR_2)_3$ fragment. Furthermore, utilizing an amido ligand itself for such a purpose would obviate the need for an external stabilization agent.

An attractive approach to stabilization of an $Nb(NR_2)_3$ species involved exploitation of the d^2 Nb center's ability to activate C-H bonds. Previous work from our group had shown that the β-hydrogen-containing *N*-isopropyl anilido ligand, N[*i*-Pr]Ar, can effectively mask three-coordinate Mo in a molybdaziridine-hydride form.[57] Indeed, the molybdaziridine-hydride

complex Mo(H)(η^2–Me_2C=NAr)(N[*i*-Pr]Ar)$_2$ (Scheme 4) is the product of amido ligand C-H activation when three-coordinate Mo(III) is ligated by three N[*i*-Pr]Ar ligands. While d^3 Mo(III) is effectively stabilized by three N[*t*-Bu]Ar ligands, proximity of β-hydrogen atoms to the Mo center results in rapid C-H oxidative addition. However, the molybdaziridine-hydride complex so obtained functions exclusively as a source of the three-coordinate species, Mo(N[*i*-Pr]Ar)$_3$, upon reaction with small molecules.[58-61] Thus the β-H elimination process is reversed upon reaction with substrate. Several examples of the chemistry available to Mo(H)(η^2–Me_2C=NAr)(N[*i*-Pr]Ar)$_2$ are depicted in Scheme 5, and it is notable that substrate insertion into the Mo-H bond *has not*, to date, been encountered.

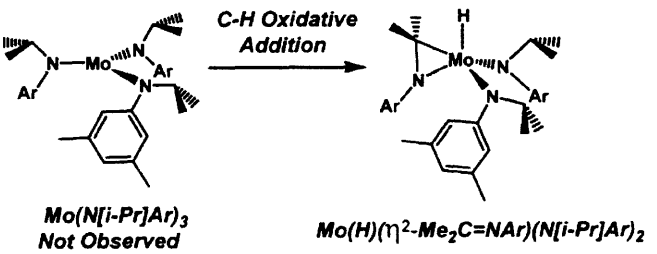

Scheme 4. Proposed tautomerization between Mo(N[*i*-Pr]Ar)$_3$ and the molybdaziridine-hydride complex Mo(H)(η^2–Me_2C=NAr)(N[*i*-Pr]Ar)$_2$

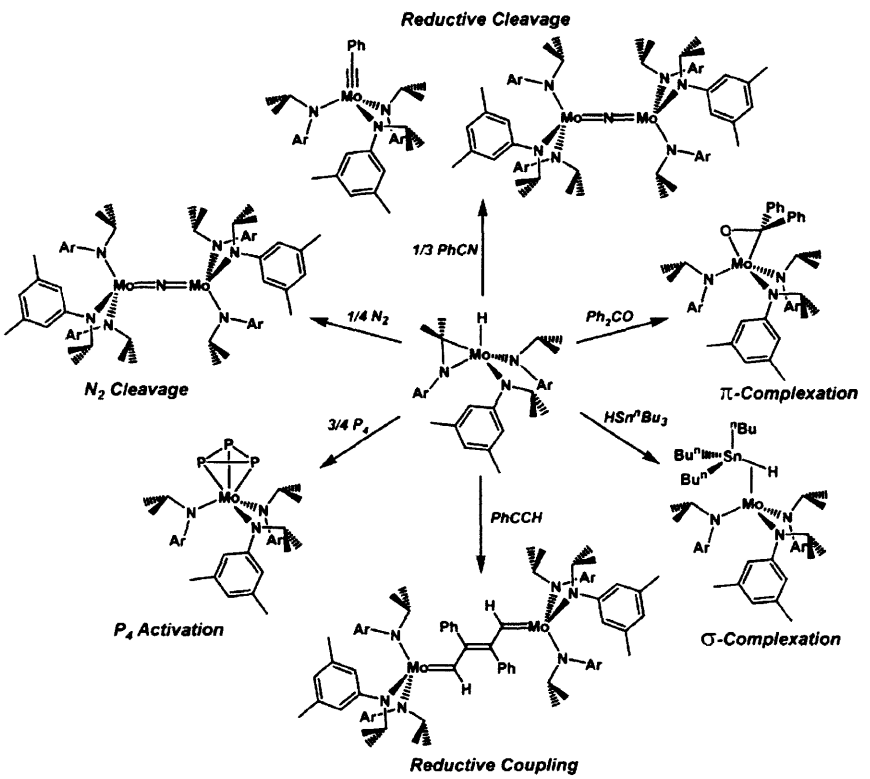

Scheme 5. Reaction pinwheel for molybdaziridine-hydride Mo(H)(η^2–Me_2C=NAr)(N[*i*-Pr]Ar)$_2$.

That a niobaziridine-hydride complex could serve as a source of the reactive $Nb(NR_2)_3$ fragment was implicated by an intriguing report from Gambarotta.[54] As shown in Scheme 6, treatment of $NbCl_4(THF)_2$ with three equivalents of the β-H-containing amide, $LiNCy_2$, provided the niobaziridine-chloride complex $Nb(Cl)(\eta^2\text{–}C_5H_{10}C{=}NCy)(NCy_2)_2$ (**A**). The latter subsequently provided the bridging N_2 complex, $(\mu_2\text{-}N_2)[Nb(NCy_2)_3]_2$ (**B**), upon treatment with $Na[HBEt_3]$ in the presence of N_2. Interestingly, the intermediacy of a niobaziridine-hydride species was not proposed in this report. However, it is conceivable that H^- for Cl^- exchange provides the niobaziridine-hydride complex, $Nb(H)(\eta^2\text{–}C_5H_{10}C{=}NCy)(NCy_2)_2$, which is responsible for the observed N_2 chemistry by serving as a source of $Nb(NCy_2)_3$.

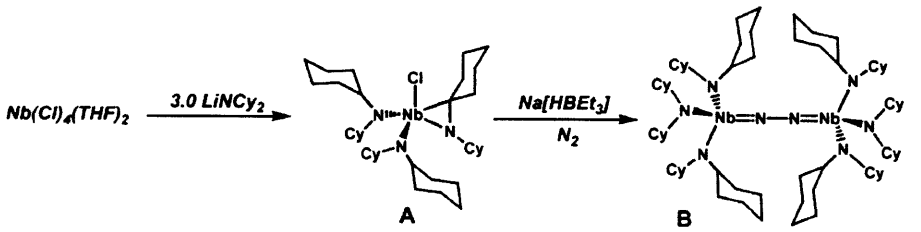

Scheme 6. Synthesis of the niobaziridine chloride **A** and subsequent N_2 chemistry. Adapted from reference 54.

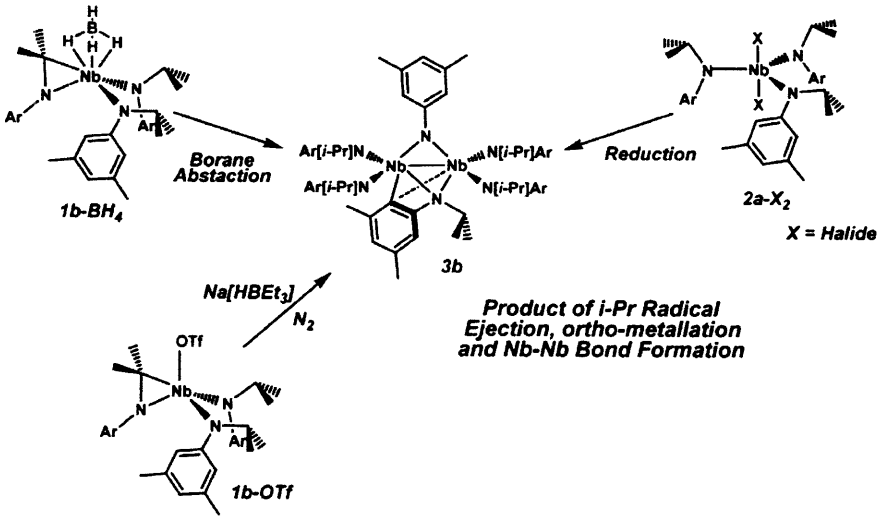

Scheme 7. Attempted Syntheses of the niobaziridine-hydride $Nb(H)(\eta^2\text{–}Me_2C{=}NAr)(N[i\text{-}Pr]Ar)_2$ (**1b**-H).

Accordingly, a program was initiated in our group to synthesize the niobaziridine-hydride complex $Nb(H)(\eta^2\text{–}Me_2C{=}NAr)(N[i\text{-}Pr]Ar)_2$ (**1b**-H), which could potentially serve as a source of three-coordinate $Nb(N[i\text{-}Pr]Ar)_3$ (**2b**) via reversible β-H elimination. However, the marked ability of the N[*i*-Pr]Ar ligand to mask a reactive three-coordinate Mo complex was not replicated for Nb. As demonstrated by Mindiola,[62,63] reduction of $Nb(X)_2(N[i\text{-}Pr]Ar)_3$ (**2b**-X_2, X = Cl, I) complexes with alkali metals did not lead to the desired niobaziridine-hydride complex **1b**-H. Instead, a complicated dimeric species was formed, which was reminiscent to that obtained in the N[*t*-Bu]Ar-ligated Nb system (**3b**, Scheme 7). Remarkably, dimer **3b** is not only a product of *iso*-propyl radical ejection concomitant with Nb-Nb bond formation, but is also a result of ortho-metallation of a N[*i*-Pr]Ar ligand. Niobaziridine ring formation was achievable by

other means and resulted in the isolation of the niobaziridine-triflate complex, Nb(OTf)(η^2–Me_2C=NAr)(N[*i*-Pr]Ar)$_2$ (**1b**-OTf, OTf = OSO_2CF_3). Complex **1b**-OTf is a pseudohalide analogue of Gambarotta's niobaziridine-chloride species, but upon reaction with Na[$HBEt_3$], dimer **3b** was produced rather than **1b**-H or an N_2 activation product (Scheme 7). Notably, complex **1b**-OTf could be smoothly transformed into the niobaziridine-borohydride complex, Nb(BH_4)(η^2–Me_2C=NAr)(N[*i*-Pr]Ar)$_2$ (**1b**-BH_4) upon treatment with $LiBH_4$. Whereas, complex **1b**-BH_4 represents a borane-adduct of the desired niobaziridine-hydride **1b**-H, borane abstraction with Lewis bases, again, resulted in N[*i*-Pr]Ar ligand degradation and the formation of **3b** (Scheme 7).

While the N[*i*-Pr]Ar ligand appeared overly susceptible to isopropyl radical ejection, a stable niobaziridine-hydride complex could potentially be obtained if a ligand resistant to radical degradation was employed. Therefore, a new β-H-containing anilido ligand, namely the *N*-neopentyl variant (N[Np]Ar), was investigated for this purpose. It was postulated that the N[Np]Ar ligand could resist radical degradation due to the greater thermodynamic barrier to neopentyl radical formation than that for either the *iso*-propyl or *tert*-butyl radical.[64] Furthermore, three neopentyl substituents would likely impart the necessary steric protection to engender the formation of a monomeric niobaziridine-hydride complex.

In this chapter, the successful isolation of the N[Np]Ar-derived, niobaziridine-hydride complex Nb(H)(η^2–*t*–Bu(H)C=NAr)(N[Np]Ar)$_2$ (**1a**-H) is described. As hoped, the N[Np]Ar ligand provides a kinetically persistent, monomeric niobaziridine-hydride complex which is resistant to radical-type degradation processes. Complex **1a**-H is shown to indeed serve as a functional equivalent of Nb(N[Np]Ar)$_3$ (**2a**) in its reaction chemistry, thereby verifying the niobaziridine-hydride functionality as an effective mask for a three-coordinate Nb *tris*-amido species. However, **1a**-H also displays reactivity typical of an early metal hydride complex, thus revealing a distinctive dichotomy in the chemistry accessible to the niobaziridine-hydride functional group.

2 Synthesis, Characterization and Thermal Behavior of the Niobaziridine–Hydride Complex Nb(H)(η^2–*t*–Bu(H)C=NAr)(N[Np]Ar)$_2$ (1a-H)

2.1 Synthesis and Characterization of the Niobaziridine-Hydride Complex Nb(H)(*t*-Bu(H)C=NAr)(N[Np]Ar)$_2$ (1a-H)

In his efforts to synthesize niobaziridine-hydride complex **1b**-H, Mindiola developed a reliable and high-yielding method for the installation of three N[*i*-Pr]Ar ligands on niobium.[57] Utilizing the trichloride complex, *mer,cis*-Nb(η^2–PhCCPh)(Cl)$_3$(THF)$_2$,[65] Mindiola found that smooth transmetallation could be achieved with 3.0 equiv of (Et_2O)Li(N[*i*-Pr]Ar). The resultant η^2-diphenylacetylene complex, (η^2–PhCCPh)Nb(N[*i*-Pr]Ar)$_3$ (**2b**-PhCCPh), was obtained in good yield without significant contamination from byproducts arising from reduction of the niobium trichloride precursor. The fact that lithium-amide reduction of Nb(η^2–PhCCPh)(Cl)$_3$(THF)$_2$ was not observed is attributed to attenuation of the electrophilicity of the Nb by the η^2–PhCCPh

ligand. The latter, being isolobal to an imido (NR) ligand, is thought raise the HOMO-LUMO gap of the $NbCl_3$ fragment, thereby rendering it less susceptible to reduction. Thus the PhCCPh ligand can be considered as a protecting group for the electrophilic Nb center. Removal of PhCCPh was achieved upon addition of elemental iodine, readily affording the bisiodide complex, $Nb(I)_2(N[i\text{-}Pr]Ar)_3$ (**2b**-I_2). The latter served as a convenient starting material for subsequent reduction studies. As depicted in Scheme 8, this synthetic route was readily extended to the formation of N[Np]Ar-ligated Nb complexes. Accordingly, the Nb(V) diiodide complex, $Nb(I)_2(N[Np]Ar)_3$ (**2a**-I_2), was obtained as an orange powder in 65-80% yield after diphenylacetylene deprotection of (η^2–PhCCPh)Nb(N[Np]Ar)$_3$ (**2a**-PhCCPh) with I_2.

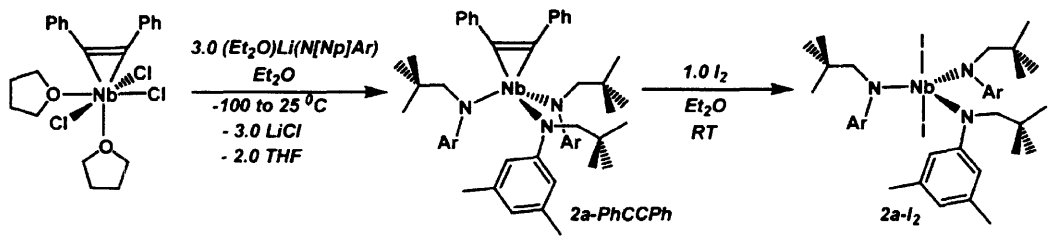

Scheme 8. Synthesis of complexes **2a**-PhCCPh and **2a**-I_2.

As was hoped, the N[Np]Ar-ligated Nb system allowed for the formation of a kinetically stable niobaziridine-hydride complex. Thus, treatment of a thawing THF solution of **2a**-I_2 with 1.25 equiv of $Mg(THF)_3$(anthracene)[66] led smoothly to the formation of the desired niobaziridine-hydride, Nb(H)(η^2-*t*-Bu(H)C=NAr)(N[Np]Ar)$_2$ (**1a**-H), as revealed by ^{1}H NMR (Scheme 9). Notably, the use of $Mg(THF)_3$(anthracene) was necessitated by the lack of clean reduction chemistry between **2a**-I_2 and common reducing agents such as Na/Hg and Mg^0. The latter observations suggest that **1a**-H is sensitive to the reaction conditions employed for its formation. After liberation of the MgI_2 and anthracene byproducts, diamagnetic **1a**-H is reproducibly obtained as large orange blocks in 50-60% yield from ca. of 12.0 g of **2a**-I_2. Once isolated, **1a**-H is freely soluble in common hydrocarbon and ethereal solvents.

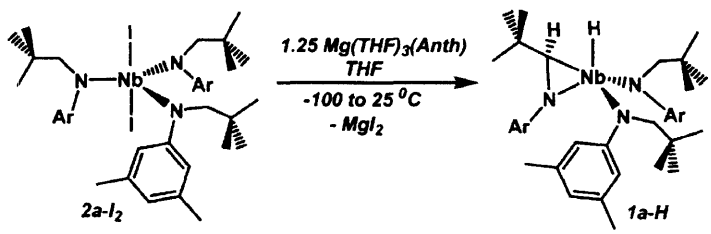

Scheme 9. Synthesis of the niobaziridine-hydride Nb(H)(η^2-*t*-Bu(H)C=NAr)(N[Np]Ar)$_2$ (**1a**-H).

A crystallographic structure determination of **1a**-H confirmed its formulation as a monomeric niobaziridine-hydride complex (Figure 4). Clearly evident from the structure of **1a**-H are the formation of the niobaziridine ring and the proximity of the crystallographically located hydrido ligand to the metallated carbon atom. A notable metrical parameter for **1a**-H is the C1-N1 bond distance of 1.407(2) Å, which is indicative of the niobaziridine functionality enjoying some η^2-imine-like character.[67] Accordingly, a considerably longer bond C-N length is observed for the intact N[Np]Ar ligands (*e.g.* d(C2-N2) = 1.472(4) Å). The ^{1}H NMR spectrum of **1a**-H,

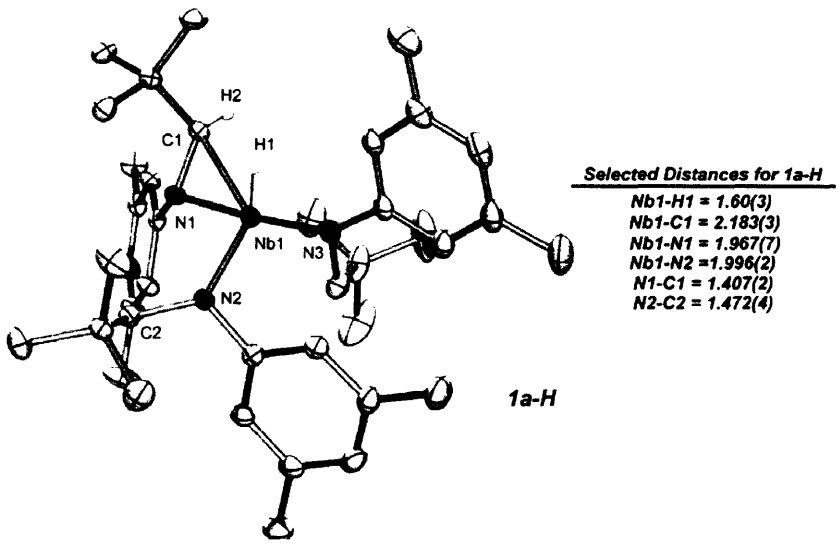

Figure 4. ORTEP diagram of niobaziridine-hydride (**1a**-H) at the 35% probability level.

consistent with its solid state structure, indicates C_1 symmetry due to formation of a stereogenic center at the carbon atom of the niobaziridine ring. A broad resonance observed at 9.24 ppm is assigned to the metal-bound hydride ligand. Such downfield shifts are typical for high-valent early transition metal hydride complexes,[68,69] and the broadness of the signal can be attributed to coupling to the quadrupolar Nb nucleus (^{93}Nb, I = 9/2, 100 %).[70,71] Furthermore, the infrared spectrum of **1a**-H displays a stretch of moderate intensity located at 1701 cm^{-1} which is assigned to the Nb-H moiety.

2.2 Solution Thermal Behavior of Complex 1a-H: Anilido Ligand C-N Oxidative Addition

Variable temperature ^{2}H NMR studies on the deuterium-labeled molybdaziridine-hydride, Mo(H)(η^2–$(CD_3)_2C$=NAr)(N[*i*-Pr-d_6]Ar)$_2$ (**4b**-H-d_{18}), revealed a chemical exchange process at temperatures greater than 75 °C.[57] This exchange process was attributed to reversible β-H elimination between **4b**-H-d_{18} and its three-coordinate tautomer, Mo(N[*i*-Pr-d_6]Ar)$_3$ (**5b**-d_{18}). Accordingly, to provide evidence for reversible β-H elimination and the existence of the three-coordinate Nb(N[Np]Ar)$_3$ (**2a**), niobaziridine-hydride **1a**-H was studied by variable temperature ^{1}H NMR. However, the spectrum of **1a**-H remained static up to 80 °C, at which temperature a new C_s symmetric product appeared concomitant with the disappearance of **1a**-H. A preparative thermolysis of **1a**-H was performed at 80 °C in C_6D_6, eliciting a color change from bright orange to pale brown. ^{1}H and ^{13}C NMR data indicated the product of thermolysis to be the neopentylimido complex, Nb(NNp)(Ar)(N[Np]Ar)$_2$ (**3a**), formally the product of C-N bond oxidative addition by putative intermediate **2a**, or alternatively the product of 1,2-aryl migration (N→Nb) via intermediate **2a** (Scheme 10). The rapid C-N oxidative addition of an anilido ligand has been observed previously when the three-coordinate Mo(N[*t*-Bu]Ar)$_3$ is subjected to one-electron oxidation. Specifically, treatment of Mo(N[*t*-Bu]Ar)$_3$ with the ferrocenium borate salt, Fc[BAr$_f$] (BAr$_f$ = B(3,5-$(CF_3)C_6H_3)_4$), led to the formation of the *tert*-butyl imido cation [Mo(N-

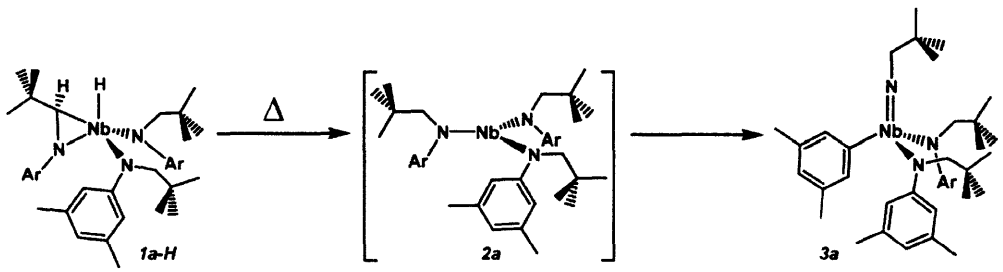

Scheme 10. Thermolytic decomposition of **1a**-H: Synthesis of the aryl imido complex **3a** by C-N oxidative addition.

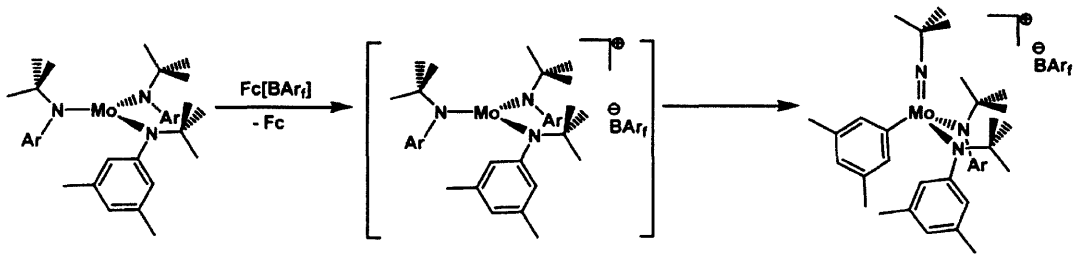

Scheme 11. Oxidatively induced C-N reductive cleavage for Mo(N[*t*-Bu]Ar)$_3$.

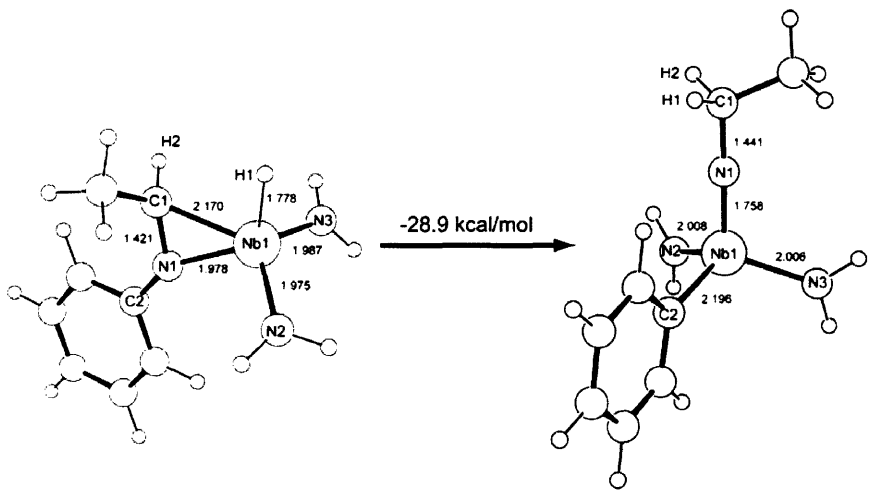

Figure 5. Optimized geometries and relative thermodynamic stabilities of models **1m-H** and **3m**.

t-Bu)(Ar)(N[*t*-Bu]Ar)$_2$]$^+$, presumably via the intermediacy of the reactive d^2 cation, [Mo(N[*t*-Bu]Ar)$_3$]$^+$ (Scheme 11).

It is noteworthy that although three-coordinate **2a** is also the likely precursor to **1a**-H, crude reaction mixtures assayed during the synthesis of **1a**-H do not indicate any formation of **3a**. However, C_6D_6 solutions of pure **1a**-H at room temperature do become enriched with **3a** over time ($t_{1/2}$ = ca. 4.5 d), pointing to the conversion of **1a**-H to **2a** by reversible β-H elimination in solution. Furthermore, thermal rearrangement of **1a**-H proceeds quantitatively to **3a**, which retains its integrity at elevated temperatures. Therefore, **1a**-H can be considered a kinetic product of ligand degradation by three-coordinate **2a**, while isomer **3a** is the thermodynamic product. The latter notion has been substantiated by DFT calculations performed on a model system for

the **1a**-H to **3a** conversion. As depicted in Figure 5, the hypothetical niobaziridine-hydride complex, Nb(H)(η^2-Me(H)C=NPh)(NH_2)$_2$ (**1m-H**), lies 28.9 kcal/mol higher in energy than its ethyl imido isomer, Nb(NEt)(Ph)(NH_2)$_2$ (**3m**). This remarkable discrepancy in energy highlights the kinetic formation of the niobaziridine-hydride functionality from three-coordinate **2a**, when clearly C-N oxidative addition is energetically preferred. Presumably, the thermodynamic gain in the formation of **3a** arises from imido-metal formation, which serves to stabilize the resultant electrophilic Nb(V) center. However, the kinetic barrier to C-N oxidative addition is evidently greater than that for C-H oxidative addition, thereby allowing niobaziridine-hydride formation to be kinetically competent for alleviation of the inherent instability of the d^2 Nb(N[Np]Ar)$_3$ fragment.

Notable from the optimized structure of model **1m-H** is the Nb-H1 bond length of 1.778 Å, which is approximately 0.2 Å greater than that found crystallographically for **1a**-H. However, X-ray diffraction is known to underestimate H-element bond lengths due to the lack of electron density in the vicinity of the hydrogen nucleus. Therefore, the computational results provide a better estimate of the Nb-H internuclear separation, as the sum of the Nb and H covalent radii attests (1.75 Å).[72] Furthermore, due absence of crystallographic data, the optimized metrical parameters of **3a-m** are suggested to reasonably approximate the molecular core of neopentyl imido **3a**.

2.3 Isotopic Labeling Studies: Evidence for Reversible β-H Elimination in Solution.

To obtain further evidence for the interconversion of complex **1a**-H and putative **2a** via reversible β-H elimination, the niobaziridine-deuteride complex, Nb(D)(η^2-*t*-Bu(D)C=NAr)(N[Np-d_2]Ar)$_2$ (**1a**-D; Np-d_2 = CD_2(*t*-Bu)) was synthesized. Selective deuteration of the methylene positions in the amine, HN(Np-d_2)Ar, was achieved according to Scheme 12, and complex **1a**-D was then prepared analogously to **1a**-H. As expected, the ^{1}H NMR spectrum of pure **1a**-D was identical to that of **1a**-H, minus the resonances originating from the methylene position of the N[Np]Ar ligand. Accordingly, these resonances appeared in the ^{2}H NMR spectrum of **1a**-D at the expected chemical shifts, with the Nb-D resonance assigned to a broad signal located at 9.20 ppm ($\nu_{1/2}$ = 8.83 Hz). As **1a**-D sat in C_6D_6 solution over time, proton incorporation into its methylene positions was not observed by ^{1}H NMR, thereby ruling out the possibility of a complicated exchange process between all C-H bonds of the N[Np]Ar ligand framework.

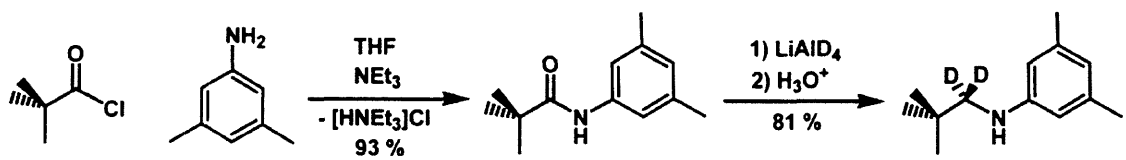

Scheme 12. Synthesis of the deuterated amine HN(Np-d_2)Ar.

During reactivity studies of complex **1a**-H (Section 2), it was found that hydride for chloride exchange could be induced upon the addition of CH_2Cl_2. The resulting niobaziridine-chloride complex, Nb(Cl)(η^2-*t*-Bu(H)C=NAr)(N[Np]Ar)$_2$ (**1a**-Cl, Scheme 13), was obtained as an *n*-pentane insoluble orange powder in *ca.* 90% yield. Thus the Nb-H moiety of **1a**-H displayed

substitution chemistry typical of an early metal hydride complex. The latter observation is in direct contrast to molybdaziridine-hydride **4b**-H, which does not display such behavior. In addition, treatment of **1a**-Cl with the borohydride reagent, Li[HBEt$_3$] in the presence of N_2, cleanly regenerated niobaziridine-hydride **1a**-H. As opposed to Gambarotta's niobaziridine-chloride complex,[57] an N_2-activation product was not obtained in the reaction between **1a**-Cl and Li[HBEt$_3$].

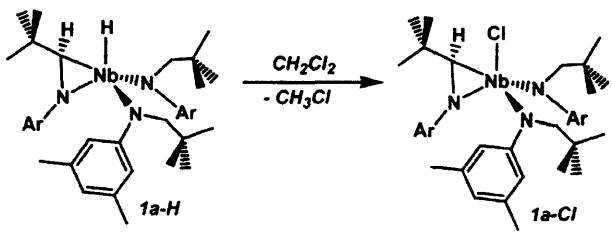

Scheme 13. Synthesis of the niobaziridine-chloride **1a**-Cl.

The analogous chloride for deuteride exchange was observed with upon treatment of **1a**-D with CD_2Cl_2, producing Nb(Cl)(η^2-*t*-Bu(D)C=NAr)(N[Np-d_2]Ar)$_2$ (**1a**-Cl-d_5) in excellent yield. Accordingly, complex **1a**-Cl-d_5 was treated at room temperature with 1.0 equiv of Li[HBEt$_3$] in THF solution. Analysis of an aliquot taken from the reaction mixture after 1 h by ^{1}H NMR clearly indicated proton scrambling into the methylene positions of the N[Np-d_2]Ar ligand (Scheme 14). Furthermore, the appearance of an Nb-H resonance was evident at ca. 9.2 ppm. Since H/D scrambling is not observed in pure **1a**-D alone, the protons incorporated into of the N[Np-d_2]Ar framework must originate from Li[HBEt$_3$]. One mechanistic scenario is that nucleophilic H^- for Cl^- substitution at Nb produces the hydride complex Nb(H)(η^2-*t*-Bu(D)C=NAr)(N[Np-d_2]Ar)$_2$ (**1a**-H-d_5), which scrambles H and D atoms due to reversible β-H elimination via the intermediacy of three-coordinate **2a**.

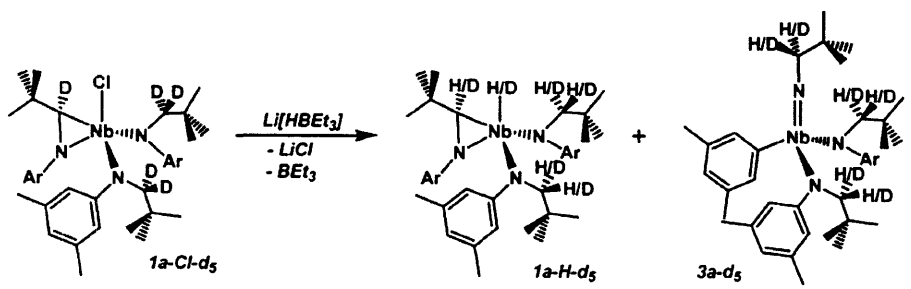

Scheme 14. H/D scrambling from the reaction between **1a**-Cl-d_5 and Li[HBEt$_3$].

However, the possibility that H^- adds directly to the carbon atom of the niobaziridine ring can not be ruled out. Such an event would produce **2a**-d_5 directly, with loss of BEt$_3$ and LiCl. If this latter mechanism is operative, niobaziridine ring closure by C-H(D) oxidative addition would produce one of six possible isotopomers of **1a**-H-d_5. If there is a significant kinetic isotope effect for C-H oxidative addition and reversible β-H elimination between **1a**-H-d_5 and **2a**-d_5 does not occur, then the unique H-atom of **1a**-H-d$_5$ would be expected to sample the hydride position with greatest probability. However, as discussed below, there is a significant H/D kinetic isotope effect in this system. While ^{1}H NMR indicates that H-atoms scramble into the methylene

positions of **1a**-H-d_5 with equal intensity, the quadrupolar coupling to Nb prevented an accurate integration of the hydride position. Although rapid and reversible β-H elimination may indeed take place between **1a**-H-d_5 and **2a**-d_5, this H/D scrambling experiment does not provide conclusive evidence for such a fact.

It is important to note that after 1 h the reaction between **1a**-Cl-d_5 and Li[HBEt$_3$] had only proceeded to 75% completion. Furthermore, during this time substantial decay of **1a**-H-d_5 to **3a**-d_5 had taken place (Scheme 14). During reactivity studies of **1a**-D, it was noted that the C-N oxidative addition process leading to **3a**-d_6 was considerably faster than for the analogous decay of perprotio **1a**-H. Whereas the relatively slow rate of formation and rapid decay of **1a**-H-d_5 precluded the determination of an equilibrium or rate constant for H/D scrambling, the kinetic isotope effect on C-N oxidative addition in the **1a**-H/D system was readily amenable for study. The rates of decay of **1a**-H and **1a**-D to the corresponding imido complex **3a** in C_6D_6 were measured by ^{1}H NMR at 75 °C. Reproducible, first order kinetics were obtained for both complexes at this temperature. As Figure 6 shows, the decay of **1a**-D is considerably faster than that for **1a**-H, resulting in an kinetic isotope effect (KIE) of $k_H/k_D = 0.40$.

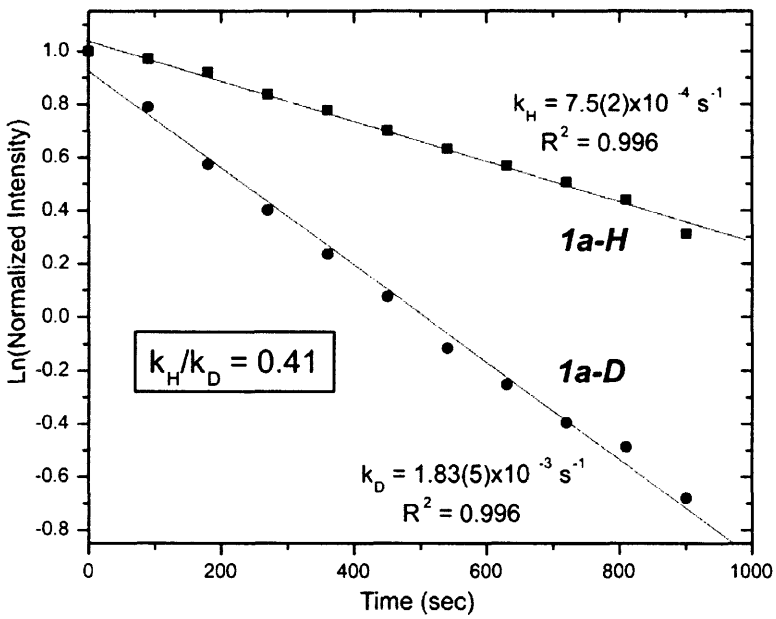

Figure 6. First order decay comparison between **1a**-H and **1a**-D at 75 °C; Ln(Normalized Intensity) vs. Time.

This large inverse KIE suggests that C-H bond making and breaking is an important component of the rate determining step in the decomposition of niobaziridine-hydride **1a**-H.[73] However, since the reaction under study is actually the formation of the imido complex **3a**, the large H/D KIE must arise from the relative ease with which reversible β-H elimination takes place between **1a**-H and **2a**. A plausible mechanistic explanation for the observed KIE is that **1a**-H and **2a** are in rapid exchange via reversible β-H elimination (k_1/k_{-1}, Scheme 15). The formation of imido **3a** is a result of a slower C-N bond cleavage process (k_2, Scheme 15), which is observable at room temperature, but naturally accelerated at elevated temperatures. Therefore, the rate of C-H oxidative addition by **2a** (k_{-1}) must be much greater than that for both C-H

reductive elimination (k_1) and C-N oxidative addition (k_2) due to fact that **1a**-H is stable in solution for extended periods ($t_{1/2}$ = ca. 4.5 d) and **2a** is unobservable. Upon deuteration, C-D oxidative addition by **2a**-d_6 is impeded by the larger C-D zero-point energy difference in the transition state relative to C-H cleavage, the direct result being a slowing of k_{-1}. Accordingly, k_2 for C-N oxidative addition becomes competitive with k_{-1} and faster formation of imido **3a**-d_6 is observed.

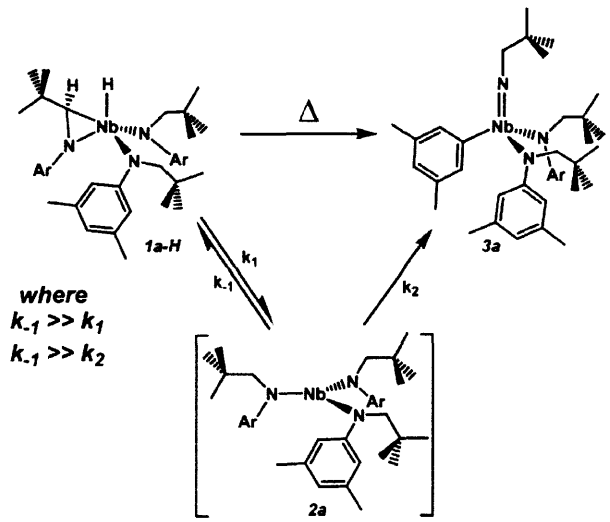

Scheme 15. Proposed mechanism for the conversion of **1a**-H to **3a** through the intermediacy of **2a**.

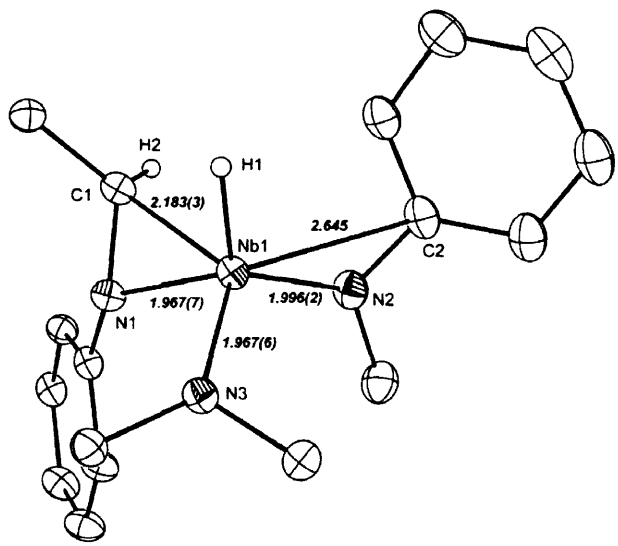

Figure 7. Partial ORTEP diagram of **1a**-H highlighting the aryl-ipso→Nb interaction.

While it is probable that three-coordinate **2a** interchanges **1a-H** and **3a** in solution, it is at best a fleeting species. Furthermore, whether unstabilized **2a** exists for a brief period in solution is a matter open to speculation. Due to is reactive nature, **2a** is most likely stabilized by agostic C-H and/or π-arene interactions from the N[Np]Ar ligand, and never present in free form.

Indeed, reversible β-H elimination between **1a**-H and **2a** may preceded by the rapid interchange of several (C-H)→Nb σ-complexes, which are well-known to be important intermediates in C-H activation processes by low-valent early metal complexes.[73-75] In addition, evidence for a π-arene→Nb interaction is observed in the solid state structure of **1a**-H, where the ipso carbon of an intact N[Np]Ar ligand is in conspicuously close contact with the Nb center (Figure 7). The latter crystallographic feature can potentially be considered as a snapshot into the C-N cleavage process by three-coordinate **2a**.

3 Divergent Reactivity of Nb(H)(η^2–*t*–Bu(H)C=NAr)(N[Np]Ar)$_2$ (1a-H) with Small Molecule Substrates

3.1 Two-Electron Reduction Reactions Mediated by Complex 1a-H

Whereas putative **2a** was not observed directly, it was hoped that **1a**-H would act as a functional equivalent of **2a** when treated with appropriate substrates. As stated above, the molybdaziridine-hydride complex **4b**-H serves exclusively as a source of the three coordinate Mo(N[*i*-Pr]Ar)$_3$ (**5b**) when treated with small molecule substrates. Furthermore, orange-brown solutions of **4b**-H left standing at room temperature are observed to gradually become purple in color, indicative of N_2 cleavage and the formation of the bridging nitrido species, (μ_2-N)[Mo(N[*i*-Pr]Ar)$_3$]$_2$ (μ_2-N)[**5b**]$_2$.[57] While N_2 activation chemistry was not observed during the synthesis and thermolysis of niobaziridine-hydride **1a**-H, the latter was found to effect the two-electron reduction of certain substrates.

To ascertain the potential of **1a**-H to serve as a source of **2a** upon reaction with small molecule substrates, chalcogen atom abstraction reactions were initially surveyed. The motivation for such a choice stemmed from the well-established tendency of several other three-coordinate, d^2 systems to elicit two-electron reduction chemistry.[13,14,33-37] Accordingly, treatment of an orange Et_2O solution of **1a**-H with an excess of N_2O resulted in a gradual color change to pale yellow over the course of 4 h. Analysis of the crude reaction mixture by ^{1}H NMR indicated the clean and quantitative formation of a new product containing a single N[Np]Ar ligand environment. Due to the well-known ability of N_2O to serve as an O-atom transfer reagent in conjunction with reducing metal centers,[76-80] the new product was likely the terminal oxo complex ONb(N[Np]Ar)$_3$ (**2a**-O, Scheme 16). An X-ray diffraction experiment confirmed this notion (Figure 8, top left), thereby establishing that the niobaziridine-hydride functional group indeed serves as an effective mask for three-coordinate **2a**.

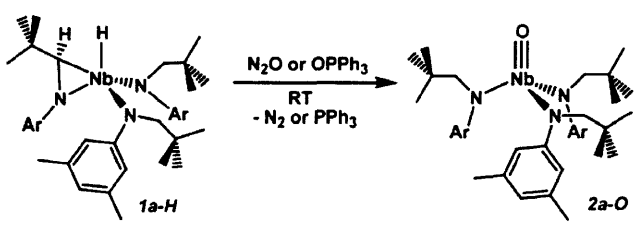

Scheme 16. Synthesis of oxo **2a**-O from **1a**-H.

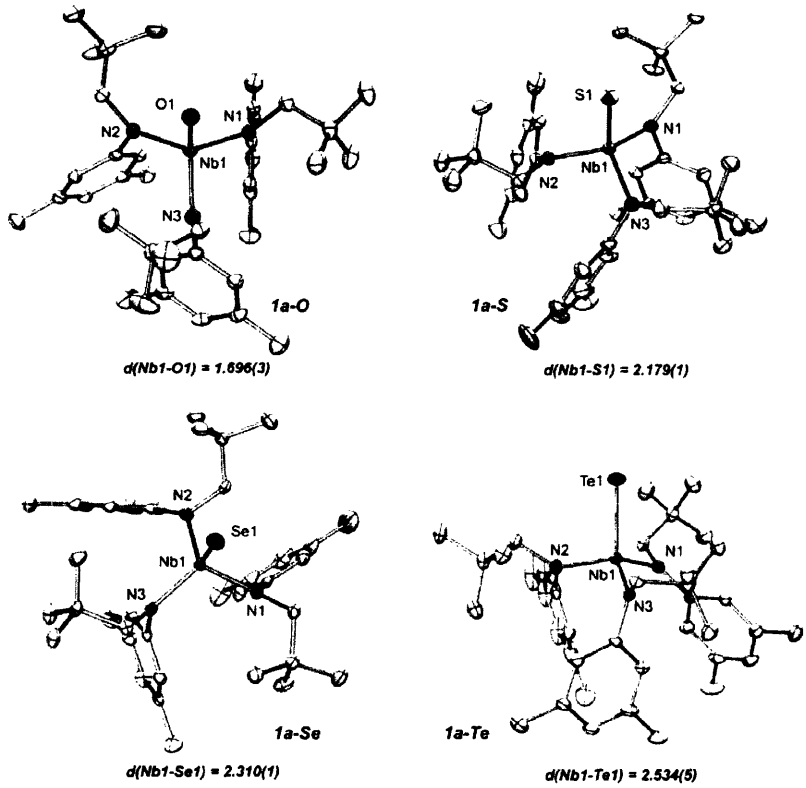

Figure 8. ORTEP diagrams of complexes **2a**-E (E = O, S, Se, Te) at the 35% probability level.

In addition, complex **1a**-H readily deoxygenates triphenylphosphine oxide ($OPPh_3$) at room temperature, cleanly affording one equiv each of oxo **2a**-O and PPh_3 (Scheme 16). In C_6D_6, the deoxygenation of 1.0 equiv $OPPh_3$ by **1a**-H is complete in ca. 8 h with only trace amounts of the imido complex **3a** having been formed. Furthermore, when carried out with a 10-fold excess of OPP_3 in C_6D_6 (0.15 mM), O-atom abstraction by **1a**-H occurred at 23 °C with pseudo-first order rate constant of $2.7(1)\text{x}10^{-4}$ s^{-1}. When a 15-fold (0.26 mM) excess of $OPPh_3$ was employed under identical conditions, the rate of reaction increased to $5.9(1)\text{x}10^{-4}$ s^{-1}. Higher $OPPh_3$ concentrations (0.301, 0.376 and 0.451 mM) did not lead to a significant increase in rate, presumably indicating that a saturation point had been reached in C_6D_6 around 0.26 mM in $OPPh_3$.

Notably, O-atom abstraction reactions from phosphine oxides by low-valent transition metal complexes are quite rare. Typically the reverse reaction, namely transfer of a terminal oxo moiety to phosphine, is encountered.[81] The only other examples where low-valent metal complexes cleave the phosphoryl P-O bond are Mayer's thermally induced deoxygenation of the chelating phosphine oxide, $Ph_2(O)P(CH_2)_2PPh_2$, by a W(II) center[82-84] and the OPR_3 (R = Me, Ph, *t*-Bu) deoxygenations by $M(silox)_3$ complexes (M = V, Nb(L), Ta; L = 4-pic, PMe_3).[36,37] While large kinetic and electronic barriers to OPR_3 deoxygenation by low-valent metal complexes can exist,[37] successful instances reflect a considerable thermodynamic driving force for metal oxo bond formation.[81] Indeed, the P-O bond strength of $OPPh_3$ has been reported as 133 kcal/mol,[81] which places a lower limit on the Nb≡O bond strength in **2a**-O. The Mo-N bond

strength in the isoelectronic complex, N≡Mo(N[*t*-Bu]Ar)$_3$, has been calculated as 155 kcal/mol,[7] and it is conceivable that the Nb≡O bond strength in **2a**-O approaches this value. It should be noted that the formation of 2 equiv of N≡Mo(N[*t*-Bu]Ar)$_3$ from three-coordinate Mo(N[*t*-Bu]Ar)$_3$ and N_2 more than compensates for the N≡N triple bond dissociation energy (226 kcal/mol). Thus a substantial thermodynamic gain is achieved from N_2 cleavage by Mo(N[*t*-Bu]Ar)$_3$.[4]

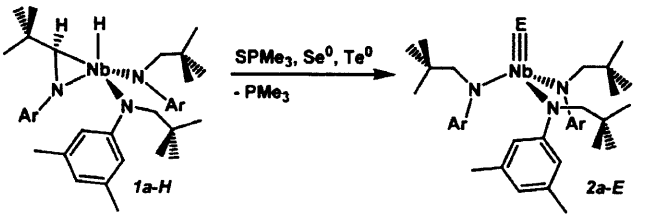

Scheme 17. Synthesis of the terminal chalcogenide complexes **2a**-E (E = S, Se, Te).

Niobaziridine-hydride **1a**-H also proves to be a convenient route to the heavier, terminal chalcogenide complexes[85] ENb(N[Np]Ar)$_3$ (**2a**-E; E = S, Se, Te) when treated with an appropriate chalcogen atom source. As shown in Scheme 17, treatment of **1a**-H with trimethylphosphine sulfide ($SPMe_3$) readily provides the sulfide complex **2a**-S, while addition of elemental Se and Te provides **2a**-Se and **2a**-Te, respectively, in excellent yields. X-ray diffraction confirmed the identity of complexes **2a**-E and revealed an isomorphous and isostructural relationship between the three heavier derivatives. As shown in Figure 8, the Nb≡E bond lengths consistently increase as the group 16 atom becomes heavier in accord with the increase in covalent radius down the group. Complex **1a**-H can engage in incomplete atom transfer reactions as well.[86,87] Thus, upon addition of the terminal phosphide complex PMo(N[*i*-Pr]Ar)$_3$ (**5a**-P)[88] to a C_6D_6 solution of **1a**-H, quantitative formation of the diamagnetic, heterodinuclear bridging phosphide complex (Ar[Np]N)$_3$Nb(μ-P)Mo(N[*i*-Pr]Ar)$_3$ is observed (**2a**(μ-P)**5a**, Figure 9). Thus, as hoped, the niobaziridine-hydride functional group in **1a**-H is indeed capable of tautomerization to the three-coordinate complex **2a**, which serves as a potent two-electron reductant. Furthermore, as revealed by the results above, complex **1a**-H is competent for the reduction of a diverse host of inorganic substrates.

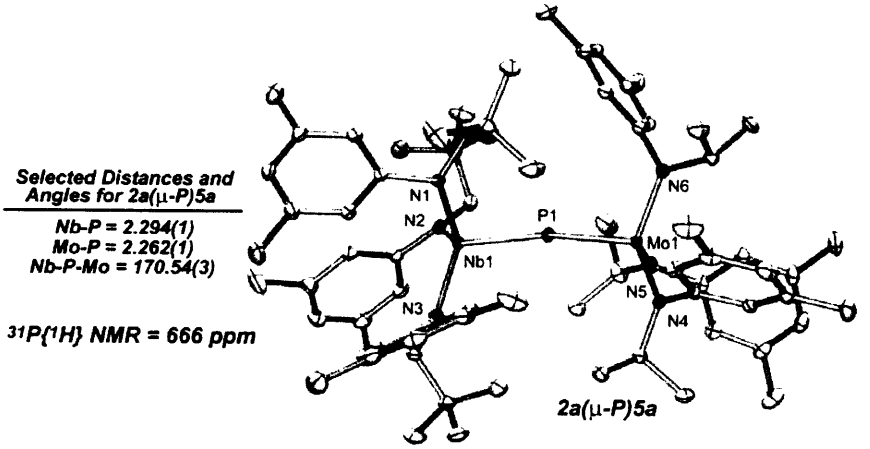

Figure 9. ORTEP diagram of **2a**(μ-P)**5a** at the 35% probability level.

3.2 Reactions of 1a-H with Unsaturated Organic Substrates: Insertion vs. Complexation

With the ability of **1a**-H to act as a source of **2a** established, reactions with organic substrates were also probed. Treatment of **1a**-H with 1.0 equiv of mesitylnitrile (MesCN, Mes = 2,4,6-$Me_3C_6H_2$) leads exclusively to the η^2-nitrile complex (η^2-MesCN)Nb(N[Np]Ar)$_3$ (**2a**-NCMes, Scheme 18), again demonstrating the accessibility of three-coordinate **2a**. Crystallographic characterization confirmed the formulation of **2a**-NCMes as an η^2-nitrile complex possessing an elongated nitrile N-C bond of 1.258(4) Å, consistent with significant π-back-donation from a reducing metal center (Figure 10).[89]

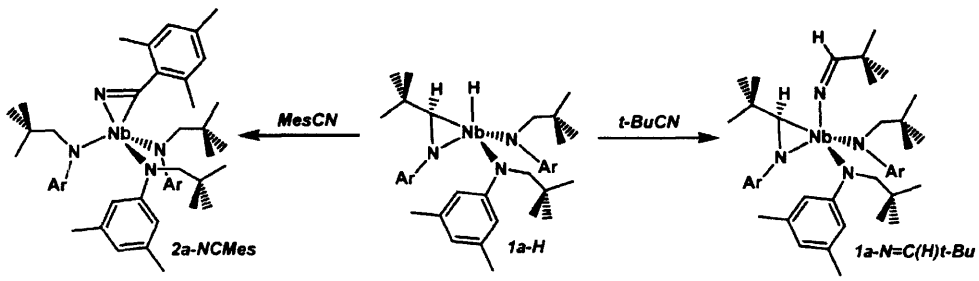

Scheme 18. Synthesis of complexes **2a**-NCMes and 1a-NC(H)*t*-Bu.

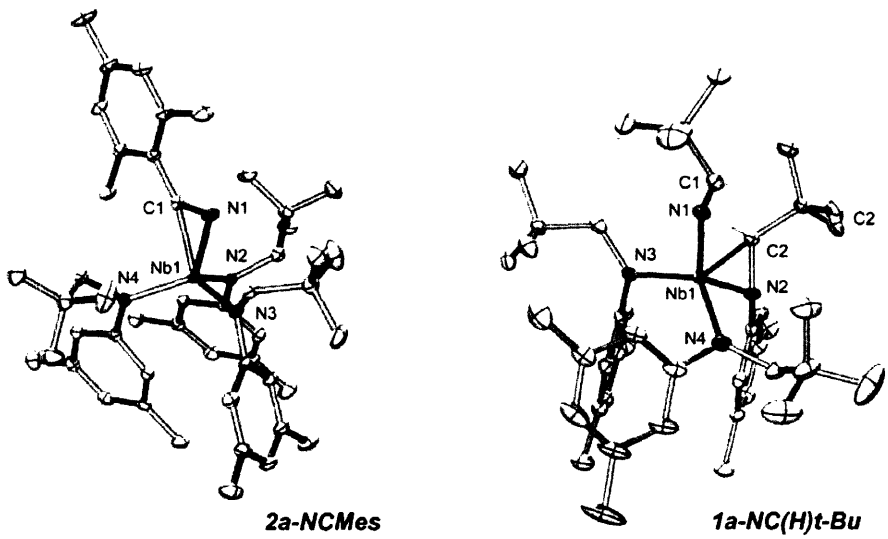

Selected Distances for 2a-NCMes
Nb1-N1 = 2.049(2)
Nb1-C1 = 1.994(2)
Nb1-N2 = 2.001(4)
N1-C1 = 1.258(5)

Selected Distances for 1a-NC(H)t-Bu
Nb1-N1 = 1.957(3)
Nb1-N2 = 1.978(3)
Nb1-C2 = 2.201(3)
N1-C1 = 1.258(5)

Figure 10. ORTEP diagrams of **2a**-NCMes and **1a**-NC(H)*t*-Bu at the 35% probability level

In contrast, when **1a**-H is treated with stoichiometric *tert*-butyl nitrile (*t*-BuCN), sole formation of the nitrile insertion[90,91] product Nb(*t*-Bu(H)C=N)(η^2-*t*-Bu(H)C=NAr)(N[Np]Ar)$_2$ (**1a**-NC(H)*t*-Bu, Scheme 18) is obtained in which the niobaziridine ring remains *intact* (Figure 10*)*. Insertion chemistry of this type was encountered by Mindiola upon borane abstraction from

the niobaziridine-borohydride complex **1b**-BH_4 in the presence of benzophenone.[63] Thus while tautomerization of niobaziridine-hydride **1a**-H to three-coordinate **2a** is possible, insertion chemistry typical of an early metal hydride is also observed. Indeed, several other unsaturated organic functional groups were found to insert into the Nb-H bond of **1a**-H. As depicted in Scheme 19, treatment of **1a**-H with benzaldehyde (PhCHO), *tert*-butyl acetylene (*t*-BuCCH), dimethylcyanamide (Me_2NCN) and diphenyldiazomethane (Ph_2CN_2)[92] resulted in the respective insertion product. A notable feature of the above insertion reactions is that they are all clean and quantitative as assayed by ^1H NMR, proceeding to completion essentially upon mixing. Contrastingly, the complexation of MesCN by **1a**-H is complete in ca. 4 h and no intermediate species are detectable by ^1H NMR during the reaction.

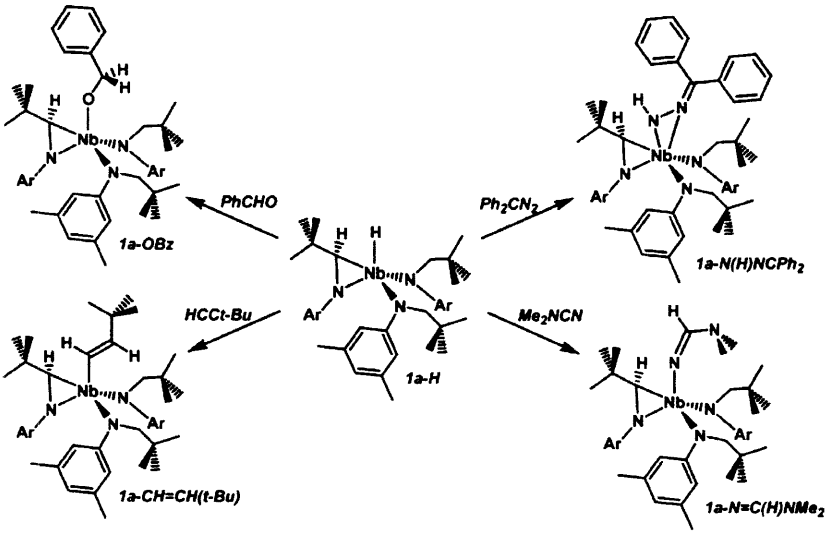

Scheme 19. Insertion chemistry of **1a**-H.

Whereas insertion chemistry appears to dominate the reactions between **1a**-H and unsaturated organic substrates, the disparate result obtained from MesCN suggests that dual pathways of reactivity are available to **1a**-H depending on the substrate employed. While it is possible that the insertion products of Scheme 19 can be converted to the corresponding η^2-bound forms via a β-H abstraction by the niobaziridine carbon atom, all retain their integrity for days at elevated temperatures (C_7H_8, 120 °C, 3 d). In no case was the formation of a complex analogous to **2a**-NCMes observed. Furthermore, **2a**-NCMes did not convert to an analogue of **1a**- NC(H)*t*-Bu or **1a**-$NC(H)NMe_2$ when similarly heated, indicating that it too is a thermodynamic product. These results suggest that the insertion chemistry observed by **1a**-H is a distinct mechanistic pathway with respect to the reaction with MesCN.

Interestingly, however, a thermally induced process was observed for the ketimido complex **1a**-NC(H)*t*-Bu. When blood red **1a**-NC(H)*t*-Bu was heated to 120 °C in C_7D_8, a dramatic color change to golden yellow was observed after 1 h. Analysis of the reaction mixture by ^1H NMR indicated the clean formation of a new C_1-symmetric product, indicating that formation of an η^2-*t*-BuCN complex again did not occur. Crystallographic characterization of this new species (Figure 11) established its identity as the cyclic imido[93,94] complex Nb(=N(*t*-Bu)HCCH(*t*-Bu)NAr)(N[Np]Ar)$_2$ (**6a**-*t*-Bu), the product of C-C bond formation via nucleophilic

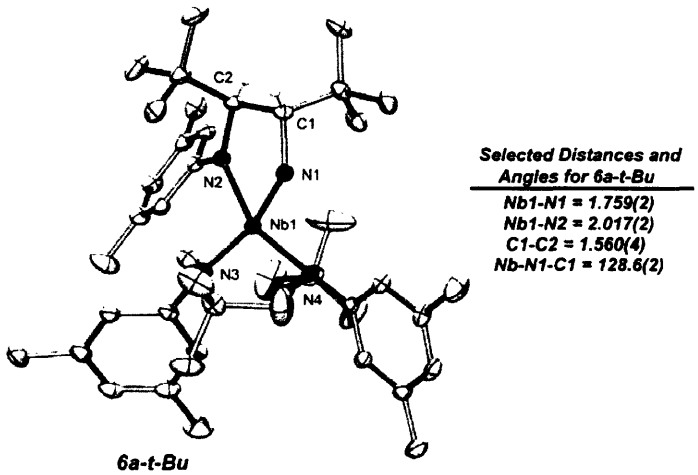

Figure 11. ORTEP diagrams of **6a**-*t*-Bu at the 35% probability level.

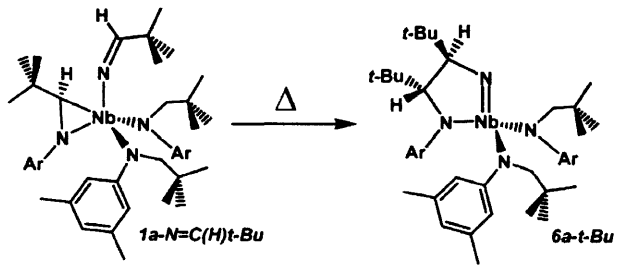

Scheme 20. Thermolysis of **1a**-NC(H)*t*-Bu: Synthesis of **6a**-*t*-Bu.

attack of the niobaziridine ring carbon on the ketimido ligand in **1a**-NC(H)*t*-Bu (Scheme 20). Although a β-H atom is available in **1a**-NC(H)*t*-Bu, nucleophilic C-C bond formation is preferentially observed. Similar results were obtained in the reactions of **1a**-H and other organonitriles. For instance, treatment of **1a**-H with benzonitrile (PhCN) rapidly resulted in the formation of the ketimido complex Nb(Ph(H)C=N)(η^2-*t*-Bu(H)C=NAr)(N[Np]Ar)$_2$ (**1a**-NC(H)Ph) as an observable intermediate (a diagnostic aldehydic proton is observed at 9.57 ppm). The latter steadily decayed at room temperature over the course of 5 h to the phenyl analogue of **6a**-*t*-Bu (**6a**-Ph, Scheme 21). When *p*-tolylnitrile (4-MePhCN) was employed under similar conditions, spontaneous niobaziridine ring expansion was also observed. Interestingly, as stated above, the amino substituted ketimido complex **1a**-NC(H)NMe$_2$ was stable at elevated temperatures for extended periods. While a β-H abstraction process is evidently disfavored, the fact that ring expansion does not occur is likely due to a fair degree of electronic saturation of the ketimido carbon by the amine lone pair. Such an effect would serve to reduce the electrophilic character of the ketimido unit and is indeed indicated in the ^{1}H NMR spectrum of **1a**-NC(H)NMe$_2$ where the amino-methyl groups appear as distinct singlets at room temperature.

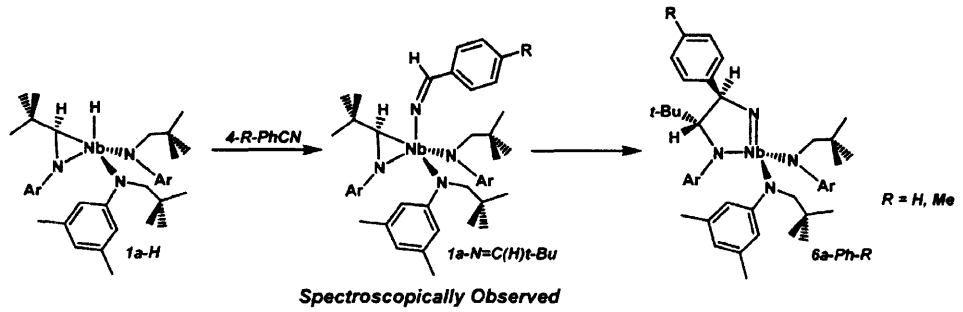

Scheme 21. Reaction Between 1a-H and para-substituted benzonitriles.

The fact that PhCN and 4-MePhCN do not produce η^2-nitrile complexes points to a critical role played by the ortho-methyl groups of MesCN in dictating the divergent reactivity of **1a**-H. An additional experiment was performed which further supported this notion. When stoichiometric *o*-tolylnitrile (2-MePhCN) was added to a C_6D_6 solution of **1a**-H, ^{1}H NMR indicated that both the ketimido complex, **1a**-NC(H)*o*-tol, and the η^2-nitrile complex, **2a**-NC(*o*-tol) were rapidly formed in a 1.0:1.5 ratio (Scheme 22). Furthermore, complex **1a**-NC(H)*o*-tol was observed rearrange to the cyclic imido species **6a**-*o*-tol over the course of 4 h, whereas the concentration of **2a**-NC(*o*-tol) remained constant. Extended heating (C_7H_8, 120 °C, ca. 1 week) did not alter the final ratio of **6a**-*o*-tol and **2a**-NC(*o*-tol), suggesting that neither species is an intermediate along the pathway to the other. While these latter results suggest that **1a**-H exhibits some form of shape-selectivity which dictates its reactivity with unsaturated substrates, the nature of this selectivity is unclear. However, it is evident that the steric properties of an incoming substrate markedly influence the behavior of the niobaziridine-hydride functional group in **1a**-H.

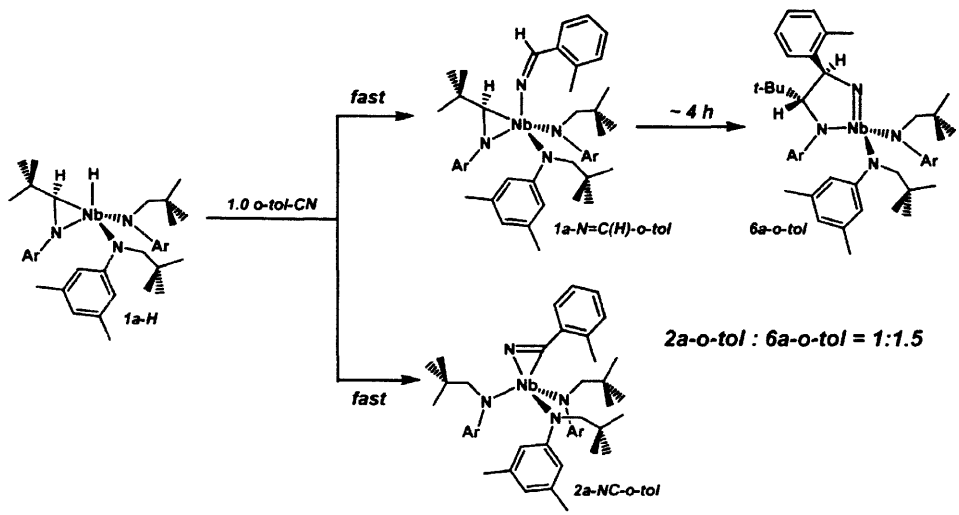

Scheme 22. Reaction Between **1a**-H and ortho-tolylnitrile.

To further explore the small molecule chemistry available to niobaziridine hydride **1a**-H, its reaction with CO was investigated. Unlike N_2O and NO, which were deoxygenated by **1a**-H, addition of excess CO to **1a**-H resulted in the rapid formation of a new C_s-symmetric product.

An X-ray diffraction experiment revealed the new product to be the enolate-imido complex, Nb(O(H)C=C(H)*t*-Bu)(NAr)(N[Np]Ar)$_2$ (**7a**, Figure 12). Complex **7a** is presumably the product of a formyl (Nb-C(O)H) intermediate, which undergoes rapid rearrangement with the niobaziridine ring accompanied by C-N bond cleavage (Scheme 23). Thus the reaction between **1a**-H and CO provides further evidence for the divergent reactivity available to the niobaziridine-hydride functional group.

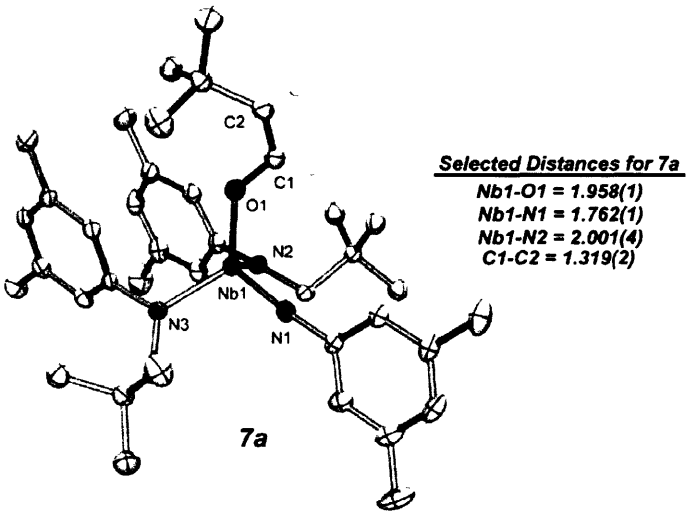

Figure 12. ORTEP diagram of complex **7a** at the 35% probability level.

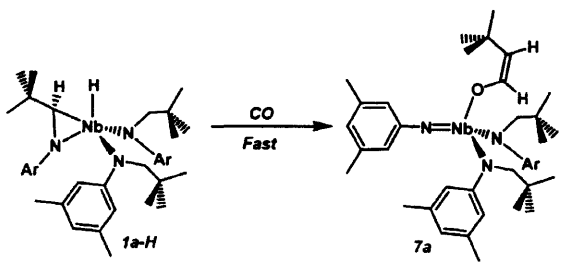

Scheme 23. Reaction of **1a**-H with CO: Formation of the enolate imido complex **7a**

3.3 Proposed Mechanism of Reaction of 1a-H with Small Molecules

While the chemistry described in section 3.2 confirms that the niobaziridine-hydride complex **1a**-H can serve as a source of three-coordinate **2a**, the insertion chemistry of section 3.2 reveals that **1a**-H also has pronounced hydridic character. The isotopic labeling studies described in section 3.1 indicate that, although a rapid equilibrium between **1a**-H and **2a** likely occurs, the latter is exceedingly reactive and likely *not* present in appreciable concentration in solution. Therefore, when a substrate such as $OPPh_3$ or MesCN is added, direct reaction with **2a** (Scheme 24, Pathway A) probably does not take place. Instead, substrates most likely first associatively bind to the five-coordinate **1a**-H to form a six-coordinate substrate→**1a**-H species (Pathway B) and one of the following processes occurs:

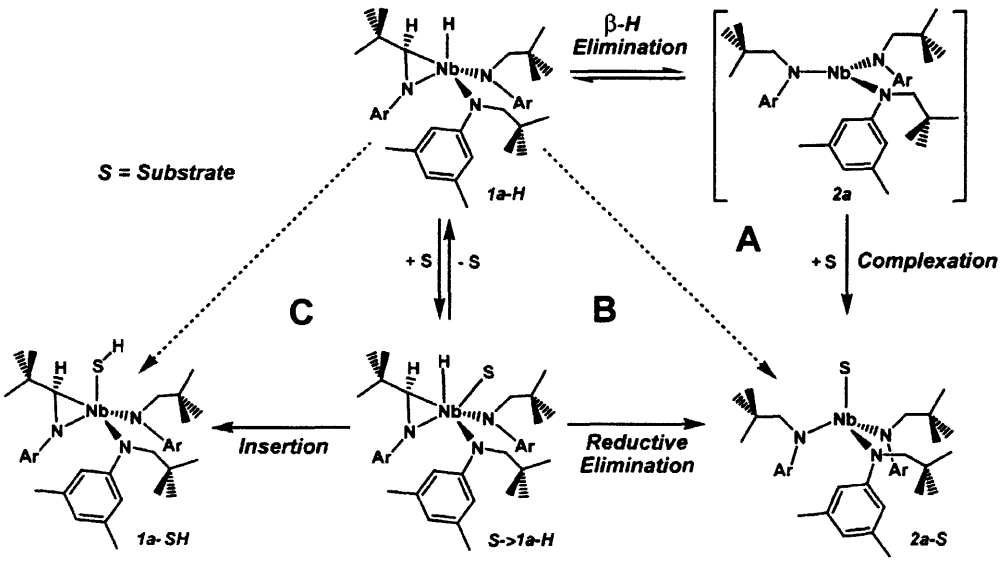

Scheme 24. Mechanistic Scheme for the reaction of **1a**-H with small molecule substrates.

1. Coordinatively Induced C-H Reductive Elimination: When a Lewis basic substrate which does not display a tendency to insert into M-H bonds (*e.g.* $OPPh_3$) associates to **1a**-H, C-H reductive elimination is induced.[95] The resultant substrate→**2a** species is then irreversibly formed or, with substrates such as $OPPh_3$, reductive scission occurs with byproduct loss. Implicit in this mechanism is that the initial substrate→**1a**-H complex may reversibly dissociate prior to coordinatively induced reductive elimination. The latter event may partially account for the slower relative rates observed for the reduction chemistry displayed by **1a**-H as compared to insertion chemistry. Furthermore, a dissociation step may possibly account for the saturation behavior observed for $OPPh_3$ deoxygenation.

2. Insertion Chemistry: When a Lewis basic substrate with a tendency to insert into M-H bonds binds the formally d^0 Nb center in **1a**-H, rapid and irreversible insertion may occur (Pathway C). However, for insertable substrates such as MesCN, and *o*-tolCN, a steric property of the substrate framework may i) inhibit the overall insertion process or ii) destabilize the transition-state of insertion in favor of the substrate→**1a**-H complex. If insertion is prevented, coordinatively induced C-H reductive elimination and substrate complexation can take place

Indirect evidence for the operation of pathway B and C, include the requisite that substrate coordination must precede the insertion of unsaturated Lewis basic substrate. Furthermore, molybdaziridine-hydride **4b**-H, which only serves as a source of the three coordinate **5b**, has been shown by stopped-flow techniques to follow pathway B in its reaction with organoisocyanides (RNC).[96] In the latter system, organoisocyanide binding to **4b**-H was determined to be rate limiting. While conclusions made for **4b**-H are not necessarily extendable to **1a**-H, the chemical similarities between the two and the aggressive insertion behavior of **1a**-H strongly suggest that it too, operates under pathway B. Again, it is interesting to note that **4b**-H has not, to date, displayed any insertion behavior in its reactions with small molecules. Whereas the factors responsible for this significant difference between **1a**-H and **4b**-H are not clear, the

relative hydridic character of the M-H bonds and the d-electron count are the most obvious candidates. Indeed, the Nb-H bond in **1a**-H will be significantly more nucleophilic than the corresponding unit in **4b**-H due to the relatively greater Lewis acidity of the former.[97] Furthermore, the fact that **4b**-H is a d^1 paramagnet may play a significant role in its chemistry. Besides providing an avenue for π-back-donation to π-acidic substrates, the unpaired spin may serve to destabilize the process of insertion into the Mo-H bond. While these arguments are all speculations at this point, it is clear that inherent electronic differences between nioba- and molybdaziridine-hydride functional groups must be responsible for their differing reactivity patterns.

4 Synthesis of Niobaziridine-Hydride Variants

4.1 Lewis Acidity Exposed: Synthesis of the Niobaziridine-Hydride Dimer [Nb(H)(Me$_2$C=NAr)(N[*i*-Pr]Ar)$_2$]$_2$ (1b)

As noted in section 2.1, niobaziridine-hydride **1a**-H was quite sensitive to the reaction conditions employed for its formation. While reductions of bisiodide **2a**-I_2 were not clean when either Na/Hg or Mg^0 were employed, the mild reduction afforded by Mg(THF)$_3$(anthracene) allowed for the isolation of **1a**-H. As a result, it was of interest to investigate whether similar reaction conditions would afford the N[*i*-Pr]Ar-ligated niobaziridine-hydride **1b**-H, or determine if **1b**-H was indeed inherently unstable.

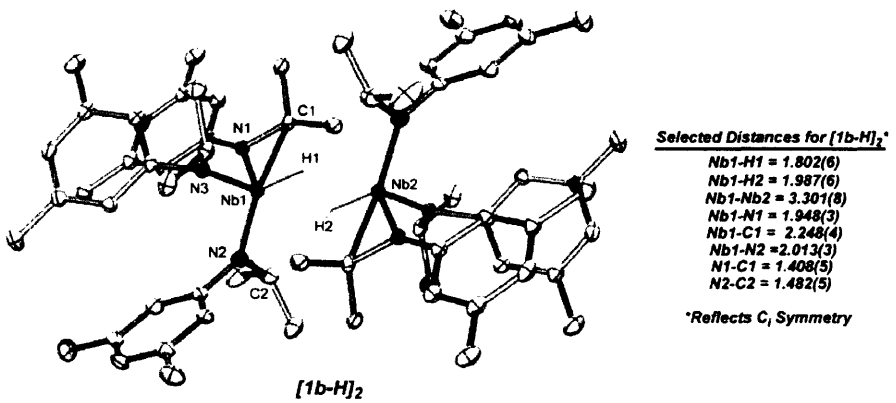

Figure 13. ORTEP diagram of complex [**1b**-H]$_2$ at the 35% probability level.

Remarkably, this strategy proved effective and the reaction between the corresponding bisiodide **2b**-I_2 and Mg(THF)$_3$(anthracene) allowed for the isolation of niobaziridine-hydride **1b**-H as dark orange crystals in ca. 30% yield. As anticipated, the C_6D_6 ^{1}H NMR spectrum of **1b**-H revealed C_s symmetry and a broad hydride resonance located at 9.2 ppm. However, a crystallographic structure determination of **1b**-H revealed a startling feature (Figure 13). Unlike niobaziridine-hydride **1a**-H, **1b**-H displays a dimeric solid state structure, in which the Nb centers are bridged by the two hydride ligands and enjoy a 3.302(3) Å separation. This structural feature of **1a**-H plainly reveals the Lewis acidity of the Nb center within the niobaziridine-hydride functional group and provides an understanding for the pronounced hydride chemistry

observed for the neopentyl variant, **1a**-H. It is important to point out that the analogous molybdaziridine-hydride **4b**-H is a monomer in the solid state, which again reflects the diminished Lewis acidity of the Mo center. Furthermore, although the Nb center in **1a**-H is Lewis acidic as well, the N[Np]Ar ligand evidently provides enough steric protection to stabilize a monomeric complex (Figure 2).

While it is presently unknown if the dimeric structure of **1b**-H (*i.e.* [**1a**-H]$_2$) is preserved in solution, the complex rapidly decomposes to the dimer **3b** at room temperature in solution over the course of hours (Scheme 25). This behavior is in direct contrast to **1a**-H, which forms the neopentyl imido complex **3a** at a considerably slower rate. Thus, while only moderately stable in solution, niobaziridine-hydride **1b**-H can be isolated.

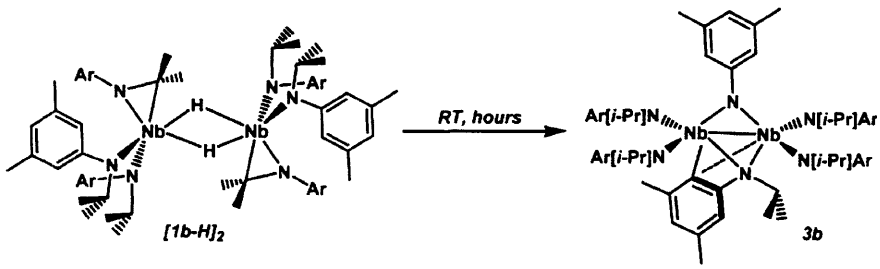

Scheme 25. Thermal decomposition of dimer [**1b**-H]$_2$ to complex **3b**.

4.2 Generality of the Niobaziridine-Hydride Functionality for the Stablization of Three – Coordinate Niobium: Synthesis of the *N*-Methyleneadamantyl Niobaziridine-Hydride 1c-H

Since the N[Np]Ar ligand provided a stable niobaziridine-hydride functionality, it was of interest to extend the general neopentyl framework to other ligand variants. While the synthesis of the N[*i*-Pr]Ar-substituted niobaziridine-hydride was possible, its relative instability compared with **1a**-H was attributed to presence of a secondary radical leaving group on the ligand framework. Therefore, the synthesis of the methylene-adamantyl anilido ligand, N[CH_2Ad]Ar (Ad = 1-adamantyl), and its corresponding niobaziridine-hydride were targeted for synthesis. As with the N[Np]Ar ligand, it was thought that the methylene group of the N[CH_2-Ad]Ar ligand would provide the Nb center with access to β-H atoms and also resist radical degradation processes. Furthermore, the large steric demand of the appended 1-Ad group was hoped to be useful for future applications.

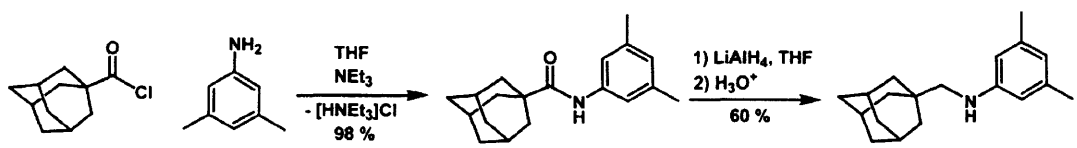

Scheme 26. Synthesis of the *N*-methyleneadamantyl aniline HN(CH_2Ad)Ar.

The amine, HN(CH_2Ad)Ar, was synthesized according to Scheme 26 and installed on Nb by the method of Mindiola. Reduction of the bisiodide complex Nb(I)$_2$(N[CH_2-Ad]Ar)$_3$ (**2c**-I_2) proceeded smoothly, providing niobaziridine-hydride **1c**-H in ca. 45% yield. The solid state

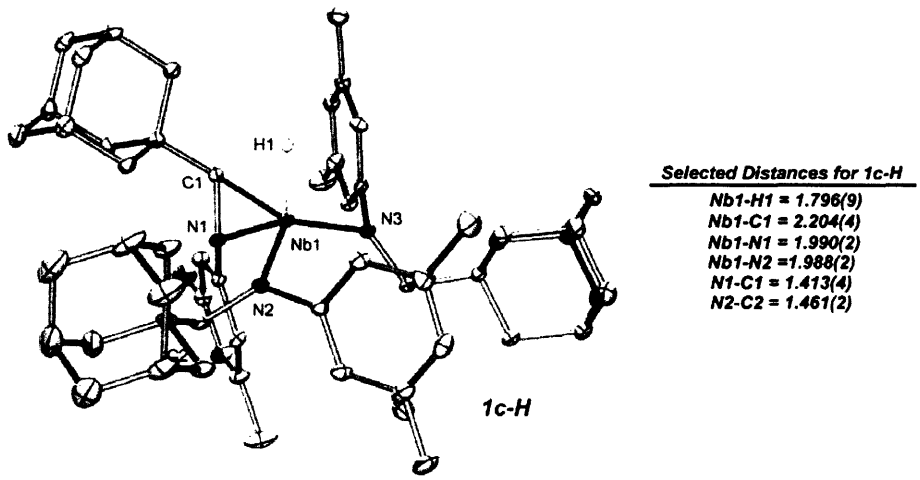

Figure 14. ORTEP diagram of complex **1c**-H at the 35% probability level.

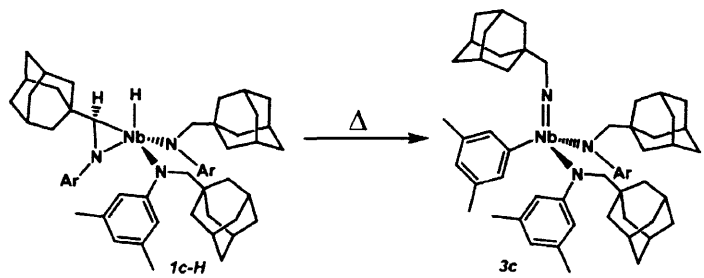

Scheme 27. Thermal decomposition **1c**-H to the aryl-imido complex **3c**.

structure of **1c**-H is shown in Figure 14 and is quite similar to that found for complex **1a**-H. Due to the adamantyl groups, **1c**-H is far less soluble in common organic solvents than is the neopentyl variant **1a**-H. Upon heating, **1c**-H forms the corresponding methyleneadamantyl imido complex, Nb(NAd)(Ar)(N[CH_2-Ad]Ar)$_2$ (**3c**) as a result of C-N bond oxidative addition by putative three-coordinate Nb(N[CH_2-Ad]Ar)$_3$ (Scheme 26). Interestingly, **1c**-H has been qualitatively observed to decompose faster than the neopentyl-variant **1a**-H, possibly due to added ring strain in the niobaziridine-hydride functional group as induced by the pendent 1-Ad substituents.

5 Conclusions and Future Work

In this chapter, the successful synthesis of the niobaziridine-hydride complex **1a**-H was described. The stability of **1a**-H arises from the neopentyl substituent of the N[Np]Ar ligand, which both resists radical degradation processes and provides the necessary steric protection to engender the formation of a mononuclear complex. Upon reaction with small molecule substrates, complex **1a**-H can act as a functional equivalent of the three-coordinate **2a**, thus

establishing the niobaziridine-hydride functionality as an effective protecting group for the reactive d^2 $Nb(NR_2)_3$ fragment. However, upon reaction with unsaturated organic substrates, insertion into the Nb-H bond in **1a**-H is observed, demonstrating divergent modes of reactivity available to the niobaziridine-hydride functional group. Insertion chemistry is not observed for molybdaziridine-hydride complex **4b**-H, which serves only as a source of the three-coordinate molybdenum complex **5b**. Additionally, unlike **4b**-H, niobaziridine-hydride **1a**-H has not exhibited reactivity toward gaseous N_2, further pointing out the inherent differences between the d^0 Nb and d^1 Mo metallaziridine-hydride functionalities.

While the niobaziridine-hydride functional group can stabilize the reactive, three-coordinate d^2 $Nb(NR_2)_3$ fragment, several questions concerning its chemistry remain. For the development of reliable two-electron reduction chemistry by complexes exemplified by **1a**-H, a thorough understanding of the factors which govern the tendency to insert unsaturated organic substrates is needed. As shown by the reaction of **1a**-H with *ortho*-tolylnitrile, a single substrate can exhibit both reduction and insertion chemistry. It is possible that modifications to the anilido ligand framework may be an effective approach to discouraging insertion reactions into the niobaziridine-hydride functionality. Accordingly, the niobaziridine-hydride complexes **1b**-H and **1c**-H may be capable of reducing small molecule substrates which display insertion chemistry with **1a**-H. Furthermore, niobaziridine-hydride variants such as **1b**-H and **1c**-H, may possess the subtle electronic properties necessary to unveil the N_2-activation chemistry available to the $Nb(NR_2)$ fragment.

6 Experimental Procedures

6.1 General Synthetic Considerations

Unless otherwise stated, all manipulations were carried out at room temperature, under an atmosphere of purified dinitrogen using a Vacuum Atmospheres glove box or Schlenk techniques. All solvents were obtained anhydrous and oxygen-free according to standard purification procedures. Benzene-d_6 (C_6D_6) and toluene-d_8 (C_7D_8) were degassed and stored in the glove box over 4 Å molecular sieves for at least 3 d prior to use. Celite 435 (EM Science) and 4 Å molecular sieves (Aldrich) were dried under vacuum at 250 °C overnight and stored under dinitrogen. Benzaldehyde and *tert*-butylnitrile were purchased from Aldrich and distilled from CaH_2 prior to use. 2,4,6-trimethylbenzonitrile (MesCN, Aldrich) was recrystallized from *n*-hexane and dried *in vacuo* prior to use. Nitrous oxide (N_2O) was obtained from BOC Gases and passed through a 1 ft column of P_2O_5 before being introduced to the reaction vessel via a Schlenk line. The compounds $Mg(THF)_3$(anthracene),[66] *mer,cis*-$Nb(Cl)_3(THF)_2$(PhCCPh),[66] (P)Mo(N[*i*-Pr]Ar)$_3$,[58] and Ph_2CN_2[98] were prepared according to literature procedures. The niobium complexes **2b**-PhCCPh and **2b**-I_2 were prepared according to the method of Mindiola.[62] All other reagents were obtained from commercial sources and used as received or purified according to standard procedures. All Glassware was oven dried at a temperature of 230 °C prior to use.

Solution ^1H, $^{13}C\{^1H\}$ and $^{31}P\{^1H\}$ NMR spectra were recorded using Varian XL-300 MHz and Varian INOVA 500 MHz spectrometers. ^1H and ^{13}C chemical shifts are reported referenced to the residual solvent resonances of 7.16 ppm (^1H) and 128.3(t) ppm (^{13}C) for benzene-d_6. $^{31}P\{^1H\}$ chemical shifts are reported referenced to the external standard H_3PO_4 (85

%, 0.0 ppm). Solution IR spectra were recorded on a Perkin-Elmer 1600 Series FTIR spectrometer. All spectra were recorded in C_6D_6 using a KBr plated solution cell. Solvent peaks were digitally subtracted from all spectra using an authentic spectrum obtained immediately prior to that of the sample. Combustion analyses were carried out by H. Kolbe Microanalytisches Laboratorium, Mülheim an der Ruhr, Germany.

6.2 Synthesis of HN(Np)Ar

The substituted aniline, HN(Np)Ar, was prepared by modifying a literature procedure for the synthesis of *N*-alkyl anilines,[99] here, employing pivaldehyde as the carbonyl-containing source. The product was typically obtained in 60% yield after vacuum distillation starting with 50 mL of pivaldehyde (460 mmol) and 36 mL of 3,5-dimethylaniline (287 mmol). ^{1}H NMR (300 MHz, C_6D_6, 23 °C): δ 6.38 (s, 1H, p-Ar), 6.19 (s, 2H, o-Ar), 3.22 (b, 1H, N*H*), 2.73 (s, 2H, N-CH_2), 2.24 (s, 6H, Ar-CH_3), 0.84 (s, 9H, *t*-Bu); ^{13}C{^{1}H} NMR (75.46 MHz, C_6D_6, 23 °C): δ 149.9 (aryl ipso), 138.7 (m-Ar), 119.8 (p-Ar), 111.6 (o-Ar), 56.2 (N*C*H$_2$), 32.3 (*C*(CH$_3$)$_3$), 28.0 (C(*C*H$_3$)$_3$), 22.1 (Ar-*C*H$_3$); FTIR (KBr windows, C_6D_6 solution): ν(N-H) 3426 cm^{-1} also 3022, 2960, 2870, 1596, 1519, 1497 1190, 690 cm^{-1}. Anal. Calcd. for $C_{13}H_{21}N$: C, 81.61; H, 11.06; N, 7.32. Found: C, 81.56; H, 10.98; N, 7.28.

6.3 Synthesis of (Et$_2$O)Li(N[Np]Ar)

To a thawing *n*-pentane solution of HN(Np)Ar (20.0 g, 104 mmol, 75 mL) was added a hexanes solution of *n*-butyl lithium (1.6 M, 78 mL, 125 mmol) dropwise over 30 min. The viscous, pale yellow reaction mixture was allowed to stir for an additional 40 min. At this point, 25 mL of diethyl ether were added to the mixture with concomitant precipitation of (Et$_2$O)Li(N[Np]Ar). The solvent was reduced to a volume of 40 mL *in vacuo*. The resulting pale yellow slurry was filtered through a sintered glass frit, affording (Et$_2$O)Li(N[Np]Ar) as a white solid in 88% yield (24.90 g) after washing with 40 mL of *n*-pentane and thorough drying under vacuum. ^{1}H NMR (300 MHz, C_6D_6, 23 °C): δ 6.39 (s, 2H, o-Ar), 6.13 (s, 1H, p-Ar), 3.38 (s, 2H, N-CH_2), 3.10 (q, 4H, J = 6 Hz, O-CH_2-CH$_3$), 2.36 (s, 6H, Ar-CH_3), 1.15 (s, 9H, *t*-Bu), 0.83 (t, 6H, J = 6 Hz, O-CH$_2$-C*H*3); ^{13}C{^{1}H} NMR (75.0 MHz, C_6D_6, 23 °C): δ 161.5 (aryl ipso), 139.3 (m-Ar), 113.2 (o-Ar), 111.1 (p-Ar), 65.8 (N-*C*H$_2$), 60.3 (O-*C*H$_2$-CH$_3$), 36.5 (*C*(CH$_3$)$_3$), 29.8 (C(*C*H$_3$)$_3$), 22.9 (Ar-*C*H$_3$), 14.8 (O-CH$_2$-*C*H$_3$); Anal. Calcd. for $C_{17}H_{30}NOLi$: C, 75.24; H, 11.14; N, 5.16; Found: C, 74.29; H, 11.59; N, 5.21.

6.4 Synthesis of Nb(PhCCPh)(N[Np]Ar)$_3$ (2a-PhCCPh)

To a diethyl ether slurry of *mer,cis*-Nb(Cl)$_3$(THF)$_2$(PhCCPh) (25.0 g, 47.9 mmol, 150 mL) at room temperature was added solid (Et$_2$O)Li(N(Np)Ar) (39.0 g, 143.7 mmol) in 3.0 g portions over the course of 1.5 h. After approximately 40 min, the mixture became dark brown and homogeneous and was allowed to stir for an additional time of 3 h. At this point, the solvent was removed *in vacuo* and the resulting dark brown residue was then extracted with two 50 mL portions of n-pentane and filtered through a sintered glass frit padded with approximately 4 cm of Celite in order to remove LiCl. The brown filtrate was evaporated to dryness *in vacuo* leaving a dark brown cake. The mixture was then slurried in 50 mL of *n*-pentane and filtered into a clean frit whereupon a yellow solid was obtained and washed with 10 mL of cold *n*-pentane. It has been our experience that this lypophilic material is not easily recrystallized from hydrocarbon or ethereal solvents and the material obtained by simple collection from the crude reaction mixture is of sufficient purity to be used in subsequent reactions. Yield: 50% based on Nb. ^{1}H NMR (500

MHz, C_6D_6, 23 °C): δ 7.75 (d, 4 H, J = 7.5 Hz, o-Ph), 7.31 (t, 4 H, J = 7.5 Hz, m-Ph), 7.08 (t, 2 H, J = 7.5 Hz, p-Ph), 6.80 (s, 6 H, o-Ar), 6.59 (s, 3 H, p-Ar), 3.82 (s, 6 H, , N-CH_2), 2.19 (s, 18 H, Ar-CH_3), 0.74 (s, 27 H, t-Bu); $^{13}C\{^1H\}$ NMR (125.66 MHz, C_6D_6, 23 °C): δ 200.0 (Ph-CC-Ph), 153.1 (aryl ipso), 143.4 (phenyl ipso), 138.8 (m-Ar), 129.2 (p-Ar), 128.5 (m-Ph), 127.4 (p-Ph), 126.0 (o-Ph), 122.8 (o-Ar), 67.1 (N-CH$_2$), 35.5 (C(CH$_3$)), 29.4 (C(CH$_3$)), 22.0 (Ar-CH$_3$). Satisfactory combustion analysis of this material has not been obtained.

6.5 Synthesis of Nb(I)$_2$(N[Np]Ar)$_3$ (2a-I$_2$)

A solution of **2a**-PhCCPh (10.0 g, 11.8 mmol) in diethyl ether (75 mL) was stirred at room temperature for 5 min. whereupon a diethyl ether solution of I_2 (3.164 g, 12.4 mmol, 10 mL) was added over 5 min. The dark yellow solution gradually became dark orange over the course of 10 min. The reaction mixture was allowed to stir for 2.5 h, after which the solvent was removed *in vacuo*. *n*-Pentane (30 mL) was added to the residue and the mixture was stirred for 5 min in order to extract liberated PhCCPh. Isolation of **2a**-I_2 was afforded by filtration of the dark orange mixture through a sintered glass frit with subsequent washing of the bright orange solid with cold *n*-pentane followed by thorough drying *in vacuo*. For instances where isolated Nb(I)$_2$(N[Np]Ar)$_3$ is contaminated with free PhCCPh, the orange solid may be allowed to precipitate from diethyl ether (~1mL/g) in the freezer (-35 °C) overnight before being collected, washed and dried again. Yield: 7.080g, 65%. ^1H NMR (300 MHz, C_6D_6, 23 °C): δ 8.04 (s, 6 H, o-Ar), 6.61 (s, 3 H, p-Ar), 3.60 (s, 6 H, N-CH_2), 2.14 (s, 18 H, Ar-CH_3), 0.585 (s, 27 H, t-Bu); $^{13}C\{^1H\}$ NMR (75.0 MHz, C_6D_6, 23 °C): δ 150.1 (aryl ipso), 139.9 (m-Ar), 130.4 (p-Ar), 124.8 (o-Ar), 76.4 (N-CH$_2$), 36.3 (C(CH$_3$)$_3$), 29.1 (C(CH$_3$)$_3$), 21.6 (Ar-CH$_3$); Anal. Calcd. for $C_{39}H_{60}N_3I_2Nb$: C, 51.05; H, 6.59; N, 4.58. Found: C, 50.61; H, 6.42; N, 4.56. This procedure can be sufficiently scaled to employ *ca.* 25 g of **2a**-PhCCPh with similar outcome.

6.6 Synthesis of Nb(H)(η^2-*t*-Bu(H)C=N(Ar))(N[Np]Ar)$_2$ (1a-H)

To a thawing THF solution of **2a**-I_2 (6.0 g, 6.53 mmol, 75 ml), 300 mg portions of Mg(THF)$_3$(anthracene) (3.418 g, 8.16 mmol) were added over a period of 10 min. The reaction mixture gradually changed in color from orange to deep purple and back to orange while being allowed to stir for a total of 3.5 h. At this point the solvent was removed *in vacuo* and the resulting orange-brown solid was extracted with two 30 mL portions of *n*-pentane and filtered through a 4 cm pad of Celite to remove salts and anthracene. The pentane filtrate was then concentrated to a volume of 10 mL, frozen and filtered while thawing through another pad of Celite in order to remove any residual anthracene. The filtrate was then dried, diethyl ether (~1mL/g) added and cooled to -35 °C for 24 h whereupon large orange blocks of pure **1a**-H were obtained and collected by vacuum filtration. Yield: 2.170 g, 52 % in two crops. ^1H NMR (500 MHz, C_6D_6, 23 °C): δ 9.25 (b, 1 H, Nb-H), 7.07 (s, 2 H, o-Ar), 7.02 (s, 2 H, o-Ar), 6.63 (s, 1 H, p-Ar), 6.59 (s, 1 H, p-Ar), 6.57 (s, 1 H, p-Ar), 6.11 (s, 2 H, o-Ar), 4.14, (s, 2 H, N-CH_2), 2.83, (d, 1 H, J = 8 Hz, N-CH_2), 2.74 (d, 1 H, J = 8 Hz, N-CH_2), 2.36 (s, 1 H, t-Bu(H)C=N), 2.35 (s, 6 H, Ar-CH_3), 2.14 (s, 6 H, Ar-CH_3), 2.13 (s, 6 H, Ar-CH_3), 1.41 (s, 9 H, t-Bu), 0.77 (s, 9 H, t-Bu), 0.46 (s, 9 H, t-Bu); $^{13}C\{^1H\}$ NMR (125.66 MHz, C_6D_6, 23 °C): δ 155.8 (aryl ipso), 144.4 (aryl ipso), 141.3 (p-Ar), 140.3 (p-Ar), 138.6 (m-Ar), 138.2 (aryl ipso), 129.0 (m-Ar), 127.7 (m-Ar), 122.9 (p-Ar), 118.4 (o-Ar), 116.7 (o-Ar), 116.5 (o-Ar), 81.9 (t-Bu(H)C=N), 68.3, (N-CH$_2$), 57.5 (N-CH$_2$), 36.4, (C(CH$_3$)$_3$), 35.0 (C(CH$_3$)$_3$), 34.4 (C(CH$_3$)$_3$), 31.7 (C(CH$_3$)$_3$), 29.3 (C(CH$_3$)$_3$), 28.6 C(CH$_3$)$_3$), 22.2 (Ar-CH$_3$), 21.9 (Ar-CH$_3$), 21.8 (Ar-CH$_3$); FTIR (KBr windows, C_6D_6 solution): ν(Nb-H) 1701 cm^{-1} also 1585, 1475, 1213, 1091, 1004, 689 cm^{-1}. Anal. Calcd. for $C_{39}H_{60}N_3Nb$:

C, 70.56; H, 9.11; N, 6.33. Found: C, 70.60; H, 9.12; N, 6.30. This procedure is optimal for the reduction of ca. 12.0 g of **2a**-I_2. A maximum yield of 64 % has been obtained in three crops. The niobaziridine-deuteride Nb(D)(η^2-*t*-Bu(D)C=N(Ar))(N[Np-d_6]Ar)$_2$ (**1a**-D) was prepared in an analogous fashion. ^{2}H NMR (76.7 MHz, C_6H_6, 23 °C): δ 9.20 (s, $\nu_{1/2}$ = 8.33 Hz, Nb-*D*), 3.83 (d, 2D, *J* = 7 Hz, N-C*D*$_2$), 2.51 (d, 2D, 7 Hz, N-C*D*$_2$), 1.86 (s, 1D, *t*-Bu(*D*)C=N).

6.7 Thermolysis of Nb(H)(η^2-*t*-Bu(H)C=N(Ar))(N[Np]Ar)$_2$ (1a-H): Synthesis of Nb(Ar)(NNp)(N[Np]Ar)$_2$ (3a)

A toluene solution of **1a**-H (200 mg, 0.30 mmol, 3 mL) was heated in a Schlenk tube at 100 °C for 1 h under an atmosphere of dinitrogen. Over this time the color of the reaction mixture changed from orange to light brown. The Schlenk tube was then transferred to the glove box where all volatile materials were removed *in vacuo*. The resulting brown residue was extracted with 2 mL of *n*-pentane and filtered through Celite. The filtrate was dried under vacuum to leave an oily brown residue which did not crystallize readily from hydrocarbon or ethereal solvents after numerous attempts. ^{1}H NMR indicated that the reaction had proceeded with complete consumption of complex **1a**-H with no additional species produced besides **3a**. ^{1}H NMR (300 MHz, C_6D_6, °C): δ 7.78 (s, 2H, Nb-Ar ortho), 6.89 (s, 1H, Nb-Ar-para), 6.79 (s, 4H, o-Ar), 6.48 (s, 2H, p-Ar), 4.18 (d, 2H, *J* = 13 Hz, N-C*H*$_2$ amido), 3.86 (s, 2H, N-C*H*$_2$ imido), 3.84 (d, 2H, *J* = 13 Hz, N-C*H*$_2$ amido), 2.34 (s, 6H, Nb-Ar-C*H*$_3$), 2.07 (s, 12H, Ar-C*H*$_3$), 1.06 (s, 9H, *t*-Bu imido), 0.94 (s, 18H, *t*-Bu); ^{13}C{^{1}H} NMR (75.0 MHz, C_6D_6, °C): δ 150.8 (amide aryl ipso), 139.7 (amide m-Ar), 136.3 (m-Ar), 135.9 (amide p-Ar), 129.9 (p-Ar), 126.0 (o-Ar), 120.3 (amide o-Ar), 77.3 (imido N-*C*H$_2$), 70.0 (amide N-*C*H$_2$), 35.9 (amide *C*(CH$_3$)$_3$), 35.0 (imido *C*(CH$_3$)$_3$), 29.0 (amide C(*C*H$_3$)$_3$), 28.4 (imido C(*C*H$_3$)$_3$), 22.1 (Ar-*C*H$_3$), 21.7 (amide Ar-*C*H$_3$). The physical properties of **3a** (i.e. oily nature and lack of crystallinity) prevented adequate purification and combustion analysis.

6.8 Synthesis of Nb(Cl)(η^2-*t*-Bu(H)C=N(Ar))(N[Np]Ar)$_2$ (1a-Cl)

To an Et_2O solution of **1a**-H (0.400 g, 0.602 mmol, 5 mL) was added excess CH_2Cl_2 (2.55 g, 30.1 mmol, 0.51 mL, 50 equiv) at room temperature. An immediate color change accompanied addition and a copious amount of precipitate was formed after ca. 10 min. The reaction mixture was allowed to stir for a total of 30 min and then all volatile materials were removed *in vacuo*. The light orange residue obtained was suspended in *n*-pentane (2 mL) and stored at -35 °C for 12 h. The orange **1a**-Cl thereby obtained was isolated by filtration followed by thorough drying *in vacuo*. Yield 0.373 g, 90% by two filtrations. ^{1}H NMR (300 MHz, C_6D_6, 23 °C): δ 7.58 (s, 2 H, p-Ar overlap), 6.76 (s, 2 H, o-Ar), 6.63 (s, 1 H, p-Ar), 6.58 (s, 2 H, o-Ar), 6.40 (bs, 2 H, o-Ar), 4.76, (d, 1 H, *J* = 14 Hz, N-C*H*$_2$), 4.39, (d, 1 H, *J* = 14 Hz, N-C*H*$_2$), 2.99 (d, 1 H, *J* = 14 Hz, N-C*H*$_2$), 2.90 (d, 1 H, *J* = 14 Hz, N-C*H*$_2$), 2.33 (s, 6 H, Ar-C*H*$_3$), 2.20 (s, 6 H, Ar-C*H*$_3$), 2.05 (s, 6 H, Ar-C*H*$_3$), 1.31 (s, 9 H, *t*-Bu), 0.82 (s, 9 H, *t*-Bu), 0.47 (s, 9 H, *t*-Bu); Anal. Calcd. for $C_{39}H_{59}N_3ClNb$: C, 67.08; H, 8.52; N, 6.02; Found: C, 66.97; H, 8.47; N, 6.10.

6.9 Synthesis of the Deuterated Amine HN(Np-*d*$_2$)Ar (Np-*d*$_2$ = CD$_2$(*t*-Bu))

Two Steps.

Step 1: Synthesis of *N*-3,5-dimethylphenylpivalamide (*t*-BuC(O)NH(3,5-$Me_2C_6H_3$): Pivaloyl chloride (*t*-BuC(O)Cl, 50.0 g, 0.414 mol, 1.2 equiv) and triethylamine (NEt_3, 41.86 g, 0.345 mol, 1.0 equiv) where added to 500 mL of anhydrous Et_2O and a positive-pressure blanket of N_2 was

applied to the reaction vessel. The cloudy white mixture was then stirred with a mechanical stirrer and cooled to 0 °C with an ice bath. Freshly distilled 3,5-dimethylaniline (34.96g, 0.345 mol) was added dropwise with a pressure-equilibrating addition funnel over the course of 1 h. A copious amount of white solid was formed from the reaction mixture after ca. 10 min. The reaction was allowed stir for a total of 3 h, at which point 300 mL of H_2O was added. The aqueous and organic phases were separated and the aqueous phase was washed with 2 x 100 mL of fresh Et_2O. The Et_2O washings were combined and evaporated leaving behind *t*-BuC(O)NH(3,5-$Me_2C_6H_3$) as a white solid. The product was slurried in 300 mL of *n*-hexane and stored at -30 °C overnight. The resultant white precipitate was filtered and washed with 50 mL of *n*-hexane. Yield 93.1%, 66.0 g. ^{1}H NMR (300 MHz, C_6D_6, 23 °C): δ 7.32 (s, 2 H, o-Ar),7.07 (s, 1 H, N-*H*) 6.59 (s, 1 H, p-Ar), 2.14 (s, 6 H, Ar-C*H*$_3$), 1.11 (s, 9 H, *t*-Bu); ^{13}C{^{1}H} NMR (75.0 MHz, C_6D_6, 23 °C): δ 175.9 (C=O) 139.3 (aryl ipso), 138.7 (m-Ar), 126.2 (p-Ar), 118.4 (o-Ar), 40.0 (*C*(CH$_3$)$_3$), 28.1 (C(*C*H$_3$)$_3$), 21.9 (Ar-*C*H$_3$); FTIR (KBr windows, C_6D_6 solution): ν(N-H) 3229 cm^{-1}, ν(C=O) 1688 also 1601, 1530, 1186.

Step 2: *N*-3,5-dimethylphenylpivalamide (32.4 g, 0.157 mol) and $LiAlD_4$ (10.0 g, 0.237 mol, 1.5 equiv) were refluxed for 16 h under N_2 in 200 mL of anhydrous THF. The reaction mixture was slowly quenched at 0 °C with 200 mL of 0.2 M HCl while under an N_2 stream. Aqueous ammonium hydroxide was then added until a pH of 10 was reached. The free amine HN(Np-*d*$_2$)Ar was then extracted with 3 x 100 mL of petroleum ether and worked up according to the procedure for the protio amine.[99] Yield: 24.68 g, 80.8 %. ^{2}H NMR (76.7 MHz, C_6H_6, 23 °C): δ 2.73 ppm.

6.10 Kinetic Measurements of the Decay of Niobaziridine-Hydride and Deuteride 1a-H and 1a-D.

All measurements were obtained by ^{1}H NMR on a Varian INOVA spectrometer operating at a resonance frequency of 500 MHz. Samples of either **1a**-H or **1a**-D were prepared in a glovebox as C_6D_6 solutions (0.015 g, 0.8 mL, 28.2 mM) which contained 5 mg of Cp_2Fe (33.6 mM) as an internal standard. The solutions, once prepared, were loaded into a sealable NMR tube. Each sample was placed in a spectrometer pre-warmed to 75 °C. Once inside the spectrometer, all samples were subjected to a 10 min. equilibration period prior to initial data collection. Raw data for each kinetic run were obtained from integration of the resonances corresponding to the *tert*-butyl substituent for both **1a**-H or **1a**-D resonating at highest field (0.46 ppm). Single pulse acquisitions were employed in all cases. All data were processed and fitted with the Mircoral Origin (v. 6.0) program suite.

6.11 Synthesis of (O)Nb(N[Np]Ar)$_3$ (2a-O)

An atmosphere of dry N_2O was introduced to a partially evacuated 50 mL Schlenk tube containing an diethyl ether solution of **1a**-H (88 mg, 0.093 mmol, 3 mL). The color of solution gradually became light brown over the course of 6 h at which point the solvent was removed *in vacuo*. The resulting yellow-brown residue was extracted with 1.5 mL of *n*-pentane and filtered through Celite. The filtrate was then evaporated to dryness in vacuo. Diethyl ether (1 mL) was added to the residue and the solution chilled at –35 °C for 1 d whereupon yellow crystals were obtained. Yield: 0.063 g, 70% in two crops. ^{1}H NMR (300 MHz, C_6D_6, 23 °C): δ 6.50 (s, 3H, p-Ar), 6.39 (s, 6H, o-Ar), 4.45 (s, 6H, N-C*H*$_2$),2.00 (s, 18H, Ar-C*H*$_3$), 1.03 (s, 27H, *t*-Bu); ^{13}C{^{1}H} NMR (75.0 MHz, C_6D_6, 23 °C): δ 153.7 (aryl ipso), 138.8 (m-Ar), 125.9 (p-Ar), 122.2 (o-Ar),

75.0 (N-CH_2), 35.7(C(CH3)$_3$), 32.0 (C(CH_3)$_3$), 21.9 (Ar-CH_3); Anal. Calcd for $C_{39}H_{60}N_3NbO$: C, 68.90; H,8.90; N, 6.18. Found: C, 68.28; H, 8.72; N, 6.14.

6.12 Deoxygenation of Triphenylphosphine oxide ($OPPh_3$) by 1a-H: Alternate Synthesis of (O)Nb(N[Np]Ar)$_3$ (2a-O)

To a benzene-d_6 solution of **1a**-H (50 mg, 0.075 mmol, 2 mL) was added a solution of triphenylphosphine oxide in benzene-d_6 (22.0 mg, 0.079 mmol, 1 mL). The reaction was monitored periodically by ^{1}H NMR and was determined to be complete after 8 h. The resulting ^{1}H NMR spectrum contained only the signature resonances for compound **2a-O** and triphenylphosphine. The presence of triphenylphosphine was confirmed by a signal at -4.8 ppm in the ^{31}P{^{1}H} NMR spectrum of the reaction mixture.

6.13 Synthesis of (S)Nb(N[Np]Ar)$_3$ (2a-S)

A diethyl ether solution of **1a**-H (200 mg, 0.301 mmol, 2 mL) was added over the course of 30 min. to a slurry of trimethylphosphine sulfide ($SPMe_3$, 0.225 g, 2.11 mmol, 7 equiv) in diethyl ether (8 mL). After 10 min. the solution became emerald green and was allowed to stir for 2.5 h, at which point all volatile materials were removed *in vacuo*. The residue was extracted with *n*-pentane (2 mL) and filtered through Celite twice, before being dried in vacuo again. The resulting light green solid was dissolved in diethyl ether (2 mL) and chilled to –35 °C for 18 h whereupon yellow orange single crystals were obtained and collected. Yield: 0.088 g, 42%. ^{1}H NMR (300 MHz, C_6D_6, 23 °C): δ 6.51 (s, 3H, p-Ar), 6.44 (s, 6H, o-Ar), 4.47 (s, 6H, N-CH_2), 2.05 (s, 18H, Ar-CH_3), 1.09 (s, 27H, *t*-Bu); ^{13}C{^{1}H} NMR (75.0 MHz, C_6D_6, 23 °C): δ 152.3 (aryl ipso), 138.6 (m-Ar), 126.5 (p-Ar), 123.4 (o-Ar), 76.9 (N-CH_2), 37.0 (C(CH_3)$_3$), 29.9 (C(CH_3)$_3$), 22.0 (Ar-CH_3); Anal. Calcd. for $C_{39}H_{60}N_3SNb$: C, 67.31; H, 8.69; N, 6.04. Found: C, 67.30; H, 8.79; N, 6.08.

6.14 Synthesis of (Se)Nb(N[Np]Ar)$_3$ (2a-Se)

To a slurry of selenium powder in benzene (45.0 mg, 0.569 mmol, 4 equiv., 3 mL) was added a benzene solution of **1a**-H (0.100 g, 0.150 mmol, 2 mL) over the course of 5 min. The reaction mixture was allowed to stir for 5 h while gradually darkening in color to a dark orange-red. All volatile materials were removed in vacuo and the resulting dark orange residue extracted with n-pentane, filtered through Celite and dried again. The resulting residue was redissolved in diethyl ether (1.5 mL) and chilled to –35 °C overnight, whereupon red single crystals were obtained and collected. Yield: 0.078 g, 70% in two crops. ^{1}H NMR (500 MHz, C_6D_6, 23 °C): δ 6.52 (s, 3H, p-Ar), 6.38 (s, 6H, o-Ar), 4.49 (s, 6H, N-CH_2), 2.04 (s, 18H, Ar-CH_3), 1.11 (s, 27H, *t*-Bu); ^{13}C{^{1}H} NMR (75.0 MHz, C_6D_6, 23 °C): δ 151.7 (aryl-ipso), 138.6 (m-Ar), 126.6 (p-Ar), 123.5 (o-Ar), 76.5 (N-CH_2), 37.3 (C(CH_3)$_3$), 30.1 (C(CH_3)$_3$), 22.0 (Ar-CH_3); Anal. Calcd. for $C_{39}H_{60}N_3SeNb$: C, 63.06; H, 8.14; N, 5.66. Found: C, 62.76; H, 8.06; N, 5.74.

6.15 Synthesis of (Te)Nb(N[Np]Ar)$_3$ (2a-Te)

Compound **2a**-Te was prepared analogously to compound **2a-Se** by substituting tellurium powder for selenium powder. The reaction was allowed to stir for 24 h resulting in a dark red brown solution. After filtration, the resulting red-brown residue was dissolved in 1 mL diethyl ether and chilled at -35 °C overnight whereupon dark red crystals were obtained. Yield: 0.071 g, 60% in two crops. ^{1}H NMR (500 MHz, C_6D_6, 23 °C): δ 6.53 (s, 3H, p-Ar), 6.36 (s, 6H, o-Ar), 4.49 (s, 6H, N-CH_2), 2.05 (s, 18H, Ar-CH_3), 1.14 (s, 27H, *t*-Bu); ^{13}C{^{1}H} NMR (125.66 MHz,

C_6D_6, 23 °C): δ 150.6 (aryl-ipso), 138.7 (m-Ar), 126.7 (p-Ar), 123.4 (o-Ar), 75.2 (N-CH_2), 37.4 ($C(CH_3)_3$), 30.4 ($C(CH_3)_3$), 21.7 (Ar-CH_3); Anal. Calcd. for $C_{39}H_{60}N_3TeNb$: C, 59.19; H, 7.64; N, 5.31. Found: C, 59.25; H, 7.58; N, 5.28.

6.16 Synthesis of (Ar[Np]N)$_3$Nb(μ-P)Mo(N[*i*-Pr]Ar)$_3$ (2a(μ-P)5a)

A diethyl ether solution of (P)Mo(N[*i*-Pr]Ar)$_3$ (115 mg, 0.188 mmol, 2.5 mL) was added dropwise over 5 min to a diethyl ether solution of **1a**-H (125 mg, 0.188 mmol, 2.5 mL). The color of the reaction mixture changed to a deep purple-red upon addition. The mixture was allowed to stir for 2 h, after which, the solvent was removed *in vacuo*. The resulting purple residue was extracted with 1.5 mL *n*-pentane and filtered through Celite. The filtrate was evaporated to dryness, redissolved in 1.5 mL *n*-hexane and allowed to sit at room temperature for 3 d whereupon a purple, microcrystalline solid was obtained and collected. Yield: 0.108 g, 45 % one crop. ^{1}H NMR (300 MHz, C_6D_6, 23 °C): δ 6.75 (s, 6H, o-Ar), 6.54 (s, 3H, p-Ar), 6.53 (s, 6H, o-Ar), 6.53 (s, 3H, p-Ar), 4.96 (sp, 3H, J = 6 Hz, N-CH(CH_3)$_2$), 2.22 (s, 18H, Ar-CH_3), 2.15 (s, 18H, Ar-CH_3), 1.57 (d, 18H, J = 6 Hz, N-CH(CH_3)$_2$), 1.09 (s, 27H, *t*-Bu); ^{13}C{^{1}H} NMR (75.0 MHz, C_6D_6, 23 °C): δ 159.3 (aryl ipso), 158.3 (aryl ipso), 138.6 (m-Ar), 137.8 (m-Ar), 127.2 (p-Ar), 125.6 (o-Ar), 125.5 (p-Ar), 121.1 (o-Ar), 82.1 (N-CH(CH_3)$_2$), 72.0 (N-CH_2), 36.5 ($C(CH_3)_3$), 30.3 ($C(CH_3)_3$), 25.0 ($C(CH_3)_2$), 22.1 (Ar-CH_3), 21.9 (Ar-CH_3); ^{31}P{^{1}H} NMR (121.4 MHz, C_6D_6, 23 °C): δ 666.6 (bs); Anal. Calcd. for $C_{72}H_{108}N_6PMoNb$: C, 67.69; H, 8.52; N, 6.58. Found: C, 67.48; H, 8.38; N, 6.34.

6.17 Synthesis of Nb(η^2-MesCN)(N[Np]Ar)$_3$ (2a-NCMes)

To a diethyl ether solution of **1a**-H (100 mg, 0.150 mmol, 2 mL) were added 1.05 equivalents of mesitylnitrile (MesCN, 23.0 mg, 0.158 mmol) in 0.5 mL of diethyl ether. A dark orange-brown solution was obtained upon addition. After filtration through Celite, the residue was dissolved in 1 mL *n*-hexane and allowed to sit at room temperature for 2 d whereupon large orange blocks were obtained and collected. Yield: 0.070 g, 55% one crop. ^{1}H NMR (300 MHz, C_6D_6, 23 °C): δ 6.98 (s, 2H, m-Mes), 6.78 (s, 6H, o-Ar), 6.54 (s, 3H, p-Ar), 3.90 (s, 6H, N-CH_2), 3.01 (s, 6H, Mes-o-Me), 2.18 (s, 3H, Mes-p-Me), 2.15 (s, 18H, Ar-CH_3), 0.78 (s, 27H, *t*-Bu); ^{13}C{^{1}H} NMR (75.0 MHz, C_6D_6, 23 °C): δ 153.2 (aryl ipso), 140.4 (m-Mes), 140.3 (Mes ipso), 138.8 (m-Ar), 132.8 (p-Mes), 130.3 (o-Mes), 126.1 (p-Ar), 121.8 (o-Ar), 65.2 (N-CH_2), 35.9 ($C(CH_3)_3$), 29.4 ($C(CH_3)_3$), 23.3 (Mes-o-CH_3), 21.9 (Ar-CH_3), 21.6 (Mes-p-CH_3); FTIR (KBr windows, C_6D_6 solution): 2951, 1587, 1475, 999 cm^{-1}. Anal. Calcd. for $C_{49}H_{71}N_4Nb$: C, 72.75; H, 8.85; N, 6.93. Found: C, 72.35; H, 9.22; N,6.97.

6.18 Synthesis of the Insertion Products 1a-NC(H)*t*-Bu, 1a-NC(H)NMe$_2$, 1a-OBz, 1a-NC(H)=C(H)*t*-Bu and 1a-N(H)NCPh$_2$

For each reaction, 1.05 equiv of reagent corresponding to 0.100 g (0.150 mmol) of **1a**-H was dissolved in 1 mL of C_6D_6. These solutions were added at room temperature to a C_6D_6 solution of **1a**-H. The reactions were monitored by ^{1}H NMR ca. 30 min after mixing and were observed to be complete. Total reaction time for each was approximately 1.5 h. The reaction mixtures were evaporated to dryness, extracted with *n*-pentane and filtered through Celite. Isolation procedures and characterization data for each are provided:

1a-NC(H)*t*-Bu: Blood-red crystals from Et_2O (- 35 °C, 1 d). Yield: 0.084 g, 75% in two crops. ^{1}H NMR (300 MHz, C_6D_6, 23 °C): δ 8.87 (s, 1H,N=C(H) *t*-Bu ketimide), 6.94 (s, 2H, o-Ar),

6.89 (s, 2H, o-Ar), 6.67 (s, 1H, p-Ar), 6.50 (s, 1H, p-Ar), 6.46 (s, 1H, p-Ar), 6.26 (s, 2H, o-Ar), 4.33 (s, 2H, N-CH_2), 3.38 (d, 1H, J = 14 Hz, N-CH_2), 3.32 (d, 1H, J = 14 Hz, N-CH_2), 3.22 (s, 1H, N=C(H)t-Bu aziridine), 2.30 (s, 6H, Ar-CH_3), 2.27 (s, 6H, Ar-CH_3), 2.09 (s, 6H, Ar-CH_3), 1.35 (s, 9H, t-Bu), 1.11 (s, 9H, t-Bu), 0.83 (s, 9H, t-Bu), 0.55 (s, 9H, t-Bu); $^{13}C\{^1H\}$ NMR (75.0 MHz, C_6D_6, 23 °C): δ 179.8 (N=C(H)t-Bu ketimide), 155.3 (aryl ipso), 150.0 (aryl ipso), 149.7 (aryl ipso), 139.2 (m-Ar), 137.8 (m-Ar), 137.7 (m-Ar), 125.7 (p-Ar), 125.4 (p-Ar), 122.3 (o-Ar), 121.2 (p-Ar), 119.8 (o-Ar), 117.1 (o-Ar), 77.9 (N=C(H)t-Bu imine), 68.9 (N-CH$_2$), 64.4 (N-CH$_2$), 40.0 (C(CH$_3$)$_3$), 38.0 (C(CH$_3$)$_3$), 35.0 (C(CH$_3$)$_3$), 34.4 (C(CH$_3$)$_3$), 31.1 (C(CH$_3$)$_3$), 29.2 (C(CH$_3$)$_3$), 28.4 (C(CH$_3$)$_3$), 26.6 (C(CH$_3$)$_3$), 21.7 (Ar-CH$_3$), 21.5 (Ar-CH$_3$), 21.3 (Ar-CH$_3$); FTIR (KBr windows, C_6D_6 solution): ν(CN) 1667 cm^{-1} also 2951, 2867, 1586, 1475, 1208, 1003, 688 cm^{-1}. Anal. Calcd. for $C_{44}H_{69}N_4Nb$: C, 70.75; H, 9.31; N, 7.50. Found: C, 70.61; H, 9.58; N, 7.48.

1a-OBz: Yellow crystals from Et_2O (-35 °C, 2 d).Yield: 0.080 g, 55%. ^1H NMR (300 MHz, C C_6D_6, 23 °C): δ 7.50 (d, 2H, J = 7.0 Hz, o-Ph), 7.28, (t, 2H, J = 7.0 Hz, m-Ph), 7.16 (t, 1H, J = 7.0 Hz, p-Ph), 6.79 (s, 2H, o-Ar), 6.75 (s, 2H, o-Ar), 6.61 (s, 3H, o-Ar *and* p-Ar), 6.53 (s, 1H, p-Ar), 6.51 (s, 1H, p-Ar), 5.70 (d, 1H, J = 13 Hz, N-CH_2), 5.59 (d, 1H, J = 13 Hz, N-CH_2), 4.08 (s, 2H, O-CH_2-Ph), 3.39 (d, 1H, J = 14 Hz, N-CH2), 3.27 (d, 1H, J = 14 Hz, N-CH_2), 3.15 (s, 1H, N=C(H)t-Bu aziridine), 2.26 (s, 6H, Ar-CH_3), 2.19 (s, 6H, Ar-CH_3), 2.15 (s, 6H, Ar-CH_3), 1.34 (s, 9H, t-Bu), 0.83 (s, 9H, t-Bu), 0.59 (s, 9H, t-Bu); $^{13}C\{^1H\}$ NMR (75.0 MHz, C_6D_6, 23 °C): δ 154.6 (aryl-ipso), 154.4 (aryl-ipso), 151.5 (aryl-ipso), 151.1 (Ph-ipso), 142.2 (m-Ph), 138.9 (m-Ar), 138.8 (m-Ar), 137.9 (m-Ar), 129.1 (o-Ph), 128.4 (p-Ph), 125.7 (p-Ar), 125.6 (p-Ar), 123.4 (p-Ar), 121.7 (o-Ar), 121.2 (o-Ar), 118.2 (o-Ar), 80.4 (O-CH$_2$-Ph), 77.7 (N=C(H)t-Bu), 67.9 (N-CH2), 66.6 (N-CH$_2$), 38.3 (C(CH$_3$)$_3$), 35.9 (C(CH$_3$)$_3$), 35.2 (C(CH$_3$)$_3$), 32.2 (C(CH$_3$)$_3$), 29.5 (C(CH$_3$)$_3$), 28.9 (C(CH$_3$)$_3$), 22.0 (Ar-CH$_3$), 21.9 (Ar-CH$_3$), 21.8 (Ar-CH$_3$); Anal. Calcd. for $C_{46}H_{66}N_3NbO$: C, 71.76; H, 8.64; N, 5.46. Found: C, 71.68; H, 8.58; N, 5.31.

1a-NC(H)NMe$_2$: Orange crystals from Et_2O (-35 °C, 2 d) Yield: 0.074 g, 68% in two crops. ^1H NMR (300 MHz, C_6D_6, 23 °C): δ 8.19 (s, 1H, N=C(H)NMe$_2$ ketimide), 7.17 (s, 2H, o-Ar), 7.02 (s, 2H, o-Ar), 6.66 (s, 1H, p-Ar), 6.60 (s, 2H, o-Ar), 6.52 (s, 1H, p-Ar), 6.50 (s, 1H, p-Ar), 4.40 (s, 2 H, N-CH_2), 3.20 (s, 2 H, N-CH_2), 3.15 (s, 1H, N=C(H)t-Bu aziridine), 2.45 (bs, 3H, NCH_3 amine), 2.38 (s, 6H, Ar-CH_3), 2.31 (s, 6H, Ar-CH_3), 2.16 (s, 6H, Ar-CH_3), 2.o5 (bs, 3H, NCH_3 amine),1.35 (s, 9H, t-Bu), 1.40 (s, 9H, t-Bu), 0.91 (s, 9H, t-Bu), 0.54 (s, 9H, t-Bu); $^{13}C\{^1H\}$ NMR (75.0 MHz, C_6D_6, 23 °C): δ 159.8 (N=C(H)NMe$_2$ ketimide), 156.5 (aryl ipso), 152.7 (aryl ipso), 152.6 (aryl ipso), 139.0 (m-Ar), 138.0 (m-Ar), 137.9 (m-Ar), 125.1 (p-Ar), 124.8 (p-Ar), 121.9 (o-Ar), 121.5 (p-Ar), 120.3 (o-Ar), 117.8 (o-Ar), 77.7 (N=C(H)t-Bu imine), 69.9 (N-CH2), 63.1 (N-CH$_2$), 38.0 (C(CH$_3$)$_3$), 36.4 (C(CH$_3$)$_3$), 35.3 (C(CH$_3$)$_3$), 32.1 (C(CH$_3$)$_3$), 29.8 (C(CH$_3$)$_3$), 29.0 (C(CH$_3$)$_3$), 22.3 (Ar-CH$_3$), 22.1 (Ar-CH$_3$), 21.9 (Ar-CH$_3$); Anal. Calcd. for $C_{42}H_{66}N_4Nb$: C, 68.73; H, 9.06; N, 9.54. Found: C, 68.65; H, 9.07; N, 9.41.

1a-C(H)=C(H)t-Bu: Orange crystals from Et_2O (- 35 °C, 3 d). Yield: 0.080 g, 71% in two crops. ^1H NMR (300 MHz, C_6D_6, 23 °C): δ 8.19 (d, 1H, J = 18 Hz, C(H)=C(H)t-Bu), 7.31 (s, 2H, o-Ar), 6.98 (s, 2H, o-Ar), 6.62 (s, 1H, p-Ar), 6.58 (s, 1H, p-Ar), 6.55 (s, 1H, p-Ar), 6.41 (s, 2H, o-Ar), 6.36 (d, 1H, J = 18 Hz, C(H)=C(H)t-Bu) 4.26 (d, 1H, J = 14 Hz, N-CH_2), 4.16 (d, 1H, J = 14 Hz, N-CH_2), 2.87 (d, 1H, J = 14 Hz, N-CH_2), 2.75 (d, 1H, J = 14 Hz, N-CH_2), 2.60 (s, 1H, N=C(H)t-Bu aziridine), 2.37 (s, 6H, Ar-CH_3), 2.26 (s, 6H, Ar-CH_3), 2.15 (s, 6H, Ar-CH_3), 1.39

(s, 9H, *t*-Bu), 1.26 (s, 9H, *t*-Bu), 0.83 (s, 9H, *t*-Bu), 0.45 (s, 9H, *t*-Bu); Anal. Calcd. for $C_{45}H_{70}N_3Nb$: C, 72.45; H, 9.46; N, 5.63. Found: C, 71.93; H, 9.28; N, 5.89.

1a-N(H)NCPh$_2$: Yellow powder from *n*-pentane (- 35 °C, 1 d). Yield 0.112 g, 88%. ^{1}H NMR (300 MHz, C_6D_6, 23 °C): δ 10.0 (s, 1H, N(*H*)NCPh$_2$), 7.93 (d, 4H, o-Ph), 7.28 (s, 2H, o-Ar), 7.24 (t, 4 H, m-Ph) 7.10 (t, 2 H, p-Ph), 7.07, (s, 1H, p-Ar), 7.00 (s, 2H, o-Ar), 6.65 (s, 2H, o-Ar), 6.63 (s, 1H, p-Ar), 6.53 (s, 1H, p-Ar), 4.09 (d, 1H, J = 8.5 Hz, N-CH_2), 3.99 (d, 1H, J = 8.5 Hz, N-CH_2), 3.05 (d, 1H, J = 9 Hz, N-CH_2), 3.00 (s, 1H, N=C(*H*)*t*-Bu aziridine), 2.54 (d, 1H, J = 9 Hz, N-CH_2), 2.31 (s, 6H, Ar-CH_3), 2.28 (s, 6H, Ar-CH_3), 2.22 (s, 6H, Ar-CH_3), 1.15 (s, 9H, *t*-Bu), 0.89 (s, 9H, *t*-Bu), 0.0.57 (s, 9H, *t*-Bu).

6.19 Synthesis of the Cyclic-Imido Complex Nb(=NC(H)*t*-BuC(H)*t*-BuNAr)(N[Np]Ar)$_2$ (6a-*t*-Bu)

A toluene solution of complex **1a**-NC(H)*t*-Bu (0.150 g, 0.200 mmol, 3 mL) was heated at 120 °C for 1.5 h. A gradual color change from blood red to bright yellow was observed over this time. The toluene solvent was removed under reduced pressure and the resulting yellow residue was extracted with *n*-pentane and filtered through Celite. The solvent was removed again and the crude solid obtained was dissolved in approximately 0.5 mL of Et_2O. Yellow plates of **6a**-*t*-Bu were obtained from this solution upon standing at - 35 °C for 3 d. Yield: 0.097 g, 65% in two crops. ^{1}H NMR (400 MHz, C_6D_6, 23 °C): δ 7.02 (s, 2H, o-Ar), 6.95 (s, 2H, o-Ar), 6.56 (s, 1H, p-Ar), 6.49 (s, 1H, p-Ar), 6.35 (s, 1H, p-Ar), 6.05 (s, 2H, o-Ar), 5.29 (s, 1H, backbone), 4.68 (d, 1H, J = 13.4 Hz, N-CH_2), 4.29 (d, 1H, J = 13.4 Hz, N-CH_2), 4.14 (s, 1H, backbone), 3.94 (d, 1H, J = 14 Hz, N-CH_2), 3.38 (d, 1H, J = 14 Hz, N-CH_2), 2.18 (s, 6H, Ar-CH_3), 2.14 (s, 6H, Ar-CH_3), 1.99 (s, 6H, Ar-CH_3), 1.26 (s, 9H, *t*-Bu), 1.14 (s, 9H, *t*-Bu), 0.99 (s, 9H, *t*-Bu), 0.84 (s, 9H, *t*-Bu); Anal. Calcd. for $C_{44}H_{69}N_4Nb$: C, 70.75; H, 9.31; N, 7.50. Found: C, 69.94; H, 9.24; N, 7.30.

6.20 Synthesis of the Cyclic-Imido Complex Nb(=NC(H)PhC(H)*t*-BuNAr)(N[Np]Ar)$_2$ (6a-Ph)

To a C_6D_6 solution of **1a**-H (0.100 g, 0.150 mmol, 2 mL) was added a C_6D_6 solution of benzonitrile (0.016 g, 0.159 mmol, 1.05 equiv, 0.5 mL). A rapid color change from orange to dark red accompanied the addition. Analysis of the reaction mixture by ^{1}H NMR after 15 min of reaction time indicated the presence of two products, with one being assigned as the ketimido insertion product Nb(N=C(H)Ph)(η^2-*t*-Bu(H)C=N(Ar))(N[Np]Ar)$_2$ (**1a**- NC(H)Ph) based on the presence of downfield singlet located at δ = 9.57 ppm. Complex **1a**- NC(H)Ph was observed to disappear over time concomitant with an increase in the resonances attributed to the other product, **6a**-Ph. Work up and isolation of **6a**-Ph was identical to that of **6a**-*t*-Bu. Yield: 0.043 g, 38%. ^{1}H NMR (400 MHz, C_6D_6, 23 °C): ^{1}H NMR (300 MHz, C_6D_6, 23 °C): δ 7.69 (d, 2H, J = 7 Hz, o-Ph), 7.29 (t, 2H, J = 6 Hz, m-Ph), 7.15 (t, 1H, J = 6 Hz, p-Ph), 6.81 (s, 2H, o-Ar), 6.54 (s, 3H, o-Ar and p-Ar), 6.39 (s, 1H, p-Ar), 6.37 (s, 1H, p-Ar), 6.22 (s, 2H, o-Ar), 5.68 (dd, 2H, J = 3 Hz, backbone), 4.64 (d, 1H, J = 13.2 Hz, N-CH_2), 4.37 (d, 1H, J = 13.2 Hz, N-CH_2), 4.07 (d, 1H, J = 13.5 Hz, N-CH_2), 3.83 (d, 1H, J = 13.5 Hz, N-CH_2), 2.14 (s, 6H, Ar-CH_3), 1.99 (s, 12H, Ar-CH_3), 1.12 (s, 9H, *t*-Bu), 1.10 (s, 9H, *t*-Bu), 0.81 (s, 9H, *t*-Bu).

6.21 Reaction of 1a-H with CO: Synthesis of the Enolate Imido Complex Nb(OC(H)=C(H)*t*-Bu)(NAr)(N[Np]Ar)$_2$ (7a)

An excess of gaseous CO was introduced to an Et_2O solution of **1a**-H (0.100 g, 0.150 mmol, 3 mL), eliciting a rapid color change from orange to pale brown. The reaction mixture was allowed to stir for 1 h at which point all volatile materials were removed *in vacuo*. The resulting pale-yellow residue was extracted with *n*-pentane and filtered through Celite. The solvent was removed again and the crude solid obtained was dissolved in approximately 0.5 mL of Et_2O. Yellow plates of **7a** were obtained from this solution upon standing at - 35 °C for several days. Yield: 0.046 g, 45%. ^{1}H NMR (400 MHz, C_6D_6, 23 °C): δ 7.29 (d, 1H, J = 6.6 Hz, enolate), 6.98 (s, 2H, p-Ar amido), 6.70 (s, 4H, o-Ar amido), 6.52 (s, 1H, p-Ar imido), 6.36 (s, 1h, o-Ar, imido), 4.45 (d, 1H, J = 6.6 Hz, enolate), 4.45 (d, 2H, J = 13 Hz, N-CH_2), 3.83 (d, 2H, J = 13 Hz, N-CH_2), 2.11 (s, 6H, Ar-CH_3 amido), 2.10 (s, 12H, Ar-CH_3 imido), 1.47 (s, 9H, *t*-Bu enolate), 0.89 (s, 18H, *t*-Bu amido). ^{13}C{^{1}H} NMR (75.0 MHz, C_6D_6, 23 °C): δ 150.2 (aryl ipso amido), 149.2 (aryl ipso imido), 139.6 (o-Ar amido), 138.5 (o-Ar imido), 126.6 (p-Ar imido), 126.0 (p-Ar amido), 123.3 (m-Ar imido), 120.8 (m-Ar amido), 117.6 (enolate), 111.8 (enolate), 72.5 (N-*C*H2), 35.6 (*C*(CH$_3$)$_3$ anilide), 32.2 (*C*(CH$_3$)$_3$ enolate), 31.8 (C(*C*H$_3$)$_3$ enolate), 28.7 (C(*C*H$_3$)$_3$ amido), 21.9 (Ar-*C*H$_3$ amido), 21.6 (Ar-*C*H$_3$ imido). FTIR (KBr windows, C_6D_6 solution): 2953, 2903, 1634, 1584, 1476, 1213, 1080, 686 cm $^{-1}$. Anal. Calcd. for $C_{40}H_{60}N_3ONb$: C, 69.44; H, 8.74; N, 6.07. Found: C, 68.34; H, 8.56; N, 5.93.

6.22 Synthesis of the Niobaziridine-Hydride Complex Nb(H)(η^2-Me$_2$C=NAr)(N[*i*-Pr]Ar)$_2$ (1b-H)

Complex **1b**-H was prepared analogously to complex **1a**-H by employing 2.5 g (2.99 mmol) of Nb(I)$_2$(N[*i*-Pr]Ar)$_3$ (**2b**-I$_2$). It was found that the total reaction time including work-up should be carried-out on the order of 2.0 h to avoid decomposition of **1b**-H to the forest green dimeric species **3b**. Dark orange single crystals of **1b**-H were obtained from a saturated Et_2O solution stored at –35 °C for 1 d in approximately 30% yield. Complex **1b**-H was found to completely decompose over the course of 1 h to forest green **3b** when heated at 65 °C and over the course of 4 h when left standing at room temperature (C_6D_6). Spectroscopic data for **3b** can be found in reference 62. Data for **1b**-H: ^{1}H NMR (300 MHz, C_6D_6, 23 °C): δ 9.23 (bs, 1H, Nb-*H*), 7.23 (s, 2H, o-Ar, aziridine), 7.15 (s, 1H, p-Ar, aziridine), 6.70 (s, 4H, o-Ar amido), 6.59 (s. 2H, p-Ar amido) 3.68 (septet, 2H, J = 4 Hz, C*H*(CH$_3$)$_2$), 2.37 (s, 6H, Ar-C*H*$_3$ aziridine), 2.07 (s, 12H, Ar-C*H*$_3$ amido), 2.02 (s, 6H, N=C(C*H*$_3$)$_2$ aziridine), 1.00 (d, 6H, J = 4 Hz, CH(C*H*$_3$)$_2$ amido), 0.96 (d, 6H, J = 4 Hz, CH(C*H*$_3$)$_2$ amido).

6.23 Synthesis of the *N*-Methyleneadamantyl Aniline HN(CH$_2$-1-Ad)Ar

Two Steps.

Step 1: Synthesis of *N*-3,5-dimethylphenyl(methyleneadamantyl) amide (1-AdC(O)NH(3,5-Me$_2$C$_6$H$_3$): 1-Adamantylcarbonyl chloride (1-AdC(O)Cl, 25.0 g, 0.124 mol, 1.2 equiv) and triethylamine (NEt$_3$, 12.598 g, 0.124 mol, 1.2 equiv) where added to 300 mL of anhydrous THF and a positive-pressure blanket of N_2 was applied to the reaction vessel. The cloudy white mixture was then stirred with a mechanical stirrer and cooled to 0 °C with an ice bath. Freshly distilled 3,5-dimethylaniline (12.578 g, 0.104 mol) was added dropwise with a pressure-equilibrating addition funnel over the course of 1 h. A copious amount of white solid was formed from the reaction mixture after ca. 10 min. The reaction was allowed stir for a total of 3

h, at which point 200 mL of Et_2O were added, followed by 300 mL of H_2O. The aqueous and organic phases were separated and the aqueous phased was washed with 2 x 100 mL of fresh Et_2O. The Et_2O washings were combined and evaporated leaving behind 1-AdC(O)NH(3,5-$Me_2C_6H_3$) as a white solid. The product was slurried in 300 mL of *n*-hexane and stored at -30 °C overnight. The resultant white precipitate was filtered and washed with 50 mL of *n*-hexane. Yield 28.7 g, 97.6%. ^{1}H NMR (300 MHz, C_6D_6, 23 °C): δ 7.39 (s, 2H, o-Ar), 6.85 (s, 1H, N-*H*) 6.62 (s, 1H, p-Ar), 2.17 (s, 6H, Ar-CH_3), 1.83 (s, 9H, 1-Ad), 1.56 (m, 5H, 1-Ad).

Step 2: *N*-3,5-dimethylphenyl(methyleneadamantyl) amide (25.0 g, 0.088 mol) and $LiAlD_4$ (6.694 g, 0.176 mol, 2 equiv) were refluxed for 24 h under N_2 in 200 mL of anhydrous THF. The reaction mixture was slowly quenched at 0 °C with 200 mL of 0.171 M HCl while under an N_2 stream. Aqueous ammonium hydroxide was then added until a pH of 10 was reached. The organic compounds were then extracted and separated from the aqueous phase with 3 x 100 mL of Et_2O. The Et_2O washings were then evaporated to dryness resulting in a white residue which was slurried in *n*-hexane (100 mL) and stored at -35 °C overnight. The resultant white precipitate was filtered and determined to be unreacted 1-AdC(O)NH(3,5-$Me_2C_6H_3$) by ^{1}H NMR. The *n*-hexane filtrate was concentrated to a volume of 50 mL and placed back at -35 °C for 2 d whereupon pure HN(CH_2-1-Ad)Ar crystallized as a colorless solid and was collected by filtration. An additional crop of HN(CH_2-1-Ad)Ar was obtained upon further concentration and cold storage of the *n*-hexane filtrate. Yield: 14.2 g, 59.7%. ^{1}H NMR (300 MHz, C_6D_6, 23 °C): δ 6.44 (s, 1H, p-Ar), 6.27 (s, 2H, o-Ar), 3.26 (s, 1H, N-*H*), 2.70 (s, 2H, N-CH_2), 2.24 (s, 6H, Ar-CH_3), 1.88 (s, 5H, 1-Ad), 1.66-1.55 (m, 5H, 1-Ad), 1.45 (s, 5H, 1-Ad).

6.24 Synthesis of (Et_2O)Li(N[CH_2-1-Ad]Ar)

The lithium salt (Et_2O)Li(N[CH_2-1-Ad]Ar) was prepared analogously to (Et_2O)Li(N[Np]Ar) (section 6.3) employing 10.0 g of HN(CH_2-1-Ad)Ar. Yield: 10.50 g, 80%. ^{1}H NMR (300 MHz, C_6D_6, 23 °C): δ 6.43 (s, 1H, o-Ar), 6.12 (s, 2H, p-Ar), 3.32 (s, 2H, N-CH_2), 3.13 (q, 4H, J = 4.0 Hz, OCH_2CH$_3$), 2.38 (s, 6H, Ar-CH_3), 2.01 (s, 5H, 1-Ad), 1.81-1.73 (m, 10H, 1-Ad), 0.86 (t, 3H, J = 4 Hz, OCH$_2$CH_3).

6.25 Synthesis of the Niobium Complexes Nb(PhCCPh)(N[CH_2-1-Ad]Ar)$_3$ (2c-PhCCPh) and Nb(I)$_2$(N[CH_2-1-Ad]Ar)$_3$ (2c-I_2)

Both **2c**-PhCCPh and **2c**-I_2 were prepared analogously to the N[Np]Ar variants (*e.g.* **2a**-PhCCPh and **2a**-I_2, respectively). Slight modifications to the procedures and characterization data are provided.

For **2c**-PhCCPh: The mixture obtained from the addition of *cis,mer*-$NbCl_3(THF)_2$(PhCCPh) and (Et_2O)Li(N[CH_2-1-Ad]Ar) in Et_2O was filtered directly to remove the LiCl byproduct. The Et_2O was subsequently removed *in vacuo* and the resulting dark yellow solid was slurried in *n*-pentane. Upon filtration of the slurry, yellow **2c**-PhCCPh was obtained in essentially pure form. Yield: ca. 90% based on 10.0 g of (Et_2O)Li(N[CH_2-1-Ad]Ar). ^{1}H NMR (300 MHz, C_6D_6, 23 °C): δ 7.75 (d, 4H, J = 4 Hz, o-Ph), 7.31 (t, 4H, J = 5 Hz, m-Ph), 7.07 (t, 2H, J = 5 Hz, p-Ph), 6.89 (s, 6H, o-Ar), 6.59 (s, 3H, p-Ar), 3.77 (s, 6H, N-CH_2), 2.25 (s, 18H, Ar-CH_3), 1.80 (s, 10H, 1-Ad), 1.57-1.49 (m, 20H, 1-Ad), 1.38 (s, 15H, 1-Ad).

For **2c**-I_2: Obtained pure as a bright orange powder by precipitation from cold *n*-pentane. Yield 85.2 % (9.119 g) relative to *cis,mer*-$NbCl_3(THF)_2$(PhCCPh) when **2a**-PhCCPh is not isolated. ^{1}H NMR (300 MHz, C_6D_6, 23 °C): δ 8.08 (s, 6H, o-Ar), 6.60 (s, 3H, p-Ar), 3.60 (s, 6H, N-CH_2), 2.19 (s, 18H, Ar-CH_3), 1.78 (s, 10H, 1-Ad), 1.52-1.47 (m, 15H, 1-Ad), 1.17 (s, 20H, 1-Ad).

6.26 Synthesis of the Niobaziridine-Hydride Complex Nb(H)(η^2-Ad(H)C=NAr)(N[CH_2-1-Ad]Ar)$_2$ (1c-H)

Complex **1c**-H was prepared analogously to complex **1a**-H employing 1.00 g (0.868 mmol) of **2c**-I_2 and 0.454 g (1.085 mmol, 1.25 equiv) of $Mg(THF)_3$(anthracene). No special handling or attention to reaction time is required. Crude **1c**-H was extracted from MgI_2 and anthracene with Et_2O due to its low solubility in *n*-pentane. The cold-filtration step was performed using Et_2O, however some anthracene remained in the sample as assayed by ^{1}H NMR. To remove the residual anthracene, crude **1c**-H was dissolved in ca. 6 mL of Et_2O and left to stand overnight at –35 °C, whereupon the residual anthracene crystallized out. Concentration of the mother liquor to approximately 4 mL, followed by storage at –35 °C, afforded pure 1c-H as a bright orange microcrystalline solid. Orange single crystals of **1c**-H were obtained from a dilute Et_2O solution left to stand at –35 °C for several weeks. Yield 0.428 g, 55%. ^{1}H NMR (300 MHz, C_6D_6, 23 °C): δ 9.34 (bs, 1H, Nb-*H*), 7.11 (s, 2H, o-Ar), 7.03 (s, 2H, o-Ar), 6.62 (s, 1H, p-Ar), 6.57 (s, 1H, p-Ar), 6.54 (s, 1H, p-Ar), 6.14 (s, 2H, o-Ar), 4.30 (s, 2H, N-CH_2), 2.70 (d, 1H, J = 13 Hz, N-CH_2), 2.62 (d, 1H, J = 13 Hz, N-CH_2), 2.33 (s, 6H, Ar-CH_3), 2.30 (s, 1H, N=C(*H*)Ad), 2.15 (s, 6H, Ar-CH_3), 2.14 (s, 6H, Ar-CH_3), 1.90-1.66 (m, 1-Ad), 1.47 – 1.32 (m, 1-Ad), 1.04 – 0.96 (m, 1-Ad). ^{13}C{^{1}H} NMR (75.0 MHz, C_6D_6, 23 °C): δ 156.3 (aryl ipso), 145.5 (aryl ipso), 141.3 (p-Ar), 140.4 (p-Ar), 138.6 (p-Ar), 128.8 (aryl ipso), 127.4 (m-Ar), 125.79 (m-Ar), 122.8 (m-Ar), 117.4 (o-Ar), 116.8 (o-Ar), 115.5 (o-Ar), 82.7 (N=*C*(H)Ad), 68.7 (N-*C*H_2), 66.3 (N-*C*H_2), 57.8 (Ad), 44.8 (Ad), 42.3 (Ad), 41.6 (Ad), 38.3 (Ad), 38.2 (Ad), 37.6 (Ad), 37.4 (Ad), 37.3 (Ad), 36.3 (Ad), 34.7 (Ad), 30.0 (Ad), 29.4 (Ad), 29.3 (Ad), 23.1 (Ar-*C*H_3), 22.3 (Ar-*C*H_3), 22.0 (Ar-*C*H_3), 21.9 (Ad), 15.9 (Ad), 14.6 (Ad).

6.27 Thermolysis of Complex 1c-H: Formation of the Aryl Imido complex Nb(NCH_2-1-Ad)(Ar)(N[CH_2-1-Ad]Ar)$_2$ (3c)

A C_6H_6 solution of complex **1c**-H (0.100 g, 0.111 mmol, 2 mL) was heated at 80°C for 40 min resulting in a color change from orange to light brown. The solvent was removed under reduced pressure and the resulting light brown residue was extracted with *n*-pentane and filtered through Celite. The solvent was removed again *in vacuo* and complex **3c** was obtained as lipophilic brown residue. Several attempts to crystallize complex **3c** from hydrocarbon and ethereal solvents were unsuccessful. ^{1}H NMR (300 MHz, C_6D_6, 23 °C): δ 8.16 (s, 2H, o-Ar-Nb), 7.86 (s, 1H, p-Ar-Nb), 6.92 (s, 4H, o-Ar), 6.51 (s, 2H, p-Ar), 4.08 (d, 2H, J = 13.5 Hz, N-CH_2), 3.80 (s, 2H, Nb=N-CH_2-Ad), 3.73 (d, 2H, J = 13.5 Hz, N-CH_2), 2.37 (s, 6H, Nb-Ar-CH_3), 2.12 (s, 12H, Ar-CH_3), 1.94-1.90 (m, 10H, 1-Ad), 1.7-1.60 (m, 35H, 1-Ad).

6.28 Computational Details

All DFT calculations were carried out utilizing the Amsterdam Density Functional (ADF) program suite,[100,101] version 2004.01.[102] The all-electron, Slater-type orbital (STO) basis sets employed were of triple-ζ quality augmented with two polarization functions and incorporated relativistic effects using the zero-order regular approximation[103,104] (ADF basis ZORA/TZ2P). The local exchange-correlation potential of Vosko et al.[105] (VWN) was augmented self-

consistently with gradient-corrected functionals for electron exchange according to Becke,[106] and electron correlation according to Perdew.[107,108] This nonlocal density functional is termed BP86 in the literature and has been shown to give excellent results both for the geometries and for the energetics of transition metal and main group systems.[109] Crystallographically determined atomic coordinates were used as input for the truncated model **1m**-H.

6.29 Crystallographic Structure Determinations

The X-ray crystallographic data collections were carried out on a Siemens Platform three-circle diffractometer mounted with a CCD or APEX-CCD detector and outfitted with a low-temperature, nitrogen-stream aperture. The structures were solved using either direct methods or the Patterson method in conjunction with standard difference Fourier techniques and refined by full-matrix least-squares procedures. A summary of crystallographic data for all complexes is given in Tables 1 – 3. The systematic absences in the diffraction data are uniquely consistent with the assigned monoclinic space groups for complexes **2a**-S, **2a**-Se, **2a**-Te, **1a**-NC(H)*t*-Bu, **6a**-*t*-Bu, **7a** and [**1b**-H]$_2$. For complex **2a**-O, the centric monoclinic setting C_2/c was chosen. No symmetry higher than triclinic was indicated in the diffraction data for complexes **1a**-H, **2a**-NCMes and **1c**-H. These choices led to chemically sensible and computationally stable refinements. An empirical absorption correction (SADABS or ψ-scans) was applied to the diffraction data for all structures. All non-hydrogen atoms were refined anisotropically. In most cases, hydrogen atoms were treated as idealized contributions and refined isotropically. The hydrido ligands of complexes **1a**-H, [**1b**-H]$_2$ and **1c**-H were located in the electron density difference map and refined isotropically. In addition, the unique hydrogen atoms of complexes **1a**-NC(H)*t*-Bu, **6a**-*t*-Bu and **7a** were located from the difference map and refined isotropically. For complex **1c**-H, two full molecules were found within the asymmetric unit and were both severely disordered. A full-molecule disorder model, where four, symmetry-inequivalent orientations of **1c**-H are present within the asymmetric unit, was successfully refined by Dr. Peter Müeller. All software used for diffraction data processing and crystal-structure solution and refinement are contained in the SAINT+ (v6.45) and SHELXTL (v6.14) program suites, respectively (G. Sheldrick, Bruker AXS, Madison, WI).

Table 1. Crystallographic Data for Complexes **1a**-H, **2a**-O, **2a**-S, **2a**-Se and **2a**-Te.

	1a-H	**2a**-O	**2a**-S	**2a**-Se	**2a**-Te
Formula	$C_{39}H_{60}N_3Nb$	$C_{39}H_{60}N_3NbO$	$C_{39}H_{60}N_3NbS$	$C_{39}H_{60}N_3NbSe$	$C_{39}H_{60}N_3NbTe$
Crystal System	Triclinic	Monoclinic	Monoclinic	Monoclinic	Monoclinic
Space Group	*P*-1	C_2/c	$P2_1/c$	$P2_1/c$	$P2_1/c$
a, Å	11.0193(7)	19.7802(18)	11.0383(9)	11.1454(8)	11.4215(5)
b, Å	11.2042(7)	12.6057(11)	10.6757(9)	10.6072(8)	10.5624(5)
c, Å	17.2591(4)	31.987(3)	33.434(3)	33.260(3)	33.1624(16)
α, deg	79.092(1)	90	90	90	90
β, deg	84.314(1)	99.542(2)	90.000(2)	90.000(1)	90.0440(10)
γ, deg	66.605(1)	90	90	90	90
V, Å^3	1919.7(2)	4865.4(12)	3939.9(6)	3932.0(5)	4000.7(3)
Z	2	8	4	4	4
radiation		Mo-K_α (λ = 0.71073 Å)			
D(calcd), g/cm^3	1.148	1.148	1.173	1.255	1.314
μ (Mo Kα), mm^{-1}	0.341	0.336	0.386	1.260	1.043
temp, K	183(2)	183(2)	183(2)	183(2)	183(2)
No. Reflections	7646	15470	15225	15365	15761
No. Ind. Ref.(R_{int})	5394(0.0617)	5587(0.0563)	5617(0.0582)	5626(0.0421)	5737(0.0431)
F(000)	712	2912	1488	1560	1632
GoF (F^2)	1.042	1.070	1.990	1.387	1.117
R(*F*), %[a]	0.0403	0.0450	0.0624	0.0651	0.0464
wR(*F*), %[a]	0.1076	0.1396	0.2329	0.1322	0.0907

[a] Quantity minimized = $wR(F^2) = \sum[w(F_o^2 - F_c^2)^2]/\sum[(wF_o^2)^2]^{1/2}$; $R = \sum\Delta/\sum(F_o)$, $\Delta = |(F_o - F_c)|$, $w = 1/[\sigma 2(F_o^2) + (aP)^2 + bP]$, $P = [2F_c^2 + \mathrm{Max}(F_o,0)]/3$

Table 2. Crystallographic Data for Complexes **2a**(μ-P)**5b**, **2a**-NCMes, **1a**-NC(H)*t*-Bu, **6a**-*t*-Bu and **7a**.

	2a(μ-P)**5b**·$(O(SiMe_3)_2)_{0.5}$	**2a**-NCMes	**1a**-NC(H)*t*-Bu	**6a**-*t*-Bu	**7a**·$(Et_2O)_{0.5}$
Formula	$C_{75}H_{117}MoN_6NbO_{0.50}PSi$	$C_{49}H_{71}N_4Nb$	$C_{44}H_{69}N_4Nb$	$C_{44}H_{69}N_4Nb$	$C_{42}H_{65}N_3O_{1.5}Nb$
Crystal System	Triclinic	Triclinic	Monoclinic	Monoclinic	Monoclinic
Space Group	*P*-1	*P*-1	$P2_1/n$	$P2_1/c$	C_2/c
a, Å	12.011(5)	10.7225(6)	19.9926(16)	10.6846(9)	38.352(2)
b, Å	12.111(8)	11.9653(7)	10.8813(9)	22.2912(19)	11.8010(7)
c, Å	29.970(12)	19.3710(11)	22.5023(18)	18.3029(16)	20.3400(13)
α, deg	84.99(3)	86.526(1)	90	90	90
β, deg	88.69(4)	77.2120(1)	116.247(1)	91.2730(10)	115.2360(10)
γ, deg	61.04(5)	72.101(1)	90	90	90
V, Å^3	3799(3)	2306.2(6)	4390.5(6)	4358.2(6)	8327.1(9)
Z	2	2	4	4	8
radiation		Mo-K_α (λ = 0.71073 Å)			
D(calcd), g/cm^3	1.188	1.165	1.130	1.138	1.163
μ (Mo Kα), mm^{-1}	0.396	0.296	0.306	0.308	0.323
temp, K	183(2)	183(2)	183(2)	183(2)	183(2)
No. Reflections	33539	9197	17271	17478	16428
No. Ind. Ref.(R_{int})	17174(0.0219)	6445(0.0633)	6298(0.0576)	6257(0.0444)	5981(0.0841)
F(000)	1450	868	1608	1608	3128
GoF (F^2)	1.063	1.203	1.182	1.054	1.035
R(*F*), %[a]	0.0392	0.0416	0.0526	0.0391	0.0484
wR(*F*), %[a]	0.0951	0.1346	0.1287	0.0966	0.1288

[a] Quantity minimized = $wR(F^2) = \sum[w(F_o^2 - F_c^2)^2]/\sum[(wF_o^2)^2]^{1/2}$; $R = \sum\Delta/\sum(F_o)$, $\Delta = |(F_o - F_c)|$, $w = 1/[\sigma 2(F_o^2) + (aP)^2 + bP]$, $P = [2F_c^2 + \mathrm{Max}(F_o,0)]/3$

Table 3. Crystallographic Data for Complexes [**1b**-H]$_2$ and **1c**-H.

	[**1b**-H]$_2$·Et$_2$O	**1c**-H
Formula	$C_{37}H_{58}N_3NbO$	$C_{57}H_{78}N_3Nb$
Crystal System	Monoclinic	Triclinic
Space Group	$P2_1/n$	P-1
a, Å	10.9912(12)	14.1236(7)
b, Å	13.9121(15)	19.7568(12)
c, Å	24.020(3)	21.3128(13)
α, deg	90	94.884(2)
β, deg	93.925(2)	104.217(2)
γ, deg	90	108.817(2)
V, Å^3	3664.2(7)	5368.5(5)
Z	4	2
radiation	Mo-K$_\alpha$ (λ = 0.71073 Å)	
D(calcd), g/cm^3	1.185	1.203
μ (Mo Kα), mm^{-1}	0.358	0.270
temp, K	183(2)	100(2)
No. Reflections	6647	20377
No. Ind. Ref.(R$_{int}$)	4626(0.0535)	12666(0.1107)
F(000)	1400	2096.0
GoF (F^2)	1.072	1.052
$R(F)$, %[a]	0.0486	0.0622
$wR(F)$, %[a]	0.1191	0.1794

[a] Quantity minimized = $wR(F^2) = \sum[w(F_o^2 - F_c^2)^2]/\sum[(wF_o^2)^2]^{1/2}$; $R = \sum\Delta/\sum(F_o)$, $\Delta = |(F_o - F_c)|$, $w = 1/[\sigma 2(F_o^2) + (aP)^2 + bP]$, $P = [2F_c^2 + \mathrm{Max}(F_o,0)]/3$

7 References

1. Cummins, C. C. *Prog. Inorg. Chem.* **1998**, *47*, 685.
2. LaPointe, R. E.; Wolczanski, P. T.; Mitchell, J. F. *J. Am. Chem. Soc.* **1986**, *108*, 6382.
3. Neithamer, D. R.; LaPointe, R. E.; Wheeler, D. S.; Richeson, D. S.; Van Duyne, G. D.; Wolczanski, P. T. *J. Am. Chem. Soc.* **1989**, *111*, 9056.
4. Laplaza, C. E.; Cummins, C. C. *Science* **1995**, *268*, 861.
5. Laplaza, C. E.; Johnson, M. J. A.; Peters, J. C.; Odom, A. L.; Kim, E.; Cummins, C. C.; George, G. N.; Pickering, I. J. *J. Am. Chem. Soc.* **1996**, *118*, 8623.
6. Laplaza, C. E.; Odom, A. L.; Davis, W. M.; Cummins, C. C.; Protasiewicz, J. D. *J. Am. Chem. Soc.* **1995**, *117*, 4999.
7. Cherry, J.-P. F.; Johnson, A. R.; Baraldo, L. M.; Tsai, Y.-C.; Cummins, C. C.; Kryatov, S. V.; Rybak-Akimova, E.V.; Capps, K. B.; Hoff, C. D.; Haar, C. M.; Nolan, S. P. *J. Am. Chem. Soc.* **2001,** *123*. 7271.
8. Steffey, B. D.; Chamberlain, L. R.; Chesnut, R. W.; Chebi, D. E.; Fanwick, P. E.; Rothwell, I. P. *Organometallics* **1989,** 8, 1419.
9. Lockwood, M. A.; Potyen, M. C.; Steffey, B. D.; Fanwick, P. E.; Rothwell, I. P. *Polyhedron*, **1995**, *14*, 3293.
10. Yu, J. S.; Fanwick, P. E.; Rothwell, I. P *J. Am. Chem. Soc.* **1990**, *112*, 8171.
11. Yu, J. S.; Felter, L.; Potyen, M. C.; Clark, J. R.; Visciglio, V. M.; Fanwick, P. E.; Rothwell, I. P. *Organometallics* **1996**, *15*, 4443
12. Rothwell, I. P. *Chem. Commun.* **1997**, 1331.
13. Ruiz, J.; Vivanco, M.; Floriani, C.; Chiesi,-Villa, A.; Guastini, C.; *Chem. Commun.* **1991**, 762.
14. Vivanco, M.; Ruiz, J.; Floriani, C.; Chiesi,-Villa, A.; Rizzoli, C. *Organometallics*, **1993**, *12*, 1802.
15. Kleckley, T. S.; Bennett, J. L.; Wolczanski, P. T.; Lobkovsky, E. B. *J.Am. Chem. Soc.* **1997**, *119*, 247.
16. Veige, A. S.; Kleckley, T. S.; Chamberlin, R. M.; Neithamer, D. R.;Lee, C. E.; Wolczanski, P. T.; Lobkovsky, E. B.; Glassey, W. V. *J. Organomet. Chem.* **1999**, *591*, 194.
17. Bonanno, J. B.; Veige, A. S.; Wolczanski, P. T.; Lobkovsky, E. *Inorg. Chem. Acta.* 2002, 345, 173.
18. Covert, K. J.; Neithamer, D. R.; Zonnevylle, M. C.; LaPointe, R. E.; Schaller, C. P.; Wolczanski, P. T. *Inorg. Chem.* **1991**, *30*. 2494.
19. Covert, K. J.; Wolczanski, P. T.; Hill, S. A.; Krusic, P. J. *Inorg. Chem.* **1992**, *31*, 64.
20. Agapie, T.; Diaconescu, P. L.; Mindiola, D. J.; Cummins, C. C. *Organometallics* **2002**, *21*, 1329.
21. Tsai, Y.-C.; Stephens, F. H.; Meyer, K.; Mendiratta, A.; Gheorghiu, M. D.; Cummins, C. C. *Organometallics* **2003**, *22*, 2902.
22. Alyea, E. C.; Basi, J. S.; Bradley, D. C.; Chisholm, M. H. *Chem. Commun.* **1968**, 495.
23. Bradley, D. C; Newing, C. W. *Chem. Commun.* **1970**, 219.
24. Bradley, D. C; , Newing, C. W.; Hursthouse, M. B. *Chem. Commun.* **1971**, 411.
25. For $V(N(SiMe_3)_2)_3$: Bradley, D. C; Copperthwaite, R. G.; *Inorg. Synth.* **1978**, *18*, 112.
26. For $Mn(N(SiMe_3)_2)_3$ and $Co(N(SiMe_3)_2)_3$: Ellison, J. J.; Power, P. P.; Schoner, S. C. *J. Am. Chem. Soc.* **1989**, *111*, 8044.
27. For $Fe(N(SiMe_3)_2)_3$: Putzer, M. A.; Neumuller, B.; Dehnicke, K.; Magull, J. *Chem. Ber.* **1996**, *129*, 175.
28. Barker, G. K.; Lappert, M. F. *J. Organomet. Chem.* **1974**, *76*, C45.
29. Barker, G. K.; Lappert, M. F. Howard, J. A. K. *J. Chem. Soc. Dalton. Trans.* **1978**, 734.

30. Latesky, S. L.; Keddington, J.; McMullen, A. K.; Rothwell, I. P.; Huffman, J. C. *Inorg. Chem.* **1985**, *24*, 995.

31. Wanandi, P. W.; Davis, W. M.; Cummins, C. C.; Russell, M. A.; Wilcox, D. E. *J. Am. Chem. Soc.* **1995**, *117*, 2210.

32. Peters, J. C.; Johnson, A. R.; Odom, A. L.; Wanandi, P. W.; Davis, W. M.; Cummins, C. C. *J. Am. Chem. Soc.* **1996**, *118*, 10175.

33. Ruppa, K. B. P.; Desmangles, N.; Gambarotta, S.; Yap, G.; Rheingold, A. L. *Inorg. Chem.* **1997**, *36*, 1194.

34. Fickes, G. M.; Davis, W. M.; Cummins, C. C. *J. Am. Chem. Soc.* **1995**, *117*, 6384.

35. Bonanno, J. B.; Henry, Neithamer, D. R.; Wolczanski, P. T.; Lobkovsky, E. *J. Am. Chem. Soc.* **1996**, *118*, 5132.

36. Veige, A. S.; Slaughter, L. M.; Wolczanski, P. T.; Matsunaga, N.; Decker, S. A.; Cundari, T. R. *J. Am. Chem. Soc.* **2001**, *123*, 6419.

37. Veige, A. S.; Slaughter, L. M.; Lobkovsky, E.; Wolczanski, P. T.; Matsunaga, N.; Decker, S. A.; Cundari, T. R. *Inorg. Chem.* **2003**, 42, 6204.

38. Chishlom, M. H.; Cotton, F. A.; Murillo, C. A; Reichert, W. W.; Shive, L. W.; Stults, B. R. *J. Am. Chem. Soc.* **1976**, *98*, 4469.

39. Chishlom, M. H.; Cotton, F. A.; Murillo, C. A; Reichert, W. W. *Inorg. Chem.* **1977**, 16, 1801.

40. Kohn, R. D.; Kociok-Kohn, G.; Maufe, M. *Chem. Ber.* **1996**, *129*, 25.

41. Cui, Q.; Musaev, D. G.; Svensson, M.; Sieber, S.; Morokuma, K. *J. Am. Chem. Soc.* **1995**, *117*, 12366.

42. Fickes, G. M.; Davis, W. M.; Cummins, C. C. *J. Am. Chem. Soc.* **1995**, *117*, 6384.

43. Zanotti-Gerosa, A.; Solari, E.; Giannini, L.; Floriani, C.; Chiesi-Villa, A.; Rizzoli, C. *J. Am. Chem. Soc.* **1998**, *120*, 437.

44. Ferguson, R.; Solari, E.; Floriani, C.; Osella, D.; Ravera, M.; Re, N.; Chiesi-Villa, A.; Rizzoli, C. *J. Am. Chem.Soc.* **1997**, *119*, 10104-10115.

45. Kawaguchi, H.; Matsuo, T. *Angew. Chem. Int. Ed. Engl.* 2002, *41*, 2792.

46. Fryzuk, M. D.; Kozak, C. M.; Bowdridge, M. R.; Jin, W.; Tung, D.; Patrick, B. O.; Rettig, S. J. *Organometallics*, **2001,** *20,* 3752.

47. Kahn, O. *Molecular Magnetism*; VCH, New York, 1993.

48. Walker, D.; Poli, R. *Inorg. Chem.* **1989**, *28*, 1793.

49. Viege, A. S.; Wolczanski, P. T.; Lobkovsky, E. B. *Angew. Chem., Int. Ed.* **2001**, *40*, 3629.

50. Fickes, M. G.; Odom, A. L.; Cummins, C. C. *Chem. Commun.* **1997**, 1994.

51. Fickes, M. G. Ph.D Thesis, Massachusetts Institute of Technology, Cambridge, MA, 1998.

52. Tayebani, M.; Fegali, K.; Gambarotta, S.; Yap, G. *Organometallics*, **1998**, *17*, 4282.

53. Tayebani, M.; Fegali, K.; Gambarotta, S.; Bensimon, C. *Organometallics*, **1997**, *16*, 5084.

54. Berno, P.; Gamboratta, S. *Organometallics* **1995**, *14*, 2159.

55. Tayebani, M.; Gambarotta, S.; Yap, G. *Organometallics*, **1998**, *17*, 3639.

56. Ruppa, B. P.; Gambarotta, S.; Yap, G. *Inorg. Chim. Acta.* **1998**, *280*, 143.

57. Tsai, Y.-C.; Johnson, M. J. A.; Mindiola, D. J.; Cummins, C. C.; Klooster, W. T.; Koetzle, T. F. *J. Am. Chem. Soc.* **1999**, *121*, 10426.

58. Cherry, J.-P. F.; Stephens, F. H.; Johnson, M. J. A.; Diaconescu, P. L.; Cummins, C. C. *Inorg. Chem.* **2001**, *40*, 6860

59. Tsai, Y.-C.; Diaconescu, P. L.; Cummins, C. C. *Organometallics* **2000**, *19*, 5260.

60. Blackwell, J. M.; Figueroa, J. S.; Stephens, F. H.; Cummins, C. C. *Organometallics* **2003**, *22*, 3351.

61. Tsai, Y.-C.; Stephens, F. H.; Meyer, K.; Mendiratta, A.; Gheorghiu, M. D.; Cummins, C. C. *Organometallics* **2003**, *22*, 2902.

62. Mindiola, D. J. Ph.D Thesis, Massachusetts Institute of Technology, Cambridge, MA, 2000.

63. Mindiola, D. J.; Cummins, C. C. *Organometallics* **2001**, *20*, 3626.

64. Heats of formation (ΔH°_{f}, kcal/mol) for the following radicals scale as follows: *tert*-C_4H_9 (7.6 +/- 1.2) < *iso*-C_3H_7 (18.2 +/- 1.5) < neo-C_5H_{11} (30.0 +/- 1.0). *CRC Handbook of Chemistry and Physics, 67th ed.* CRC Press, Florida, 1987.

65. Hartung, J. B.; Pedersen, S. F.; *Organometallics* **1990**, *9*, 1414.

66. Freeman, P. K.: Hutchinson, L. L. *J. Org. Chem.* **1983**, *48*, 879.

67. Tunge, J. A.; Czerwinski, C. J.; Gately, D. A.; Norton, J. R.; *Organometallics* **2001**, *20*, 254.

68. Templeton, J. C.; Craig, P. C.; Pregosin, P. S.; Ruegger, H. *Magn. Reson. Chem.* **1993**, 31, 58.

69. Holmes, S. M.; Schafer, D. F.; Wolczanski, P.T.; Lobkovski, E. B. *J. Am. Chem. Soc.* **2001**, *123*, 10571 and references therein.

70. Besescker, C. J.; Klemperer, W. G.; Maltbie, D. J.; Write, D. A. *Inorganic Chemistry* **1985**, *24*, 1027.

71. Harris, R. K.; Mann, B. E., Eds. *NMR and the Periodic Table*; Academic Press: London, 1978.

72. Pauling, L. *The Nature of the Chemical Bond*, 3rd ed.; Cornell University Press, 1960, Ch. 11, p. 405.

73. Churchill, D. G.; Janak, K. E.; Wittenberg, J. S.; Parkin, G.; *J. Am. Chem. Soc.* **2003**, *125*, 1403.

74. Bullock, M. R.; Headford, C. E. L.; Kegley, S. E.; Norton, J. R.; *J. Am. Chem. Soc.* **1985**, *107*, 727.

75. Headford, C. E. L.; Hennessy, K. M.; Kegley, S. E.; Norton, J. R.; *J. Am. Chem. Soc.* **1989**, *111*, 3897.

76. Smith, M. R.; Matsunaga, P. T.; Andersen, R. A. *J. Am. Chem. Soc.* **1993**, *115*, 7049.

77. Koo, K. M.; Hillhouse, G. L.; Rheingold, A. L. *Organometallics* **1995**, *14*, 456.

78. Vaughan, G. A.; Hillhouse, G. L.; Rheingold, A. L. *J. Am. Chem. Soc.* **1990**, *112*, 7994.

79. Matsunaga, P. T.; Hillhouse, G. L.; Rheingold, A. L. *J. Am. Chem. Soc.* **1993**, *115*, 2075.

80. Howard, W.; Parkin, G. *J. Am. Chem. Soc.* **1994**, *116*, 606.

81. Holm, R. H. *Chem. Rev.* **1987**, *87*, 1401.

82. Hall, K. A.; Mayer, J. M. *J. Am. Chem. Soc.* **1992**, *114*, 10402-10411.

83. Brock, S. L.; Mayer, J. M. *Inorg. Chem.* **1991**, *30*, 2138.

84. Bryan, J. C.; Geib, S. J.; Rheingold, A. L.; Mayer, J. M. *J. Am. Chem. Soc.* **1987**, 109, 2826.

85. Parkin, G. *Prog. Inorg. Chem.* **1998**, *47*, 1.

86. Woo, L. K. *Chem. Rev.* **1993**, *93*, 1125.

87. Johnson, M. J. A.; Lee, P. M.; Odom, A. L.; Davis, W. M.; Cummins, C. C. *Angew. Chem. Int. Ed. Engl.* **1997**, *36*, 87.

88. Cherry, J.-P. F.; Stephens, F. H.; Johnson, M. J. A.; Diaconescu, P. L.; Cummins, C. C. *Inorg. Chem.* **2001**, *40*, 6820.

89. Etienne, M.; Cafagna, C.; Lorente, P.; Mathieu, R.; de Muontauzon, P. J. *Organometallics* **1999**, *18*, 3075 and references therein.

90. Alelyunas, Y. W.; Guo, Z.; LaPointe, R. E.; Jordan, R. F. *Organometallics* **1993**, *12*, 544.

91. Churchill, M. R.; Wasserman, H. J.; Belmonte, P. A.; Schrock, R. R. *Organometallics*, **1982**, *1*, 559.

92. Floriani has reported that Ph_2CN_2 readily undergoes α-N insertion into the Zr-H bond of Schwartz's reagent ($Cp_2Zr(H)Cl$), see: Gambarotta, S.; Floriani, C.; Chiesi-Villa, A.; Guastini, C. *Inorg. Chem.* **1983**, *22*, 2029.

93. Gray, S. D.; Weller, K. J.; Bruck, M. A.; Briggs, P. M.; Wigley, D. E. *J. Am. Chem. Soc.* **1995**, *117*, 10678.

94. Gountchev, T. I.; Tilley, T. D. *J. Am. Chem. Soc.* **1997**, *119*, 12831.

95. Jones, W.D.: Hessell, E. T. J. *Am. Chem. Soc.* **1992**; *114*, 6087.

96. Stephens, F. H.; Figueroa, J. S.; Cummins, C. C.; Kryatova, O. P.; Kryatov, S. V.; Rybak-Akimova, E. V.; McDonough, J. E.; Hoff, C. D. *Organometallics* **2004**, *23*, 3126-3138.

97. Labinger, J. A.; Bercaw, J. E. *Organometallics*, **1988**, 7, 926.

98. Smith, L. I.; Howard, K. L. *Organic Syntheses*; Wiley: New York, 1955; Collect. Vol. 111, pp 351-2.

99. Micovic, I. V.; Ivanovic, M. D.; Piatak, D. M.; Bojic, V. D.; *Synthesis* **1991**, 1043.

100. te Velde, G.; Bickelhaupt, F. M.; van Gisbergen, S. J. A.; Fonseca Guerra, C.; Baerends, E. J.; Snijders, J. G.; Ziegler, T. *J. Comput. Chem.* **2001**, *22*, 931.

101. Fonseca Guerra, C.; Snijders, J. G.; te Velde, G.; Baerends, E. J. *Theor. Chem. Acc.* **1998**, *99*, 391.

102. *ADF2004.01*; SCM, Theoretical Chemistry, Vrije Universiteit, Amsterdam, The Netherlands, http://www.scm.com.

103. van Lenthe, E.; Baerends, E. J.; Snijders, J. G. *J. Chem. Phys.* **1993**, *99*, 4597.

104. van Lenthe, E. The ZORA Equation. Thesis, Vrije Universiteit Amsterdam, Netherlands, 1996.

105. Vosko, S. H.; Wilk, L.; Nusair, M. *Can. J. Phys.* **1980**, *58*, 1200.

106. Becke, A. *Phys. Rev. A* **1988**, *38*, 3098.

107. Perdew, J. P. *Phys. Rev. B* **1986**, *34*, 7406.

108. Perdew, J. P. *Phys. Rev. B* **1986**, *33*, 8822.

109. See, for example: Deng, L.; Schmid, R.; Ziegler, T. *Organometallics* **2000**, *19*, 3069.

Chapter 2. Activation of Elemental Phosphorus: Synthesis of an Anionic Terminal Phosphide of Niobium

Joshua S. Figueroa

Department of Chemistry, Room 6-332
Massachusetts Institute of Technology
Cambridge, Massachusetts

May 9th 2005

CONTENTS

List of Figures

List of Schemes

List of Tables

1 Introduction

Stemming mainly from its role as an integral constituent of life, the synthetic and industrial utilization of phosphorus has received immense attention for over a century. In 1985, the industrial reduction of phosphate rock (apatite, $Ca_3(PO_4)_2$) to both phosphoric acid (H_3PO_4) and elemental, white phosphorus (P_4) exceeded an astounding 150 million tons world wide.[1] While the vast majority of H_3PO_4 produced annually is used for agricultural fertilizers, P_4 represents the major commercial P-atom source for organophosphorus compounds utilized by the food, detergent, specialty chemical and pharmaceutical industries.[2-4] Typically, incorporation of phosphorus into organic compounds is achieved by substitution reactions employing phosphorus trichloride (PCl_3),[3,4] which is a toxic, moisture-sensitive, volatile liquid.[5] Nevertheless, PCl_3 is produced industrially by the large-scale treatment of P_4 with Cl_2 gas in refluxing PCl_3.[2,3] Not surprisingly therefore, the harsh and energy-intensive conditions required for the commercial production of organophosphorus compounds has spurred long-standing interest in the mild and controlled activation of P_4.[6,7]

Low-valent transition metal complexes have received considerable attention as agents for P_4–activation.[8-16] However, the inherent reactivity of P_4, coupled with the proclivity of P-atoms to catenate, often leads to multiple products upon its reaction with low-valent metal centers.[6,8,13,17,18] Indeed, the mild activation of P_4 by transition metal complexes, in which several bonds of the P_4 tetrahedron are broken in a well-defined, selective and reproducible manner, is rare. Our group's interest in this area stems from the exclusive formation of the phosphido complex, P≡Mo(N(*t*-Bu)Ar)$_3$, upon reaction at room temperature between P_4 and the 3-coordinate, d^3 Mo(N(*t*-Bu)Ar)$_3$.[19] While this chemistry, along with a concurrent report by Schrock,[20] established the terminal phosphido (P^{3-}) functionality as a ligand, it also provided a distinctive paradigm for transition metal-based activation of P_4. Thus the juxtaposition of a highly reducing metal center and a constrained ancillary-ligand environment can provide for the facile cleavage of P_4 while inhibiting unwanted side reactions.

Herein is reported a remarkably efficient niobium-based system for the activation and functionalization of P_4. As shown in the preceding chapter, the niobaziridine-hydride complex, Nb(H)(*t*-Bu(H)C=NAr)(N[Np]Ar)$_2$ (**1a**-H) can act as a functional equivalent of the 3-coordinate, d^2 species Nb(N[Np]Ar)$_3$ (**2a**). As such, complex **1a**-H is shown to effect the selective reduction of the P_4 tetrahedron under mild conditions. This chemistry has resulted in the isolation of an unprecedented terminal phosphido anion of niobium which is the first example of P^{3-} ligation to a transition metal outside of group 6. Additionally, the phosphido anion so obtained readily allows for the functionalization of the P^{3-} moiety within the protective coordination sphere of niobium. This feature has allowed for the synthesis of several novel and diverse phosphorus-containing ligands. In this chapter, exploitation of this phosphido anion towards the synthesis of novel transition metal-supported main group compounds of unique composition and bonding is described. In the following chapter, the utility of the phosphido anion in the construction of synthetically valuable P_4-derived organophosphorus compounds is addressed.

2 Results and Discussion

2.1 Activation of Elemental Phosphorus (P_4) by Niobaziridine-Hydride 2a-H: Synthesis of the Bridging Diphosphide (μ_2:η^2,η^2-P_2)[Nb(N[Np]Ar)$_3$]$_2$ ((μ-P_2)[2a])

As shown in Chapter 1, the niobaziridine-hydride (**1a**-H) can serve as a synthon for the reactive 3-coordinate d^2 species Nb(N[Np]Ar)$_3$ upon treatment with certain substrates. Since substrate coordination is a likely prerequisite to the reduction chemistry exhibited by **1a**-H, its reaction with P_4 was explored due to the well-established ability of P_4 to act as a Lewis basic ligand.[6,21] Gratifyingly, combination of C_6D_6 solutions of **1a**-H and P_4 (0.25 equiv) at room temperature resulted in an immediate color change from orange to forest green. Analysis of the reaction mixture by ^{1}H NMR after 15 min indicated the quantitative consumption of **1a**-H concomitant with the appearance of a new species possessing three-fold symmetry. Accordingly, the $^{31}P\{^1H\}$ NMR spectrum of the same reaction mixture revealed a broad resonance centered at 399.0 ppm consistent with the formation a low-coordinate phosphorus species. Furthermore, unreacted P_4 (- 545 ppm, C_6D_6) was not detected by $^{31}P\{^1H\}$ NMR.

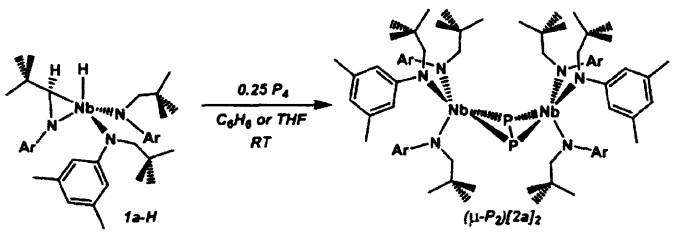

Scheme 1. Activation of P_4 by Complex **2a**-H: Synthesis of (μ_2:η^2,η^2-P_2)[Nb(N[Np]Ar)$_3$]$_2$ ((μ-P_2)[**2a**]$_2$).

Crystallographic structure determination of the product from the reaction of **1a**-H and P_4 established its identity as the diniobium, bridging diphosphide complex, (μ_2:η^2,η^2-P_2)[Nb(N[Np]Ar)$_3$]$_2$ ((μ-P_2)[**2a**]$_2$, Scheme 1). Complex (μ-P_2)[**2a**]$_2$ was obtained reproducibly in ca. 55 % yield as a forest green crystalline solid by low-temperature crystallization from Et_2O. Thus the reaction can be viewed as a $2e^-$ per Nb reduction of the P_4 tetrahedron and is reminiscent of the mild activation of P_4 reported for the d^3 Mo(III) trisamide system.[19,22] In addition, the reaction between **1a**-H and P_4 is selective inasmuch as (μ-P_2)[**2a**]$_2$ the only new product obtained when either an excess or deficiency of P_4 is used. Whether fleeting intermediates exist during the reaction is a matter open to speculation at this point.

The molecular structure of (μ-P_2)[**2a**]$_2$ (Figure 1) shows the P_2 unit to be disposed in a side-on and butterfly conformation relative to the Nb-Nb vector (Nb1-P1-P2-Nb2 dihedral angle = 135.61(5)°). Furthermore, the Nb1-Nb2 distance of 4.2052(8) Å obviates the existence of a M-M bond. It is notable that a P_2 unit unsupported by a M-M bond is a rarely documented functionality in early transition metal chemistry.[6,8] The only structurally characterized early metal example is Scherer's (μ_2:η^2,η^2-P_2)[Cp*Re(CO)$_2$]$_2$ obtained as a minor product from the reaction of P_4 with the corresponding Re=Re dimer.[23] Additionally, Stephan has provided inconclusive evidence for the formation of the related (μ_2:η^2,η^2-P_2)[Cp*$_2$Zr]$_2$ by a method independent of P_4.[24] Unsupported μ_2:η^2,η^2-P_2 complexes are

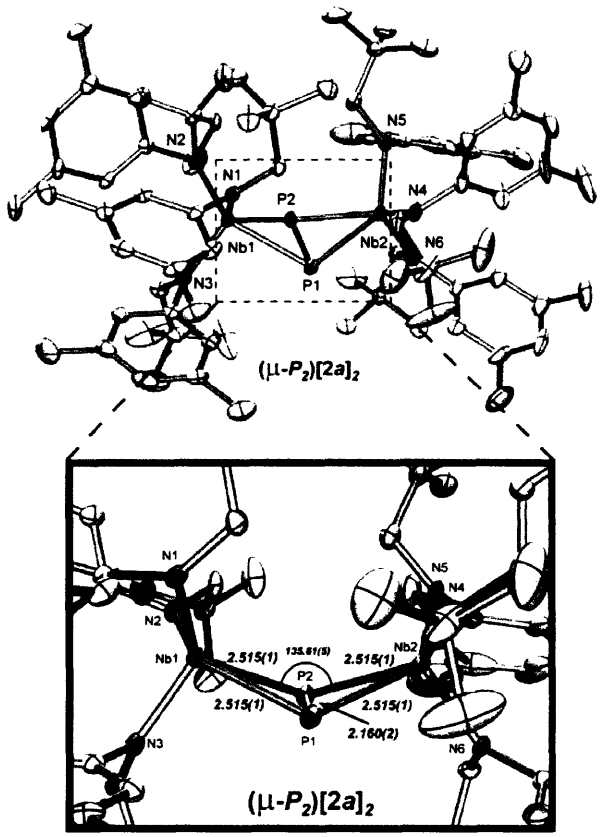

Figure 1. ORTEP Diagram of $(\mu\text{-}P_2)[\mathbf{2a}]_2$ at the 35% probability level.

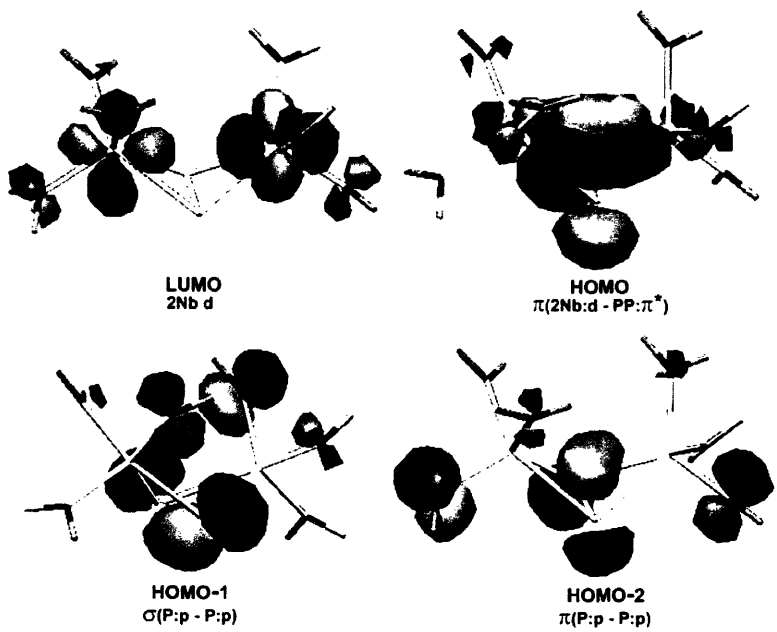

Figure 2. Calculated Frontier Molecular Orbitals for $(\mu_2{:}\eta^2,\eta^2\text{-}P_2)[Nb(NH_2)_3]_2$ ($(\mu\text{-}P_2)[\mathbf{2m}]_2$).

known for the 14-e$^-$ late metal fragments $[Ni(PR_3)_2]$ and $[Pt(PR_3)_2]$,[25] to which d^2 $Nb(N[Np]Ar)_3$ is isolobal.

Interestingly however, the P1-P2 distance in $(\mu\text{-}P_2)$[**2a**]$_2$ (2.150(2) Å) is ca. 0.11 Å shorter than that expected for a P-P single bond (d(P-P) in P_4 (g) = 2.21 Å),[2,26] thus indicating P-P multiple bond character in the P_2 unit itself. Density functional theory calculations on the model construct $(\mu_2\text{:}\eta^2,\eta^2\text{-}P_2)[Nb(NH_2)_3]_2$ ($(\mu\text{-}P_2)$[**2m**]$_2$) are consistent with this notion. Shown in Figure 2 are the frontier molecular orbitals calculated for model $(\mu\text{-}P_2)$[**2m**]$_2$. The HOMO-2 orbital is dominated by a π-type orbital formed from the in-phase combination of adjacent phosphorus p-orbitals in the P_2 unit. The out-of-phase combination of these same orbitals resembles a typical π* orbital and accordingly engages in a 2e$^-$ back-bond with both Nb centers (HOMO).

2.2 Reductive Cleavage of $(\mu\text{-}P_2)$[2a]$_2$: Synthesis of the Anionic Terminal Phosphide of Niobium, $[P{\equiv}Nb(N[Np]Ar)_3]^-$ ([2a-P]$^-$)

It was recognized that the P_2 unit in $(\mu\text{-}P_2)$[**2a**]$_2$ could be further reduced by two electrons to afford a species featuring a terminal, uninegative phosphorus atom bound to a single niobium center. Such a species would also be isoelectronic to the neutral terminal phosphido complexes obtained from the Mo(III) trisamide system.[19,22] Accordingly, treatment of a green THF solution of $(\mu\text{-}P_2)$[**2a**]$_2$ with an excess of 1.0% sodium amalgam gradually produced a dark orange mixture over 2.5 h. Analysis of the crude reaction mixture by $^{31}P\{^1H\}$ NMR spectroscopy indicated the presence of a new signal centered near δ = 1010 ppm, characteristic of early-transition-metal phosphido species containing one-coordinate phosphorus.[19,20,22,27] Solvent removal followed by diethyl ether extraction and crystallization produced the hydrocarbon-soluble, sodium etherate dimer $[Na(Et_2O)$[**2a**-P]$]_2$ (Scheme 2), as yellow-orange blocks in 65% yield. Crystallographic characterization of $[Na(Et_2O)$[**2a**-P]$]_2$ confirmed that the reductive scission of the P_2 unit in $(\mu\text{-}P_2)$[**2a**]$_2$ had indeed taken place (Figure 3). The square Na_2P_2 core of $[Na(Et_2O)$[**2a**-P]$]_2$ is a structural feature similarly possessed by the isoelectronic molybdenum carbido[28] and niobium nitrido[29] anions prepared previously in our group.

The $^{31}P\{^1H\}$ NMR spectrum of pure $[Na(Et_2O)$[**2a**-P]$]_2$ in C_6D_6 solution gives rise to a broad signal located at δ = 949.2 ppm ($\nu_{1/2}$ = 495 Hz), which shifts to 1019.8 ppm ($\nu_{1/2}$ = 166 Hz) when the spectrum is obtained in THF solution. Whereas the broad nature of the signals is caused by relaxation effects owing to the quadrupolar niobium nucleus,[30] the chemical shift difference presumably arises from formation of a monomeric $Na(THF)_x$[**2a**-P] species in THF solution (Scheme 2). Such downfield movement in ^{31}P chemical shift in polar solvents may be attributed to diminished Na–P contact ion pairing, with concomitant strengthening of $P_{(p\pi)}\rightarrow Nb_{(d\pi)}$ bonding interactions as the electropositive niobium center compensates for the buildup of negative charge.[31] The resulting stabilization of the $P_{(p\pi)}$ orbital affects its corresponding $P_{(p\pi^*)}$ component similarly, thus narrowing the energy gap between phosphorus-based occupied and virtual MO's.[32] Consequently, greater magnetic-field induced mixing of these MO's is achieved, providing for increasingly downfield ^{31}P chemical shifts.[33,34] Complete sequestration of the sodium counter ion from the phosphorus nucleus can

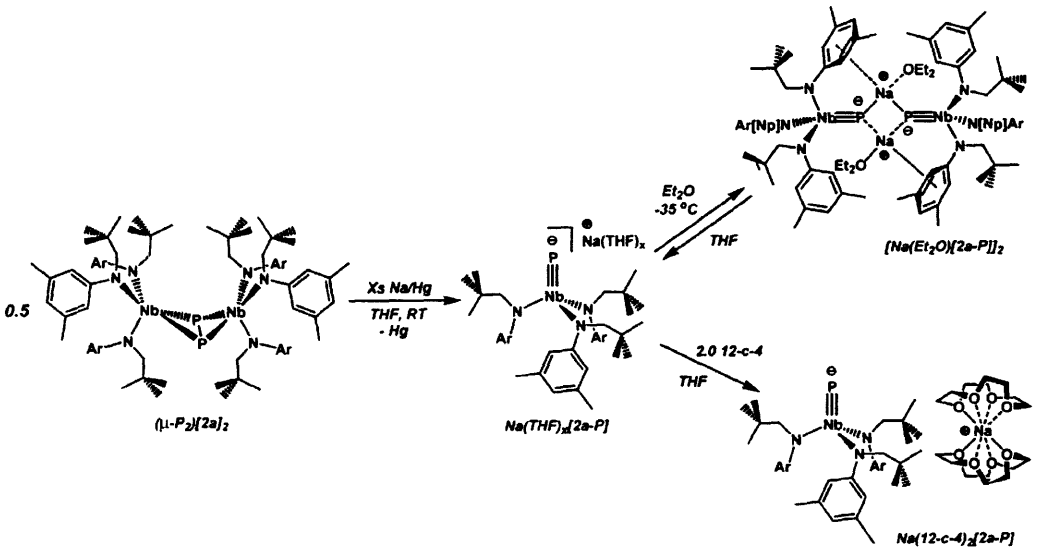

Scheme 2. Synthesis of the Terminal Phosphido Anion $[P{\equiv}Nb(N[Np]Ar)_3]^-$ ([**2a**-P]$^-$).

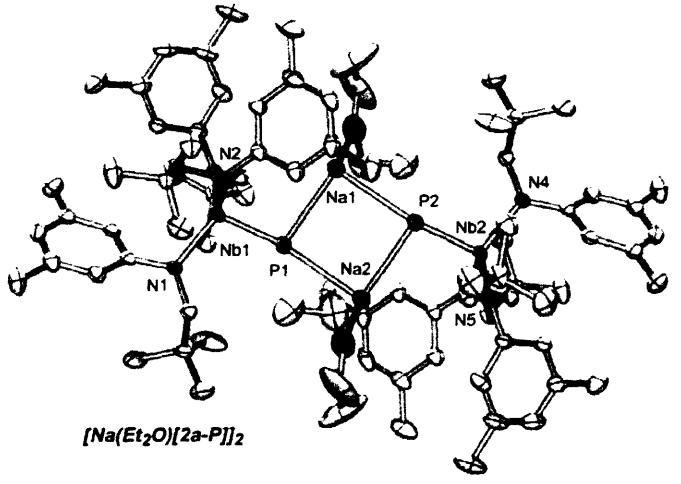

Figure 3. ORTEP Diagram of $[Na(Et_2O)[\mathbf{2a}\text{-P}]]_2$ at the 35% Probability Level. Selected Bond Distances [Å]: Nb1-P1 = 2.2029(11). P1-Na1 = 2.8857(18).

be achieved by treatment of a THF solution of $[Na(Et_2O)[\mathbf{2a}\text{-P}]]_2$ with 2.0 equivalents of the crown ether 12-crown-4 (12-c-4, Scheme 2). The resulting hydrocarbon insoluble salt, Na(12-c-4)$_2$[**2a**-P], gives rise to a single ^{31}P NMR signal at 1110.2 ppm ($\nu_{1/2}$ = 170 Hz, THF-d_8), further emphasizing the downfield progression of chemical shift as the $[P{\equiv}Nb(N[Np]Ar)_3]^-$ unit becomes discrete and separated from its counter ion.

Crystallization from a THF/*n*-pentane mixture produced red-orange plates of Na(12-c-4)$_2$[**2a**-P] in 80% yield. The single crystal X-ray structure of Na(12-c-4)$_2$[**2a**-P] (Figure 4) clearly shows the anion–cation separation imposed by 2.0 equivalents of 12-c-4 and confirms the terminal nature of the phosphido substituent. The Nb1-P1 bond length of 2.186(2) Å in

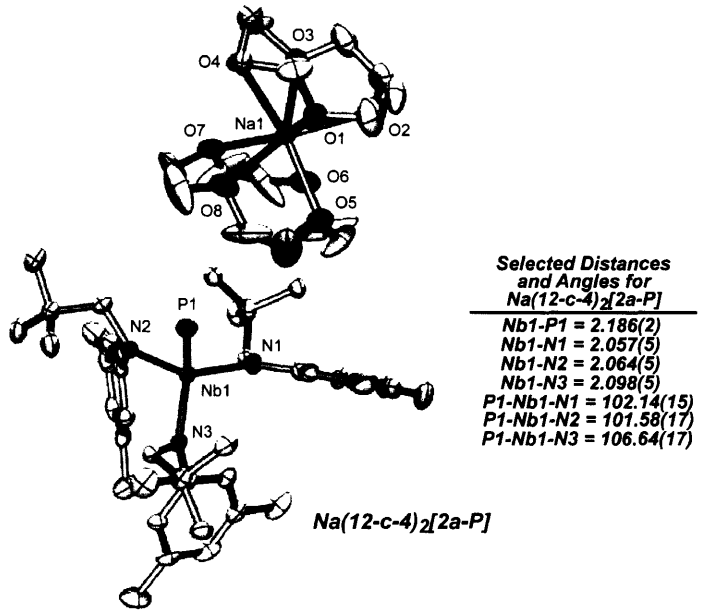

Figure 4. ORTEP Diagram of Na(12-c-4)$_2$[**2a**-P] at the 35% Probability Level.

Na(12-c-4)$_2$[**2a**-P] is short when compared to the related four coordinate, tantalum phosphinidene complex, [PhP=Ta(OSi-*t*-Bu$_3$)$_3$] (Ta=P 2.317(4) Å),which can be viewed as containing a short Ta=P double bond.[35] However, the Nb1-P1 bond length in Na(12-c-4)$_2$[**2a**-P] agrees well with the Mo≡P triple bonds in P≡Mo(N[*t*-Bu]Ar)$_3$[19] (2.119(4) Å) and P≡Mo(N[*i*-Pr]Ar)$_3$[22] (2.116(3) Å), when the 0.07 Å difference in covalent radius between Nb and Mo is considered.[22] Thus, Na(12-c-4)$_2$[**2a**-P] can be considered as containing a Nb≡P triple bond,[36] the notion of which has also been substantiated by DFT calculations on the model complex [P≡Nb(NH$_2$)$_3$]$^-$ ([**2m**-P]$^-$). As shown in Figure 5, the calculated frontier orbitals of [**2m**-P]$^-$ in C_{3v} symmetry portray the classic 2π + 1σ triple bond formalism. The degenerate HOMO of *E* symmetry is comprised of almost exclusively orthogonal $P_p \rightarrow Nb_d$ π interactions. Furthermore, the degenerate LUMO calculated for [**2m**-P]$^-$ corresponds to an antibonding P–Nb$_d$ orbital of π* character (not shown). It is also noteworthy that Na(12-c-4)$_2$[**2a**-P] is the first definitive example of a terminal phosphide complex of a transition metal outside of group 6.[36,37]

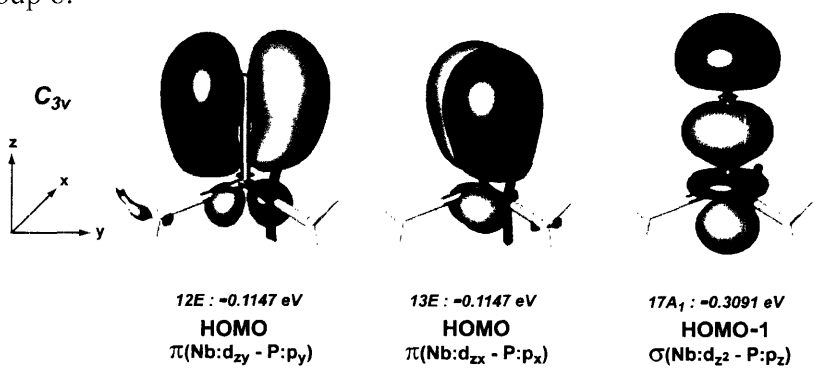

Figure 5. Calculated Frontier Molecular Orbitals for [P≡Nb(NH$_2$)$_3$]$^-$ ([**2m**-P]$^-$).

2.3 Electrophilic Addition to Phosphido Anion [2a-P]$^-$: A New Route to Terminal Phosphinidene Complexes of Niobium

The negative charge of [**2a**-P]$^-$ offers a powerful avenue for the construction of terminal phosphinidene ligands from a P_4-derived phosphorus atom. This is in contrast to the P_4-derived terminal phosphido complexes of group 6,[19,20,22,38-41] which are less-easily derivatized owing to the neutrality of the of the phosphido ligand. The rich chemistry exhibited by early transition metal terminal phosphinidenes has been delineated since Lappert's seminal report of the terminal phosphinidene complexes $Cp_2M{=}PR$ (M = Mo, W; R = 2,4,6-*t*-$Bu_3C_6H_2$, $CH(SiMe_3)_2$).[42,43] Yet in the overwhelming majority of these complexes reported to date, the phosphinidene unit is delivered to the metal with the P-R bond already *intact*.[44,45] The only exception is Schrock's report that the treatment of LiP(H)Ph-derived terminal phosphinidene complex $(N_3N)Ta{=}PPh$ (N_3N = $[N(CH_2CH_2NSiMe_3)_3]^{3-}$) with Li^0 metal induces P-C bond cleavage. The resulting compound, $(N_3N)Ta{=}PLi$, was obtained as a mixture with PhLi, but underwent P-E bond formation (E = C, Si) when treated with various electrophiles.[37]

The terminal phosphorus atom in [**2a**-P]$^-$ readily provides new examples of terminal phosphinidenes[44,46] upon salt metathesis reactions with electrophiles. For example, treatment of thawing THF solutions of $Na(THF)_x$[**2a**-P] with 0.95 equivalents of trimethylsilyl or trimethylstannyl chloride produced the trimethylsilyl $Me_3SiP{=}Nb(N[Np]Ar)_3$ (**2a**-$PSiMe_3$), and trimethylstannyl, $Me_3SnP{=}Nb(N[Np]Ar)_3$ (**2a**-$PSnMe_3$), phosphinidene complexes in 75% and 85% yield, respectively (Scheme 3). The $^{31}P\{^1H\}$ NMR spectral resonances for **2a**-$PSiMe_3$ (δ = 528.6 ppm) and **2a**-$PSnMe_3$ (δ = 607.0 ppm) indicate bent phosphinidene moieties typical for four-coordinate early-transition metal phosphinidene complexes supported by hard, π-donating, ancillary ligands.[44] A solid-state structural determination of **2a**-$PSnMe_3$ (Figure 6) confirmed this spectroscopic assignment and revealed an elongated Nb1-P1 bond (2.2731(8) Å) relative to that in $Na(12\text{-c-}4)_2$[**2a**-P], consistent with formulation of this product as a doubly bonded Nb=P terminal phosphinidene. Furthermore, the P1-Sn1 bond length of 2.4778(8) Å matches the sum of covalent radii for these atoms, attesting to a single bond between tin and phosphorus in **2a**-$PSnMe_3$.[26]

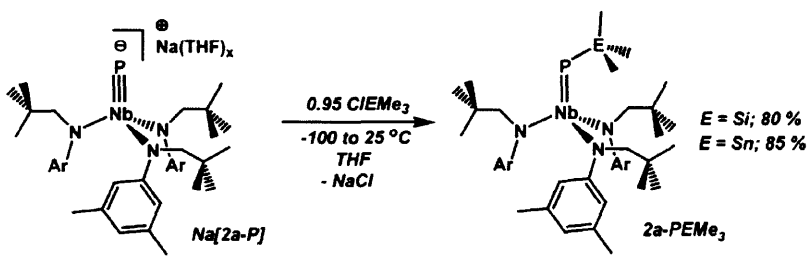

Scheme 3. Synthesis of the Terminal Phosphinidene Complexes **2a**-$PEMe_3$ from Anion [**2a**-P]$^-$.

It is noteworthy that the stannylphosphinidene ligand in **2a**-$PSnMe_3$ has no precedent. Presumably, this is a result of a lack of suitable reagents for the transfer of a "$PSnR_3$" group to a metal acceptor, which highlights the synthetic versatility of [**2a**-P]$^-$ for the construction of new phosphinidene ligands. Accordingly, addition of triphenylstannyl chloride to $Na(THF)_x$[**2a**-P] readily afforded the triphenylstannyl phosphinidene complex

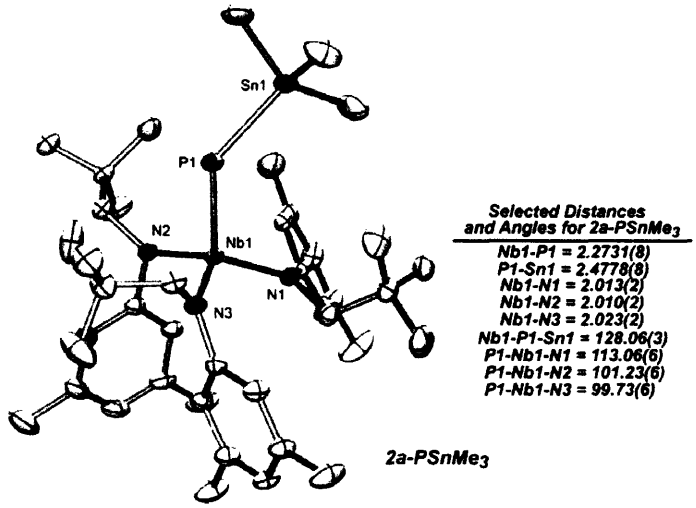

Figure 6. ORTEP Diagram of **2a**-$PSnMe_3$ at the 35% Probability Level.

$Ph_3SnP{=}Nb(N[Np]Ar)_3$ (**2a**-$PSnPh_3$) in excellent yield as determined by ^1H NMR spectroscopy. Terminal phosphinidene **2a**-$PSnPh_3$ is characterized by a downfield $^{31}P\{^1H\}$ NMR resonance of 579.1 ppm ($^1J_{SnP}$ = 646.1 Hz), which is in good agreement with **2a**-$PSnMe_3$ (P-$^{117/119}$Sn coupling is unresolved in **2a**-$PSnMe_3$).

Whereas the formation of terminal phosphinidenes from electrophiles containing one halide leaving group is fairly general, the Nb≡P$^-$ unit in [**2a**-P]$^-$ has been found to be extremely susceptible to over-halogenation processes. Thus treatment of [**2a**-P]$^-$ with an excess of 1.0 equiv of monohalide-containing electrophiles invariably leads to significant formation of the bishalide complex $Nb(X)_2(N[Np]Ar)_3$ (**2a**-X_2, X = halide). Low temperatures, while necessary for successful substitution of [**2a**-P]$^-$ with sub-stoichiometric quantities of electrophile, do not inhibit niobium halide formation. Furthermore, [**2a**-P]$^-$ is incompatible with high local concentrations of halide, thereby necessitating slow addition of electrophilic reagents. Attempts to doubly-substitute a dichloride-containing electrophile (*e.g.* Ph_2SnCl_2, Ph_2SiCl_2, $PhPCl_2$) with 2.0 equiv of [**2a**-P]$^-$ also leads to **2a**-Cl_2 as the predominant product (an exception is discussed in section 2.6). Whether the formation of **2a**-Cl_2 in these latter reactions is a result of β-Cl elimination from a species of the type [R_n(Cl)E-P=Nb(N[Np]Ar)$_3$], followed by a second chlorination at Nb, is presently unclear.

2.4 Phosphorus-Phosphorus Multiple Bond Formation: Synthesis of η^2–Phosphinophosphinidenes of Niobium

The previous section demonstrated the potential of forming new niobium phosphinidenes containing P-E single bonds. However, it was also of interest to examine the ability of the Nb≡P$^-$ unit in anion [**2a**-P]$^-$ to engage in multiple bonding with an incoming electrophile. In this regard, phosphinophosphinidenes (PPR_2)[47] were intriguing as synthetic targets. The parent phosphinophosphinidenes, PPH_2, is a neutral isomer of diphosphene (HP=PH) and has been the subject of several theoretical investigations[47-50] concerning the electronic structure of low-coordinate phosphorus species.[51] Accordingly, interest in phosphinophosphinidenes

arises from the continuum of resonance forms which can be evoked to describe the nature of the P-P interaction (Scheme 4).[48] Such descriptions include the singly-bound phosphinidene form (**A**), analogous to both carbene (CR_2) and nitrene (NR) species. However, resonance forms reminiscent of both alkenes (**B**) and alkynes (**C**) can also be considered and the P-P bond order is thought to be exquisitely sensitive to the nature of the R groups. Indeed, the difluoro-variant, PPF_2, has been studied computationally and was proposed to contain a P-P triple bond largely fortified by the presence of the electron-withdrawing fluoro substituents.[48]

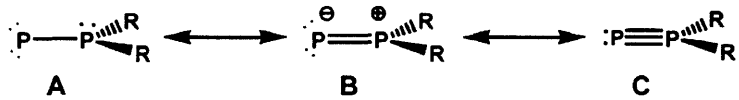

Scheme 4. Three Possible Resonance Forms for P–P Bonding in Phosphinophosphinidenes.

Not surprisingly therefore, diorgano-substituted phosphinophosphinidenes have generated interest as π-electron ligands capable of η^2-binding to transition-metal centers.[47,49,52] A prototypical example is the structurally characterized complex [(η^2-*t*-Bu_2PP)Pt(PPh_3)$_2$].[52,53] Fritz and co-workers have pioneered the synthesis of such complexes by utilization of the "phosphinophosphinidene transfer" reagent, *t*-Bu_2PP=PX(*t*Bu_2) (X=Me or Br), in conjunction with low-valent late metal centers (Scheme 5).[49,54-58] However, the use of a phosphinophosphinidene transfer reagent is the only reported synthetic entry to complexes of phosphinophosphinidenes and it is currently solely applicable to the di-*tert*-butyl variant (PP(*t*-Bu)$_2$). Thus it was hoped that the facile functionalization of anion [**2a**-P]$^-$ would allow for the synthesis of early metal examples of PPR_2, but also provide insight into the effects of diverse organic substituents on the coordinated PPR_2 moiety. Potentially, altering the organic substituents of a coordinated PPR_2 molecule could lead to changes in coordination mode or reactivity patterns.

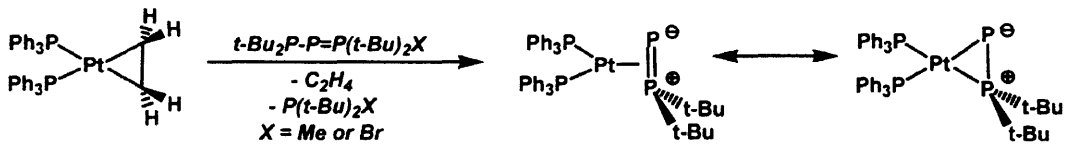

Scheme 5. Utilization of Fritz's Phosphinophosphinidene Transfer Reagent in the Synthesis of η^2–PP(*t*-Bu)$_2$ Platinum Complexes. Adapted from Reference 47.

Treatment of a thawing THF solution of Na(THF)$_x$[**2a**-P] with 0.95 equivalents of di-*tert*-butylchlorophosphine (*t*-Bu_2PCl) readily provided the orange phosphinophosphinidene complex, (η^2-*t*-Bu_2PP)Nb(N[Np]Ar)$_3$ (**2a**-P(t-Bu)$_2$) in 65% yield (Scheme 6). Formation of phosphinophosphinidene **2a**-PP(t-Bu)$_2$ from [**2a**-P]$^-$ and *t*-Bu_2PCl represents a synthetic method complementary to Fritz and co-workers' use of a transfer reagent in which the P-P bond is already *intact*.[52-58] However, the functionalization of [**2a**-P]$^-$ with R_2PCl electrophiles has indeed been found to be applicable to the synthesis of novel, Nb-complexed R_2PP derivatives. Thus, treatment of Na(THF)$_x$[**2a**-P] with diphenylchlorophosphine (Ph_2PCl) afforded the red diphenylphosphinophosphinidene complex, (η^2-Ph_2PP)Nb(N[Np]Ar)$_3$] (**2a**-$PPPh_2$) in 60% isolated yield (Scheme 6).

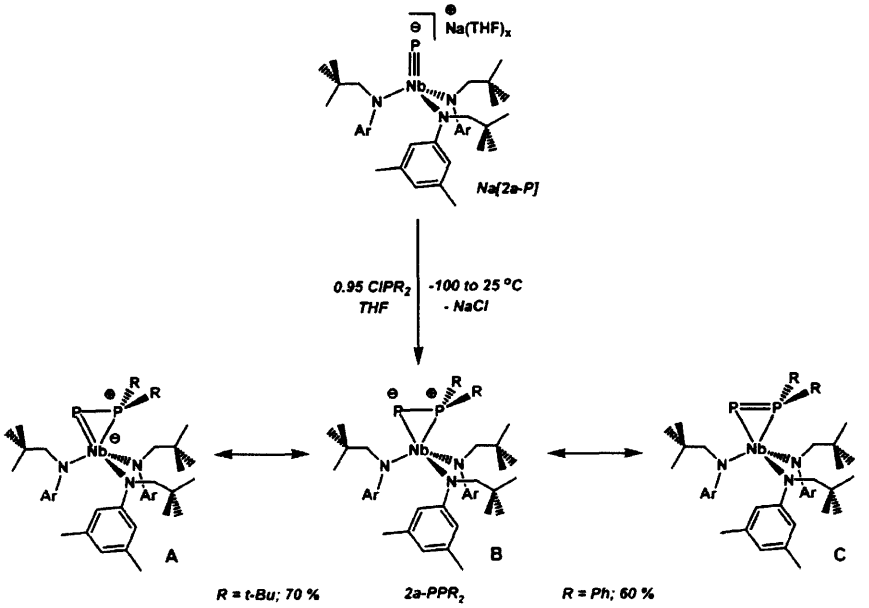

Scheme 6. Synthesis of Phosphinophosphinidene Complexes **2a**-PPR_2.

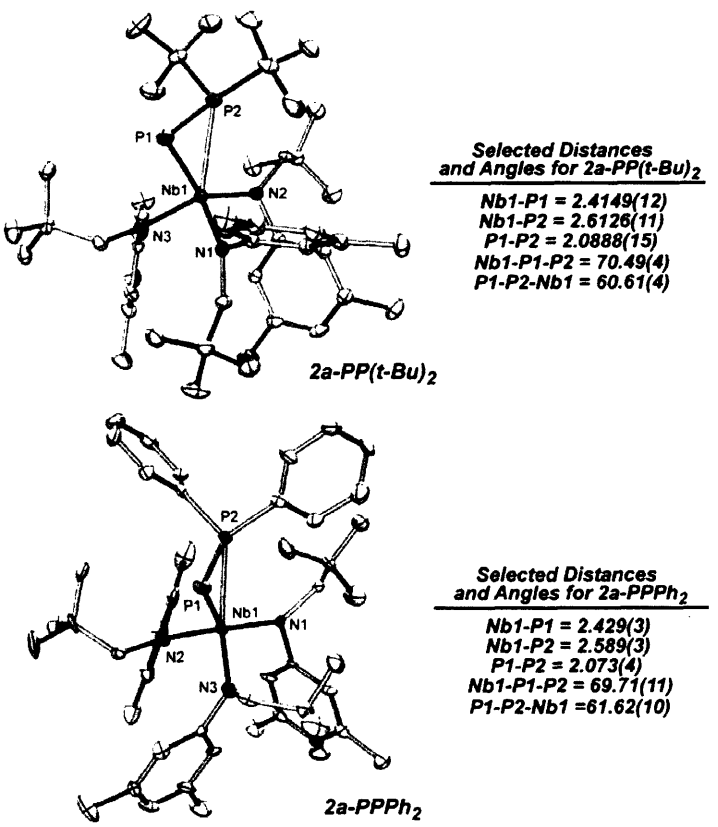

Figure 7. ORTEP Diagrams of 2a-$PP(t\text{-}Bu)_2$ and **3**-PPh_2 at the 35% Probability Level.

The solid-state structures of **2a**-PP(t-Bu)$_2$ and **2a**-PPPh$_2$ (Figure 7) clearly show the η^2-interaction of the R_2PP unit with the niobium center. The Nb1-P1 bond lengths for both **2a**-PP(t-Bu)$_2$ and **2a**-PPPh$_2$ (2.4149(12) and 2.429(3) Å, respectively) are much longer than typically found in early-transition metal phosphinidene complexes[44] and more closely approximate an Nb–P single bond.[26] Contrastingly, the P1–P2 separations of 2.0888(15) and 2.073(4) Å in **2a**-PP(t-Bu)$_2$ and **3**-PPh$_2$, respectively are approximately 0.13 Å shorter than expected for a P–P single bond (2.21 Å),[2] lending credence to the notion of multiple-bond character in the R_2PP unit. Thus substantial electronic reorganization of the Nb≡P$^-$ unit ensues upon addition of a formally $[PR_2]^+$ fragment to [**2a**-P]$^-$.

The $^{31}P\{^1H\}$ NMR spectrum of **2a**-PP(t-Bu)$_2$ (C_6D_6) exhibits two sets of doublets located at δ = 405.5 and 80.6 ppm for the phosphinidene (P_α) and phosphino (P_β) P-atoms, respectively, with a large $^1J_{PP}$ coupling constant of 425 Hz also reflective of multiple-bonding interactions[59] (P_α = 401.3 ppm, P_β = 19.0 ppm, $^1J_{PP}$ = 439 Hz for **3**-PPh$_2$). NMR calculations carried out on the hypothetical construct, (η^2-Me$_2$PP)Nb(NH$_2$)$_3$, (next section) support the assignment of a downfield shift for P_α relative to P_β in this system. However, the highly downfield signals for P_α in **2a**-PP(t-Bu)$_2$ and **2a**-PPPh$_2$ are in stark contrast to the mononuclear (η^2–*t*-Bu$_2$PP)PtL$_2$ (L = phosphine) complexes of Fritz,[52-58] in which P_α resonates *upfield* of P_β. The $P_\beta > P_\alpha$ pattern of chemical shifts for (η^2–*t*-Bu$_2$PP)PtL$_2$ indicates a small contribution from P_α in the frontier-orbital region of these complexes.[33,34] This is reasonable due to the fact that filled, non-bonding metal d-orbitals are typically energetically highest lying in square planar-Pt complexes.[60] As a result, a substantial energy gap between magnetically coupled, occupied and unoccupied P_α-based orbitals probably exists. Therefore, the paramagnetic contribution to the NMR shielding of P_α may not be substantial, affording an upfield chemical shift.[30] Conversely, complexes **2a**-PP(t-Bu)$_2$ and **2a**-PPPh$_2$ do not possess non-bonding d-electrons. The latter fact highlights a major electronic difference between these early and late transition metal PPR_2 systems which is evidently manifested in their respective spectroscopic signatures. Pikies has recently employed Fritz's transfer reagent for the synthesis of the d^0 zirconium η^1-phosphinophosphinidene, Cp*$_2$Zr(η^1-PP(*t*-Bu)$_2$)(PMe$_2$Ph),[61] in which the phosphinidene P-atom give rise to a large downfield ^{31}P chemical shift (745 ppm).

2.5 Electronic Structure of Terminal and η^2–Phosphino Phosphinidenes of Niobium

To elucidate the electronic structure of the phosphinidene complexes discussed in the previous sections, the model complexes Me$_3$SiP=Nb(NH$_2$)$_3$ (**2m**-PSiMe$_3$) and (η^2-Me$_2$PP)Nb(NH$_2$)$_3$ (**2m**-PPMe$_2$) were subject to geometry optimization at the density functional level. Of particular interest were the orbital interactions associated with η^2–phosphinophosphinidene ligation and P-P multiple bonding in complexes **3**-PR$_2$. However, the terminal phosphinidene system was also considered computationally for comparison. The optimized structures of both models **2m**-PSiMe$_3$ and **2m**-PPMe$_2$ were in excellent agreement with their experimental counterparts **2a**-PSnMe$_3$ and **2a**-PP(t-Bu)$_2$, respectively.

The frontier molecular orbitals calculated for **2m**-PSiMe$_3$ were consistent with its formulation as a doubly-bound terminal phosphinidene complex (Figure 8).[44] The HOMO-1 is

The frontier molecular orbitals calculated for **2m**-$PSiMe_3$ were consistent with its formulation as a doubly-bound terminal phosphinidene complex (Figure 8).[44] The HOMO-1 is a bonding orbital of Nb dz^2 and P py character, which constitutes the Nb-P σ-interaction, whereas the HOMO of **2m**-$PSiMe_3$ is a pure Nb–P π-orbital comprised of both Nb dxz and P px contributions. In addition, the LUMO of **2m**-$PSiMe_3$ is the π* complement to the π-orbital of the HOMO. It is noteworthy that the corresponding P pz orbital is low in energy and is engaged in σ-bonding to Si. Furthermore, the orbital of P py parentage in HOMO-1 contains considerable electron density positioned distal to the Nb center. This feature is typical of d^0 early transition metal bent phosphinidene complexes and can be considered to partially account for their nucleophilic character.[44] However, it is important to note that, at least for **2m**-$PSiMe_3$, this electronic feature should not be viewed as a lone pair,[44] but rather an extension of a MO which also contains significant Nb-P σ-bonding character. Indeed, the remaining two valence electrons for P reside in a low energy s-orbital which can be considered as part of the phosphorus atomic core. The latter fact reflects the tendency of the 2nd row and heavier main-group atoms to use predominantly p-orbitals for bonding in low-coordinate compounds.[62,63]

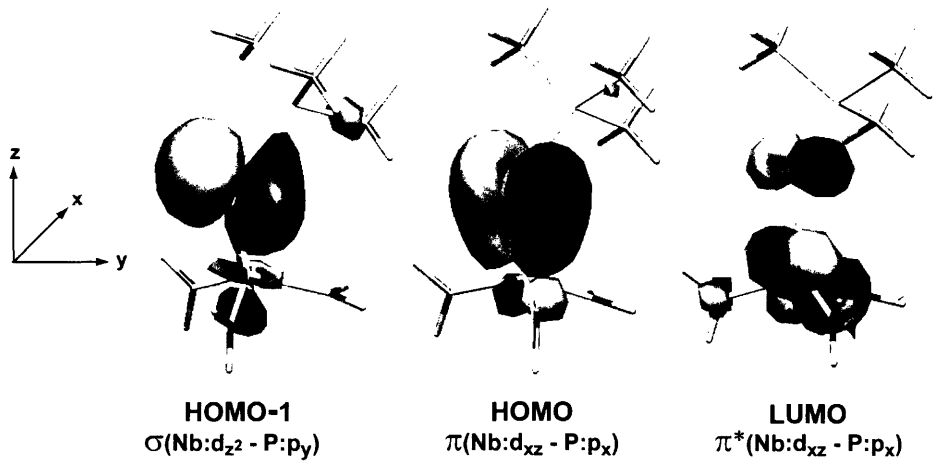

Figure 8. Calculated Frontier Molecular Orbitals for $Me_3SiP{=}Nb(NH_2)_3$ (**2m**-$PSiMe_3$).

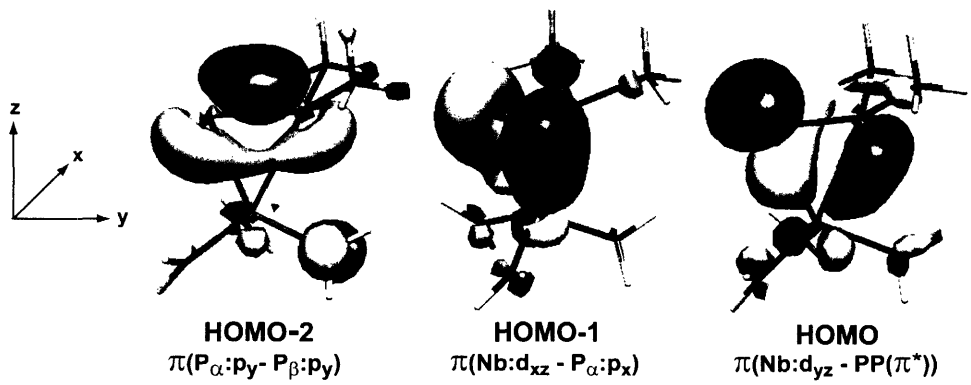

Figure 9. Calculated Frontier Molecular Orbitals for (η^2-$PPMe_2$)$Nb(NH_2)_3$ (**2m**-$PPMe_2$).

(Figure 9) is characteristic of a π-backbonding interaction from a formally d^2 Nb^{III} center to a π* orbital of the $PPMe_2$ ligand, in accord with the standard Dewar-Chatt-Duncanson model of π-complexation.[64,65] Additional evidence for multiple bond character in the η^2–$PPMe_2$ ligand in **2m**-$PPMe_2$ is garnered from inspection of HOMO-2, which is essentially a P_α-P_β π-interaction composed of adjacent P pz orbitals. However, as revealed by HOMO-1, substantial double bond character reminiscent of a terminal phosphinidene species[44] remains in the Nb-P_α interaction of **2m**-$PPMe_2$. In addition, the large lobe on P_α distal to the Nb atom in the HOMO of **2m**-$PPMe_2$ is similar to that discussed above for **2m**-$PSiMe_2$, further pointing to the terminal phosphinidene character in these Nb-complexed PPR_2 compounds. Thus as depicted in Scheme 6, resonance forms which account for both a multiply bound PPR_2 unit (**C**) and terminal phosphinidene Nb=P interactions (**A**) contribute to the overall electronic structure in complexes **2a**-PPR_2. Nevertheless, the foregoing calculations strongly support the notion that Nb-P_α multiple bonding in [**2a**-P]$^-$ can be redistributed onto a β-atom upon functionalization.

2.6 Phosphorus–Based Electronic Reorganization Exploited: Synthesis of Novel Complexed Phosphorus–Containing Molecules.

As shown from the synthesis of the stannyl and phosphinophosphinidene complexes above, anion [**2a**-P]$^-$ possesses enormous potential for the construction of novel phosphorus-containing ligands. In general, the isoelectronic nitrido[29,66,67] and carbido[28,31] anions synthesized in our group have allowed for "ground-up" construction of metallo–functional groups unavailable by alternative synthetic methods. For example, functionalization the group 5 (V, Nb) nitrido anions have afforded the first examples of triflimide (M=N(SO_2CF_3))[29] and iminophosphinimide (M=N-P=NR)[66] coordination complexes. In addition, the molybdenum carbido anion has afforded an unprecedented anionic, complexed, phosphaisocyanide ligand ([Mo-C≡PR]$^-$),[68] although its formulation as such is a point of contention.[69] While [**2a**-P]$^-$ can be added to this class of functionalizable terminal anions, the propensity to redistribute Nb≡P multiple bonding distinguishes it from both the nitrido and carbido species which have not, to date, displayed such behavior. As described below, this tendency has allowed for the isolation of some remarkable Nb-complexed, phosphorus-containing molecules.

2.6.1 Synthesis of a Niobium-Complexed Diphospha–Organoazide: A Potential Diphosphorus (P≡P) Eliminator.

Interest in V and Nb iminophosphinimide (M=N-P=NR) complexes[66] arose from the prospect that such species could thermally eliminate the P≡N molecule concomitant with metal-imido formation (M=NR).[70] While the iminophosphinimides were found to be thermally robust, this chemistry was inspired from reports of N_2 extrusion from group 5 arylazide (ArN_3) complexes to form the corresponding arylimidos.[71,72] Accordingly, the prospect that phosphido anion [**2a**-P]$^-$ could provide a diphospha–organoazide (PPNR), complex was appealing. The resultant Nb-complexed species (*e.g.* Nb-PPNR) could potentially serve as a condensed phase source of the reactive diatomic diphosphorus molecule (P≡P) via Nb=NR formation. Indeed, the P_2 molecule is known to be available from P_4 only at exceedingly high temperatures (~900 °C).[2,5] Furthermore, the fact that diphospha–organoazides are unknown as free or stabilized species served as additional impetus to explore their chemistry.

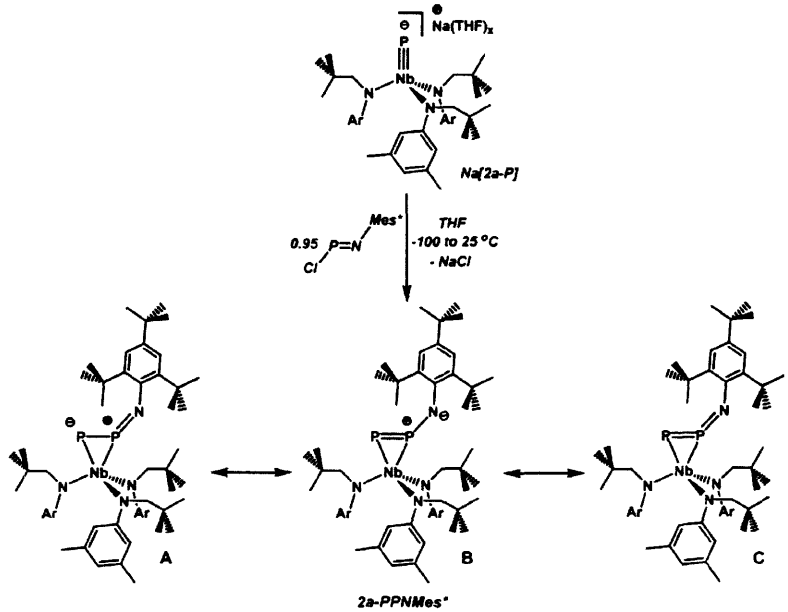

Scheme 7. Synthesis of the Diphosphaoranoazide Complex **2a**-PPMes*.

To obtain a PPNR complex from anion [**2a**-P]$^-$, the 2,4,6-tri-*tert*-butylphenyl-substituted chloroiminophosphine, ClP=NMes* (Mes* = 2,4,6-*t*-$Bu_3C_6H_2$), first synthesized by Niecke was employed.[73] Burford has subsequently shown that ClP=NMes* readily serves as a source of the one-coordinate phosphinium ion [P≡NMes*]$^+$ when treated with suitable chloride ion abstraction reagents.[74,75] Therefore, it was hoped that smooth substitution of ClP=NMes* could be achieved when treated with anion [**2a**-P]$^-$. Indeed, slow addition of a thawing THF solution of ClP=NMes* to a cold THF solution of Na(THF)$_x$[**2a**-P] provided the orange-red diphospha–arylazide complex, (η^2-*P,P*-Mes*NPP)Nb(N[Np]Ar)$_3$ (**2a**-PPNMes*) in 60% yield after removal of NaCl and crystallization (Scheme 7). A crystallographic structure determination of **2a**-PPNMes* confirmed its formulation as a diphospha–arylazide complex with an η^2-P-P bonding mode and an uncoordinated NMes* unit (Figure 10).

As with complexes **3**-PR_2, the addition of a [P≡NMes*]$^+$ fragment to anion [**2a**-P]$^-$ evokes P-P multiple bond formation at the expense of Nb-P multiple bonding. Structural parameters in support of this claim for **2a**-PPNMes* include a Nb1-P1 distance of 2.5653(6) Å, which again, falls outside of the range expected for a terminal phosphinidene complex.[44] Furthermore, the P1-P2 bond distance of 2.0173(8) Å in **2a**-PPNMes is considerably shorter than expected for a P-P single bond (2.21 Å).[2] The notion of P-P multiple bonding is also reflected in the $^{31}P\{^1H\}$ spectrum (C_6D_6) of **2a**-PPNMes (Figure 11), where the $^1J_{PP}$ coupling constant is an astounding 650 Hz.[59] Also notable in the $^{31}P\{^1H\}$ spectrum of **2a**-PPNMes is the asymmetric doublet-of-doublets splitting pattern for the P_α and P_β atoms. While both

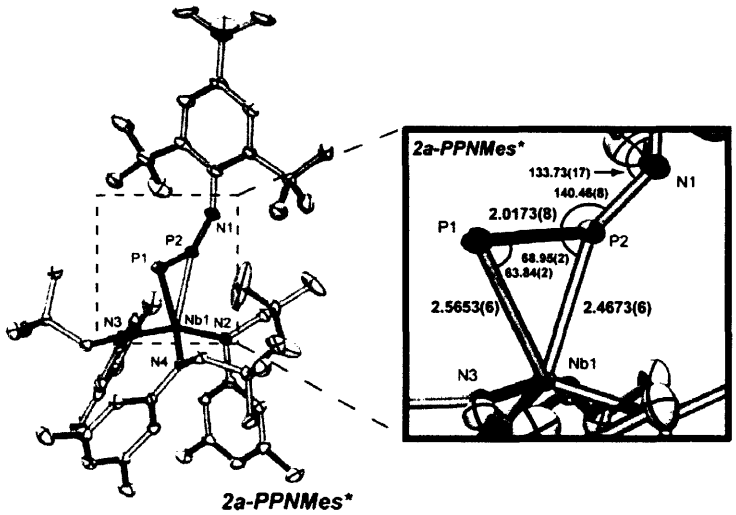

Figure 10. ORTEP Diagram of **2a**-PPNMes* at the 35% Probability Level.

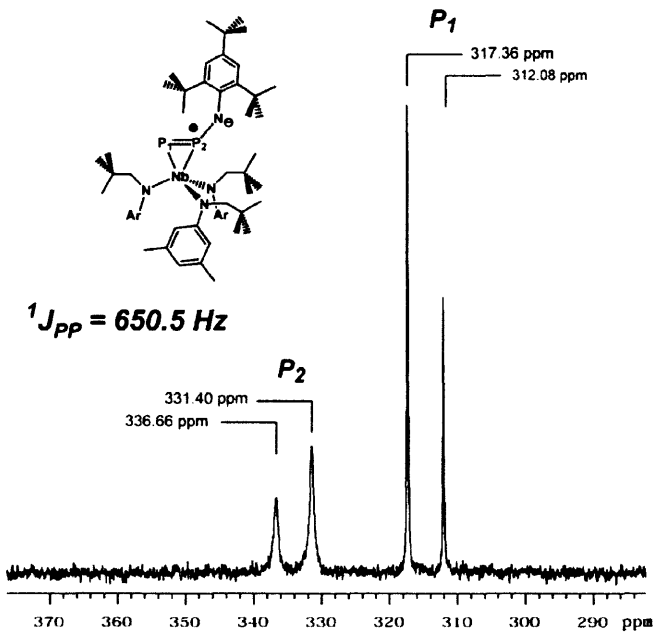

Figure 11. $^{31}P\{^1H\}$ NMR spectrum of **2a**-PPNMes* in C_6D_6 at 121.0 MHz.

resonances should experience broadening due to coupling to the quadrupolar Nb nucleus ($^{93}Nb = I = 9/2$, 100%),[30] the additional broadening of the low-field resonance is attributed to ^{14}N–coupling (I =1, 99.63%)[30] to the P_β nuclei. That a large P_β-N coupling in **2a**-PPNMes* can be observed spectroscopically is also supported by its solid state structure, where a fair degree of P_β–N1 multiple bonding is indicated (d(P2-N1) = 1.5565(19), $r_{cov}P + r_{cov}N$ = 1.80 Å).[26] Thus resonance forms including **A** and **C** in Scheme 7 may reasonably approximate the bonding in **2a**-PPNMes*.

To test for the possibility of P_2 extrusion, thermolysis studies of **2a**-PPNMes* were performed. Heating a red-orange C_6D_6 solution of **2a**-PPNMes* at 65 °C for 1.0 h, resulted in a color change to dark yellow-brown. Analysis of the thermolysis mixture by ^1H NMR revealed that a new three-fold symmetric product containing the Mes* substituent had cleanly formed. In addition, the corresponding $^{31}P\{^1H\}$ spectrum indicated complete disappearance of the resonance associated with **2a**-PPNMes*. Crystallographic analysis on yellow crystals obtained from the thermolysis mixture established the identity of the new product as the imido complex, $(Mes*N)Nb(N[Np]Ar)_3$ (**2a**-NMes*, Figure 12). Thus the thermodynamic driving force of Nb-imido formation indeed provides for the elimination of the P_2 unit in **2a**-PPNMes* (Scheme 8).

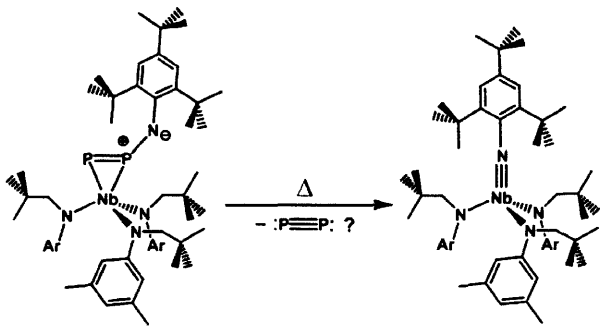

Scheme 8. Synthesis of Imido **2a**-NMes* by the Thermolysis of **2a**-PPNMes*.

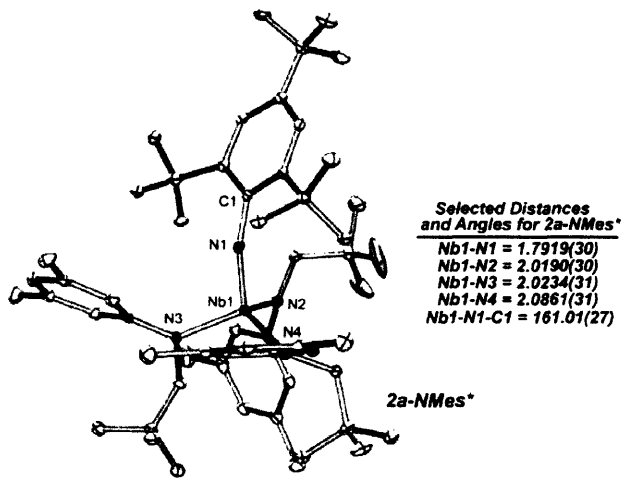

Figure 12. ORTEP Diagram of **2a**-NMes* at the 35% Probability Level.

It is tempting to suggest that the P_2 unit in **2a**-PPNMes* is ejected as the diphosphorus molecule (P≡P). However, such a notion has not been confirmed. Whereas the resonance for **2a**-PPNMes* reproducibly disappears upon thermolysis, $^{31}P\{^1H\}$ NMR does not indicate the formation of a new major phosphorus-containing product. However, when the reaction mixture is assayed by $^{31}P\{^1H\}$ NMR for long periods of time, a multitude of complex phosphorus resonances appear in the region between +300 and –200 ppm. These phosphorus-containing species presumably arises from reaction between the liberated 'P_2' fragment and solvent or complexes **2a**-PPNMes* and **2a**-NMes*. Indeed, small unidentified resonances are

present in the aliphatic region in the ^{1}H NMR spectrum of **2a**-NMes* obtained from the thermolysis of **2a**-PPNMes* in deuterated solvents. Furthermore, P_4 (δ = –545 ppm, C_6D_6) is not observed after thermolysis of **2a**-PPNMes*, but it is known that condensation of P≡P gas does not result in the formation of P_4.[2] Instead, an amorphous brown form of phosphorus is obtained, which may additionally account for the species obtained upon thermolysis of **2a**-PPNMes*. Attempts to trap the incipient P_2 unit by performing the thermolysis of **2a**-PPNMes* in neat cyclopentadiene (C_5H_6) has lead to the observation of single phosphorus-containing molecule by $^{31}P\{^{1}H\}$ NMR. This compound may be a Diels-Alder-type cycloaddition product of P_2, however efforts to isolate and characterize it have been unsuccessful to date. While the latter result is promising, additional work must be done before complex **2a**-PPNMes* can be claimed to serve as solution-phase reagent for the production of the diphosphorus molecule.

2.6.2 Triatomic *cyclo*-EP_2 Rings (E = Ge, Sn, Pb) as Bridging Ligands: Complexed Main-Group Cyclopropenium Analogues

Three-membered, 2π-electron rings comprised of main group elements are of interest as compact manifestations of 4n+2 Hückel aromaticity, with n = 0.[76] The cyclopropenium ion, [*cyclo*-C_3H_3]$^+$, serves as the prototypical organic representative of this class.[77-79] However, the prospect of isolobal heteroatom substitution of one or more CH units of the cyclopropenium ring has spurred both theoretical[80-87] and experimental[88-91] investigations seeking to extend the concept of π-delocalization throughout the p-block of the periodic table.

In the context of expanding the chemistry of anion [**2a**-P]$^-$, its reaction with divalent group 14 salts was investigated. From these studies, novel three-membered, 2π-electron rings of the formulation *cyclo*-EP_2 (E = Ge, Sn, and Pb) were produced owing to the propensity of anion [**2a**-P]$^-$ to undergo electronic rearrangement when functionalized. While these *cyclo*-EP_2 rings are expected to be reactive entities in the free state, anion [**2a**-P]$^-$ allows for the synthesis of stabilized versions due to complexation by two sterically protective Nb(N[Np]Ar)$_3$ fragments. Interestingly, this particular family of *cyclo*-EP_2 triangles has not been considered previously in either free or complexed form. Furthermore, divalent group 14 atoms have received relatively little attention as components of three-membered, 2π-electron rings. In fact, only the neutral cyclopropene carbene (*cyclo*-:C(C_2H_2)), diazacyclopropene carbene (*cyclo*-:CN_2) and silacyclopropenylidene (*cyclo*-:Si(C_2H_2)) molecules have been considered theoretically,[92,93] with three-membered rings containing the heavier group 14 atoms having been to date completely neglected.

When equimolar quantities of Na(THF)$_x$[**2a**-P] and $SnCl_2$ were combined in cold THF solution, $^{31}P\{^{1}H\}$ NMR spectroscopy revealed a single new resonance centered at δ = 47.2 ppm, well up-field of the range expected for an early transition metal phosphinidene complex.[44] X-ray structural analysis on a crystal harvested from the reaction mixture established the identity of complex (SnP_2)[**2a**]$_2$ as containing a central *cyclo*-SnP_2 ring and as the product of net double [P≡Nb(N[Np]Ar)$_3$]$^-$ addition to $SnCl_2$. A purposeful synthesis was then devised and also extended to the Ge– and Pb–containing derivatives. Accordingly, slow addition of 0.47 equiv of the corresponding divalent group–14 salt (Ge = $GeCl_2$(dioxane), Sn = $SnCl_2$, Pb = $Pb(OTf)_2$ (OTf = OSO_2CF_3)) to Na(THF)$_x$[**2a**-P] in cold THF solution,

provided dark red $(GeP_2)[\mathbf{2a}]_2$ and forest green $(SnP_2)[\mathbf{2a}]_2$ and $(PbP_2)[\mathbf{2a}]_2$ in moderate isolated yields (Ge = 65%, Sn = 40%, Pb = 30%) after salt removal and crystallization from Et_2O (Scheme 9).

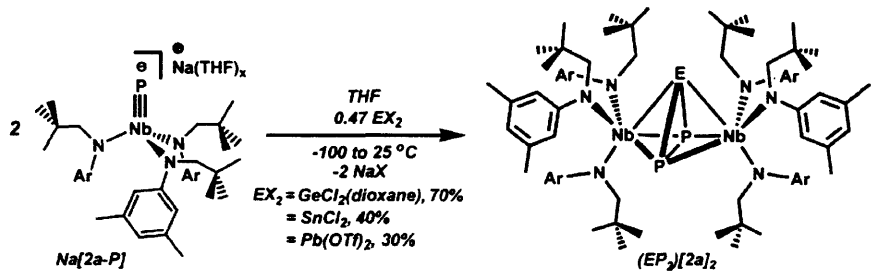

Scheme 9. Synthesis of μ_2:η^3,η^3-*cyclo*-EP_2 Complexes $(EP_2)[\mathbf{2a}]_2$.

Upon isolation, diamagnetic complexes $(EP_2)[\mathbf{2a}]_2$ are obtained as crystalline solids which are soluble in ethereal and aromatic solvents. While $(GeP_2)[\mathbf{2a}]_2$ and $(SnP_2)[\mathbf{2a}]_2$ retain their integrity in solution at elevated temperatures (C_6D_6, 80-100 °C, 2d), complex $(PbP_2)[\mathbf{2a}]_2$ was found to decompose at room temperature in solution to Pb^0 and the bridging diphosphide, $(\mu\text{-}P_2)[\mathbf{2a}]_2$, over several hours. The absence of light did not retard the decomposition process for $(PbP_2)[\mathbf{2a}]_2$ and considering its fragile nature, it is remarkable that the present synthesis permitted its isolation in pure form. Accordingly, an alternate synthesis of $(SnP_2)[\mathbf{2a}]_2$ was attempted by treatment of $(\mu\text{-}P_2)[\mathbf{2a}]_2$ with an excess of Sn^0 dust in THF solution. However, no reaction was observed when intermittently assayed for 24 h, highlighting the synthetic entry to complexes $(EP_2)[\mathbf{2a}]_2$ provided by anion $[\mathbf{2a}\text{-}P]^-$. Furthermore, it is notable that the synthesis of complexes $(GeP_2)[\mathbf{2a}]_2$ and $(SnP_2)[\mathbf{2a}]_2$ proceed from $[\mathbf{2a}\text{-}P]^-$ and group-14 di-chlorides without considerable formation of the bis-chloride complex $\mathbf{2a}\text{-}Cl_2$. Indeed, $SnCl_2$ and $GeCl_2$(dioxane) are the only dihalide species which react smoothly with anion $[\mathbf{2a}\text{-}P]^-$ to date.

Depicted in Figure 13 are the solid-state, molecular structures for complexes $(EP_2)[\mathbf{2a}]_2$. Evident for each is the μ_2:η^3,η^3 disposition of the *cyclo*-EP_2 ring between the two niobium centers. For $(SnP_2)[\mathbf{2a}]_2$ and $(PbP_2)[\mathbf{2a}]_2$, the *cyclo*-EP_2 units are near-perfect isosceles triangles, where the $\angle$P-E-P angle in $(PbP_2)[\mathbf{2a}]_2$ (48.85(5)°) is slightly more acute than that in $(SnP_2)[\mathbf{2a}]_2$ (51.23(7)°) as a result of the larger covalent radius of Pb. Indeed, the average E-P bond distances in $(SnP_2)[\mathbf{2a}]_2$ and $(PhP_2)[\mathbf{2a}]_2$ ($(SnP_2)[\mathbf{2a}]_2$ = 2.571 Å, $(PbP_2)[\mathbf{2a}]_2$ = 2.677 Å) scale with the difference in covalent radii between Sn and Pb and reflect values typical of Sn–P and Pb–P single bonds.[26] Additionally, the P–P distances of 2.223(2) Å and 2.213(3) Å for$(SnP_2)[\mathbf{2a}]_2$ and $(PbP_2)[\mathbf{2a}]_2$, respectively, are in the range typical of P–P single bonds,[2,51] indicating a saturated electronic framework for these *cyclo*-EP_2 rings when sandwiched between two reducing d^2 niobium centers. Complex $(GeP_2)[\mathbf{2a}]_2$ however, was found to crystallize in the cubic space group $P2_13$ with its Nb–Nb vector coincident with a crystallographic C_3 axis. Unfortunately this morphology resulted in crystallographically imposed, three-fold compositional disorder of the ring atoms in the *cyclo*-GeP_2 unit. Consequently, chemically suspect metrical parameters were obtained for the complexed GeP_2 ring, where the edge distance of 2.460 Å clearly exceeds the value for a P–P

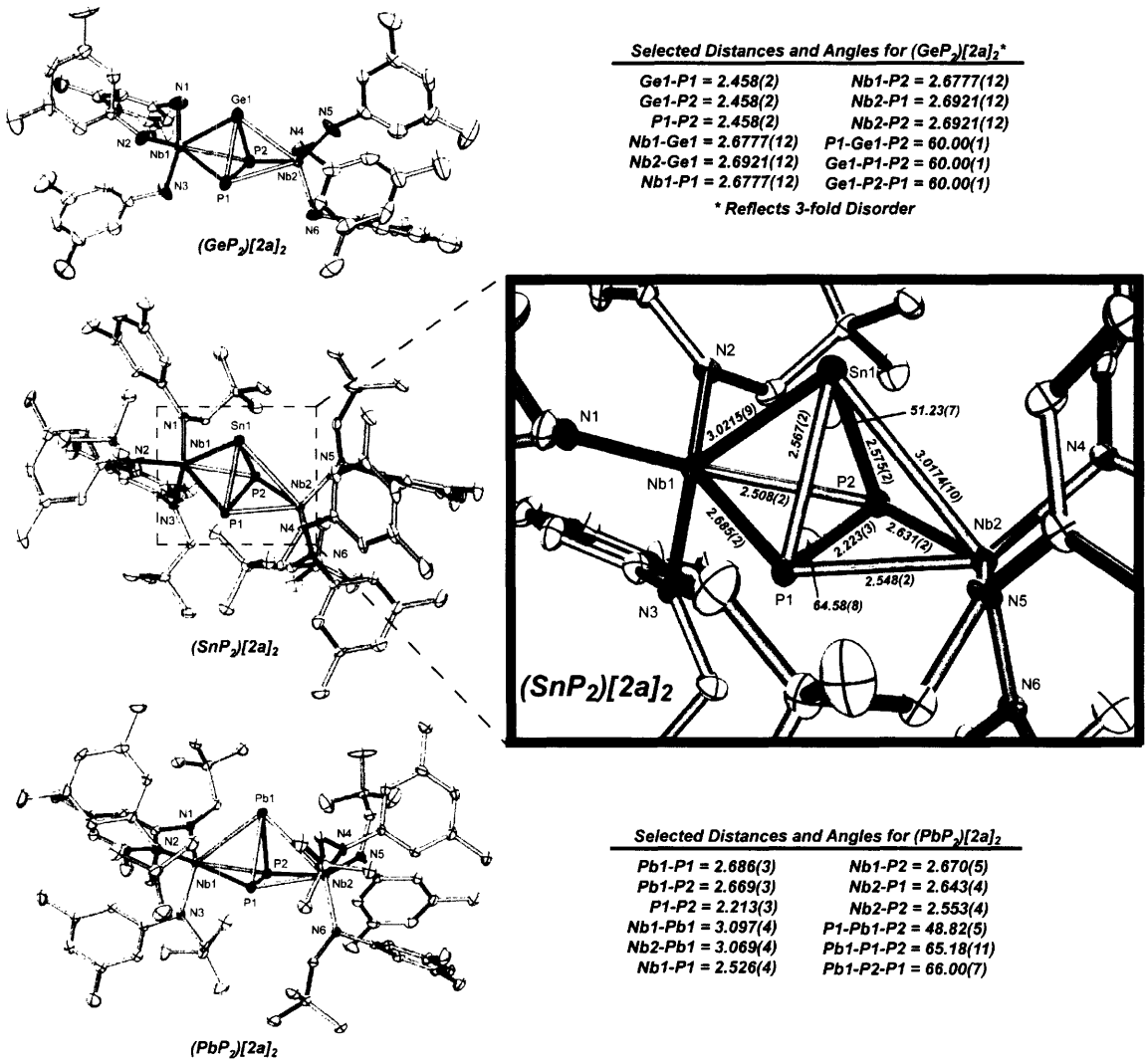

Figure 13. ORTEP Diagrams of Complexes $(EP_2)[\mathbf{2a}]_2$ at the 35% Probability Level. Neopentyl Residues of $(EP_2)[\mathbf{2a}]_2$ have been removed for Clarity.

single bond and reflects structural dominance by the larger, Ge component.

To garner further insight into the geometrical structure of complex $(GeP_2)[\mathbf{2a}]_2$, the model construct, $(\mu_2{:}\eta^3,\eta^3\text{-}cyclo\text{–}GeP_2)[Nb(NH_2)_3]_2$ ($(GeP_2)[\mathbf{2m}]_2$), was subject to full geometry optimization at the density functional level. Using the experimental metrical parameters of $(GeP_2)[\mathbf{2a}]_2$ as input, $(GeP_2)[\mathbf{2m}]_2$ converged to a geometry with interatomic P–P (2.242 Å) and P–Ge (2.4465 Å av.) separations consistent with both P–P and P–Ge single bonds (Figure 14).[2,51] All other overall structural features for $(GeP_2)[\mathbf{2m}]_2$ were likewise consistent with those found experimentally for $(SnP_2)[\mathbf{2a}]_2$ and $(PbP_2)[\mathbf{2a}]_2$. Furthermore, the calculated structural parameters for models $(SnP_2)[\mathbf{2m}]_2$ and $(PbP_2)[\mathbf{2m}]_2$ were in excellent agreement with their experimental counterparts. Therefore, it is proposed that $(GeP_2)[\mathbf{2m}]_2$ represents the molecular geometry for complex $(GeP_2)[\mathbf{2a}]_2$ in the absence of crystallographic disorder.

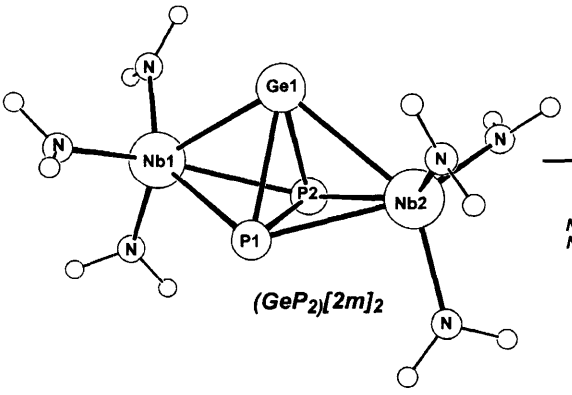

Selected Distances and Angles Calculated for $(GeP_2)[2m]_2$	
Ge1-P1 = 2.447	Nb1-P2 = 2.583
Ge1-P2 = 2.446	Nb2-P1 = 2.597
P1-P2 = 2.242	Nb2-P2 = 2.609
Nb1-Ge1 = 2.704	P1-Ge1-P2 = 54.55
Nb2-Ge1 = 2.713	Ge1-P1-P2 = 62.75
Nb1-P1 = 2.597	Ge1-P2-P1 = 62.70

Figure 14. Optimized Molecular Geometry of Model $(\mu_2{:}\eta^3,\eta^3\text{-}cyclo\text{–}GeP_2)[Nb(NH_2)_3]_2$ ($(GeP_2)[\mathbf{2m}]_2$).

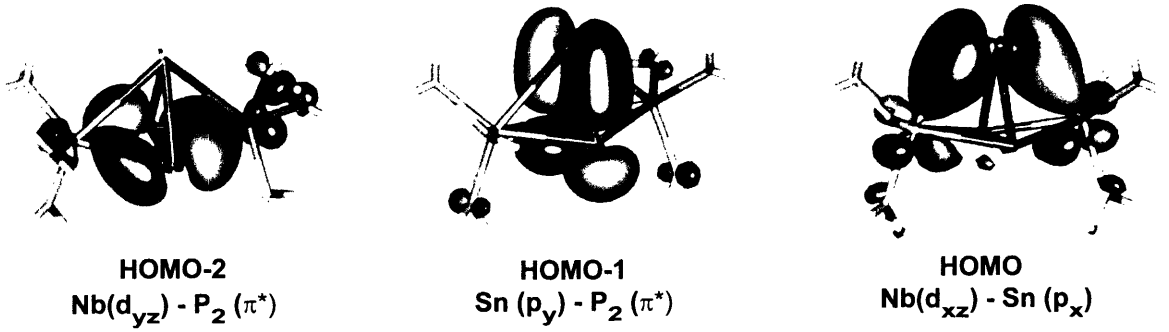

Figure 15. Calculated Frontier Molecular Orbitals for $(\mu_2{:}\eta^3,\eta^3\text{-}cyclo\text{–}SnP_2)[Nb(NH_2)_3]_2$ ($(SnP_2)[\mathbf{2m}]_2$).

Of particular interest are the electronic structure attributes attendant with *cyclo*-EP_2 complexation in complexes $(EP_2)[\mathbf{2a}]_2$. Depicted in Figure 15 are the highest-lying occupied molecular orbitals calculated for $(SnP_2)[\mathbf{2m}]_2$ which are qualitatively representative for all complexes $(EP_2)[\mathbf{2m}]_2$. Whereas the HOMO–1 is part of the σ-framework of the *cyclo*-SnP_2 unit, complexation by the Nb centers consists of a pair of mutually orthogonal $2e^-$ π-backbonds. One of these (HOMO) involves the out-of-plane Sn valence p orbital as the acceptor component, while the other (HOMO-2) utilizes a P–P π* orbital as the acceptor component. Accordingly, a pair of d^2 niobium trisamide fragments is seen to be electronically complementary to a formally neutral *cyclo*-EP_2 ring. However, summation of the calculated multipole-derived charge (MDC-q)[94] on the ring atoms in $(EP_2)[\mathbf{2m}]_2$ indicate that each *complexed cyclo*-EP_2 unit bears a net charge of approximately −1.0 (Table 1). Thus, although formally neutral as free entities, complexation by two electropositive d^2 Nb centers renders these *cyclo*-EP_2 rings moderately anionic. The latter interpretation is consistent with the saturated nature of the *cyclo*-EP_2 framework as determined crystallographically for $(SnP_2)[\mathbf{2a}]_2$ and $(PbP_2)[\mathbf{2a}]_2$.

Table 1. Calculated Multipole Derived Charges at the Quadrupole Level (MDC-q, a.u.) for the *cyclo*-EP_2 Ring Atoms in Models $(EP_2)[\mathbf{2m}]_2$

Model	Atom	MDC-q
$(GeP_2)[\mathbf{2m}]_2$	Ge	-0.390652
	P	-0.400260
	P	-0.396022
		$\Sigma_{MDC\text{-}q}$ = **−1.186**
$(SnP_2)[\mathbf{2m}]_2$	Sn	-0.185777
	P	-0.365193
	P	-0.366728
		$\Sigma_{MDC\text{-}q}$ = **−0.917**
$(PbP_2)[\mathbf{2m}]_2$	Pb	-0.057589
	P	-0.381398
	P	-0.399759
		$\Sigma_{MDC\text{-}q}$ = **−0.837**

It is noteworthy that the net negative charge calculated for the *cyclo*-EP_2 rings in models $(EP_2)[\mathbf{2m}]_2$ decreases in the order Ge > Sn > Pb according to the decrease in electronegativity of the group 14 atom.[95-97] Indeed, the negative charge on phosphorus is calculated to remain relatively constant between models $(EP_2)[\mathbf{2m}]_2$ (−0.384 ± 0.016 a.u) and variation in net charge between each *cyclo*-EP_2 ring is dictated by the charge on E (MDC-q (a.u.) = −0.390, Ge; −0.185, Sn; −0.057, Pb , Table 1). A similar dependence on the identity of the group 14 atom is observed experimentally in the solution $^{31}P\{^1H\}$ spectra of complexes $(EP_2)[\mathbf{2a}]_2$ (δ ^{31}P = −15.7 ppm, $(GeP_2)[\mathbf{2a}]_2$; 47.8 ppm, $(SnP_2)[\mathbf{2a}]_2$; 115.2 ppm, $(PbP_2)[\mathbf{2a}]_2$). The downfield progression of resonances is qualitatively attributed to the increase in the paramagnetic component (σ_{para}) of the total ^{31}P shielding tensor ($\sigma_{total} = \sigma_{para} + \sigma_{dia} + \sigma_{so}$; dia = diamagnetic, so = spin orbit) as the group 14 atom becomes less electronegative.[98,99] NMR calculations performed on models $(EP_2)[\mathbf{2m}]_2$ are consistent with this suggestion, revealing that variation in σ_{para} dominates σ_{total} and increases in the order Pb > Sn > Ge (Table 2). Accordingly, the σ_{dia} was found to be essentially invariant between models $(EP_2)[\mathbf{2m}]_2$ (961.9 ± 0.5 ppm) and σ_{so} made a negligible contribution (13 – 21 ppm, Table 2). Mapping the principal components of σ_{para} onto the molecular frame of $(EP_2)[\mathbf{2m}]_2$ (Figure 16) reveals that $R(\sigma_{11})$ (R = rotation operator) mediates an occupied-virtual coupling between the Nb_2-P_2 π^* backbond (occupied) and the σ^* framework (virtual) of the EP_2 ring, in the presence of the applied magnetic field. Accordingly, the electronic origin of the ^{31}P deshielding as influenced[32-34] by the identity of the group 14 atom in complexes $(EP_2)[\mathbf{2a}]_2$ can be readily visualized.

Table 2. Calculated ^{31}P Shielding Tensors (σ, ppm) for Models $(EP_2)[\mathbf{2m}]_2$.

Model	σ_{para}	σ_{dia}	σ_{so}	σ_{total}
$(GeP_2)[\mathbf{2m}]_2$	σ_{11} = -851.197	σ_{11} = 955.281	σ_{11} = 15.313	**424.343**
	σ_{22} = -547.304	σ_{22} = 964.028	σ_{22} = 22.268	
	σ_{33} = -277.160	σ_{33} = 966.957	σ_{33} = 24.839	
	Av. = **-558.553**	Av. = **962.089**	Av. = **20.807**	
$(SnP_2)[\mathbf{2m}]_2$	σ_{11} = -946.556	σ_{11} = 956.206	σ_{11} = 14.141	**354.640**
	σ_{22} = -628.033	σ_{22} = 962.727	σ_{22} = 20.393	
	σ_{33} = -305.986	σ_{33} = 966.926	σ_{33} = 24.099	
	Av. = **-626.858**	Av. = **961.953**	Av. = **19.545**	
$(PbP_2)[\mathbf{2m}]_2$	σ_{11} = -1097.637	σ_{11} = 955.379	σ_{11} = -17.986	**292.291**
	σ_{22} = -645.882	σ_{22} = 963.550	σ_{22} = 19.754	
	σ_{33} = -304.679	σ_{33} = 968.257	σ_{33} = 36.118	
	Av. = **-682.733**	Av. = **962.395**	Av. = **12.629**	

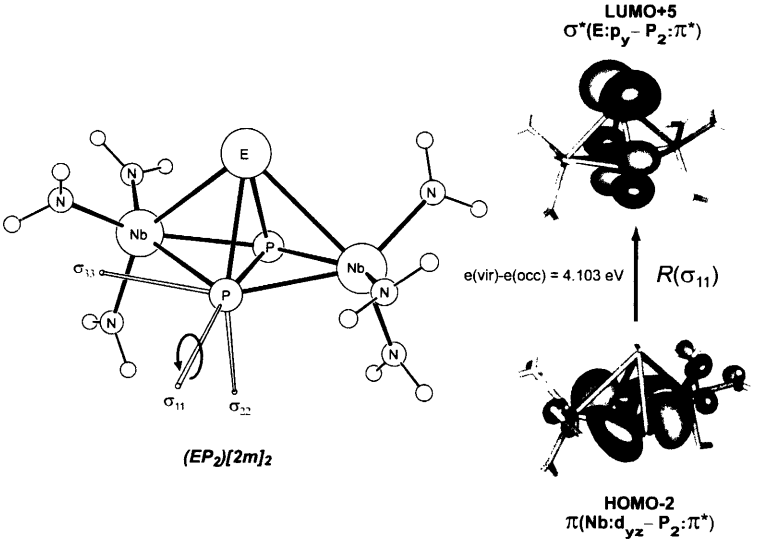

Figure 16. (Left) Principal components of σ_{para} mapped onto the molecular frame of models $(EP_2)[\mathbf{2m}]_2$. (Right) Principal magnetic coupling of occupied (occ) and virtual (vir) orbitals about the rotation operator $R(\sigma_{11})$ accounting for the influence of the E atom on the ^{31}P paramagnetic shielding tensor. e = energy.

Complex $(SnP_2)[\mathbf{2a}]_2$ also gives rise to a broad, upfield ^{119}Sn NMR signal located at δ = −696.4 ppm ($\nu_{1/2}$ = 1300.8 Hz C_6D_6, 20 °C). Typical ^{119}Sn chemical shifts for divalent Sn species are significantly deshielded relative to that of$(SnP_2)[\mathbf{2a}]_2$, falling in the range of 2300 to 700 ppm.[100,101] Large downfield shifts in SnR_2 compounds are a result of mixing occupied σ-SnR molecular orbitals with the normally empty p-orbital of Sn(II) within an applied magnetic field.[96] The disparate ^{119}Sn NMR spectroscopic behavior of $(SnP_2)[\mathbf{2a}]_2$ is readily rationalized by the ground-state electronic saturation of the empty p-orbital of Sn by the two Nb centers (HOMO, Figure 15). Unfortunately, attempts to locate the corresponding ^{203}Pb NMR shift for $(PbP_2)[\mathbf{2a}]_2$ were unsuccessful due to its rapid decomposition in solution.

2.6.3 Computational Investigations of Free *cyclo*-EP_2 Rings

Since theoretical studies on free divalent group-14 *cyclo*-EP_2 rings have not been reported, preliminary DFT calculations on this system were performed. Of particular interest was the extent of which 4n+2 Hückel aromaticity could be considered as present in these 2π-electron three-membered rings. While Hückel aromaticity was defined for π-ring systems composed of degenerate CH units (*e.g.* benzene),[76] theoretical studies have suggested that π-delocalization is an important component in heteroatom-containing rings as well. Indeed, the borirene molecule, *cyclo*–HB(HCCH), has been proposed to have substantial aromatic character,[81,88] albeit less so than the parent cyclopropenium ion (*cyclo*-$[C_3H_3]^+$). Furthermore, aromatic stabilization has been suggested for the azirinyl ion, *cyclo*-$[HCN_2]^+$, but again, much less so than in borirene and cyclopropenium due to polarization of the π-system toward the electronegative N atoms.[81,91] Typically, π-delocalization is less pronounced in systems containing adjacent light and heavy main-group elements due to mismatch in orbital energies.[82,102]

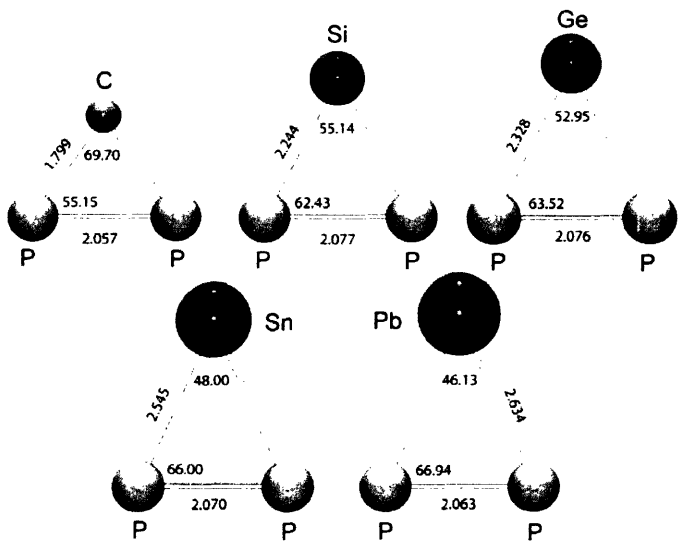

Figure 17. Optimized Geometries for All Group-14 *cyclo*-EP_2 Rings

Depicted in Figure 17 are the optimized geometries for the entire series of group-14 *cyclo*-EP_2 triangles calculated in C_{3v} symmetry. Each triatomic ring represents a minimum on the potential energy surface as verified by a harmonic frequencies calculation. For each ring, the E-P bond distance is only slightly shorter than the value expected for a single bond, indicating that significant E-P multiple bonding is not present. This is in contrast to other heteroatom containing three-membered rings for which π-delocalization is thought to be important. For example, the analogous C-B bond in borirene is ca. 10% shorter than expected for a B-C single bond.[81] In addition, the P-P separation in each *cyclo*-EP_2 ring is consistent with a corresponding P-P bond order of ca. 2.0.[51,103] Interestingly however, with the exception of carbon, the P-P bond distance is seen to decrease as the E atom becomes heavier, signifying an increase in P-P bond order. Presumably, the short P-P bond observed for *cyclo*-CP_2 is a manifestation of the geometrical constraints of the ring, which should be most

pronounced for the relatively small carbon atom. However, an explanation for the increase in P-P multiple bonding in the heavier congeners is revealed from inspection of an interaction diagram for the molecular orbitals of the *cyclo*-EP_2 system.

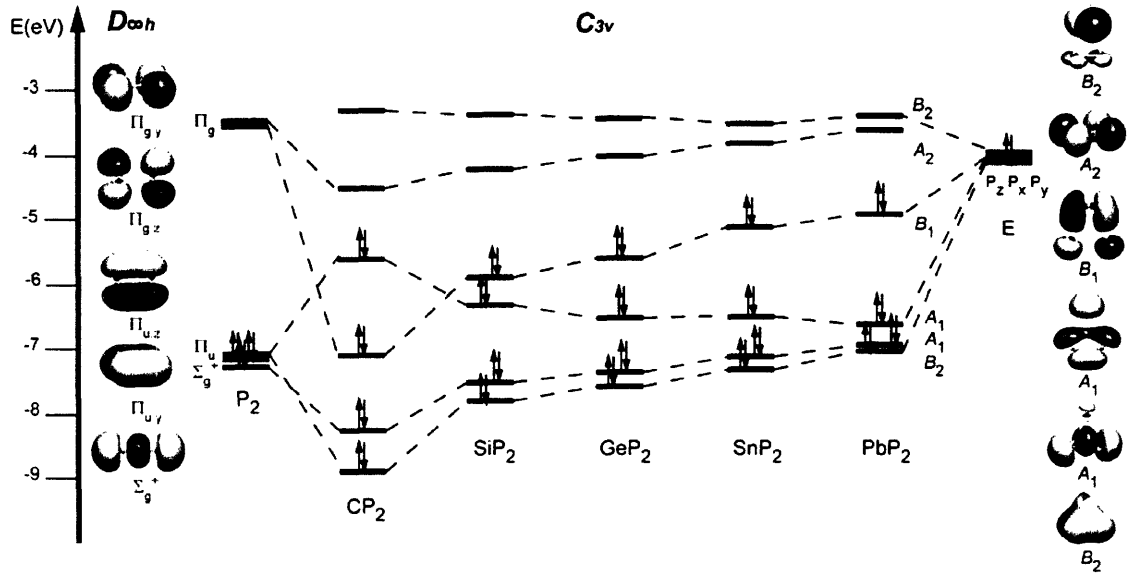

Figure 18. Interaction diagram for the construction of *cyclo*-EP_2 rings from a singlet E atom and the diphosphorus molecule (P_2).

Shown in Figure 18 is a quantitative interaction diagram for the construction of each *cyclo*-EP_2 from the diphosphorus molecule (P≡P, $D_{\infty h}$) and a singlet (^{1}A) divalent group-14 atom. On left are the molecular orbitals calculated for *cyclo*-GeP_2 in C_{3v} symmetry which are qualitatively representative of the entire group-14 series. In accord with expectations, the HOMO-LUMO gap for *cyclo*-PbP_2 is the smallest relative to the lighter congeners, indicating it should be the least stable (and most reactive) system. Of particular note is the orbital of B_2 symmetry which accounts for out-of-plane π interaction for the 2π-electron rings. As is clearly seen, this orbital is most stabilized for E = C and increases steadily in energy as the E atom becomes heavier. Indeed, for E = Pb, this B_2 orbital approaches the energy of the localized π-orbital in the P_2 molecule (Π_u, right), indicating its stabilization via delocalization into the empty, out-of-plane p orbital on Pb is insignificant. Thus the shortening of the P-P bond in the *cyclo*-EP_2 rings can be viewed as a result of B_2 orbital becoming more characteristic of localized P-P π bond as the E atom becomes heavier. Presumably, the energy mismatch between P p and E p orbitals is responsible for preventing π-delocalization in the heavier *cyclo*-EP_2 rings.[86,98]

B_2 Orbital	EP_2	CP_2	SiP_2	GeP_2	SnP_2	PbP_2
	% E p_y	25.21	16.29	15.86	12.69	11.29
	% 2P p_y	72.28	80.97	80.66	84.01	85.90

Figure 19. Individual B_2 π-Orbital Calculated for the *cyclo*-EP_2 Rings.

Figure 18 depicts the individual B_2 orbital for the *cyclo*-EP_2 rings along with the values for the corresponding atomic orbital parentages (%) obtained from the DFT calculations. In accord with the interaction diagram of Figure 17, out-of-plane π-delocalization is most pronounced for *cyclo*-CP_2. Furthermore, the contribution of the C p_y orbital to the B_2 MO (25.21%) is close to the maximum value of 33.3% as seen for the *cyclo*-$[C_3H_3]^+$.[81,87] However, a sharp drop-off in the participation of the E p_y orbital is observed for Si – Pb, where the B_2 orbital of *cyclo*-PbP_2 indeed resembles the localized P-P π-bond of diphosphorus. Therefore, these calculations suggest that the aromatic character of the free group-14 *cyclo*-EP_2 rings may be significant for E = C, but is increasingly less so in the heavier analogues. However, a more detailed computational analysis of this systems is necessary to support these preliminary findings.

3 Conclusions and Future Work

The activation of elemental phosphorus (P_4) by the niobaziridine-hydride complex **1a**-H has been shown to be exceedingly mild, providing the bridging diphosphide complex (μ-P)[**2a**]$_2$ in excellent yield. Complex (μ-P)[**2a**]$_2$ can be subsequently reduced with Na/Hg to afford the terminal phosphido anion [**2a**-P]$^-$, which is best formulated as containing a Nb-P triple bond. Due to its uninegative charge, anion [**2a**-P]$^-$ is readily functionalized upon addition of electrophiles. Most interestingly, the terminal Nb≡P$^-$ unit in [**2a**-P]$^-$ has demonstrated a propensity to undergo electronic rearrangement in a manner which exchanges Nb-P multiple bonding for phosphorus-element multiple bonding. This feature of anion [**2a**-P]$^-$ has allowed for the synthesis of novel, low-coordinate phosphorus compounds within the protective coordination sphere of a niobium trisamide fragment. It should be noted, that several of the complexed phosphorus compounds accessible via anion [**2a**-P]$^-$ are not available from alternate synthetic routes. Thus, anion [**2a**-P]$^-$ represents a powerful new reagent in low-coordinate phosphorus chemistry.

Due to the ability of anion [**2a**-P]$^-$ to readily effect phosphorus-element multiple bonding, a host of synthetic opportunities exist. An intriguing prospect in this regard is the combination of anion [**2a**-P]$^-$ with the terphenyl, group-14 monochloride complexes (ArECl, E = Ge, Sn) pioneered by Power[104] for synthesis of complexed, organo-phosphagermynes and stannynes (*i.e.* P≡GeAr and P≡SnAr). Species of the type E≡SnAr (E = Ge, Sn) are isolable to the diorganophosphinophosphinidenes discussed in this chapter and theoretical studies have

suggested that the P≡E unit can be kinetically stabilized by a terphenyl substituent.[105,106] Furthermore, utilization of anion [**2a**-P]$^-$ for the synthesis of complexed, phosphorus-group 16 multiply bonded species (*i.e.* P=TeR) can also be envisioned.

While the synthetic potential of anion [**2a**-P]$^-$ for construction of *complexed* low-coordinate phosphorus compounds is evident, a methodology for the liberation of the newly formed phosphorus compound from the Nb center is needed. A 'decomplexation' methodology is imperative for subsequent studies of the chemistry [**2a**-P]$^-$-derived, low-coordinate phosphorus compounds in free form. Potentially, addition of N_2O or an electron-withdrawing olefin may effectively sequester the Nb(N[Np]Ar)$_3$ fragment from its complexed, phosphorus-containing unit.

4 Experimental Procedures

4.1 General Synthetic Considerations

Unless otherwise stated, all manipulations were carried out at room temperature, under an atmosphere of purified dinitrogen using a Vacuum Atmospheres glove box or Schlenk techniques. All solvents were obtained anhydrous and oxygen-free according to standard purification procedures. Tetrahydrofuran-d_8 (THF-d_8) was vacuum transferred from Na metal and stored in the glove box over 4 Å molecular sieves for at least 3 d prior to use. Benzene-d_6 (C_6D_6) was degassed and stored similarly. Celite 435 (EM Science) and 4 Å molecular sieves (Aldrich) were dried under vacuum at 250 °C overnight and stored under dinitrogen. Elemental phosphorus (P_4) was recrystallized from toluene (C_7H_8) and stored under dinitrogen prior to use. Lead(II) triflate ($Pb(OTf)_2$) was prepared by treating $PbCl_2$ with 2.0 equiv of $LiN(SiMe_3)_2$ in *n*-pentane (to form $Pb(N(SiMe_3)_2)_2$), followed by protonolysis with triflic acid (HO_3SCF_3). Solid, colorless $Pb(OTf)_2$ was isolated by filtration and washing with *n*-pentane. The chloroiminophosphine, ClP=NMes*, was prepared as specified in the literature.[69] All other reagents were obtained from commercial sources and used as received or purified according to standard procedures. All glassware was oven dried at a temperature of 230 °C prior to use.

Solution ^{1}H, ^{13}C{^{1}H}, ^{31}P{^{1}H} and ^{119}Sn{^{1}H} NMR spectra were recorded using Varian XL-300 MHz and Varian INOVA 500 MHz spectrometers. ^{1}H and ^{13}C chemical shifts are reported referenced to the residual solvent resonances of 7.16 ppm (^{1}H) and 128.3(t) ppm (^{13}C) for benzene-d_6 or 1.73 ppm (^{1}H) and 67.57 ppm (^{13}C) for THF-d_8. ^{31}P{^{1}H} chemical shifts are reported referenced to the external standard H_3PO_4 (85 %, 0.0 ppm). ^{119}Sn{^{1}H} chemical shifts are reported referenced to the external standard $SnMe_4$ (neat, 0.0 ppm). Solution IR spectra were recorded on a Perkin-Elmer 1600 Series FTIR spectrometer. All spectra were recorded in C_6D_6 using a KBr plated solution cell. Solvent peaks were digitally subtracted from all spectra using an authentic spectrum obtained immediately prior to that of the sample. Combustion analyses were carried out by H. Kolbe Microanalytisches Laboratorium, Mülheim an der Ruhr, Germany.

4.2 Synthesis of (μ_2:η^2,η^2-P_2)[Nb(N[Np]Ar)$_3$]$_2$ ((μ-P_2)[2a]$_2$)

To a benzene solution of **1a**-H (300 mg, 0.452 mmol, 5.0 mL) was added over the course of 5 min to a benzene solution of white phosphorus (P_4) (16.8 mg, 0.135 mmol, 0.3 equiv, 5.0 mL). The reaction mixture turned dark green upon mixing and was allowed to stir for an additional 1.5 h. at which point all volatile materials were removed *in vacuo*. The resulting dark green residue was extracted with diethyl ether (6 mL), filtered through Celite and dried again *in vacuo*. The residue was redissolved in diethyl ether (3 mL) and chilled to –35 °C for one week whereupon small, dark green single crystals were obtained and collected. Yield: 0.375 g, 60 %. ^{1}H NMR (500 MHz, C_6D_6, 23 °C): δ 6.98 (bs, 12H, o-Ar), 6.59 (s, 6H, p-Ar), 4.23 (bs, 12H, N-C*H*$_2$), 2.25 (s, 36H, Ar-C*H*$_3$), 0.97 (s, 54H, *t*-Bu); ^{13}C{^{1}H} NMR (125.66 MHz, C_6D_6, 23 °C): δ 154.2 (aryl ipso), 138.1 (m-Ar), 126.6 (o-Ar), 124.4 (p-Ar), 73.4 (N-*C*H$_2$), 37.3 (*C*(CH$_3$)$_3$), 30.5 C(*C*H$_3$)$_3$), 22.1 (Ar-*C*H$_3$); ^{31}P{^{1}H} NMR (202.6 MHz, C_6D_6, 23°C): δ 399.3 (bs); FTIR (KBr windows, C_6D_6 solution): 2951, 1600, 1586, 1475, 1365, 1062, 1001, 686 cm^{-1}. Anal. Calcd. for $C_{78}H_{120}N_6P_2Nb_2$: C, 67.42; H, 8.70; N, 6.05. Found: C, 67.21; H, 8.58; N, 5.87.

4.3 Synthesis of [Na(Et$_2$O)[PNb(N[Np]Ar)$_3$]]$_2$ ([Na(Et$_2$O)][2a-P]]$_2$)

To a green THF solution of (μ-P_2)[**2a**]$_2$ (1.00g, 1.50 mmol, 10 mL) was added 1.0% sodium amalgam (Na: 0.115 g, 3.3 equiv/Nb) and stirred vigorously for 2.5 h while gradually changing in color to dark orange. The resulting solution was decanted from the amalgam, filtered through Celite and evaporated to dryness. The dark orange residue was then extracted with Et_2O (5 mL) and cooled at –35 °C for 3 d whereupon large yellow-orange crystals were obtained. Yield: 0.759 g, 64% in two crops. ^{1}H NMR (300 MHz, C_6D_6, 23 °C): δ 6.98 (s, 6H, o-Ar), 6.39 (s, 3H, p-Ar), 4.45 (s, 6H, N-C*H*$_2$), 2.00 (s, 18H, Ar-C*H*$_3$), 1.03 (s, 27H, *t*-Bu); ^{13}C{^{1}H}NMR (75.0 MHz, C_6D_6, 23 °C): δ 153.7 (aryl ipso), 138.8 (m-Ar), 125.9 (p-Ar), 122.2 (o-Ar), 75.0 (N-*C*H$_2$), 35.7 (*C*(CH$_3$)$_3$), 32.0 (C(*C*H$_3$)$_3$), 21.9 (Ar-*C*H$_3$); ^{31}P{^{1}H} NMR (202.6 MHz, 23 °C): δ 949.5 (C_6D_6, bs, $\nu_{1/2}$ = 496.0 Hz), 1019.8 (THF, bs, $\nu_{1/2}$ = 166 Hz, formulated as Na(THF)$_x$[**2a**-P]; Combustion analysis not obtained due to repeated and non-stoichiometric desolvation of etherate.

4.4 Synthesis of Na(12-crown-4)$_2$[PNb(N[Np]Ar)$_3$] Na(12-c-4)$_2$[2a-P]

To a THF solution of Na(THF)$_x$[**2a**-P] (0.100 g, 0.115 mmol, 5 mL) was added a THF solution of 12-crown-4 (0.040 g, 0.231 mmol, 2 mL) over the course of 5 min. The reaction mixture was allowed to stir for 30 min, after which it was concentrated to a volume of 2 mL and filtered through a small plug of Celite. N-Pentane (2 mL) was added and the resulting solution was stored at –35 °C overnight whereupon small red-orange crystals were obtained. Yield: 0.099 g, 80%. ^{1}H NMR (500 MHz,THF-d$_8$, 23 °C): δ 6.48 (s, 6H, o-Ar), 6.03 (s, 6H, p-Ar), 4.42 (s, 6H, N-C*H*$_2$), 3.66 (s, 32H,12-c-4), 1.95 (s, 18H, Ar-C*H*$_3$), 0.94 (s, 27H, *t*-Bu); ^{13}C{^{1}H}NMR (125.7 MHz, THF-d$_8$, 23 °C): δ 158.4 (aryl ipso), 137.0 (m-Ar), 120.9 (o-Ar), 120.0 (p-Ar), 76.5 (N-*C*H$_2$), 66.7 (12-c-4), 36.7 (*C*(CH$_3$)$_3$), 30.6 (C(*C*H$_3$)$_3$), 22.0 (Ar-*C*H$_3$); ^{31}P{^{1}H} NMR (202.6 MHz, THF-d$_8$, 23 °C): δ 1110.8 (bs, $\nu_{1/2}$ = 170 Hz) Anal. Calcd. for $C_{55}H_{92}N_3O_8PNaNb$: C, 61.73; H, 8.66; N, 3,93; Found: C, 61.19; H, 8.42; N, 4.07.

4.5 Synthesis of Phosphinidene Complexes 2a-PEMe$_3$ and 2a-PP(t-Bu)$_2$.

Separately, a 5 mL THF solution of Na(THF)$_x$[**2a**-P] (0.250 g, 0.316 mmol) and a 2 mL THF solution containing 0.95 equiv of the corresponding electrophile (ClSiMe$_3$ – **2a**-PSiMe$_3$,

$ClSnMe_3$ – **2a**-$PSnMe_3$, $ClP(t\text{-}Bu)_2$ – **2a**-$PP(t\text{-}Bu)_2$, $ClPPh_2$ – **2a**-$PPPh_2$) were frozen in a glove box cold well (liquid N_2). Upon removal from the cold well, approximately 0.6 mL of the thawing solution containing the electrophile was added dropwise over 1 min. to the thawing solution of $Na(THF)_x$[**2a**-P], eliciting a color change from dark yellow to red-orange. The reaction mixture was allowed to stir for an additional 3 min. whereupon both solutions were placed back into the cold well. This procedure was repeated two more times until complete addition of the electrophile was achieved. The reaction mixture was then allowed to warm to room temperature and stirred for an additional 30 min. before being evaporated to dryness in vacuo. The resulting residue was extracted with *n*-pentane (3 mL), filtered through Celite and the filtrate evaporated to dryness in vacuo. The resulting residue was then dissolved in a minimum of Et_2O, except for **2a**-$PP(t\text{-}Bu)_2$, which was dissolved in a minimum of *n*-pentane. These solutions were chilled at –35 °C for 1 – 2 d whereupon crystals were obtained.

2a-$PSiMe_3$: Orange crystals, 75%. ^1H NMR (300 MHz, C_6D_6, 23 °C): δ 6.60 (s, 6H, o-Ar), 6.52 (s, 6H, p-Ar), 4.44 (s, 6H, N-CH_2), 2.11 (s, 18H, Ar-CH_3), 1.08 (s, 27H, *t*-Bu), 0.60 (s, 9H, $Si(CH_3)_3$); $^{13}C\{^1H\}$NMR (125.7 MHz, C_6D_6, 23 °C); δ153.2 (aryl ipso), 138.8 (m-Ar), 126.0 (p-Ar), 121.5 (o-Ar), 77.9 (N-CH_2), 36.2 ($C(CH_3)_3$), 30.0 ($C(CH_3)_3$), 21.8 (Ar-CH_3); 5.5 ($Si(CH_3)_3$); $^{31}P\{^1H\}$ NMR (202.5 MHz, C_6D_6, 23 °C): δ 526.4 (bs); Anal. Calcd. for $C_{42}H_{69}N_3PSiNb$: C, 65.68; H; 9.06, N, 5.47. Found: C, 65.50; H, 8.98; N, 5.50.

2a-$PSnMe_3$: Red crystals, 88%. ^1H NMR (500 MHz, C_6D_6, 23 °C): δ 6.69 (s, 6H, o-Ar), 6.49 (s, 6H, p-Ar), 4.42 (s, 6H, N-CH_2), 2.11 (s, 18H, Ar-CH_3), 1.05 (s, 27H, *t*-Bu), 0.62 (s, 9H, $Sn(CH_3)_3$, $^2J_{HSn}$ = 26.4 Hz (^{119}Sn), $^2J_{HSn}$ = 25.2 Hz (^{117}Sn)); $^{13}C\{^1H\}$NMR (125.7 MHz, C_6D_6, 23 °C); δ 152.9 (aryl ipso), 138.7 (m-Ar), 126.1 (p-Ar), 122.4 (o-Ar), 75.6 (N-CH_2), 37.0 ($C(CH_3)_3$), 30.2 ($C(CH_3)_3$), 21.8 (Ar-CH_3); –1.2 ($Sn(CH_3)_3$); $^{31}P\{^1H\}$ NMR (202.5 MHz, C_6D_6, 23 °C): δ 607.0 (bs, $^{117/119}Sn$ coupling was not resolved); Anal. Calcd. for $C_{42}H_{69}N_3PSnNb$: C, 58.75; H, 8.10; N, 4.89. Found: C, 58.43; H, 8.00; N, 4.94.

2a-$PP(t\text{-}Bu)_2$: Orange crystals, 60%. ^1H NMR (500 MHz, C_6D_6, 23 °C): δ 6.68 (s, 6H, o-Ar), 6.58 (s, 6H, p-Ar), 4.22 (s, 6H, N-CH_2), 2.19 (s, 18H, Ar-CH_3), 1.41 (d, 18H, $P(C(CH_3)_3)_2$, $^3J_{HP}$ = 14.5 Hz), 0.90 (s, 27H, *t*-Bu); $^{13}C\{^1H\}$NMR (125.7 MHz, C_6D_6, 23 °C); δ 156.3 (aryl ipso), 137.6 (m-Ar), 125.7 (p-Ar), 124.3 (o-Ar), 76.6 (N-CH_2), 38.3 ($P(C(CH_3)_3)_2$, $^1J_{CP}$ = 6.23 Hz), 36.3 ($C(CH_3)_3$), 32.8 ($P(C(CH_3)_3)_2$, $^2J_{CP}$ = 7.54 Hz), 29.9 ($C(CH_3)_3$), 21.5 (Ar-CH_3); $^{31}P\{^1H\}$ NMR (202.5 MHz, C_6D_6, 23 °C): δ 405.5 (d, $^1J_{PP}$ = 425.1 Hz), 80.6 (d, $^1J_{PP}$ = 425.1 Hz); Anal. Calcd. for $C_{47}H_{78}N_3P_2Nb$: C, 67.20; H, 9.36; N, 5.00. Found: C, 66.91; H, 9.03; N, 4.97.

2a-$PPPh_2$: Red crystals, 65%. ^1H NMR (500 MHz, C_6D_6, 23 °C): δ 7.85 (m, 4H, o-Ph), 7.09 (m, 4H, m-Ph), 7.01 (m, 2H, p-Ph), 6.78 (s, 6H, o-Ar), 6.52 (s, 3H, p-Ar), 3.90 (s, 6H, N-CH_2), 2.15 (s, 18H, Ar-CH_3), 0.79 ((s, 27H, *t*-Bu); $^{13}C\{^1H\}$NMR (75.0 MHz, C_6D_6, 23 °C); δ 155.3 (aryl ipso), 139.2 (Ph ipso), 138.0 (m-Ar), 133.8 (m-Ph), 129.2 (p-Ph), 128.7 (o-Ph), 126.2 (o-Ar), 124.2 (p-Ar), 73.9 (N-CH_2), 36.3 ($C(CH_3)_3$), 30.0 ($C(CH_3)_3$), 21.9 (Ar-CH_3); $^{31}P\{^1H\}$ NMR (121.5 MHz, C_6D_6, 23 °C): δ 388.5 (d, $^1J_{PP}$ = 439.8 Hz), 16.1 (d, $^1J_{PP}$ = 439.8 Hz); Anal. Calcd. for $C_{51}H_{70}N_3P_2Nb$: C, 69.61; H, 8.02; N, 4.68. Found: C, 69.88; H, 7.89; N, 4.63.

4.6 Synthesis of (η^2-*P,P*–PPNMes*)Nb(N[Np]Ar)$_3$ (2a-PPNMes*, Mes* = 2,4,6-tri-*tert*-butylphenyl).

Separately, a 5 mL THF solution of Na(THF)$_x$[**2a**-P] (0.487 g, 0.616 mmol) and a 2 mL Et_2O solution of ClP=NMes* (0.190 g, 0.585 mmol, 0.95 equiv) were frozen in a glove box cold well (liquid N_2). Upon removal from the cold well, approximately 0.6 mL of the thawing solution containing Cl–P=NMes* was added dropwise over 1.0 min. to the thawing solution of Na(THF)$_x$[**2a**-P], eliciting a color change from dark yellow to red-orange. The reaction mixture was allowed to stir for an additional 3 min. whereupon both solutions were placed back into the cold well. This procedure was repeated two more times until complete addition of Cl–P=NMes* was achieved. The reaction mixture was then allowed to warm to room temperature and stirred for an additional 30 min. before being evaporated to dryness in vacuo. The resulting residue was extracted with *n*-pentane (3 mL), filtered through Celite and the filtrate evaporated to dryness in vacuo. The resulting lipophilic, orange-brown residue was then dissolved in 2 mL of *n*-pentane and chilled at –35 °C for 2 d, effecting the precipitation of pure **2a**-PPNMes* (^{1}H NMR) as a red-orange powder (55% average yield). Analytically pure, single crystals of **2a**-PPNMes* were obtained by recrystallization of powdered **2a**-PPNMes* from Et_2O at –35 °C. ^{1}H NMR (500 MHz, C_6D_6, 20 °C): δ 7.74 (s, 2H, m-Mes*), 6.59 (s, 9H, o- and p-Ar), 4.12 (s, 6H, N-CH_2), 2.12 (s, 18H, Ar-CH_3), 1.92 (s, 18H, o-(C(CH_3)$_3$)$_2$Mes*), 1.47 (s, 9H, p-(C(CH_3)$_3$)Mes*), 0.82 (s, 27H, *t*-Bu); ^{31}P{^{1}H} NMR (121.5 MHz, C_6D_6, 20 °C): δ 324 (dd, $^1J_{PP}$ = 650.5 Hz); Anal. Calcd. for $C_{57}H_{89}N_4P_2Nb$: C, 69.49; H, 9.11; N, 5.69.

4.7 Thermolysis of (η^2-*P,P*–PPNMes*)Nb(N[Np]Ar)$_3$: Synthesis of Mes*N=Nb(N[Np]Ar)$_3$ (2a-NMes*, Mes* = 2,4,6-tri-*tert*-butylphenyl).

A THF solution of **2a**-PPNMes* (0.250 g, 0.253 mmol, 4 mL) was added to a thick-walled, glass reaction vessel, which was subsequently heated to 70 °C for 45 min. During heating, the reaction mixture changed in color from red-orange to yellow-orange, concomitant with the formation of a small amount of brown-black precipitate. All volatile materials were removed in vacuo and the resulting brown residue was extracted with *n*-pentane (3 mL) and filtered through Celite. The filtrate was concentrated to a volume of 1 mL and stored at –35 °C for 3 d, whereupon golden yellow single crystals of **2a**-NMes* were obtained and collected. Yield: 48%. ^{1}H NMR (500 MHz, C_6D_6, 20 °C): δ 7.44 (s, 2H, m-Mes*), 7.02 (s, 6H, o-Ar), 6.55 (s, 3H, p-Ar), 3.90 (s, 6H, N-CH_2), 2.21 (s, 18H, Ar-CH_3), 1.69 (s, 18H, o-(C(CH_3)$_3$)$_2$Mes*), 1.35 (s, 9H, p-(C(CH_3)$_3$)Mes*), 0.89 (s, 27H, *t*-Bu); Anal. Calcd. for $C_{57}H_{89}N_4Nb$: C, 69.49; H, 9.11; N, 5.69.

4.8 Synthesis of (μ_2:η^3,η^3-*cyclo*–EP$_2$)[Nb(N[Np]Ar)$_3$]$_2$ Complexes ((EP$_2$)[**2a**]$_2$; E =Ge, Sn, Pb).

Separately, a 5 mL THF solution of Na(THF)$_x$[**2a**-P] (0.300 g, 0.380 mmol) and a 2 mL THF solution containing 0.47 equiv of the corresponding divalent group 14 salt ($GeCl_2$·dioxane for (GeP$_2$)[**2a**]$_2$, $SnCl_2$ for (SnP$_2$)[**2a**]$_2$ and Pb(OTf)$_2$ for (PbP$_2$)[**2a**]$_2$) were frozen in a glove box cold well. Upon removal from the cold well, approximately 0.6 mL of the thawing solution containing the salt was added dropwise over 1 min to the thawing solution of Na(THF)$_x$[**2a**-P]. The reaction mixture was allowed to stir for an additional 3 min whereupon both solutions were placed back into the cold well. This procedure was repeated two more times until complete addition of the divalent group-14 salt was achieved. The reaction mixture was then

allowed to warm to room temperature and stirred for an additional 30 min before being evaporated to dryness in vacuo. The residue was extracted with *n*-pentane (3 mL), filtered through Celite and the filtrate evaporated to dryness again in vacuo. Crystallizations of each complex were effected by storing a saturated Et_2O solution at a temperature of –35 °C for 1–3 d.

(GeP_2)[**2a**]$_2$: Red crystals, 70%. ^{1}H NMR (500 MHz, C_6D_6, 20 °C): δ 6.69 (s, 6H, o-Ar), 6.60 (s, 3H, p-Ar), 4.42 (s, 6H, N-CH_2), 2.20 (s, 18H, Ar-CH_3), 1.02 (s, 27H, *t*-Bu); ^{13}C{^{1}H}NMR (125.7 MHz, C_6D_6, 20 °C); δ155.9 (aryl ipso), 137.7 (m-Ar), 126.4 (p-Ar), 125.2 (o-Ar), 80.3 (N-*C*H$_2$), 37.3 (*C*(CH$_3$)$_3$), 30.8 (C(*C*H$_3$)$_3$), 21.9 (Ar-*C*H$_3$); ^{31}P{^{1}H} NMR (202.5 MHz, C_6D_6, 20 °C): δ –15.7 (s); Anal. Calcd. for $C_{78}H_{120}N_6P_2GeNb$: C, 64.07; H; 8.27, N, 4.97. Found: C, 65.50; H, 8.98; N, 5.22.

(SnP_2)[**2a**]$_2$: Green crystals, 40%. ^{1}H NMR (500 MHz, C_6D_6, 20 °C): δ 6.76 (s, 6H, o-Ar), 6.60 (s, 3H, p-Ar), 4.35 (s, 6H, N-CH_2), 2.22 (s, 18H, Ar-CH_3), 1.02 (s, 27H, *t*-Bu); ^{13}C{^{1}H}NMR (125.7 MHz, C_6D_6, 20 °C); δ156.2 (aryl ipso), 137.7 (m-Ar), 126.3 (p-Ar), 125.0 (o-Ar), 80.0 (N-*C*H$_2$), 37.4 (*C*(CH$_3$)$_3$), 30.8 (C(*C*H$_3$)$_3$), 21.9 (Ar-*C*H$_3$); ^{31}P{^{1}H} NMR (202.5 MHz, C_6D_6, 20 °C): δ 47.8 (t, $^1J_{SnP}$ = 205.2 Hz); ^{119}Sn NMR (186.5 MHz, C_6D_6, 20 °C): δ –696.4 (bs, $\nu_{1/2}$ = 1300.8 Hz); Anal. Calcd. for $C_{78}H_{120}N_6P_2SnNb$: C, 62.11; H; 8.02, N, 5.57. Found: C, 61.75; H, 7.91; N, 5.66.

(PbP_2)[**2a**]$_2$: Green crystals, 30%. ^{1}H NMR (500 MHz, C_6D_6, 20 °C): δ 6.78 (s, 6H, o-Ar), 6.62 (s, 3H, p-Ar), 4.45 (s, 6H, N-CH_2), 2.23 (s, 18H, Ar-CH_3), 1.02 (s, 27H, *t*-Bu) ^{31}P{^{1}H} NMR (202.5 MHz, C_6D_6, 20 °C): δ 115.2 (s with shoulders); Due to the rapid decomposition of **1**-Pb, satisfactory ^{13}C{^{1}H} NMR data and combustion analysis were not obtained.

4.9 Computational Details

All DFT calculations were carried out utilizing the Amsterdam Density Functional (ADF) program suite,[107,108] version 2004.01.[109] The all-electron, Slater-type orbital (STO) basis sets employed were of triple-ζ quality augmented with two polarization functions and incorporated relativistic effects using the zero-order regular approximation[110,111] (ADF basis ZORA/TZ2P). The local exchange-correlation potential of Vosko et al.[112] (VWN) was augmented self-consistently with gradient-corrected functionals for electron exchange according to Becke,[113] and electron correlation according to Perdew.[114,115] This nonlocal density functional is termed BP86 in the literature and has been shown to give excellent results both for the geometries and for the energetics of transition metal and main group systems.[116] Crystallographically determined atomic coordinates were used as input for all geometry optimized structures, which were then subjected to a harmonic frequency calculation to ensure they represented local minima on the potential energy surface. Pictorial orbital representations from the ADF results were generated using either the program MOLEKEL[117] aided with the use of the ADF DENSF utility or the program Molden[118] aided by the ADF ADFrom utility. The output generated from geometry optimization calculations were used as input for the ADF NMR program.[98] A second round of single point calculations were performed on the optimized atomic coordinates obtained from the ADF output with the inclusion of spin-orbit coupling. The spin-orbit-included results were subsequently input to

the NMR program to obtain the spin-orbit component to the calculated ^{31}P chemical shielding tensor.

4.10 Crystallographic Structure Determinations.

The X-ray crystallographic data collections were carried out on a Siemens Platform three-circle diffractometer mounted with a CCD or APEX-CCD detector and outfitted with a low-temperature, nitrogen-stream aperture. The structures were solved using either direct methods or the Patterson method in conjunction with standard difference Fourier techniques and refined by full-matrix least-squares procedures. A summary of crystallographic data for all complexes is given in Tables 3 – 5. The systematic absences in the diffraction data are uniquely consistent with the assigned monoclinic space groups for complexes (μ-P)[**2a**]$_2$, [Na(Et_2O)[**2a**-P]]$_2$, (SnP_2)[**2a**]$_2$ and (PbP_2)[**2a**]$_2$. The diffraction data for complex **2a**-$PPPh_2$ were uniquely consistent with the orthorhombic space group Pbca. No symmetry higher than triclinic was indicated in the diffraction data for Na(12-c-4)[**2a**-P], **2a**-$PSnMe_3$, **2a**-PP(*t*-Bu)$_2$, **2a**-PPNMes* and **2a**-NMes. Complex (GeP_2)[**2a**]$_2$ was refined in the chiral, cubic space group $P2_13$ (flack parameter = -0.01(3)). These choices led to chemically sensible and computationally stable refinements. An empirical absorption correction (SADABS or ψ-scans) was applied to the diffraction data for all structures. All non-hydrogen atoms were refined anisotropically. All hydrogen atoms were treated as idealized contributions and refined isotropically. The unit cell for both (SnP_2)[**2a**]$_2$ and (PbP_2)[**2a**] contained molecules of diethyl ether possessing two-site positional disorder. The disordered molecules were modeled and refined anisotropically in the case of (SnP_2)[**2a**]$_2$, and isotropically without hydrogen atoms for (PbP_2)[**2a**]$_2$. These models led to noticeable improvements in the final residual values for each structure.

Complex (GeP_2)[**2a**]$_2$ was found to possess compositional disorder in the cyclo-GeP_2 ring due to coincidental alignment of the Nb–Nb vector with a three-fold axis of the $P2_13$ space group. Approximation of each ring position as $Ge_{0.33}P_{0.67}$ resulted in the best fit to the diffraction data, whereas other Ge_xP_y permutations adversely affected the refinement statistics and led to significant residual electron density in the difference map surrounding the area of interest. The pictorial representation of (GeP_2)[**2a**]$_2$ found in the text is that in which both P and Ge have been fixed to share the same atomic coordinate with site occupancy factor (SOF) of $Ge_{0.33}P_{0.67}$. Free refinement of each atom with the same SOF resulted in a separation of atomic coordinates, where P converged to a position 0.34 Å closer to the Nb-Nb vector relative to Ge (Figure 20). However, invocation of crystallographic symmetry generates two concentric equilateral triangles, where the inner, 3P-ring contains an anomalously short P–P bond length of 2.156 Å (Figure 20). This latter model improved the final residual value, R_1, by approximately 0.3 % and has been deposited with the Cambridge Crystallographic Data Center (CCDC). Although the atomic positions in (GeP_2)[**2a**]$_2$ could be separated and refined freely, the crystallographically imposed three-fold symmetry prevents an accurate elucidation of the molecular geometry by masking small translations of the Nb(N[Np]Ar)$_3$ fragment relative to the central GeP_2 ring via lattice-averaging of three equally probable orientations in the crystal. Therefore, the site-fixed and freely refined models lead to anomalously long and short P–P bond lengths, respectively, because alignment of the Nb–Nb vector with a crystallographic three-fold axis disallows the translational movement evidently required to reveal a chemically sensible molecular geometry.

In addition, $(GeP_2)[\mathbf{2a}]_2$ contained two-site positional disorder for the methylene carbons of the neopentyl residues, resulting in two corresponding tetrahedral conformations of the *tert*-butyl substituents. Modeling this disorder resulted in a final occupancy ratio of 65:35 for the two conformations as dictated by the refinement statistics and led to improved residual values. All software utilized for diffraction data processing and crystal-structure solution and refinement were contained in the SHELXTL (v6.14) program suite (G. Sheldrick, Bruker XRD, Madison, WI).

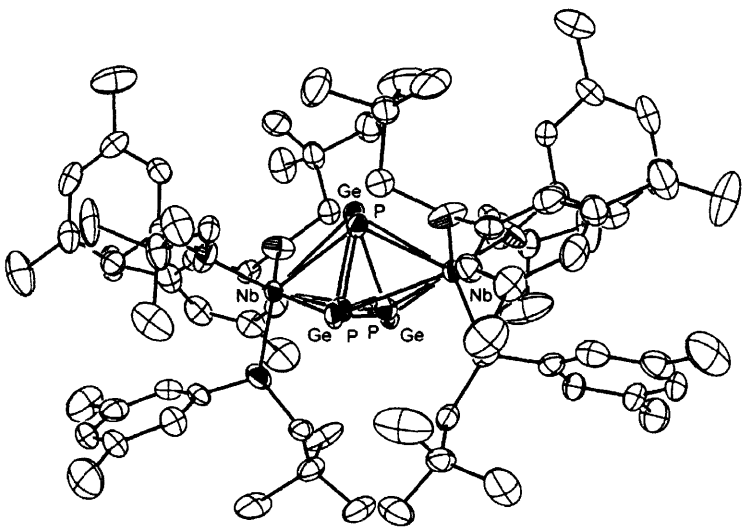

Figure 20. ORTEP diagram of the freely-refined crystallographic model of $(GeP_2)[\mathbf{2a}]_2$. Note that crystallographic symmetry generates two-concentric triangles for the cyclo-GeP_2 unit. Only the major-occupancy component of the disordered neopentyl groups is shown. Thermal Ellipsoids are drawn at the 35% probability level.

Table 3. Crystallographic Data for Complexes (μ-P)[**2a**]$_2$, [Na(Et$_2$O)[**2a**-P]]$_2$, Na(12-c-4)[**2a**-P], **2a**-PSnMe$_3$ and **2a**-PP(*t*-Bu)$_2$

	(μ-P)[**2a**]$_2$	[Na(Et$_2$O)[**2a**-P]]$_2$	Na(12-c-4)[**2a**-P]	**2a**-PSnMe$_3$	**2a**-PP(*t*-Bu)$_2$
Formula	$C_{78}H_{120}N_6NbP_2$	$C_{43}H_{70}N_3NaPNb$	$C_{55}H_{93}N_3PO_8NaNb$	$C_{43}H_{69}N_3PSiNb$	$C_{47}H_{78}N_3P_2Nb$
Crystal System	Monoclinic	Monoclinic	Triclinic	Triclinic	Triclinic
Space Group	$P2_1/c$	$P2_1/n$	P-1	P-1	P-1
a, Å	13.931(2)	14.9081(10)	13.3942(9)	10.9652(6)	11.4084(6)
b, Å	16.519(3)	18.7760(13)	13.7318(9)	11.5308(7)	13.0157(6)
c, Å	34.582(5)	16.7805(11)	18.3879(12)	18.4233(10)	18.0594(9)
α, deg	90	90	93.9330(10)	82.4880(10)	75.4330(10)
β, deg	92.088(3)	95.4020(10)	108.5770(10)	88.4380(10)	77.5930(10)
γ, deg	90	90	90.7220(10)	79.5050(10)	68.9620(10)
V, Å^3	7953(2)	4676.2(5)	3196.1(4)	2270.8(2)	2399.3(2)
Z	4	4	2	2	2
radiation	Mo-K$_\alpha$ (λ = 0.71073 Å)				
D(calcd), g/cm^3	1.161	1.123	1.187	1.256	1.163
μ (Mo Kα), mm^{-1}	0.371	0.332	0.272	0.886	0.035
temp, K	183(2)	183(2)	183(2)	183(2)	183(2)
No. Reflections	31335	17328	12890	8524	9261
No. Ind. Ref.(R$_{int}$)	10395 (0.0682)	6097(0.0536)	8289(0.0809)	5829(0.0181)	6206(0.0361)
F(000)	2968	1696	1228	896	904
GoF (F^2)	1.208	1.059	1.010	1.081	1.052
$R(F)$, %[a]	0.0523	0.0422	0.0824	0.0247	0.0457
$wR(F)$, %[a]	0.0939	0.1098	0.1966	0.0613	0.1057

[a] Quantity minimized = $wR(F^2) = \sum[w(F_o^2 - F_c^2)^2]/\sum[(wF_o^2)^2]^{1/2}$; $R = \sum\Delta/\sum(F_o)$, $\Delta = |(F_o - F_c)|$, $w = 1/[\sigma 2(F_o^2) + (aP)^2 + bP]$, $P = [2F_c^2 + \mathrm{Max}(F_o,0)]/3$

Table 4. Crystallographic Data for Complexes **2a**-PPPh$_2$, **2a**-PPNMes*, **2a**-NMes and (GeP$_2$)[**2a**]$_2$

	2a-PPPh$_2$	**2a**-PPNMes*·(Et$_2$O)	**2a**-NMes*	(GeP$_2$)[**2a**]$_2$
Formula	$C_{51}H_{70}N_3P_2Nb$	$C_{57}H_{79}N_4P_2Nb$	$C_{57}H_{79}N_4Nb$	$C_{78}H_{120}GeN_6Nb_2P_2$
Crystal System	Orthorhombic	Triclinic	Triclinic	Cubic
Space Group	*P*bca	*P*-1	*P*-1	$P2_13$
a, Å	21.3714(14)	11.7432(8)	12.3211(5)	20.1101(4)
b, Å	18.9237(12	16.4705(11)	13.4990(5)	20.1101(4)
c, Å	24.3094(17)	17.3764(12)	17.1933(7)	20.1101(4)
α, deg	90	69.6728(10)	88.4280(10)	90
β, deg	90	78.3227(10)	88.6190(10)	90
γ, deg	90	86.7900(10)	71.9150(10)	90
V, Å^3	9831.4(11)	3086.0(4)	2716.97(19)	8132.8(3)
Z	8	2	2	4
radiation	Mo-K$_\alpha$ (λ = 0.71073 Å)			
D(calcd), g/cm^3	1.189	1.140	1.116	1.194
μ (Mo Kα), mm^{-1}	0.345	0.287	0.259	0.725
temp, K	183(2)	100(2)	100(2)	193(2)
No. Reflections	27290	56680	15868	55637
No. Ind. Ref.(R$_{int}$)	4588 (0.0896)	13572(0.0377)	9255(0.0504)	4639(0.0840)
F(000)	3744	1144	980	3096
GoF (F^2)	1.485	1.125	1.025	1.029
$R(F)$, %[a]	0.0966	0.0432	0.0520	0.0372
$wR(F)$, %[a]	0.1880	0.1071	0.1193	0.0729

[a] Quantity minimized = $wR(F^2) = \sum[w(F_o^2 - F_c^2)^2]/\sum[(wF_o^2)^2]^{1/2}$; $R = \sum\Delta/\sum(F_o)$, $\Delta = |(F_o - F_c)|$, $w = 1/[\sigma 2(F_o^2) + (aP)^2 + bP]$, $P = [2F_c^2 + \mathrm{Max}(F_o,0)]/3$

Table 5. Crystallographic Data for Complexes $(SnP_2)[\mathbf{2a}]_2$ and $(PbP_2)[\mathbf{2a}]_2$

	1-Sn·$(Et_2O)_{0.5}$	**1**-Pb·$(Et_2O)_{1.5}$
Formula	$C_{80}H_{125}N_6Nb_2O_{0.50}P_2Sn$	$C_{84}H_{125}N_6Nb_2O_{1.5}P_2Pb$
Crystal System	Monoclinic	Monoclinic
Space Group	$P2_1/n$	$P2_1/c$
a, Å	12.2374(9)	18.47(3)
b, Å	32.877(3)	21.51(3)
c, Å	20.8487(15)	22.43(3)
α, deg	90	90
β, deg	100.3670(10)	107.24(6)
γ, deg	90	90
V, Å^3	8251.0(11)	8511(22)
Z	4	4
radiation	Mo-K_α (λ = 0.71073 Å)	
D(calcd), g/cm^3	1.244	1.325
μ (Mo Kα), mm^{-1}	0.656	2.321
temp, K	193(2)	193(2)
No. Reflections	33365	128630
No. Ind. Ref.(R_{int})	11724(0.1038)	22856(0.0769)
F(000)	3252	3508
GoF (F^2)	1.063	1.033
$R(F)$, %[a]	0.0747	0.0420
$wR(F)$, %[a]	0.1170	0.1060

[a] Quantity minimized = $wR(F^2) = \sum[w(F_o^2 - F_c^2)^2]/\sum[(wF_o^2)^2]^{1/2}$; $R = \sum\Delta/\sum(F_o)$, $\Delta = |(F_o - F_c)|$, $w = 1/[\sigma 2(F_o^2) + (aP)^2 + bP]$, $P = [2F_c^2 + \text{Max}(F_o,0)]/3$.

5 References

1. Becker, P. *Phosphates and Phosphoric Acid*, Marcel Dekker, New York, 1988.
2. Greenwood, N. N.; Earnshaw, A. *Chemistry of the Elements*, 2nd ed.; Butterworth-Heinemann, Oxford, 1997; Chapter 12, pp. 473-497.
3. Engel, R. *Synthesis of Carbon Phosphorus Bonds*, 2nd ed.; CRC Press, Boca Raton, 2004.
4. Quin, L. D. *A Guide to Organophosphorus Chemistry*; Wiley, New York, 2000.
5. Cotton, F. A.; Wilkinson, G. *Advanced Inorganic Chemistry*, 5th ed.; Wiley, New York, 1988; Chapter 11, pp. 391-395.
6. Ehses, M; Romerosa, A.; Peruzzini, M. *Top. Curr. Chem.* **2002**, *220*, 107.
7. Peruzzini, M.; De los Rios, I.; Romerosa, A.; Vizza, F. *Eur. J. Inorg. Chem.* **2001**, *3*, 593.
8. Scherer, O. J. *Acc. Chem. Res.* **1999**, *32*, 751.
9. Goh, L. Y.; Chu, C. K.; Wong, R. C. S.; Hambley, T. W. *Chem. Commun.* **1979**, 1951.
10. Chisholm, M. H.; Folting, K.; Huffman, J. C. Koh, J. J. *Polyhedron*, **1985**, *4*, 893.
11. Schmid, G.; Kempny, H. P *Z. Anorg. Allg. Chem.* **1977**, *432*, 160.
12. Vizi-Orosz, *J. Organomet. Chem.* **1976**, *111*, 61.
13. Lindsell, W. E.; McCullough, K. J.; Welch, A. J. *J. Am. Chem. Soc.* **1983**, *105*, 4487.
14. Scherer, O. J.; Vondung, J.; Wolmershauser, G. *Angew. Chem. Int. Ed. Engl.* **1989**, *28*, 1355.
15. Di Varia, M.; Midollini, S.; Sacconi, L. *J. Am. Chem. Soc.* **1979**, *101*, 1757.
16. Di Varia, M.; Stoppioni, P. *Polyhedron*, **1987**, *6*, 351.
17. Chisholm, M. H.; Folting, K.; Pasterczyk, J. W. *Inorg. Chem.* **1988**, *27*, 3057.
18. Chisholm, M. H.; Huffman, J. C.; Pasterczyk, J. W. *Inorg. Chem.* **1988**, *27*, 3057.
19. Laplaza, C. E.: Cummins, C. C.; Davis, W. M. *Angew. Chem. Int. Ed. Engl.* **1995**, *34*, 2042.
20. Zanetti, N. C.; Schrock, R. R.; Davis, W. M. *Angew. Chem. Int. Ed. Engl.* **1995**, *34*, 2044.
21. Dapporto, P.; Midollini, S.; Sacconi, L. *Angew. Chem. Int. Ed. Engl.* **1979**, *18*, 469.
22. Cherry, J.-P. F.; Stephens, F. H.; Johnson, M. J. A.; Diaconescu, P. L.; Cummins, C. C. *Inorg. Chem.* **2001**, *40*, 6860.
23. Scherer, O. J.; Eshes, M.; Wolmershauser, G. *Angew. Chem. Int. Ed. Engl.* **1998**. *37*, 507.
24. Fermin, M. C.; Ho, J.; Stephan, D. W. *Organometallics* **1995**, *14*, 4247.
25. Schaffer, H.; Binder, D.; Fenske, D. *Angew. Chem. Int. Ed. Engl.* **1985**, *24*, 893.
26. Pauling, L. *The Nature of the Chemical Bond*, 3rd ed.; Cornell University Press, 1960, Ch. 11, p. 405.
27. Wu, G.; Rovnyak, D.; Johnson, M. J. A.; Zanetti, N. C.; Musaev, D. G.; Morokuma, K.; Schrock, R. R.; Griffin, R. G.; Cummins, C. C. *J. Am. Chem. Soc.* **1996**, *118*, 10654.
28. Peters, J. C.; Odom, A. L.; Cummins, C. C. *Chem. Commun.* **1997**, 1995.
29. Fickes, M. G.; Odom, A. L.; Cummins, C. C. *Chem. Commun.* **1997**, 1993.
30. Harris, R. K.; Mann, B. E. Eds. *NMR and the Periodic Table*, Academic Press,London, 1978.
31. Greco, J. B.; Peters, J. C.; Baker, T. A.; Davis, W.M.; Cummins, C. C.;Wu, G. *J. Am. Chem. Soc.* **2001**, *123*, 5003.
32. Ruiz-Morales, Y.; Schreckenbach, G.; Ziegler, T. *Organometallics* **1996**, *15*, 3920.

33. Ruiz-Morales, Y.; Schreckenbach, G.; Ziegler, T. *J. Phys. Chem.* **1996**, *100*, 3359.
34. Ruiz-Morales, Y.; Schreckenbach, G.; Ziegler, T, *J. Chem. Phys.* **1996**, *104*, 8605.
35. Bonanno, J. B.; Wolczanski, P. T.; Lobkovsky, E. B. *J. Am. Chem.Soc.* **1994**, *116*, 11159.
36. Johnson, B. P.; Balazs, G.; Scheer, M. *Top. Curr. Chem.* **2004**, *232*, 1.
37. Freundlich, J. S.; R. R. Schrock, R. R.; Davis, W. M. *J. Am. Chem. Soc.* **1996**, *118*, 3643.
38. Stephens, F. H.; Figueroa, J. S.; Diaconescu, P. D.; Cummins, C. C. *J. Am. Chem. Soc.* **2003**, *125*, 9264.
39. Scheer, M.; Muller, J.; Haser, M. *Angew. Chem. Int. Ed. Engl.* **1996**, *35*, 2492.
40. Scheer, M.; Muller, J.; Baum, G.; Haser, M. *Chem. Commun.* **1998**, 1051.
41. Scheer, M.; Kramkowski, P.; Schuster, K. *Organometallics*, **1999**, *18*, 2874.
42. Hitchcock, P. B.; Lappert, M. F.; Lueng, W.-P. *Chem. Commun.* **1987**, 1282.
43. Bohra, P.; Hitchcock, P. B.; Lappert, M. F.; Lueng, W.-P. *Polyhedron*, **1989**, *8*, 1184.
44. Cowley, A. H. *Acc. Chem. Res.* **1997**, *30*, 445.
45. Basuli, F.; Bailey, B. C.; Huffman, J. C.; Baik, M.-H.; Mindiola, D. J. *J. Am. Chem. Soc.* **2004**, *126*, 1924.
46. Cowley, A. H.; Barron, A. R. *Acc. Chem. Res.* **1988**, *21*, 81.
47. Trinquier, G.; Bertrand, G. Inorg. Chem. **1985**, *24*, 3842.
48. Jin, S.; Colegrove, B. T.; Schaefer III, H. F. *Inorg. Chem.* **1991**, *30*, 2969.
49. Creve, S.; Pierloot, K.; Nguyen, M. T.; Vanquickborne, L. G. *Eur. J. Inorg. Chem.* **1999**, 107.
50. Grigoleit, S.; Alijah, A.; Rozhenko, A. B.; Streubel, R.; Schoeller, W. W. *J. Organomet. Chem.* **2002**, *643– 644*, 223.
51. Regitz, M; Scherer, O. J.; Eds. *Multiple bonds and low coordination in Phosphorus chemistry*; Thieme Verlag, New York, **1990**.
52. Olkowska-Oetzel, J; Pikies, J. *Appl. Organomet. Chem.* **2003**, *17*, 28.
53. Krautscheid, H.; Matern, E.; Kovacs, I.; Fritz, G.; Pikies, J. *Z. Anorg. Allg. Chem.* **1997**, *623*, 1917.
54. Krautscheid, H.; Matern, E.; Fritz, G.; Pikies, J. *Z. Anorg. Allg. Chem.* **1998**, *624*, 501.
55. Krautscheid, H.; Matern, E.; Fritz, G.; Pikies, J. *Z. Anorg. Allg. Chem.* **1998**, *626*, 1617.
56. Krautscheid, H.; Matern, E.; Fritz, G.; Pikies, J. *Z. Anorg. Allg. Chem.* **2000**, *626*, 253.
57. Krautscheid, H.; Matern, E.; Pikies, J.; Fritz, G. *Z. Anorg. Allg. Chem.* **2000**, *626*, 2133.
58. Matern, E.; Pikies, J.; Fritz, G. *Z. Anorg. Allg. Chem.* **2000**, *626*, 2136.
59. Shah, S.; Protasiewicz, J. D. *Coord. Chem. Rev.* **2000**, *210*,181.
60. Albright, T. A.; Burdett, J. K.; Whangbo, M. –H. *Orbital Interactions in Chemistry*, Wiley, New York, 1985.
61. Pikies, J.; Baum, E.; Matern, E.; Chojnacki, J.; Grubba, R.; Robaszkiewicz, A. *Chem. Commun.* **2004**, 2478.
62. Power, P. P. *Chem. Rev.* **1999**, *99*, 3463.
63. Power, P. P. *Chem. Commun.* **2003**, 2091.
64. Dewar, M. J. S *Bull. Soc. Chim. Fr.* **1951**, *79*, 18.
65. Chatt, J.; Duncanson, L. A. *J. Chem. Soc.* **1953**, 2939.

66. Brask, J. K.; Fickes, M. G.; Sangtrirutnugul, P.; Dura-Vila, V.; Odom, A. L.; Cummins, C. C. *Chem. Commun.* **2001**, 1671.

67. Brask, J. K.; Dura-Vila, V.; Diaconescu, P. L.; Cummins, C. C. *Chem. Commun.* **2002**, 902.

68. Agapie, T.: Diaconescu, P. L.; Cummins, C. C. *J. Am. Chem. Soc.* **2002**, *124*, 2412.

69. Weber, L. *Eur. J. Inorg. Chem.* **2003**, 1843.

70. Wigley, D. E. *Prog. Inorg. Chem.* **1994**, *42*, 239.

71. Fickes, M. G; Davis, W. M.; Cummins, C. C. *J. Am. Chem. Soc.* **1995**, *117*, 6384.

72. Proulx, G.;Bergman, R. G *J. Am. Chem. Soc.*, **1995**, *117*, 6382.

73. Niecke, E.; Nieger, M.; Reichert, F. *Angew. Chem. Int. Ed. Engl.* **1988**, *27*, 1715

74. Burford, N.; Phillips, A. D.; Spinney, H. A.; Robertson, K. N.; Cameron, T. S.; McDonald, R. *Inorg. Chem.* **2003**, *42*, 4949.

75. Burford, N.; Dyker, C. A.; Phillips, A. D.; Spinney, H. A.; Decken, A.; McDonald, R.; Ragogna, P. J.; Rheingold, A. L. *Inorg. Chem.* **2004**, *43*, 7502.

76. Garratt, P. J. *Aromaticity*; Wiley, New York, **1986**; pp. 137-141.

77. Breslow, R.; Groves, J. T.; Ryan, G. *J. Am. Chem. Soc.* 1967, 89, 5048.

78. Farnum, G.; Mehta, G.; Silberman, R. S. *J. Am. Chem. Soc.* **1967**, *89*, 5049.

79. Breslow, R.; Groves, J. T. *J. Am. Chem. Soc.* **1970**, *92*, 984.

80. Wong, M. W.; Radom, L. *J. Am. Chem. Soc.* **1989**, *111*, 6976.

81. Byun, Y.-G.; Seabo, S.; Pittman, C. U., Jr. *J. Am. Chem. Soc.* **1991**, *113*, 3689.

82. Flores, J. R.; Largo, A. *J. Phys. Chem.* **1992**, *96*, 3015.

83. Schoeller, W. W.; Tubbesing, U. *THEOCHEM*, **1995**, *343*, 49.

84. Xie, Y.; Schreiner, P. R.; Schaefer, H. F.; Li, X.-W.; Robinson, G. H. *J. Am. Chem. Soc.* **1996**, *118*, 10635.

85. Eisfeld, W.; Regitz, M. *J. Org. Chem.* **1998**, *63*, 2814.

86. Xie, Y.; Schreiner, P. R.; Schaefer, H. F.; Li, X.-W.; Robinson, G. H. *Organometallics*, **1998**, *17*, 114.

87. Salcedo, R.; Olvera, C. *THEOCHEM*, **1999**, *460*, 221.

88. *cyclo*-BC_2: (a) Eisch, J. J.; Shafii, B.; Rheingold, A. L. *J. Am. Chem. Soc.* **1987**, *109*, 2526. (b) Eisch, J. J.; Shafii, B.; Odom J. D.; Rheingold, A. L. *J. Am. Chem. Soc.* **1990**, *112*, 1847.

89. [*cyclo*-PC_2]$^+$: Laali, K. K.; Geissler, B.; Wagner, O.; Hoffmann, J.; Armbrust, R.; Eisfeld, W.; Regitz, M. *J. Am. Chem. Soc.* **1994**, *116*, 9407.

90. [*cyclo*-Ga_3]$^{2-}$: Li, X.-W.; Pennington, W. T.; Robinson, G. H. *J. Am. Chem. Soc.* **1995**, *117*, 7578.

91. [*cyclo*-CP_2]$^+$: (a) Bourissou, D.;Bertrand, G. *Top. Cur. Chem.* **2002**, *220*, 1. (b) Bourissou, D.; Canac, Y.; Collado, M. I.; Barceirdo, A.; Bertrand, G. *J. Am. Chem. Soc.* **1997**, *119*, 9923. (c) Bourissou, D.; Canac, Y.; Gornitzka, H.; Barceirdo, A.; Bertrand, G. *Eur. J. Inorg. Chem.* **1999**, 1479.

92. Jursic, B. S. *THEOCHEM*, **1999**, *491*, 33.

93. Frenking, G.; Remington, R. B.; Schaefer, H. F., III *J. Am. Chem. Soc.* **1986**, *108*, 2169.

94. Swart, M.; van Duijnen, P. T.; Snijders, J. G. *J. Comput. Chem.* **2001**, 79.

95. Luo. Y.-R.; Benson, S. W *J. Phys. Chem.* **1989**, *93*, 7333.

96. Kapp, J.; Remko, M.; Schleyer, P. v. R. *Inorg. Chem.* **1997**, *36*, 4241.

97. Suresh, C. H.; Koga, N. *J. Am. Chem. Soc.* **2002**, *124*, 1790.

98. Schreckenbach, G.; Ziegler, T. *J. Phys. Chem.* **1995**, *99*, 606.

99. Gilbert, T. M.; Ziegler, T. *J. Phys. Chem. A.* **1999**, *103*, 7537.

100. Eichler, B. E.; Phillips, B. L.; Power, P. P.; Augustine, M. P. *Inorg. Chem.* **2000**, *39*, 5450.

101. Eichler, B. E.; Phillips, A. D.; Haubrich, S. T.; Mork, B. V.; Power, P. P. *Oranometallics*, **2002**, *21*, 5622.

102. Cotton, F. A.; Cowley, A. H.; Feng, X. *J. Am. Chem. Soc.* **1998**, *120*, 1795.

103. Nixon, J. F. *Chem. Rev.* **1988**, *88*, 1327.

104. Simons, P. S.; Pu, L.; Olmstead, M. M.; Power, P. P *Organometallics*, **1997**, *16*, 1920.

105 . Hu, Y. –H.; Su, M. –D. *Chem. Phys. Let.* **2003**, *378*, 289.

106 . Lai, C. –H.; Su, M. –D.; Chu, S. –Y. *J. Phys. Chem. A* **2002,** *106,* 575.

107. te Velde, G.; Bickelhaupt, F. M.; van Gisbergen, S. J. A.; Fonseca Guerra, C.; Baerends, E. J.; Snijders, J. G.; Ziegler, T. *J. Comput. Chem.* **2001**, *22*, 931.

108. Fonseca Guerra, C.; Snijders, J. G.; te Velde, G.; Baerends, E. J. *Theor. Chem. Acc.* **1998**, *99*, 391.

109. *ADF2004.01*; SCM, Theoretical Chemistry, Vrije Universiteit, Amsterdam, The Netherlands, http://www.scm.com.

110. van Lenthe, E.; Baerends, E. J.; Snijders, J. G. *J. Chem. Phys.* **1993**, *99*, 4597.

111. van Lenthe, E. The ZORA Equation. Thesis, Vrije Universiteit Amsterdam, Netherlands, 1996.

112. Vosko, S. H.; Wilk, L.; Nusair, M. *Can. J. Phys.* **1980**, *58*, 1200.

113. Becke, A. *Phys. Rev. A* **1988**, *38*, 3098.

114. Perdew, J. P. *Phys. Rev. B* **1986**, *34*, 7406.

115. Perdew, J. P. *Phys. Rev. B* **1986**, *33*, 8822.

116. See, for example: Deng, L.; Schmid, R.; Ziegler, T. *Organometallics* **2000**, *19*, 3069.

117. Flukiger, P.; Luthi, H. P.; Portmann, S.; Weber, J. *MOLEKEL 4.3*; Swiss Center for Scientific Computing, Manno, 2000; http://www.cscs.ch/molekel.

118. Schaftenaar, G.; Noordik, J. H. *J. Comput.-Aided Mol. Design* **2000**, 14, 123.

Chapter 3. Isovalent Pnictogen for O(Cl) Exchange Mediated by Terminal Pnictide Anions of Niobium

Joshua S. Figueroa

Department of Chemistry, Room 6-332
Massachusetts Institute of Technology
Cambridge, Massachusetts

May 9th 2005

CONTENTS

List of Figures

List of Schemes

List of Tables

1 Introduction

The metathetical transfer of N or P atoms from d^0 metal nitrido[1-8] or phosphido[9-14] complexes to organic acceptors represents a potentially powerful approach to the construction of organonitrogen and organophosphorus compounds. Furthermore, the utility of d^0 pnictido complexes as reagents in synthesis becomes especially attractive if pnictido–metal formation is coupled to element activation (*e.g.* N_2[15-24] and P_4[9,13]). While the end-on Lewis-basicity of d^0 pnictido complexes is well-documented,[1,2,8,9,25-27] reactivity manifolds exemplary of metathetical exchange are much less developed. Chisholm however, has recently reported a ^{15}N-label swap between $MeC{\equiv}^{15}N$ and $PhC{\equiv}N$ catalyzed by the nitrido complex $N{\equiv}W(O\text{-}t\text{-}Bu)_3$, [28] thereby establishing metal-mediated N-atom metathetical exchange as a viable process. Postulated in that work is the existence of 4-membered metallacyclic intermediates which furnish new M≡N and C≡N triple bonds by retro–[2+2] fragmentation. Such 4-membered intermediates are analogous to those invoked for the isoelectronic process of alkyne metathesis by Schrock-type alkylidyne complexes.[29] Similarly, Schrock has shown that terminal phosphinidenes of tantalum undergo isovalent PR for O metathesis upon reaction with aldehydes,[30] where again, 4-membered metallacycles were postulated as key intermediates. While this latter reaction furnishes phosphaalkenes,[31] it demonstrates that metathetical exchange of M-P for C-P multiple bonding is possible on a d^0 metal platform.

With the synthesis of the d^0 phosphido anion [**1a**-P]$^-$, has emerged new potential for the construction of low-coordinate organophosphorus compounds derived from elemental phosphorus (P_4). In this chapter, the phosphido anion [**1a**-P]$^-$ is shown to readily transform acid chlorides (RC(O)Cl) into phosphaalkynes (RC≡P), in a reaction thermodynamically driven by the release of chloride ion and formation of the oxoniobium(V) complex **1a**-O (Chapter 2). This isovalent P for O(Cl) exchange is found to proceed in a metathetical fashion, where a C-P triple bond is furnished from a 4-membered niobacyclic intermediate and is thus mechanistically analogous to alkyne metathesis. Furthermore, the conversion of oxo **1a**-O into the niobaziridine-hydride (**1a**) has been achieved, thus providing a viable system for mild P_4 activation, P-atom transfer to organic substrates and efficient metal-complex regeneration.

This synthetic methodology has been extended to the formation of organonitrile compounds derived from dinitrogen gas (N_2). Despite its overwhelming abundance, N_2 is underutilized as an N-atom source in synthesis. This limitation arises from the scope of methods available for scission of the strong (226 kcal/mol) N≡N triple bond and subsequent N-atom transfer to organic substrates.[32] However as shown here, the N_2-derived nitrido anion $[N{\equiv}Nb(N[Np]Ar)_3]^-$ ([**1a**-N]$^-$), effects the conversion of acid chlorides substrates into their corresponding organonitriles. The recycling of oxo **1a**-O is applicable as well, thereby affording a synthetic dinitrogen fixation system for the production of synthetically valuable organonitrogen compounds.

2 Phosphaalkynes from Acid Chlorides via Isovalent P for O(Cl) Exchange

Since the discovery of phosphaacetylene (HC≡P) by Gier in 1961,[33] phosphaalkynes have played a pivotal role in the development of modern organophosphorus chemistry.[31,34] From seminal

investigations into multiple bonding between phosphorus and carbon,[35-39] an advanced methodology for construction of low-coordinate organophosphorus compounds of vast synthetic utility has developed.[34] The reactive and unsaturated nature of phosphaalkynes has been exploited in both organic[34,40] and polymer chemistry,[41] providing novel and efficient routes to phosphorus-containing heterocycles and polymers with unique electronic and physical properties. Additionally, with the advent of kinetically stabilized phosphaalkynes (*e.g.* *t*-BuC≡P) in the early 1980's,[42] a burgeoning field of phosphaalkyne coordination chemistry has materialized,[43,44] enabling the synthesis of complexed organophosphorus compounds unstable as free species.

However, wide-spread synthetic utilization of phosphaalkynes is limited by the harsh conditions required for their preparation.[34,45] Indeed, most methods involve high-temperature (T > 150 °C), base-induced siloxane-elimination from silyl-substituted phosphaalkenes. The latter are often obtained from the reaction of acid chlorides with $P(SiMe_3)_3$, which is hazardous both to prepare and handle. In addition, many organic substituents are incompatible with such synthetic conditions, resulting in low - if any - yields of the desired phosphaalkynes.[34] Recent advances have been made in developing both mild and catalytic reactions for phosphaalkyne synthesis; however most are only applicable to a very limited number of organic substituents.[46,47] Therefore, the development of new reactions tailored to provide phosphaalkynes in a manner both preparatively mild and tolerant of diverse organic functionality are of interest.

Herein are presented studies toward the development of a new and general phosphaalkyne synthesis which serves to meet the aforementioned goals. As demonstrated in Chapter 2, the propensity of the phosphido anion [**1a**-P]$^-$ to undergo electronic rearrangement at phosphorus provides a starting point for the formation of P-C multiple bonds under mild synthetic conditions. Furthermore, the synthesis of [**1a**-P]$^-$ from niobaziridine-hydride **1a**-H and P_4 offers the potential to couple phosphaalkyne synthesis with a mild element activation event, thus obviating the need for aggressive P-atom transfer reagents such as $P(SiMe_3)_3$.

2.1 Synthesis and Characterization of Niobacyclobutene Complexes (R(O)C=P)Nb(N[Np]Ar)$_3$ (R = *t*-Bu, 2-*t*-Bu; 1-Ad, 2-1-Ad)

To test the utility of anion [**1a**-P]$^-$ for formation of the P≡C functionality, kinetically stabilized phosphaalkynes were initially targeted. As shown by Becker,[42,48] Nixon[49] and others,[50] stabilization of the inherently reactive P≡C triple bond is best achieved through the use of sterically demanding aryl or tertiary alkyl substituents. While the latter both provide steric protection, tertiary alkyl substituents also serve to diminish the electrophilic character of the C≡P unit with respect to spontaneous self-polymerization. Similar effects are achieved through the use of sterically-demanding amino-groups (NR_2).[51-53]

Treatment of Na(THF)[**1a**-P] with either pivaloyl chloride (*t*-BuC(O)Cl) or adamantoyl chloride (1-AdC(O)Cl) in cold THF solution elicited a color change from dark yellow to red over the period of 1.0 h. Removal of solvent and NaCl, followed by crystallization from Et_2O produced the cherry–red metallacycles, (*t*-BuC(O)P)Nb(N[Np]Ar)$_3$ (**2**-*t*-Bu) and (1-AdC(O)P)Nb(N[Np]Ar)$_3$ (**2**-1-Ad) in 70 and 80% yield, respectively (Scheme 1). Crystallographic structure determination of complexes **2**-*t*-Bu and **2**-1-Ad revealed

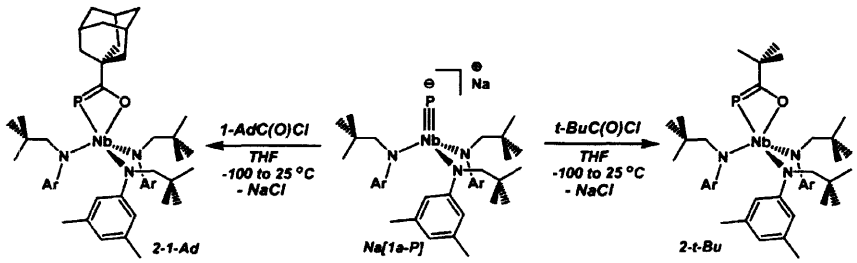

Scheme 1. Synthesis of Niobacyclobutene Complexes **2**-1-Ad and **2**-*t*-Bu.

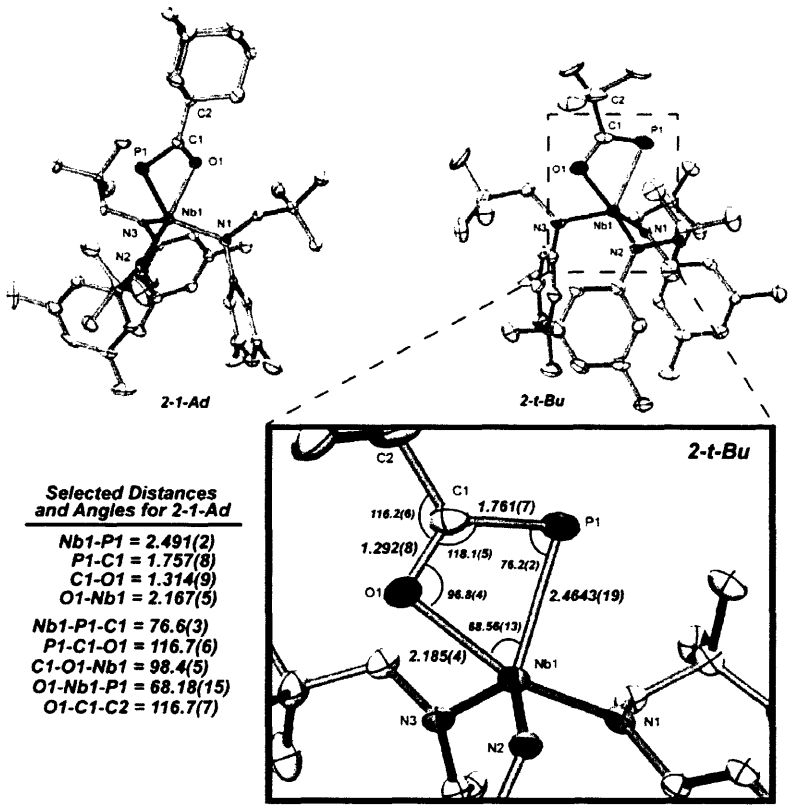

Figure 1. ORTEP Diagrams of **2**-1-Ad and **2**-*t*-Bu at the 35% Probability Level.

four–membered, Nb–P–C–O rings containing both Nb–P and Nb–O linkages (Figure 1). Whereas complexes **2**-*t*-Bu and **2**-1-Ad can be viewed as acylphosphinidenes[54] (Nb=PC(=O)R) with bending at phosphorus[55] and carbonyl oxygen coordination, **2**-*t*-Bu and **2**-1-Ad are best formulated as heteroatom–substituted, niobacyclobutene (Nb-P=C(-O)R) complexes. Thus, as exhibited in Nb-complexed phosphinophosphinidenes (Chapter 2), considerable electronic rearrangement at phosphorus occurs upon acylation of the $Nb{\equiv}P^-$ fragment. Structural parameters in support of a niobacyclobutene formulation for **2**-*t*-Bu (structural parameters for **2**-*t*-Bu and **2**-1-Ad are essentially identical, Figure 1) include an elongated carbonyl C–O distance of 1.314(4) Å and a shortened P-C distance of 1.757(7) Å. The latter parameter is in the range typical for phosphaalkene P-C double bonds,[31] while the former parameter exceeds the maximum value expected for a carbonyl group. Furthermore, the Nb-P distance of 2.491(2) Å is

substantially longer than expected for a doubly-bound terminal phosphinidene,[55] more closely approximating a Nb-P single bond.[56]

Formulation of complexes **2**-*t*-Bu and **2**-1-Ad as niobacyclobutene species also finds support from their spectroscopic signatures. In C_6D_6 solution, the $^{31}P\{^1H\}$ NMR resonances for **2**-*t*-Bu (261 ppm) and **2**-1-Ad (258 ppm) are upfield of the chemical shift range characteristic of early transition metal, terminal phosphinidene complexes,[55] while lying in the range typical for phosphaalkenes.[31] The $^{13}C\{^1H\}$ NMR resonances of 260 ppm (**2**-*t*-Bu and **2**-1-Ad) for the metallacyclic carbon, with associated large $^1J_{PC}$ coupling constants of 113 Hz (**2**-*t*-Bu) and 107 Hz (**2**-1-Ad), are likewise strongly suggestive of the presence of P-C multiple bonding in these niobacycles. In addition, the increase in P-C bond order at the expense of carbonyl C=O bonding is reflected in the infrared spectrum of complexes **2**, where no carbonyl stretching vibrations in the normal region (1700-1500 cm^{-1}) are observed. Difference FTIR experiments conducted on **2**-1-Ad and its ^{13}C-labled isotopomer (1-Ad^{13}C(O)P)Nb(N[Np]Ar)$_3$, failed to conclusively identify a C-O stretching vibration, presumably due to vibronic coupling of several normal modes associated with the niobacyclobutene unit.

2.2 Fragmentation of Niobacyclobutene Complexes 2-*t*-Bu and 2-1-Ad: Formation of the Kinetically Stabilized Phosphaalkynes *t*-BuC≡P and 1-AdC≡P

Although isolable and amenable to characterization, niobacycles **2** are valence-isoelectronic to the metallacyclic intermediates postulated by Chisholm in explanation of N≡W(O-*t*-Bu)$_3$-catalyzed N-atom exchange between organonitriles.[28] Accordingly, niobacycles **2** have been found to readily undergo fragmentation in solution, thereby demonstrating both the ability of the d^0 Nb-trisamide platform to mediate C-P triple bond formation and the feasibility of a metathetical route to phosphaalkynes. For instance, cherry-red C_6D_6 solutions of **2**-*t*-Bu left standing at room temperature are observed to gradually pale in color to the characteristic yellow of oxo **1a**-O over several hours. Intermittent assays of these solutions by either ^1H or $^{31}P\{^1H\}$ NMR spectroscopy revealed the disappearance of **2**-*t*-Bu concomitant with formation of **1a**-O and the phosphaalkyne *t*-BuC≡P (**3**-*t*-Bu, Scheme 2).[42,45] Similar results were obtained for **2**-1-Ad, which generated oxo **6** and 1-AdC≡P (**3**-1-Ad).[34,48] The known phosphaalkynes **3** were readily identified by their characteristic ^1H and ^{31}P resonances, and the use of ^{13}C-labeled **1**-1-Ad produced 1-Ad^{13}C≡P, with C-P coupling constants in excellent agreement with literature values (Figure 2).[34]

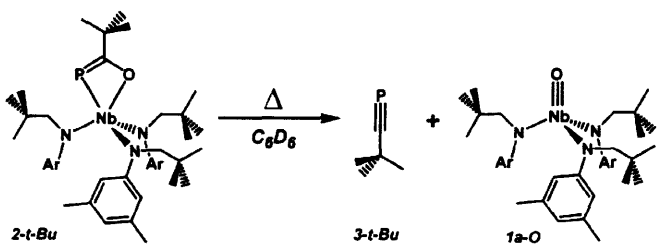

Scheme 2. Thermolysis of Niobacyclobutene Complex **2**-*t*-Bu: *tert*-Butyl Phosphaalkyne Ejection.

^1H NMR spectra for the conversion of **2**-*t*-Bu to products **3**-*t*-Bu and **1a**-O clearly demonstrate the phosphaalkyne ejection process (Figure 3). Spectrum **A** contains resonances

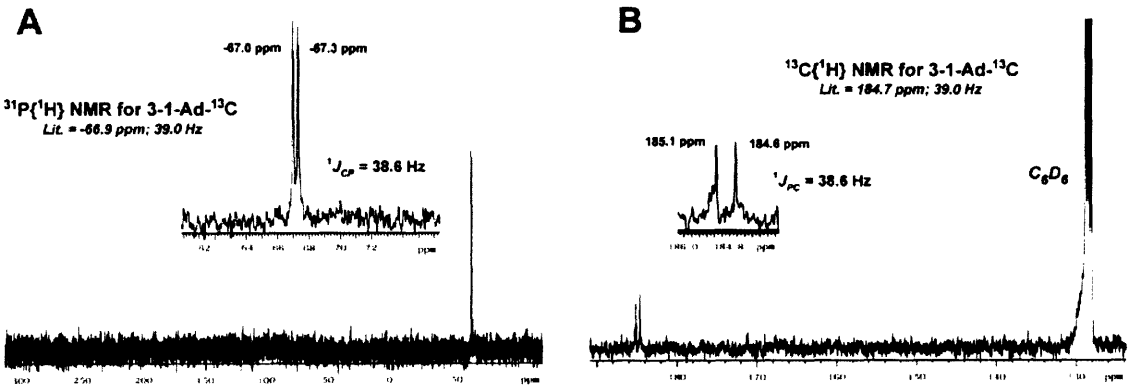

Figure 2. (**A**) $^{31}P\{^{1}H\}$ spectrum (C_6D_6) for **3**-1-Ad-^{13}C after thermolysis of **2**-1-Ad-^{13}C. Note: **2**-1-Ad-^{13}C is not present in the spectrum. (**B**) Partial $^{13}C\{^{1}H\}$ spectrum (C_6D_6) for **2**-1-Ad-^{13}C after thermolysis of **2**-1-Ad.

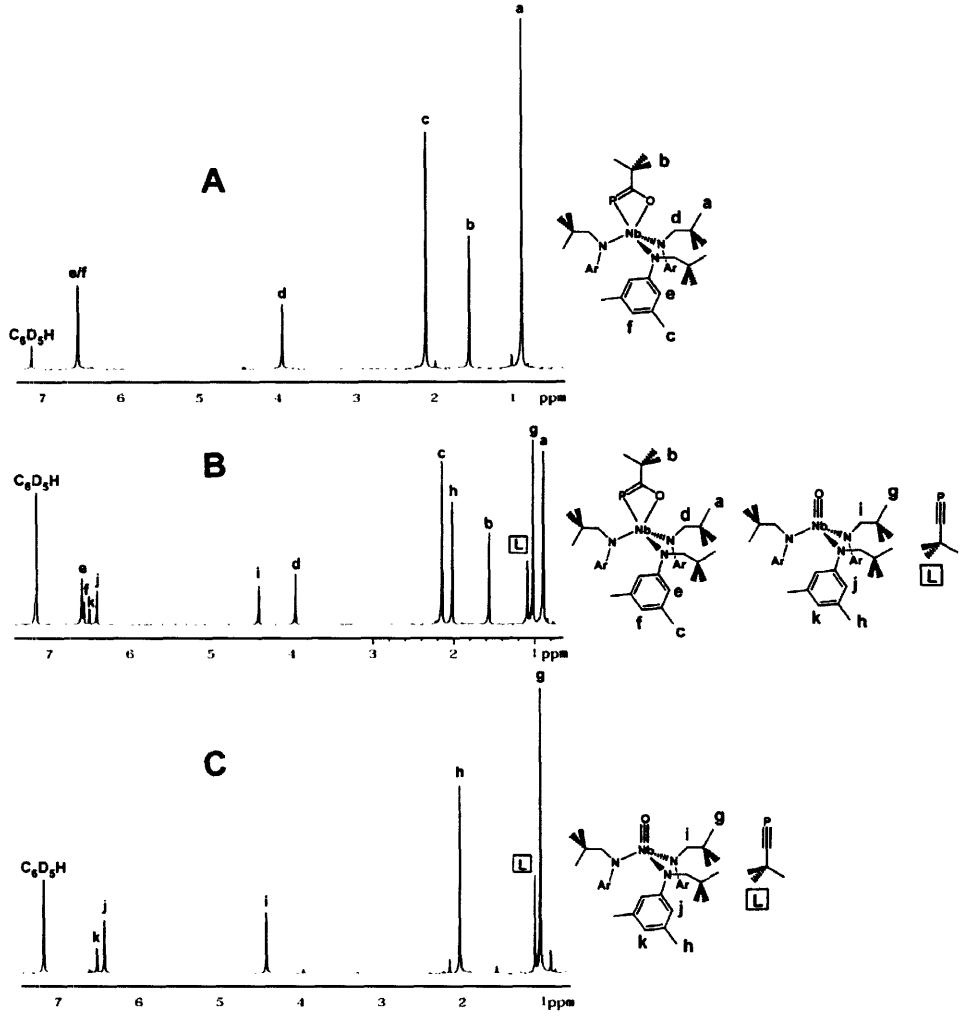

Figure 3. (**A**) Room temperature ^{1}H NMR spectrum of **2**-*t*-Bu prior to thermolysis. (**B**) Room temperature ^{1}H NMR spectrum (C_6D_6) of **2**-*t*-Bu after heating for 45 min at 45 °C. The spectrum contains near equimolar quantities of **2**-*t*-Bu, **3**-*t*-Bu and **1a**-O. (**C**) Room temperature ^{1}H NMR spectrum (C_6D_6) of **3**-*t*-Bu and **1a**-O after heating for 4 h at 45 °C where essentially complete consumption of **2**-*t*-Bu has been achieved. Peak assignments are provided.

corresponding to **2**-*t*-Bu prior to heating, while **B** represents the same sample after immersion in a 45 °C oil bath for 1 h. Apparent in **B** is the clean generation of both **3**-*t*-Bu and **1a**-O without formation of side-products, indicating that reactants and products are compatible during the thermolysis reaction. Complete consumption of **2**-*t*-Bu is achieved at 45 °C in an additional 2.5 h, over which time clean thermolysis behavior is maintained (**C**). Monitoring the thermolysis of **2**-*t*-Bu by $^{31}P\{^{1}H\}$ NMR also revealed a smooth transformation. Figure 4 shows a time profile corresponding to the **2**-*t*-Bu → **3**-*t*-Bu + **1a**-O conversion at 45 °C in C_6D_6 as monitored by $^{31}P\{^{1}H\}$ NMR. Clearly evident is the smooth decay of the resonance at 261 ppm (**2**-*t*-Bu) occurring simultaneously with the appearance of a resonance located at −64 ppm (**3**-*t*-Bu, Lit. (20 °C) = −69 ppm[34,42,45]). No additional signals ascribable to either intermediate species or side-products are observed in the $^{31}P\{^{1}H\}$ NMR spectrum over the range +700 to −300 ppm during the reaction. The fragmentation of **2**-1-Ad to **3**-1-Ad and oxo **1a**-O showed identical spectral behavior when monitored over time by $^{31}P\{^{1}H\}$ NMR spectroscopy. Upon complete thermolysis, solutions containing equimolar amounts of phosphaalkynes **3** and **1a**-O stored at room temperature do not revert to the corresponding niobacycle **2** when monitored for several weeks. Thus the fragmentation of niobacycles **2** is irreversible under the conditions probed, with phosphaalkynes **3** and oxo **1a**-O evidently incapable of reforming the latter by P≡C/Nb≡O [2+2]-cycloaddition.

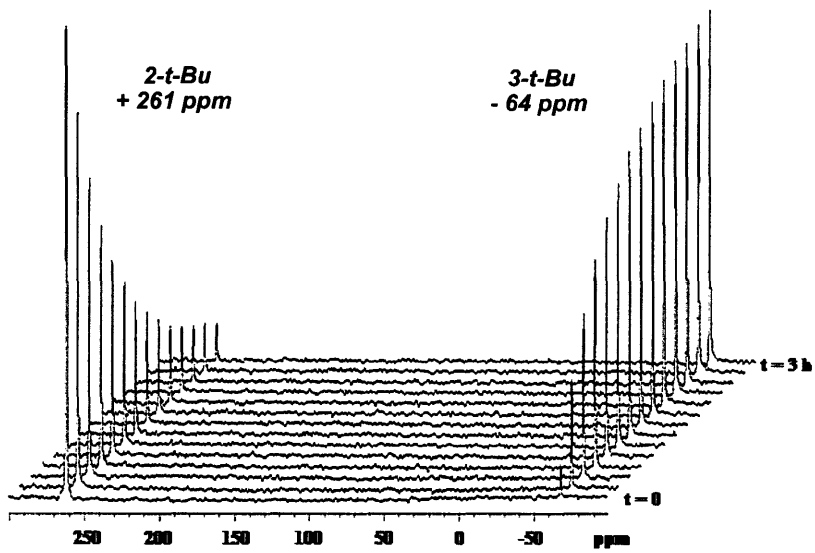

Figure 4. $^{31}P\{^{1}H\}$ NMR Time-Profile for the Reaction **2**-*t*-Bu → **3**-*t*-Bu + **1a**-O (C_6D_6).

For synthetic purposes, thermolysis of solutions containing **2**-*t*-Bu or **2**-1-Ad at 85 °C provides **1a**-O and the corresponding phosphaalkyne within 1 h. After thermolysis of a solution containing **2**-*t*-Bu, colorless solutions of the phosphaalkyne, **3**-*t*-Bu, are obtained by simple vacuum transfer. This procedure affords solutions of pure **3**-*t*-Bu (Figure 5) in yields greater than 90%, on scales from 20 to 200 mg of **2**-*t*-Bu (^{1}H NMR integration vs. internal standard). After vacuum transfer, golden yellow **1a**-O was recovered in near quantitative yield and found to be essentially pure as assayed by ^{1}H NMR (contaminated with ca. 1% HN(Np)Ar).

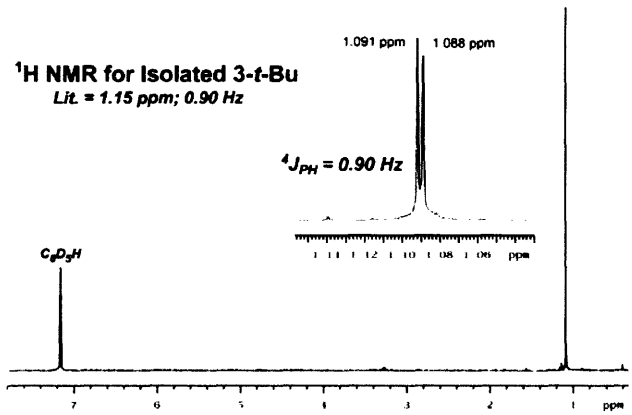

Figure 5. Room Temperature ^{1}H NMR Spectrum (C_6D_6) of *t*-BuCP (**3**-*t*-Bu) Obtained After Vacuum Transfer.

2.3 Kinetic Studies of Phosphaalkyne Ejection from the Niobacyclobutene Complex 2-*t*-Bu

The fact that no intermediates are observed during the **2** → **3** + **1a**-O reaction, coupled with the C-P multiple bond character present in niobacycles **2**, suggests that phosphaalkyne formation may proceed by an intramolecular retro-[2+2] fragmentation. Furthermore, inasmuch as they are isolable, niobacycles **2** may themselves represent intermediates along the phosphaalkyne ejection pathway. To establish an intramolecular mechanism as potentially operative and to obtain activation parameters for phosphaalkyne formation, kinetic studies on the fragmentation of niobacycle **2**-*t*-Bu were performed.

The clean thermolytic fragmentation of **2**-*t*-Bu was ideally suited for a kinetic investigation. While the UV-Vis spectral signatures of both d^0 complexes **2**-*t*-Bu and **1a**-O were nearly identical, their *t*-Bu resonances were resolved in C_6D_6 to allow for accurate integration by ^{1}H NMR. As shown in Figure 6, clean first-order kinetic behavior was observed for the decay of **2**-*t*-Bu over the temperature range 308 – 338 K. Furthermore, the rate of decay for **2**-*t*-Bu at 318 K was identical at initial concentrations of 1.9 mM and 3.2 mM, supporting the notion of phosphaalkyne ejection by a unimolecular process. Activation parameters $\Delta H^{\ddagger}$ = 24.9 ± 1.4 kcal/mol and $\Delta S^{\ddagger}$ = 2.4 ± 4.3 cal/mol K were obtained for the temperature range studied (Figure 7a) and it is interesting to note that a considerable enthalpic cost is required to initiate the retro-[2+2] fragmentation process. However, the small entropic barrier indeed supports the proposal that niobacycles **2** are intermediates on the phosphaalkyne formation pathway, requiring little reorganization to reach the transition state for fragmentation.

As stated in the previous section, the presence of the newly generated phosphaalkyne is compatible with both **2**-*t*-Bu and **1a**-O during the fragmentation process. A plot comparing the decrease in relative intensity of **2**-*t*-Bu vs. time with the corresponding increase of oxo **1a**-O as measured at 308 K is shown in Figure 7b. Notable is the simultaneous disappearance and appearance of **2**-*t*-Bu and **1a**-O, respectively, suggesting that formation of the latter is not delayed by the formation of an additional, unobserved species. While the possibility that a Lewis acid/base adduct of the type **3**-*t*-Bu→**1a**-O may exist immediately following phosphaalkyne ejection, its presence is undetectable by NMR. To date, no evidence has been

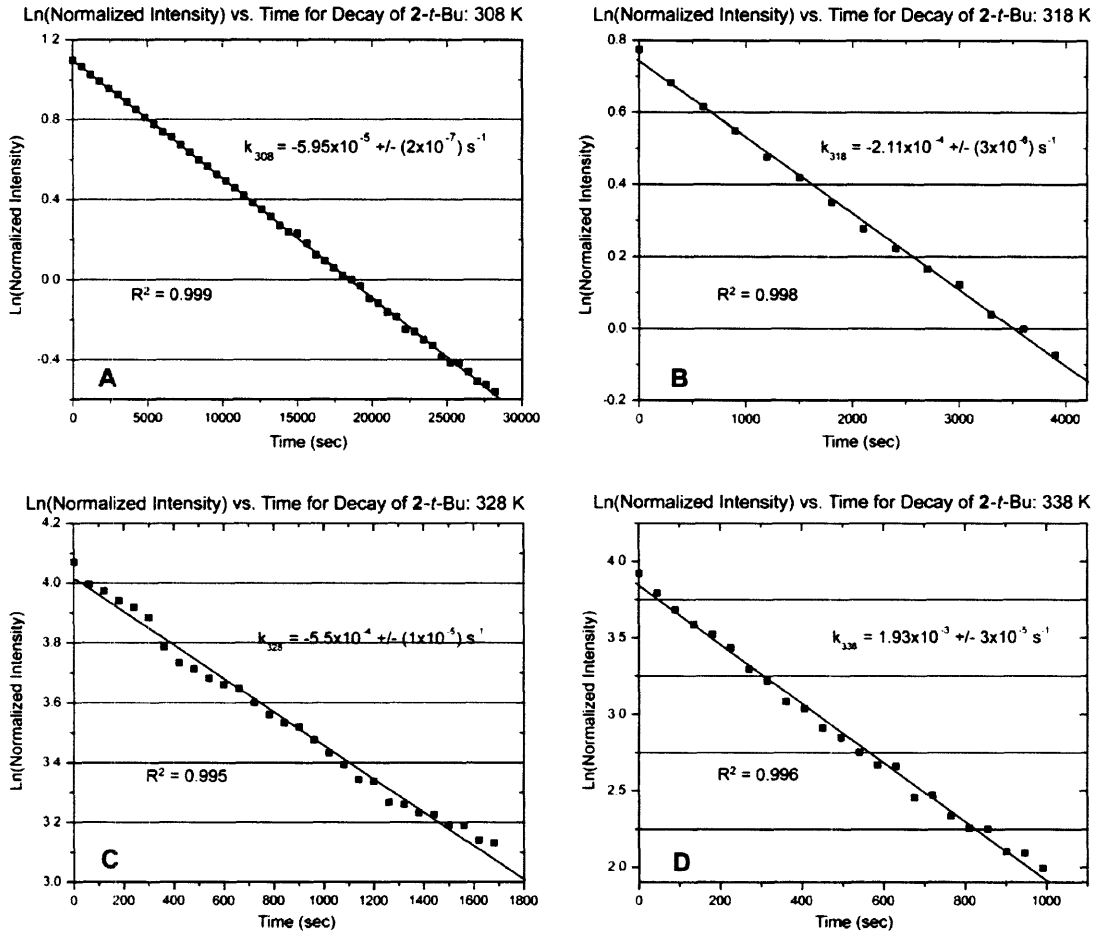

Figure 6. Logarithmic First–Order Fits for the Decay of **2**-*t*-Bu vs. time at 308 (**A**), 318 (**B**), 328 (**C**) and 338 (**D**) K. Rate constants and R^2 statistics are provided.

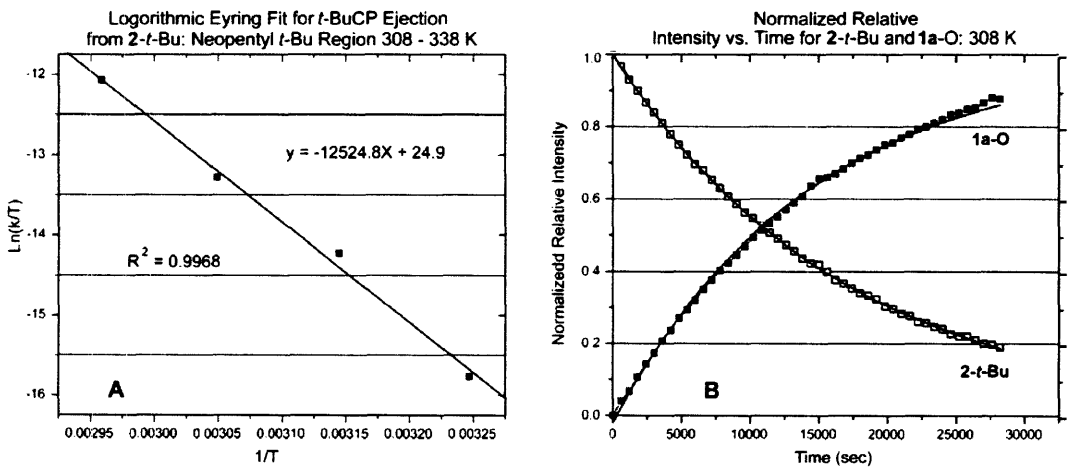

Figure 7. (**A**) Logarithmic Fit to the Eyring Equation for Decay of **2**-*t*-Bu over the Temperature Range 308 – 338 K. Linear Equation and R^2 Statistic are Provided. (**B**) Comparative Time-Profile of Normalized Relative Intensity for the Decay of **2**-*t*-Bu and Increase of **1a**-O.

Table 1. Rates and Free Energies of Activation for *t*-BuC≡P Ejection from **2**-*t*-Bu at Various Temperatures

Temperature (K)	Rate Constant, k (s^{-1})	$\Delta G^{\ddagger}$ (kcal/mol)
308	$5.95(2) \times 10^{-5}$	24.16
318	$2.11(3) \times 10^{-4}$	24.13
328	$5.5(1) \times 10^{-4}$	24.11
338	$1.93(3) \times 10^{-3}$	24.09

obtained for the propensity of **1a**-O to bind a Lewis basic ligand. In addition, the smooth, consistent decay of **2**-*t*-Bu precludes an inhibitory role for the newly generated **3**-*t*-Bu, unless the unlikely situation whereby **3**-*t*-Bu binds and dissociates to both **1**-*t*-Bu and **1a**-O at the same rate is occurring.

2.4 Deoxygenative Recycling of the Oxoniobium(V) Complex 1a-O: Synthetic Cycle for P_4-Derived Phosphaalkynes

Since oxo **1a**-O is the ultimate Nb product of phosphaalkyne ejection, its conversion to niobaziridine hydride **1a** was of particular interest in order to establish anion [**1a**-P]$^-$ as a reusable reagent for C≡P triple bond formation. The direct deoxygenation of **1a**-O by an external reagent seemed unlikely due to the marked oxygen-atom abstraction ability of the d^2 Nb(N[Np]Ar)$_3$ fragment (Chapter 1). Therefore, the incorporation of the terminal oxygen atom in **1a**-O into a psuedohalide leaving group by electrophilic attack was adopted as a synthetic strategy. Such a transformation would allow for reduction to niobaziridine hydride **1a** in a subsequent step.

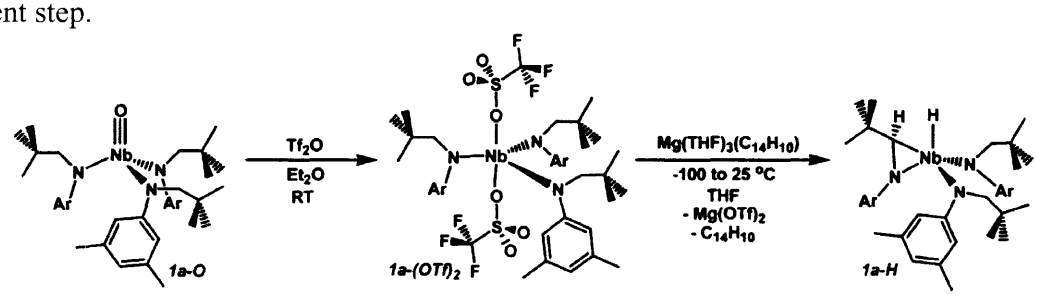

Scheme 3. Synthesis of **1a**-(OTf)$_2$ and Subsequent Reduction to Niobaziridine-Hydride **1a**-H.

Remarkably, oxo **1a**-O was found to be quantitatively converted to the bistriflate complex Nb(OTf)$_2$(N[Np]Ar)$_3$ (**1a**-(OTf)$_2$, Scheme 3, Tf = SO_2CF_3) upon treatment with the potent electrophile triflic anhydride[57] (Tf_2O, 1.0 equiv) in Et_2O. Bistriflate **1a**-(OTf)$_2$ is a bright orange, ether-insoluble, crystalline solid isolated in 90% yield by simple filtration of the reaction mixture. The formation of **1a**-(OTf)$_2$ from **1a**-O and Tf_2O is noteworthy in that the electrophilic potency of the latter converts the normally inert $Nb^V{\equiv}O$ unit into a common leaving group. Although limited to just a few cases, examples where a d^0 early transition metal oxo has been transformed into a good leaving group have been reported.[58-60] An X-ray structural study performed on **1a**-(OTf)$_2$ confirmed its formulation as a molecular bistriflate complex (Figure 8). The trigonal bipyramidal coordination geometry observed for **1a**-(OTf)$_2$ is consistent with the molecular structure of the related, 5-coordinate Nb(V) halide complexes Nb(Cl)$_2$(N[*i*-Pr]Ar)$_3$,[61] Nb(Cl)$_2$(N[Np]Ar)$_3$[62] and Nb(I)$_2$(N[Np]Ar)$_3$.[62] The solid state, equatorial conformation of the anilido ligands in these complexes is interpreted as providing maximum out-of-plane $N_{p\pi} \rightarrow Nb_{d\pi}$

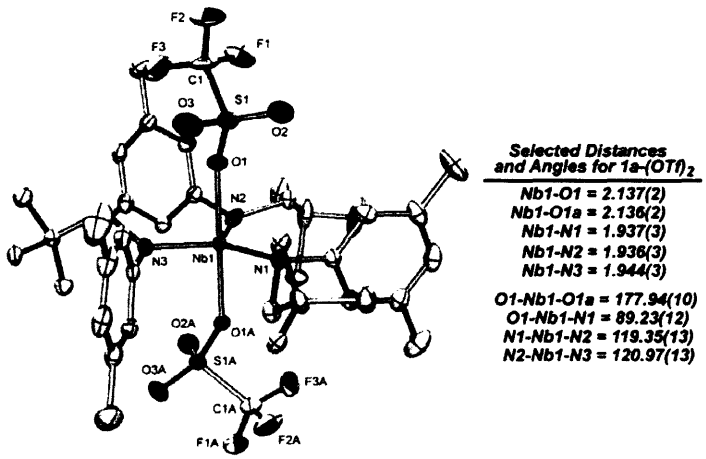

Figure 8. ORTEP Diagram of **1a**-$(OTf)_2$ at the 35% Probability Level.

bonding surrounding the σ-bound halide or pseudohalide ligands. This effect serves to stabilize the complexes by quenching the Lewis acidity of the Nb center.

As expected, bistriflate **1a**-$(OTf)_2$ serves as an ideal synthetic precursor to niobaziridine-hydride **1a**-H. Reduction of **1a**-$(OTf)_2$ with Mg(anthracene)$(THF)_3$[63] in THF (Scheme 3) affords **1a** in comparable yields to the same procedure employing $Nb(I)_2(N[Np]Ar)_3$ (**1a**-$(I)_2$, Chapter 1). Subsequent treatment of **1a** with P_4 restores its use for subsequent phosphaalkyne formation. A synthetic cycle illustrating the step-wise synthesis of P_4-derived phosphaalkynes from niobaziridine-hydride **1a**-H is shown in Scheme 4. Furthermore, this system establishes a paradigm for the conversion of a thermodynamically stable entity (*e.g.* **1a**-O), to a species capable of element activation (**1a**-H). Such a feature is a critical requirement for the development of a catalytic system based on the chemistry of Scheme 4.

2.5 Isovalent Exchange as a Route to Novel Substituted Phosphaalkynes

The results of the preceding sections demonstrate the ability of phosphido anion [**1a**-P]$^-$ to mediate P≡C triple bond formation in a manner both preparatively milder and mechanistically distinct from existing phosphaalkyne syntheses.[34] Kinetically-stabilized **3**-*t*-Bu and **3**-1-Ad are accessible from [**1a**-P]$^-$ via isovalent P for O(Cl) exchange, representing a significant improvement over the high-temperature procedures typically used for their preparation.[45,48] Furthermore, the high-yield recycling of oxo **1a**-O allows for an efficient synthetic procedure with respect to the metal-based reagents. To further expand the scope of this new reaction, the ability to generate phosphaalkynes inaccessible from existing synthetic procedures was investigated.

Initial attempts to generate novel phosphaalkynes focused on organic substituents which, again, would provide kinetic stabilization to the newly formed P≡C unit. Indeed, evidence for the formation of the known phosphaalkynes MeC≡P[64] and PhC≡P[65]has been obtained upon combination of anion [**1a**-P]$^-$ and the corresponding acid chloride (MeC(O)Cl and PhC(O)Cl, respectively). The Me and Ph-substituted niobacycles were only marginally stable as compared to **2**-*t*-Bu and **2**-1-Ad, but MeC≡P and PhC≡P were identifiable spectroscopically. However, the

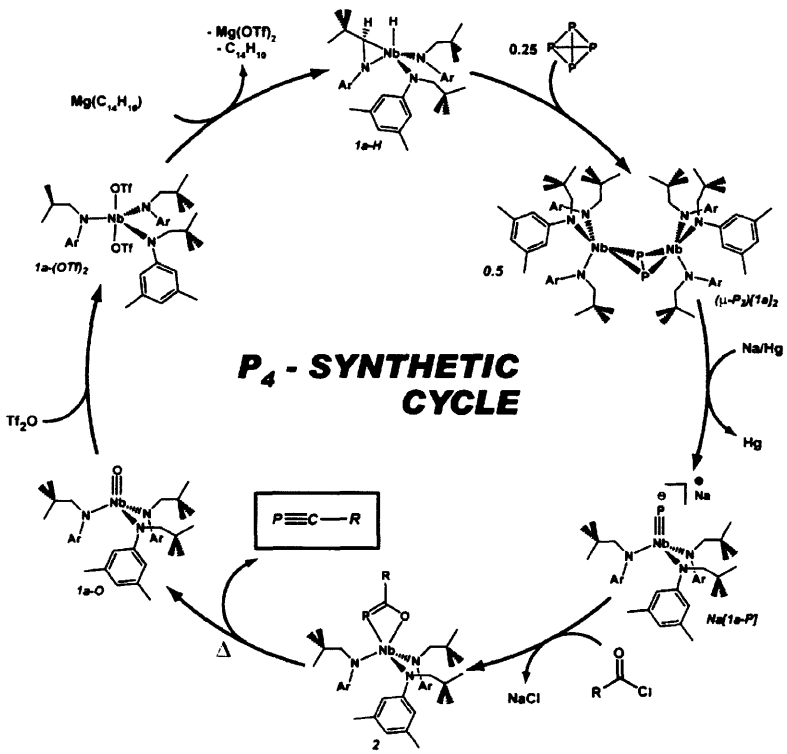

Scheme 4. Synthetic Cycle for the Metathetical Formation of P_4-Derived Phosphaalkynes.

MeC≡P and PhC≡P so generated reacted quickly with both the corresponding niobacycle and oxo **1a**-O, ultimately resulting in complex and intractable mixtures. Both MeC≡P and PhC≡P are known to be exceedingly reactive, decomposing to polymer and other unidentified products at temperatures above -30 °C.[34,64-66]

2.5.1 Bis-Phosphaalkynes

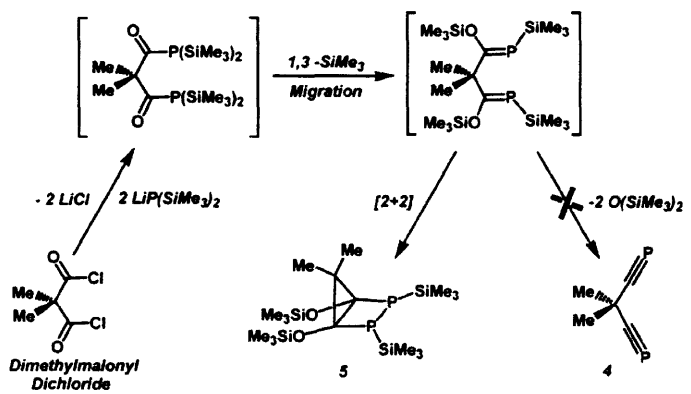

Scheme 5. Regitz'Attempted Synthesis of Bis-Phosphaalkyne **4**. Adapted from Reference 68.

Realizing that bisphosphaalkyne compounds have been difficult to obtain by traditional methods,[67] their synthesis was targeted by P for O(Cl) exchange. An attempt to generate the

bisphosphaalkyne (**4**, Scheme 5) corresponding to dimethylmalonyl dichloride ($Me_2C(C(O)Cl)_2$) by siloxane-elimination was reported by Regitz.[68] However, as outlined in Scheme 5, the 2,3-diphosphabicyclo[2.1]pentane **5** was formed instead due to preferential [2+2] P=C cycloaddition rather than siloxane elimination. It was reasoned that Nb-mediated P for O(Cl) isovalent exchange could provide bisphosphaalkyne **4** without interference from the intramolecular cycloaddition reaction of Scheme 5. While **4** can be considered as a kinetically stabilized phosphaalkyne by virtue of a central tertiary carbon atom, treatment of anion [**1a**-P]$^-$ with 0.5 equiv of dimethylmalonyl dichloride resulted in the formation of products attributable to oxidation of the Nb≡P$^-$ unit. This observation is attributed to the electron-withdrawing ability of the geminal-disubstituted dimethylmalonyl dichloride. Therefore, the adamantane cage, with its discrete tertiary carbon atoms, was investigated as a scaffold on which to construct the bis-C≡P functionality by P for O(Cl) isovalent exchange.

Accordingly, treatment of anion [**1a**-P]$^-$ with 0.5 equiv of adamantane-1,3-dicarbonyl chloride (1,3-$(C(O)Cl)_2$Ad) in cold THF solution resulted in the smooth formation of the adamantane-bridging bisniobacycle, **6** (Scheme 6). In contrast to the reaction between [**1a**-P]$^-$ and dimethylmalonyl dichloride, crude reaction mixtures assayed by ^{1}H NMR during the formation of **6** did not indicate the presence of species attributable to electron transfer. Complex **6** is reproducibly isolated as an orange-red powder in ca. 60% yield by precipitation from cold *n*-pentane. To date, crystals suitable for crystallographic analysis have not been obtained, but the $^{31}P\{^1H\}$ NMR signature (δ = 260.0 ppm) of **6** agrees well with that of its mononiobacyclic analogue, **2**-1-Ad (δ =258.2 ppm). Furthermore, combustion analysis for **6** is consistent with its formulation.

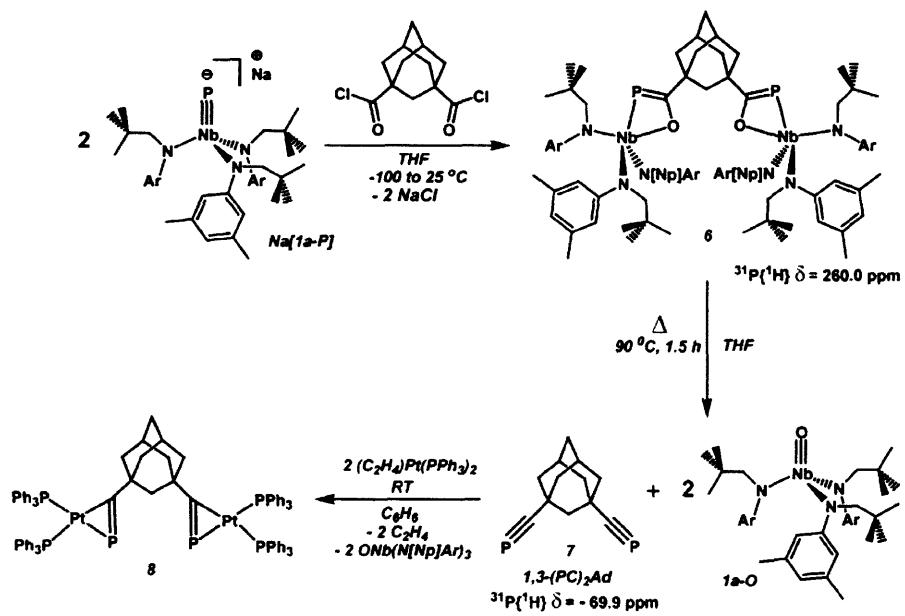

Scheme 6. Synthesis and Complexation of Bis-Phosphaalkyne **7**.

Formation of the bisphosphaalkyne, 1,3-$(P{\equiv}C)_2$Ad (**7**), from bisniobacycle **6** was achieved by thermolysis of the latter in THF solution at 90 °C (Scheme 6). Analysis of the resulting mixture by ^{1}H NMR indicated the clean formation of oxo along with new resonances assignable to an adamantyl group. The corresponding $^{31}P\{^1H\}$ NMR spectrum revealed complete consumption of **6** and a single new resonance centered at –64.4 ppm. This ^{31}P NMR signal is in excellent agreement with those for the related tertiary alkyl-substituted **3**-1-Ad and **3**-*t*-Bu,[34,45] and thus provides strong evidence for the successful synthesis of the bisphosphaalkyne, 1,3-$(P{\equiv}C)_2$Ad (**7**). Moreover, **7** displayed solution stability properties consistent with its formulation as a kinetically-stabilized phosphaalkyne. Accordingly, the ^{31}P NMR resonance assigned to **7** remained unchanged in solution over the course of ca. 2 weeks as it stood at room temperature in the presence of oxo **1a**-O.

Several attempts to separate bisphosphaalkyne **7** from **1a**-O by fractional crystallization or chromatography were unsuccessful. Therefore, complexation of **7** by a low-valent transition metal complex was employed as a separation technique. Nixon has shown that the platinum-ethylene complex, $(C_2H_4)Pt(PPh_3)_2$,[69] readily binds kinetically stabilized phospha-[49] and arsaalkynes[70] in an η^2 fashion with concomitant loss of free ethylene. Repeated fractional crystallizations of oxo **1a**-O from Et_2O (n ≥ 3, ca. 75% of **1a**-O removed) was found to sufficiently enrich the solution in bisphosphaalkyne **7**. Addition of off-white $(C_2H_4)Pt(PPh_3)_2$ to a brown C_6H_6 solution of the **7**-enriched mixture elicited an immediate color change to dark yellow. While effervescence attributable to the formation of C_2H_4 gas was not observed, $^{31}P\{^1H\}$ NMR provided substantial evidence for the formation of the bisphosphaalkyne complex 1,3-$((\eta^2{-}P{\equiv}C)Pt(PPh_3)_2)_2$Ad (**8**, Scheme 6). Addition of *n*-pentane to the reaction mixture precipitated **8** as a golden-yellow powder in 84% isolated yield from $(C_2H_4)Pt(PPh_3)_2$.

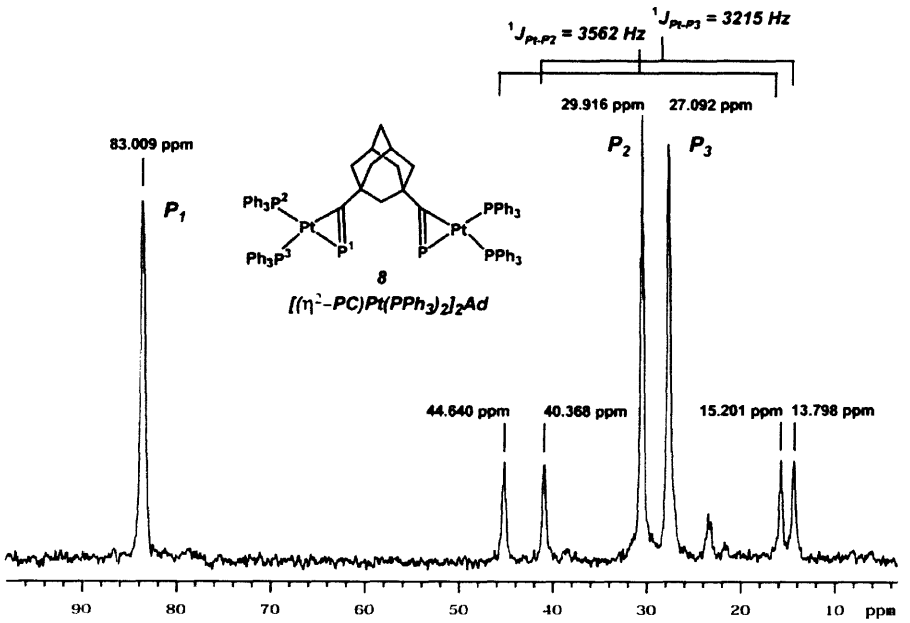

Figure 9. $^{31}P\{^1H\}$ NMR Spectrum (C_6D_6) of Bisphosphaalkyne Complex **8** at 121.1 MHz.

Although complex **8** could not be crystallographically characterized, the $^{31}P\{^{1}H\}$ NMR spectrum of **8** (Figure 9), is consistent with the ABX spin-pattern expected for a square planar, $Pt(PPh_3)_2$–bound phosphaalkyne complex.[43,49] Interestingly, no ^{195}Pt coupling was observed for the phosphaalkyne P-atoms in the $^{31}P\{^{1}H\}$ NMR spectrum of **8**, which contrasts with that observed by Nixon for the related (η^2–*P,C*–*t*-BuC≡P)$Pt(PPh_3)_2$ ($^{1}J_{Pt\text{-}P}$ = 62 Hz).[49] Exceedingly small values for $Pt\text{-}P_{alkyne}$ coupling are characteristic of Pt-bound phosphaalkyne complexes and are readily attributable to the low s-orbital character in the P_{alkyne}-Pt bond.[43] Though not unambiguously characterized to date, the synthesis of **7** and its diplatinum derivative provide a promising beginning for the construction of novel phosphaalkyne compounds using anion [**1a**-P]$^-$.

2.5.2 Amino-Substituted Phosphaalkynes.

To further extend the generality of phosphaalkyne formation by anion [**1a**-P]$^-$, carbonyl-containing compounds other than acid chlorides were surveyed as potential substrates. Whereas esters such as methyl pivalate (*t*-BuC(O)OMe) did not react with anion [**1a**-P]$^-$, mesityl isocyanate (MesNCO, Mes = 2,4,6-$Me_3C_6H_2$) readily formed an adduct with the latter to provide $Na[(MesNC(O)P)Nb(N[Np]Ar)_3]$ (Na[**9**], Scheme 7), as hydrocarbon-insoluble, brick-red powder. Crystallographic characterization of Na[**9**] (as its *tris*-THF solvate, Figure 10) revealed a niobacyclic framework similar to that found in the neutral derivates **2**-*t*-Bu and **2**-1-Ad. However, the P-C (1.821(9) Å) and Nb-P (2.394(2) Å) internuclear separations in [**9**]$^-$ are longer and shorter, respectively, than those in **2**-*t*-Bu and **2**-1-Ad. While the P-C bond length in [**9**]$^-$ indicates the presence of a long double bond ($r_{cov}C + r_{cov}P$ = 1.87 Å; r_{cov} = covalent radius),[56] the Nb-P separation suggests that substantial multiple bonding between Nb and P is conserved. The $^{31}P\{^{1}H\}$ NMR resonance of 456.8 ppm for [**9**]$^-$ is consistent with this notion. The latter can be considered as indicative of a bonding formulation for [**9**]$^-$ intermediate between that of a terminal phosphinidene[55] and a niobacyclobutene species of the type exemplified by **2**-*t*-Bu (261 ppm) and **2**-1-Ad (258 ppm).

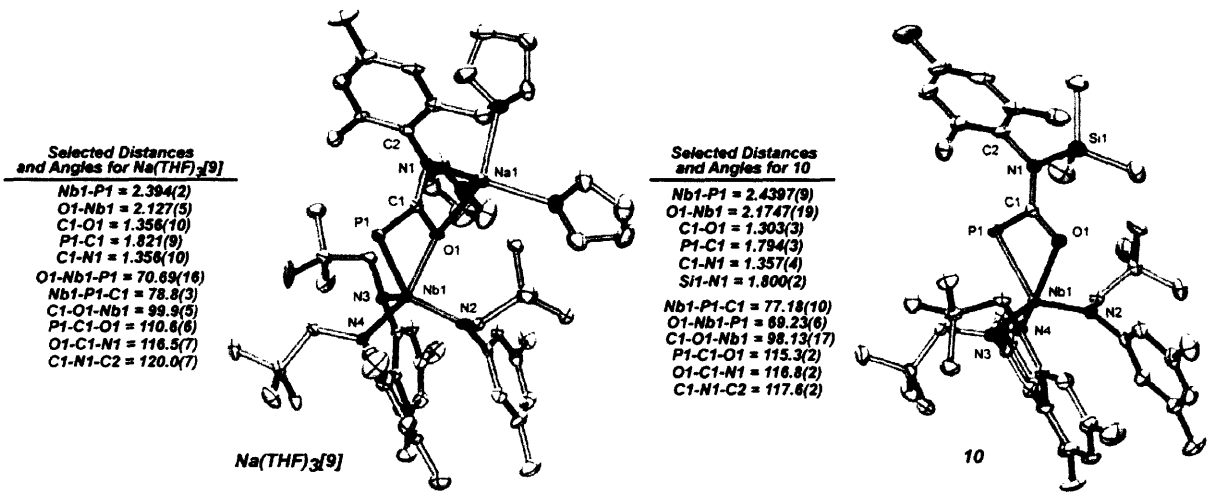

Figure 10. ORTEP Diagram of $Na(THF)_3$[**9**] and **10** at the 35% Probability Level.

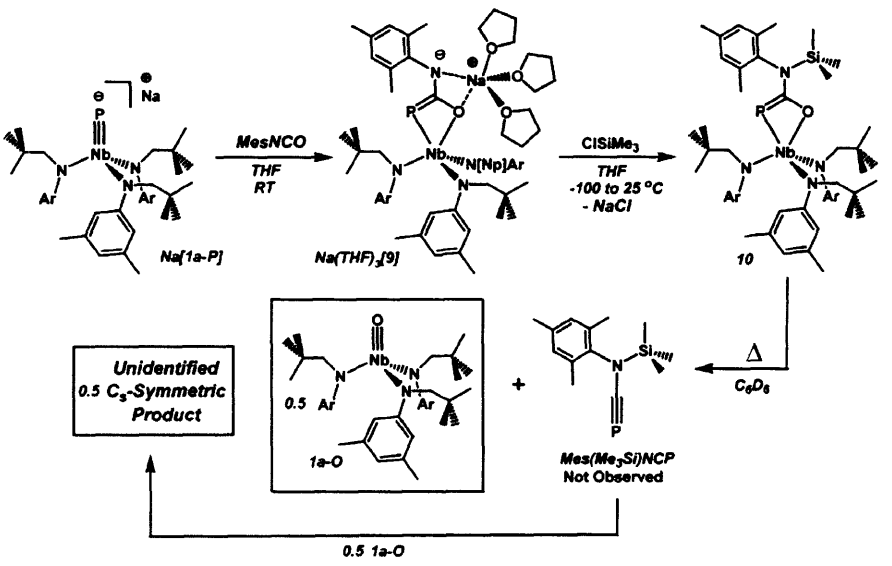

Scheme 7. Synthesis and Thermal Behavior of Anion $[\mathbf{9}]^-$ and Silylated Derivative **10**.

Also notable from the structure of $Na(THF)_3[\mathbf{9}]$ is the 120.0(7)° C1-N1-C2 angle, which suggests that the negative charge of the complex is localized on the N1 atom. Accordingly, treatment of Na[**9**] with $ClSiMe_3$ allowed for its exocyclic derivatization and formation of the cherry-red, amino-substituted niobacycle, **10** (Scheme 7). As expected, silylation of anion **9** at nitrogen completes its electronic reorganization to a niobacyclobutene species. Thus, the crystallographically-determined metrical parameters of **10** (Figure 10) agree well with both **2**-*t*-Bu and **2**-1-Ad, despite the presence of an electron-donating amino-group on the niobacyclic ring. In addition, the upfield movement of the ^{31}P resonance of **10** (336.3 ppm) is also indicative of decreased Nb-P multiple bonding relative to anion $[\mathbf{9}]^-$.

Niobacycle **10** represents a precursor to amino-substituted phosphaalkynes via isovalent exchange. It is notable that only three stable R_2N-C≡P compounds have been reported to date ((*i*-Pr)$_2$N-C≡P,[51,52] (*i*-Pr)(Me_3Si)N-C≡P[53] and (2,2,6,6–Me_4piperidino)–1–C≡P[71]) and only one of these, namely (*i*-Pr)(Me_3Si)N-C≡P, contains two different substituents. However, liberation of the P≡C(N(R^1)R^2) unit from the metal center was not straight forward for the case of **10**. Heating **10** at 80 °C in C_6D_6 (Scheme 7) produced a mixture 1:1 of oxo **6** and an unidentified C_s symmetric species as indicated by ^1H NMR. Monitoring the reaction by $^{31}P\{^1H\}$ NMR after heating for 30 minutes revealed the presence of a signal located at -137 ppm, characteristic of amino-substituted phosphaalkynes.[51-53] However, this signal disappears, giving rise to a singlet centered at δ = 95.2 ppm assigned to the C_s product observed by ^1H NMR. A possible explanation for these observations is that the newly generated P≡C(N(Mes)$SiMe_3$) inserts into two N[Np]Ar ligands of oxo **1a**-O. Such a situation would account for the C_s symmetry of the new product, the single resonance found in the $^{31}P\{^1H\}$ NMR of the reaction mixture and the remaining 0.5 equiv of **1a**-O. Furthermore, insertion chemistry of this type is plausible due to the well-established tendency of CO_2, to which P≡C(N(Mes)$SiMe_3$) is valence isoelectronic, to insert into metal-amido bonds.[72]

Given the facility with which anionic niobacycles exemplified by Na[**9**] can be synthesized and derivatized, their utility for the formation of amino-substituted phosphaalkynes is evident. However, conditions must be found which circumvent side reactions during liberation of the reactive P≡C(N(R^1)R^2) molecule. It is also noteworthy that Na[**9**]-type anions potentially offer access to [P≡CNR]$^-$ salts, which have been recently shown to exhibit rich reactivity manifolds when prepared by other methods.[73]

3 Heterodinuclear Niobium/Molybdenum Dinitrogen Cleavage and N for O(Cl) Isovalent Exchange: Synthesis of N_2-Derived Organonitriles

As demonstrated above, the phosphido anion [**1a**-P]$^-$ successfully allows the formation of phosphaalkynes by P for O(Cl) metathesis. The niobium-containing product obtained after phosphaalkyne generation, namely oxo **1a**-O, was also shown to be readily recycled back to starting material. Consequently, it was of interest to extend this synthetic methodology to the construction of organonitriles (N≡CR) from the analogous nitrido niobium anion [N≡Nb(N[Np]Ar)$_3$]$^-$ ([**1a**-N]$^-$). Furthermore, it was highly desirable that anion [**1a**-N]$^-$ be derived from N_2 gas. While N_2 reduction to ammonia has received considerable attention of late,[74-81] there remains interest in direct incorporation of N_2-derived nitrogen atoms into organic molecules without the intermediacy of ammonia.[82-90] However, existing methods for the metal-mediated transfer of N-atoms derived from N_2 to organic substrates often proceed with destruction of the resultant metal complex.[74,80-81] Accordingly, a synthetic system allowing for N-atom transfer, nitrile formation and conservation of the metal complex would provide an efficient and atom-economical N_2-fixation methodology.

In addition, through the use of $^{15}N_2$ gas, the coupling of metal-mediated N_2 cleavage and isovalent exchange can provide facile synthetic access to ^{15}N-labled organonitriles. This application is particularly appealing due to the utility of ^{15}N as a spectroscopic handle in biological nuclear magnetic resonance[91,92] (NMR) and electron double nuclear resonance (ENDOR) investigations. Indeed, ^{15}N-labled organonitriles have been employed in ENDOR studies as substrates for the nitrogenase FeMo-cofactor,[93] in addition to serving as valuable synthons to many biologically-active heterocycles.[94-100] Whereas $^{15}N_2$ gas is among the least expensive commercial sources of ^{15}N atoms, its utilization in organic synthesis is currently inhibited by a paucity of effective synthetic N_2-fixation systems.[101]

Like the phosphorus chemistry above, activation of N_2 by a niobium trisamide system is expected to result in the formation of a dinuclear bridging N_2 complex. The latter would presumably provide a nitrido niobium anion in a subsequent reduction step. Indeed, Gambarotta has provided evidence for the bimolecular activation of N_2 by a Nb(NR_2)$_3$ species in a system that is explicable in terms of the existence of a niobaziridine-hydride intermediate.[102] However, the niobaziridine-hydride complex **1a**-H *has not* exhibited any reactivity towards N_2 to date. Complex **1a**-H has been subjected to numerous experimental conditions aimed at encouraging its reaction with N_2. Such experiments have included (i) stirring **1a**-H at low temperatures where N_2 is known to be at high concentration in solution, (ii) exposure of solutions of **1a**-H to high pressures of N_2, (iii) addition of Lewis basic additives to solutions of **1a**-H in order to promote niobaziridine ring opening[103]and (iv) addition of neutral, transition metal dinitrogen complexes[104] which could transfer coordinated N_2 to **1a**-H in solution. However, in each case, no

reaction with N_2 was observed. Furthermore, the factors responsible for the lack of reactivity between **1a**-H and N_2 are presently unclear.

Despite the unsuccessful studies aimed at the direct activation of N_2 by **1a**-H, the formation of N_2-derived organonitriles by N for O(Cl) isovalent exchange on a d^0 Nb platform remained a priority. Therefore, the heterodinuclear Nb/Mo N_2-cleavage system developed by Mindiola was exploited in order to access an N_2-derived nitrido niobium anion.[61,105] Unfortunately, the use of this particular heterodinuclear N_2-cleavage system suffers in terms of atom-economy from loss the of one N-atom as a neutral nitrido molybdenum(VI) complex.[105] To partially overcome this limitation, new expedient and high-yielding syntheses of both the Nb and Mo precursors for heterodinuclear N_2 cleavage have been developed. These studies, along with the development of a Nb-based system for formation of N_2-derived organonitriles by isovalent N for O(Cl) exchange, are presented below.

3.1 Molybdenum-Based Systems for Dinitrogen Uptake: Improved Syntheses of Molybdenum Dinitrogen Anions

In the previous report of Nb/Mo heterodinuclear N_2 cleavage by Mindiola et al.,[105] the molybdenum dinitrogen anion $[(N_2)Mo(N[t\text{-Bu}]Ar)_3]^-$ ([**11a**-N_2]$^-$)[17] was combined with the chloro-Nb^{IV} complex, Nb(Cl)(N[*i*-Pr]Ar)$_3$ (**1b**-Cl),[106] as shown in Scheme 8. The resulting Nb/Mo heterodinuclear N_2 complex **12a** was subsequently reduced by KC_8[107] to afford one equiv each of the terminal nitrides N≡Mo(N[*t*-Bu]Ar)$_3$ (**11a**-N)[15-17] and [N≡Nb(N[*i*-Pr]Ar)$_3$]$^-$ ([**1b**-N]$^-$).[105] Because the synthesis of Na[**11a**-N_2] required an exceedingly long addition time (t > 10 h) of the *tris*anilide Mo(N[*t*-Bu]Ar)$_3$ (**11a**)[15-17] to sodium amalgam (Na/Hg),[17] a more convenient route to its formation was sought.

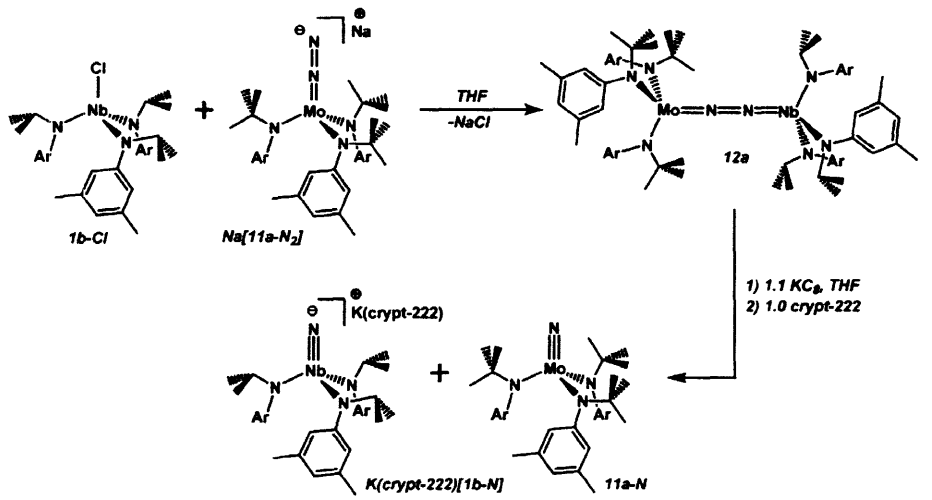

Scheme 8. The Nb/Mo Heterodinuclear N_2 Cleavage System Reported by Mindiola et al.

The trimethylsilyldiazenido complex, $(Me_3SiN_2)Mo(N[t\text{-Bu}]Ar)_3$ (**11a**-N_2SiMe_3),[17] was chosen for this purpose due to its availability in ^{15}N-labeled form and facile, one-pot synthesis from **11a**, N_2 and chlorotrimethylsilane (Me_3SiCl). It was found that treatment of **11a**-N_2SiMe_3 with sodium methoxide (NaOMe, 5.0 equiv) readily provides the target salt, Na[**11a**-N_2], in 75-

80% yields after workup and crystallization (Scheme 9). The yields of Na[**11a**-N_2] obtained by this desilylation route are comparable to those reported previously[17], but the necessity for slow addition of **11a** to Na/Hg is obviated.

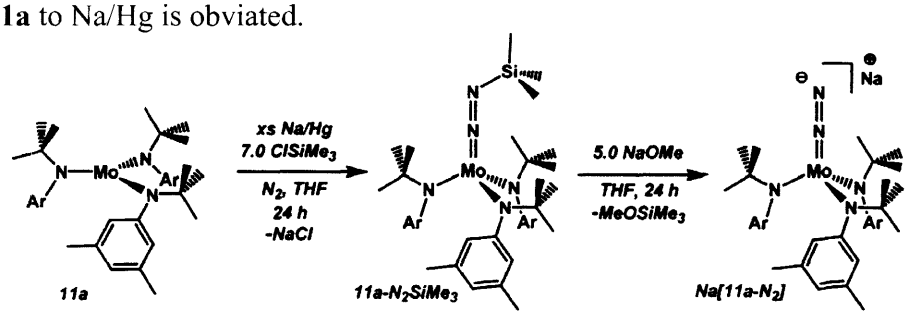

Scheme 9. Synthesis of Na[**11a**-N_2] via desilylation of **11a**-N_2SiMe_3.

In the course of studying the chemistry of molybdenum complexes supported by the N[Np]Ar ligand, another system was discovered which provides convenient, one-step access to a molybdenum dinitrogen anion. The molybdaziridine-hydride complex, Mo(H)(*t*-Bu(H)C=NAr)(N[Np]Ar)$_2$ (**11b**-H, Figure 11), is a purple-black, ground-state paramagnet (μ_{eff} = 1.64 μ_B) closely related to its diamagnetic niobium analogue **1a**-H. Complex **11b**-H is readily synthesized on a multigram scale in ca. 50% isolated yield by combination of $MoCl_3(THF)_3$ and (Et_2O)Li(N[Np]Ar) in Et_2O solution. Unlike **11a** and the *N*-isopropylanilide ligated Mo(H)(Me_2C=NAr)(N[*i*-Pr]Ar)$_2$ (**11c**),[108-112] complex **11b** does not effect the six-electron reduction of N_2 in solution at room temperature or below.[103,108] Instead, **11b** is stable for days in solution with respect to N_2 scission, but readily forms the dinitrogen-containing salt, Na[(N_2)Mo(N[Np]Ar)$_3$] (Na[**11b**-N_2]) when stirred over excess Na/Hg in the presence of N_2 (Scheme 10). Diamagnetic Na[**11b**-N_2] is obtained as a cherry-red crystalline solid after crystallization from *n*-pentane and gives rise to an intense ν_{NN} stretch at 1730 cm^{-1} in C_6D_6 solution (ν_{NN} = 1674 cm^{-1} for Na[**11b**-$^{15}N_2^-$]). The direct formation of Na[**11b**-N_2] from **11b** is notable inasmuch as analogues **11a** and **11c** both form the corresponding nitrido complexes (**11a**-N and (μ-N)[**11c**]$_2$) when subject to an identical synthetic regimen.[17,103] While the factors governing this dichotomy are presently unclear, small variations of the ancillary ligand framework have been shown to greatly influence the chemistry exhibited by these molybdenum anilido complexes.[108,113]

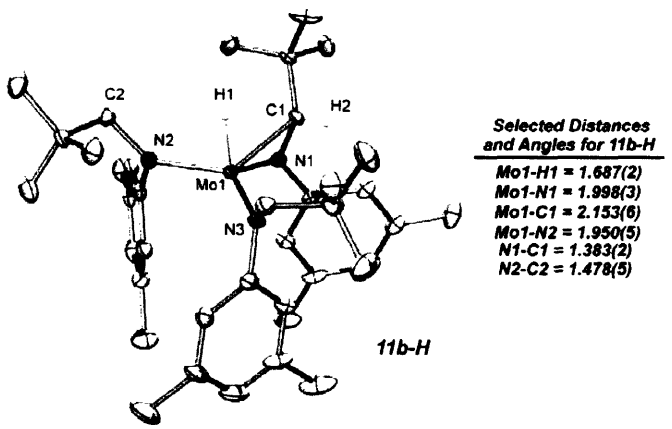

Figure 11. ORTEP Diagram of **11b**-H at the 35% Probability Level.

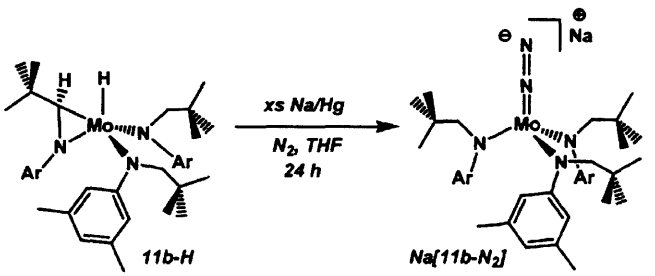

Scheme 10. Synthesis of N_2 anion Na[**11b**-N_2].

3.2 Synthesis of Dinitrogen-Bridged Mo/Nb Complexes and Heterodinuclear Dinitrogen Cleavage

While the N[*i*-Pr]Ar-ligated Nb^{IV} complex **1b**-Cl[106] was employed previously for heterodinuclear N_2 cleavage,[105] a platform encouraging metathetical exchange at the Nb center was sought. Therefore, the *N*-neopentylanilide (N[Np]Ar) system was chosen for this purpose based on the greater access it provides to the Nb center. Accordingly, reduction of the orange diiodide complex, **1a**-$(I)_2$ (Chapter 1), with 0.55 equiv of Mg(anthracene)$(THF)_3$[63] in THF solution provided the purple-brown monoiodide, Nb(I)(N[Np]Ar)$_3$ (**1a**-I) in 35% yield after crystallization from *n*-pentane. X-ray crystallography confirmed the formulation of **1a**-I as a 4-coordinate monoiodide complex, which is monomeric despite the large apparent accessibility to the Nb center (Figure 12). The overall solid-state structure of **1a**-I is otherwise unremarkable except for the pseudo-C_s symmetry exhibited by the three N[Np]Ar ligands. This latter feature is consistent with **1a**-I being a 3-fold symmetric, Nb^{IV} d^1 paramagnet (μ_{eff} = 1.81 μ_B), and accordingly susceptible to a first-order Jahn-Teller distortion.

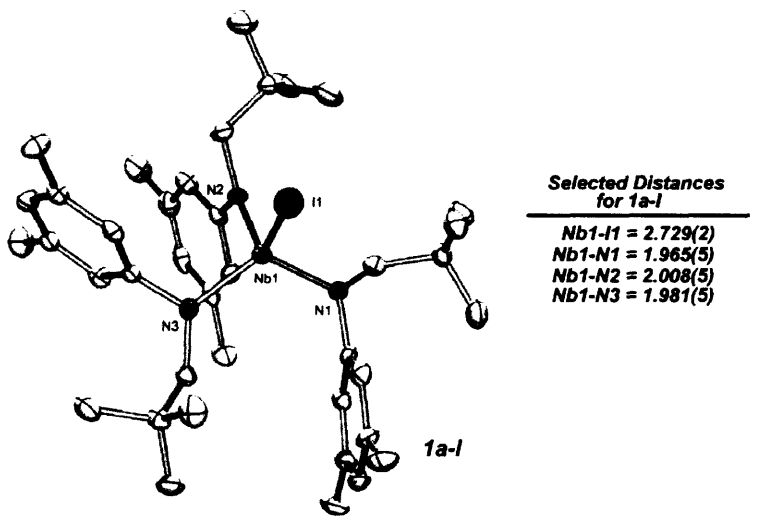

Figure 12. ORTEP Diagram of **1a**-I at the 35% Probability Level.

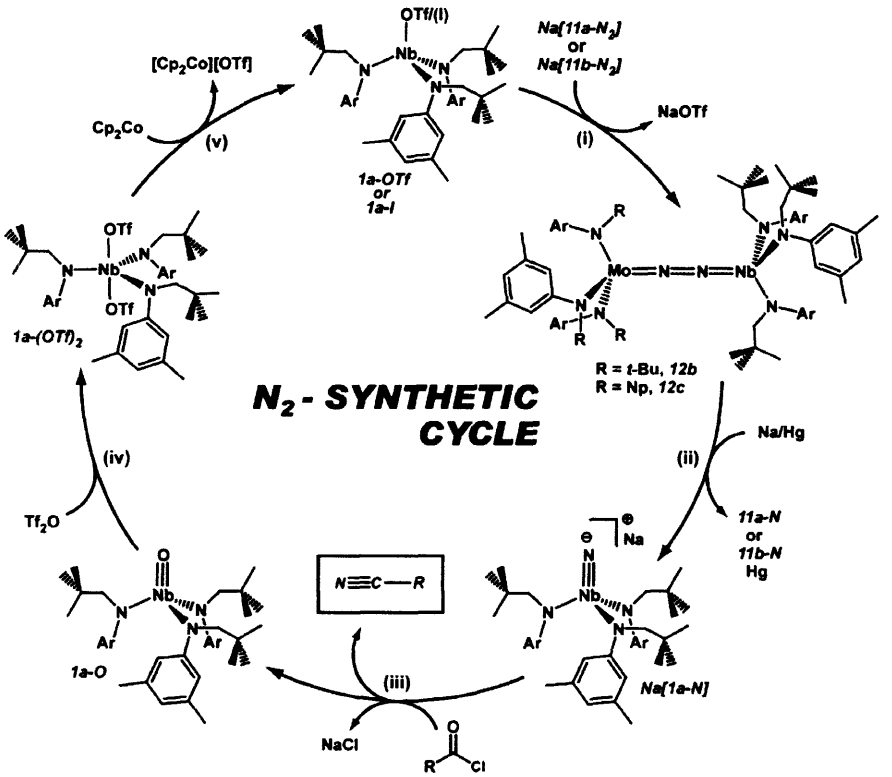

Scheme 11. Synthetic Cycle for the Metathetical Formation of N_2-Derived Organonitriles.

Dinitrogen anions [**11a**-N_2]$^-$ and [**11b**-N_2]$^-$ are transformed to the heterodinuclear Nb/Mo N_2 complexes (Ar[Np]N)$_3$Nb(μ-N_2)Mo(N[*t*-Bu]Ar)$_3$ (**12b**) and (Ar[Np]N)$_3$Nb(μ-N_2)Mo(N[Np]Ar)$_3$ (**12c**), respectively, when treated with **1a**-I (Scheme 11, reaction i). Paramagnetic **12b** and **12c** are obtained as green-brown crystalline solids after recrystallization from *n*-pentane. Each possesses solution magnetic and spectroscopic properties similar to those reported for the Nb/Mo heterodinuclear N_2 complex **12a**.[105] While both **12b** and **12c** can be isolated in ca. 50% recrystallized yields, the crude materials obtained after removal of NaOTf have been found to be of sufficient purity for subsequent reactions. Accordingly, scission of the dinitrogen units in **12b** and **12c** is effected by addition of excess Na/Hg in THF solution, providing an orange solution containing the Na(THF)$_x$ salt of the niobium nitrido anion [**1a**-N]$^-$ and the molybdenum nitrido complexes **11a**-N[15-17] or **11b**-N, respectively (Scheme 11, reaction ii). Cleavage of the N_2 unit in derivatives **12** upon reduction is readily rationalized by formation of the dinuclear anion [(Ar[Np]N)$_3$Nb(μ-N_2)Mo(N[R]Ar)$_3$]$^-$. The latter is isoelectronic to the homobimetallic N_2 complex (Ar[R]N)$_3$Mo(μ-N_2)Mo(N[R]Ar)$_3$[15-17] and similarly possesses an unstable $(\pi_0)^4(\pi_1)^4(\pi_2)^2$ electronic configuration across the M(μ-N_2)M core with respect to nitrido metal formation.[16] Consequently, the **12**/Na reaction system exemplifies the only such heterodinuclear N_2 scission process to date, despite the growing number of reported heterodinuclear N_2 complexes.[17,114-123]

Due to its disparate solubility properties in hydrocarbon solvents, nitrido anion salt Na[**1a**-N] is readily separable from the neutral derivatives **11**-N. Addition of *n*-pentane to the crude solid obtained from reduction of **12c** solubilizes **11b**-N, while precipitating the desolvated

salt, Na[**1a**-N], as an off-white powder. Filtration of the mixture affords essentially pure Na[**1a**-N] in 80 – 85% yield on a scale of up to 2.0g of **12c**. The same procedure liberates Na[**1a**-N] from **11a**-N in comparable yield. Subsequent evaporation of the filtrate and recrystallization of the residue from Et_2O, recovers molybdenum complexes **11a**-N and **11b**-N as yellow-orange crystals in 80% and 72% yields, respectively. The molecular structures of Na[**1a**-N] (as its *tris*-THF solvate) and **11b**-N were determined by X-ray diffraction (Figure 13), which confirmed their formulation. Furthermore, when prepared from $^{15}N_2$, both Na[**1a**-^{15}N] (δ = 754 ppm, Figure 14**A**) and **11b**-^{15}N (δ = 870 ppm) give rise to highly downfield ^{15}N NMR resonances typical of triply-bound, d^0 nitrido metal species.[28,105,124-129]

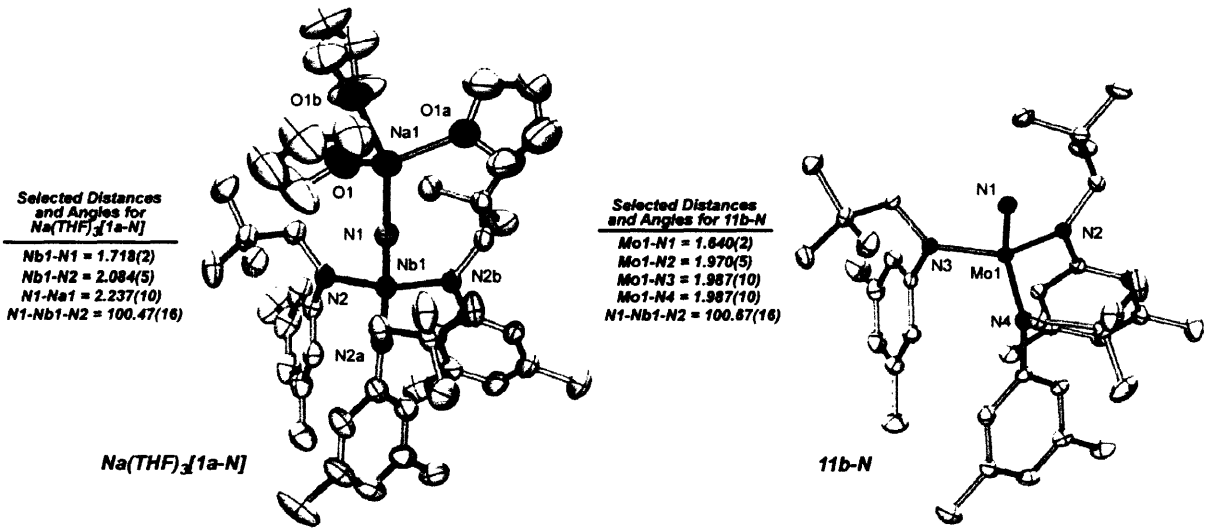

Figure 13. ORTEP Diagrams of Na(THF)$_3$[**1a**-N] and **11b**-N at the 35% Probability Level.

3.3 Synthesis of N_2-Derived Organonitriles from the Nitrido Anion [1a-N]$^-$ and Acid Chloride Substrates by isovalent N for O(Cl) Exchange

Nitrido anion [**1a**-N]$^-$ was competent for the conversion of a variety of acid chlorides into their corresponding organonitriles (Scheme 11, reaction iii). For example, treatment of a THF-d_8 solution of Na[**1a**-N] with pivaloyl chloride (*t*-BuC(O)Cl, 0.95 equiv) at room temperature elicited a rapid color change from pale yellow to orange. Analysis of the reaction mixture by ^{1}H NMR spectroscopy after 15 min indicated complete consumption of Na[**1a**-N], concomitant with the formation of **1a**-O and pivalonitrile (*t*-BuC≡N, δ = 1.32 ppm, THF-d_8) in nearly quantitative yield. Similar results were obtained for acid chlorides, RC(O)Cl, where R = Ph, 1-Ad (Ad = adamantyl), Me and HC=CH$_2$.

The volatile organonitriles (*e.g.* R = *t*-Bu, Me and HC=CH$_2$), were isolated from the reaction mixture by simple vacuum transfer, providing THF-d_8 solutions of the pure compounds in ca. 90% yields relative to Na[**1a**-N] (^{1}H NMR vs. Cp_2Fe). Notably, excessive thermal input was not needed to liberate the newly generated RC≡N from **1a**-O and ^{1}H NMR analysis gave no indication for the formation of RC≡N→**1a**-O Lewis base/acid adducts. After vacuum transfer and removal of NaCl, oxo **1a**-O was recovered essentially pure as assayed by ^{1}H NMR. As in

Nb-mediated phosphaalkyne synthesis (above), addition of Tf_2O to **1a**-O effected its conversion to bistriflate **1a**-$(OTf)_2$ (Scheme 11, reaction iv). The latter is subsequently reduced to the green brown monotriflato complex Nb(OTf)(N[Np]Ar)$_3$ (**1a**-OTf) by Cp_2Co or Mg(anthracene)$(THF)_3$ (Scheme 11, reaction v). Monotriflate **1a**-OTf is readily substituted for **1a**-I in the synthesis of the heterodinuclear N_2 complexes **12**, thus establishing the synthetic cycle for Nb-mediated nitrile formation (Scheme 11).

When ^{15}N-labeled Na[**1a**-^{15}N] was treated with the same acid chlorides, the corresponding ^{15}N-organonitriles were smoothly generated. Vacuum transfer of the volatile ^{15}N-organonitriles into sealable NMR tubes allowed for their analysis by ^{15}N NMR spectroscopy, whereas the ^{15}N NMR spectra of ^{15}N-benzonitrile and ^{15}N-adamantylnitrile (R = C_6H_5 and 1-Ad, respectively) were recorded in the presence of oxo **1a**-O. In all cases, only one resonance was observed over the range 200 – 900 ppm, highlighting the efficiency of ^{15}N-atom transfer from Na[**1a**-^{15}N] to acid chloride substrates.

Listed in Table 2 are the experimentally determined solution ^{15}N chemical shifts (δ) for the ^{15}N-organonitriles generated from Na[**1a**-^{15}N] in this study and the corresponding ^{15}N NMR spectra are depicted in Figure 14. Whereas ^{15}N chemical shift data are available for both ^{15}N-acetonitrile[130] and ^{15}N-benzonitrile,[131,132] those of ^{15}N-pivalonitrile, ^{15}N-1-adamanylcarbonitrile and ^{15}N-acrylonitrile (Figure 14) have evidently not been reported. However, as Table 2 shows, the new ^{15}N chemical shift data reported here exhibit the expected qualitative trend based on inductive effects. Although the ^{31}P nucleus is more sensitive to inductive effects, increasingly electron-releasing substituents promote a similar upfield progression of ^{31}P resonances in phosphaalkynes.[34,51-53,72] In addition, treatment of Na[**1a**-^{15}N] with ^{13}C-labled acetylchloride ($H_3C^{13}C(O)Cl$) afforded doubly labeled (^{15}N/^{13}C) acetonitrile ($H_3C^{13}C{\equiv}^{15}N$, Figure 14**F**), the ^{15}N NMR chemical shift and coupling constants ($^1J_{CN}$ and $^3J_{HN}$) of which were in excellent agreement with literature values.[130] Similar treatment of Na[**1a**-^{15}N] with ^{13}C-labled 1-adamantylchloride (1-Ad^{13}C(O)Cl)[133] produced ^{15}N/^{13}C-1-adamantylcarbonitrile (1-Ad$^{13}C{\equiv}^{15}N$, Figure 14**E**), thereby providing another example of a doubly labeled organonitrile from Na[**1**-^{15}N].

3.4 Reaction Sequence Leading to Organonitrile Formation from [1a-N]$^-$ and Acid Chlorides

The reaction between RC(O)Cl and Na[**1a**-N] in THF is rapid, proceeding to products RC≡N, **1a**-O and NaCl within minutes at room temperature or below. To date, no evidence for the presence of intermediate species during the organonitrile formation process has been obtained. This contrasts with the related tungsten-mediated organonitrile synthesis developed recently in our group.[134] In that case, treatment of the neutral nitrido complex, N≡W(N[*i*-Pr]Ar)$_3$, with RC(O)Cl provided the linear acylimido[135-138] species R(O=)CN=W(Cl)(N[*i*-Pr]Ar)$_3$ as an observable intermediate prior to fragmentation to RC≡N and oxo-chloride, W(O)(Cl)(N[*i*-Pr]Ar)$_3$.[134] It was postulated that bending the linear acylimido moiety at nitrogen afforded an unobserved tungstacyclobutene species susceptible to retro-[2+2] fragmentation in a manner reminiscent of alkyne metathesis by Schrock-type alkylidyne complexes.[29] A similar intramolecular mechanism was proposed for thiocyanate ion ([SCN]$^-$) formation upon reaction

Table 2. Solution ^{15}N NMR Data for ^{15}N-Labeled Organonitriles ($^{15}N{\equiv}CR$).[a]

Nitrile	R	δ (ppm)	^{15}N-Coupling Constants (Hz)
1-Adamantylcarbonitrile-$^{13}C/^{15}N$[b]	1-Ad	244.1	$^{1}J_{CN}$ = 15.2
Pivalonitrile-^{15}N	*t*-Bu	244.2	
Acetonitrile$^{13}C/^{15}N$	CH_3	247.9[c]	$^{1}J_{CN}$ = 17.0, $^{3}J_{HN}$ = 1.67
Benzonitrile-^{15}N[b]	C_6H_5	259.2[d]	
Acrylonitrile-^{15}N	$HC{=}CH_2$	260.0	$^{3}J_{HN}$ = 1.33, $^{5}J_{HN(trans)}$ = 0.24[e]

[a] All spectra were acquired in THF-d_8 at 20.1 °C on an instrument operating at 60.84 MHz (^{1}H = 600.2 MHz). [b] Spectrum acquired in the presence of **1a**-O. [c] Literature value for $^{15}N{\equiv}^{13}C{-}CH_3$ δ = 245.0 ppm (neat).[130] [d] Literature value for $^{15}N{\equiv}C{-}C_6H_5$ = 258.4 ppm in CH_2Cl_2[131,132] [e] The $^{5}J_{HN}(cis)$ coupling was not resolved.

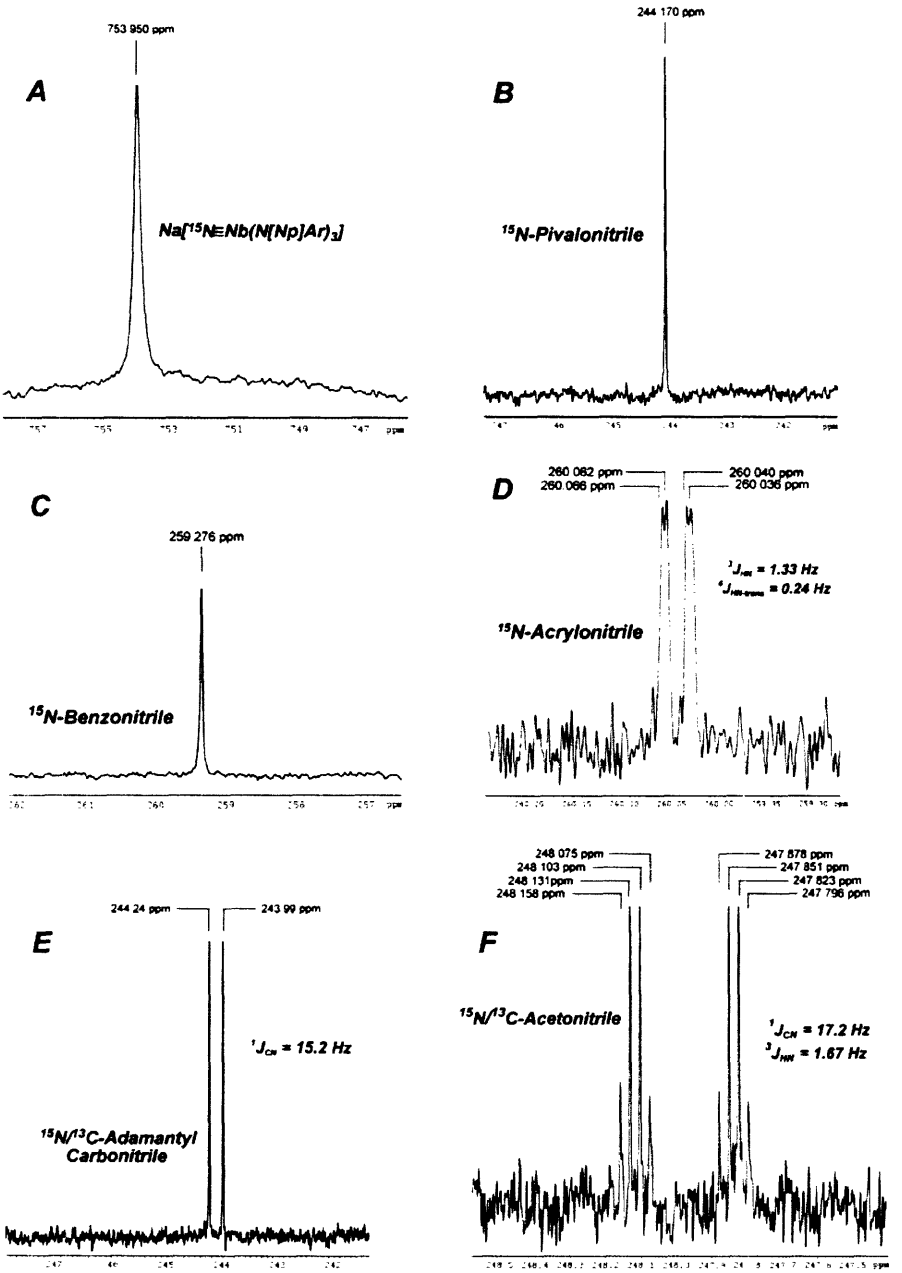

Figure 14. Solution ^{15}N NMR Spectra (THF-d_8) for Na[**1a**-^{15}N] and ^{15}Labeled Organonitriles.

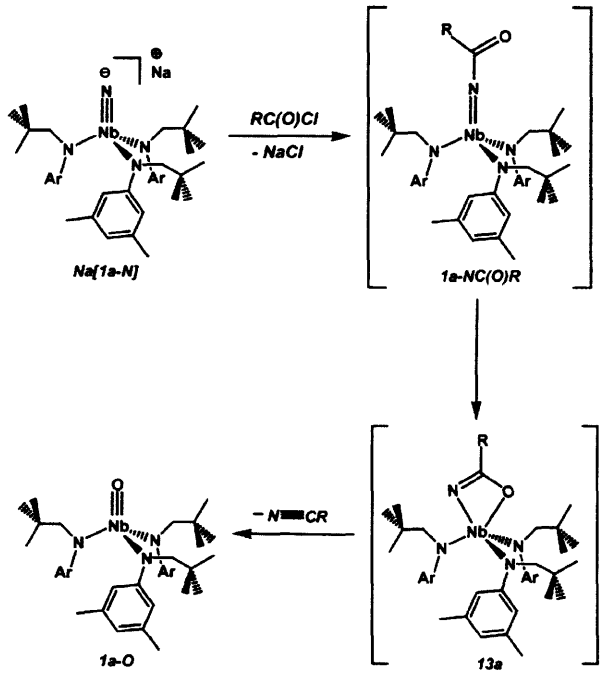

Scheme 12. Proposed Reaction Sequence Leading to Metathetical Organonitrile Formation from Na[**1a**-N] and Acid Chloride Substrates.

of the nitrido vanadium anion $[N{\equiv}V(N[t\text{-Bu}]Ar)_3]^-$ and CS_2.[139] Furthermore, Bergman has recently reported the conversion of amides to organonitriles where intramolecular retro-[2+2] fragmentation of a d^0 zirconium-acylimido is proposed to be mechanistically operative.[140,141]

While reaction between Na[**1a**-N] and RC(O)Cl presumably affords a linear acylimido species (**1a**-NC(O)R, Scheme 12), intramolecular niobacyclobutene formation (**13a**, Scheme 12) and retro-[2+2] fragmentation are evidently unimpeded by the *tris*-N[Np]Ar ligand set. However, to model these events, it was of interest to find a niobium platform capable of stabilizing an incipient linear acylimido complex. It was reasoned that the *tris*-N[*t*-Bu]Ar ligand set would provide a kinetically persistent acylimido due to its greater steric demand in the vicinity of the metal center relative to that of *tris*-N[Np]Ar. Accordingly, the nitrido niobium salt, $Na[N{\equiv}Nb(N[t\text{-Bu}]Ar)_3]$ (Na[**1c**-N]),[142] prepared in the context of isocyanate decarbonylation rather than N_2 cleavage, was employed. Treatment of Na[**1c**-N] with 0.95 equiv of pivaloyl chloride afforded the pale-yellow complex t-Bu(O)CN=Nb(N[*t*-Bu]Ar)$_3$ (**1c**-NC(O)*t*-Bu, Scheme 13) in 77% yield and an X-ray diffraction study confirmed its identity as a linear acylimido-niobium species (Figure 15).

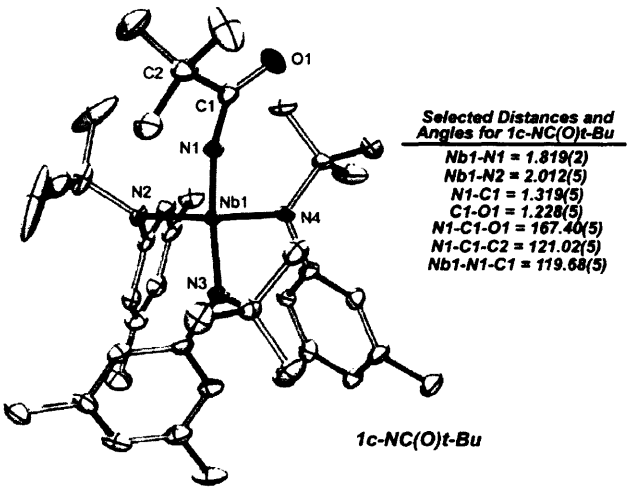

Figure 15. ORTEP Diagram of **1c**-NC(O)*t*-Bu at the 35% Probability Level.

As expected, complex **1c**-NC(O)*t*-Bu was stable at room temperature in C_6D_6 solution. However, upon heating at 80 °C for 1 h, pivalonitrile (*t*-BuC≡N, δ = 0.76 ppm, C_6D_6) and the oxo niobium complex O≡Nb(N[*t*-Bu]Ar)$_3$[143] (**1c**-O, Scheme 13) were cleanly generated. Thus while the linear acylimido functionality on Nb can be kinetically stabilized by three ancillary *tert*-butyl substituents, subsequent organonitrile formation is not prohibited. Furthermore, no intermediates were observed spectroscopically during the **1c**-NC(O)*t*-Bu → *t*-BuC≡N + **1c**-O conversion, indicating that formation of products occurs quickly upon coordination of acylimido oxygen atom to the Nb center. Therefore, the rapid metathetical exchange processes observed for the N[Np]Ar-ligated [**1a**-N]$^-$ can be considered a result of an unhindered coordination environment about Nb. This notion is further substantiated by the observed formation of [SCN]$^-$ from CS_2 and [N≡V(N[*t*-Bu]Ar)$_3$]$^-$,[139] despite occurring on the smaller and seemingly inaccessible C_{3v}-symmetric vanadium center.[144]

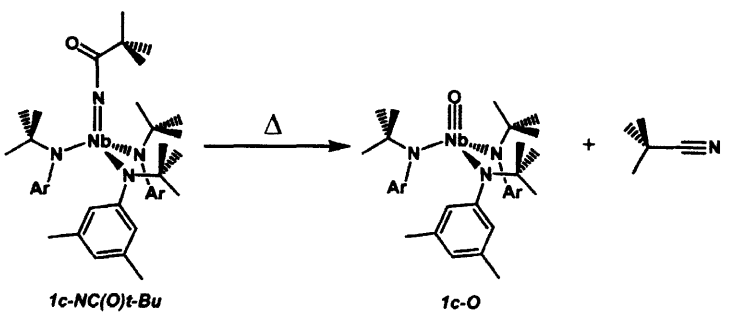

Scheme 13. Thermolysis of **1c**-NC(O)*t*-Bu: Formation of *t*-BuC≡N and oxo **1c**-O

3.5 Calculated Thermodynamic Parameters for Organonitrile Nitrile Formation

To elucidate in further detail the reaction sequence leading to organonitrile formation, DFT calculations were performed on a representative model system (**14m**). As shown in Figure 16, the direct conversion of the linear acylimido complex, $H_3C(O)CN{=}Nb(NH_2)_3$ (**14m-A**), to

products $O{\equiv}Nb(NH_2)_3$ (**14m-O**) and $H_3CC{\equiv}N$ is calculated to be favorable by 7.99 kcal/mol. Also shown is the relative enthalpic change associated with isomerization of **14m-A** to the corresponding 4-membered niobacycle, **14m-B**. While the calculated structures of both **4m-A** and **14m-O** showed excellent agreement to their experimental counterparts (*e.g.* **1c**-NC(O)*t*-Bu and **1a**-O, Chapter 1), that of **14m-B** represented a minimum on the potential energy surface. Interestingly, the **14m-A** → **14m-B** isomerization process, characterized by bending of **14m-A** at the acylimido nitrogen, is disfavored by only 2.68 kcal/mol. Although not observed experimentally, these calculations suggest formation of an intermediate akin to **14m-B** is not prevented by an insurmountable energetic barrier. Furthermore, retro-[2+2] fragmentation of **14m-B** to **14m-O** and $H_3CC{\equiv}N$ is enthapically favored by 10.67 kcal/mol. It is interesting to note that formation of $H_3CC{\equiv}P$ and oxo **14m-O** from the phosphorus-containing niobacycle $(H_3C(O)C{=}P)Nb(NH_2)_3$ is calculated to be enthalpically favored by only 1.73 kcal/mol. While the Nb≡P bond dissociation energy is expected to be lower than that the of Nb≡N bond, the enthalpically preferred formation of nitriles relative to phosphaalkynes reflects a significant energetic compensation gained in the formation of a strong C≡N triple bond.

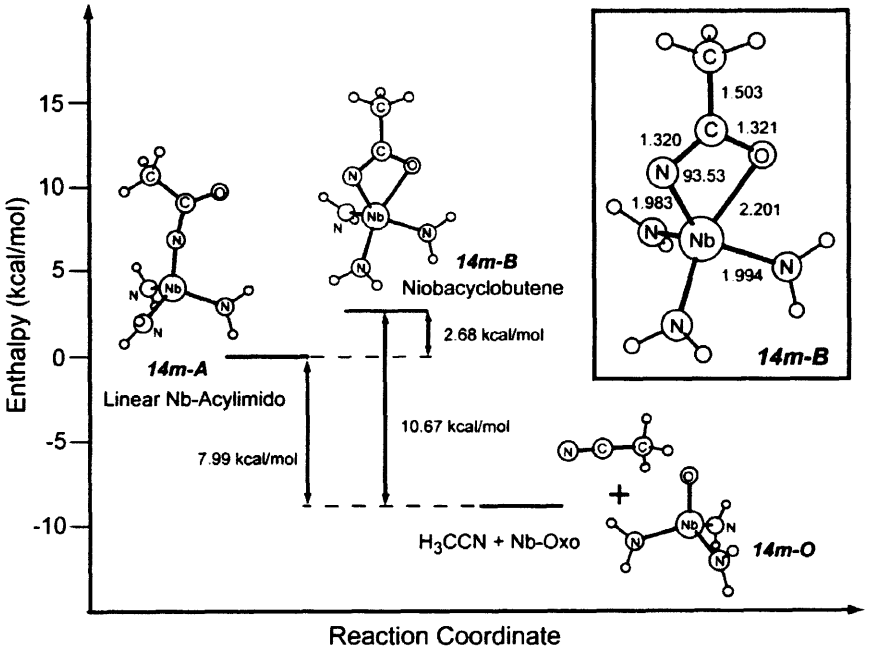

Figure 16. Calculated relative enthalpic values for the conversion of model **14m-A** to products **14m-O** and MeC≡N. The niobacyclobutene species **14m-B** (inset) was found as a stationary point on the potential energy surface.

That niobacycle **14m-B** can furnish an organonitrile by retro-[2+2] fragmentation is readily rationalized from inspection of its geometric structure. The optimized geometry of **14m-B** is consistent with its formulation as a niobacyclobutene (Nb-N=C(R)O, Figure 15, inset), rather than a bent acylimido (Nb=N-C(=O)R) complex. Thus significant electronic reorganization in the acylimido functionality is initiated by coordination of oxygen to the Nb center. Calculated metrical parameters in support of this claim include a shortening of the N-C

bond length in **14m-B** relative to **14m-A** (1.320 Å vs. 1.386 Å) and a considerable lengthening of the corresponding C-O bond (1.321 Å vs. 1.227 Å). Additionally, the Nb-N bond length of 1.983 Å in **14m-B** clearly exceeds the range expected for a Nb^{V}-imido complex,[145] falling closer to that expected for an amido[146] or ketimido ligand.[111,146-147] Coupled with the acute niobacyclic Nb-N-C angle (93.53°), the foregoing geometric parameters of **14m-B** provide a reasonable picture for the exchange of C-O and M-N multiple bonds for that of C-N and M-O within the coordination sphere of niobium. Notably, Chisholm has also identified computationally a 4-membered intermediate for N≡W(O-*t*-Bu)$_3$–catalyzed N-atom exchange between organonitriles with gross structural features similar to those of **14m-B**.[28]

4 Conclusions and Future Work

The work described in this chapter has demonstrated the propensity of low-coordinate, d^0 pnictido niobium complexes to mediate the transfer of pnictogen atoms to organic substrates. Specifically, the phosphido anion [**1a**-P]$^-$ has been shown to transform acid chlorides into phosphaalkynes by an isovalent P for O(Cl) exchange reaction, which swaps Nb≡P and C≡P triple bonds. This new heteroatom exchange reaction has provided for the construction of P_4-derived phosphaalkynes under mild synthetic conditions and represents a marked improvement in the synthesis of RC≡P compounds. The ultimate Nb-containing product of this reaction sequence, the oxo complex **1a**-O, has been shown to be converted back to the niobaziridine-hydride complex **1a**-H through the synthetic intermediacy of the bistriflate species **1a**-$(OTf)_2$. Thus anion [**1a**-P]$^-$ can be considered as a recyclable reagent for the formation of phosphaalkynes.

In addition, N_2-derived organonitriles have been synthesized in an analogous N for O(Cl) exchange mediated by the nitrido niobium anion [**1a**-N]$^-$. The nitrido ligand of the latter is obtained from N_2 in a heterodinuclear Mo/Nb N_2 cleavage process utilizing a Mo trisanilide system as a reaction partner. Strong evidence has been obtained for the formation of phosphaalkynes and organonitriles from the intramolecular retro-[2+2] fragmentation of niobacyclobutene intermediates. Thus the isovalent pnictogen for O(Cl) exchange reactions described here are mechanistically analogous to alkyne metathesis by Schrock-type alkylidyne complexes. Furthermore, these reactions establish a new paradigm for utilization of d^0 pnictido complexes obtained from element activation reactions in organic synthesis.

While this work lays the foundation for the formation of organo-phosphorus and nitrogen compounds from d^0 phosphido and nitrido complexes, respectively, much work remains before a truly efficient synthetic methodology is realized. Paramount to this goal is the development of a separation technique for the isolation of non-volatile organopnictogen compounds from oxo **1a**-O without affecting the integrity either species. Further, the scope of organic substrates suitable for isovalent exchange must be expanded. Such possibilities include the use of γ-halocarbonyl compounds (*i.e.* $R(O)C(CH_2)_2CH_2X$, x =halide), which could provide synthetically useful 5-membered cyclic imines and phosphaalkenes. Lastly, and of crucial importance, the well-defined bimetallic activation of N_2 by a niobium[148,149] trisamide system must be discovered and harnessed.

5 Experimental Procedures

5.1 General Synthetic Considerations

Unless otherwise stated, all manipulations were carried out at room temperature, under an atmosphere of purified dinitrogen using a Vacuum Atmospheres glove box or Schlenk techniques. All solvents were obtained anhydrous and oxygen-free according to standard purification procedures. Tetrahydrofuran-d_8 (THF-d_8) was vacuum transferred from Na metal and stored in the glove box over 4 Å molecular sieves for at least 3 d prior to use. Benzene-d_6 (C_6D_6) was degassed and stored similarly. Celite 435 (EM Science) and 4 Å molecular sieves (Aldrich) were dried under vacuum at 250 °C overnight and stored under dinitrogen. Gaseous $^{15}N_2$ (99.9% ^{15}N) was purchased from Cambridge Isotope Laboratories in 100 mL break-seal containers. Solid NaOMe was slurried in anhydrous THF under an N_2 atmosphere for 24h, before being dried at ca. 180 °C under vacuum for an additional 24 h. Pivaloyl chloride (*t*-BuC(O)Cl) was distilled from CaH_2 prior to use. Ferrocene (Cp_2Fe) was sublimed and stored under dinitrogen prior to use. The reagents $Mg(THF)_3$(anthracene),[63] 1-Adamantoyl chloride-^{13}C (1-Ad^{13}C(O)Cl)[133], $(C_2H_4)P(PPh_3)_2$[68] and $MoCl_3(THF)_3$[150] were prepared as specified in the literature. Adamantane-1,3-dicarbonyl chloride (1,3-$(C(O)Cl)_2$Ad) was prepared by refluxing adamantane-1,3-dicarboxylic acid in neat thionyl chloride (SO_2Cl_2) for 3 h, followed by recrystallization from Et_2O under N_2. All other reagents were obtained from commercial sources and used as received. All Glassware was oven dried at a temperature of 230 °C prior to use.

Solution ^1H, $^{13}C\{^1H\}$, $^{19}F\{^1H\}$ and $^{31}P\{^1H\}$ NMR spectra were recorded using Varian XL-300 MHz and Varian INOVA 500 MHz spectrometers. ^1H and ^{13}C chemical shifts are reported referenced to the residual solvent resonances of 7.16 ppm (^1H) and 128.3(t) ppm (^{13}C) for benzene-d_6 or 1.73 ppm (^1H) and 67.57 ppm (^{13}C) for THF-d_8. $^{31}P\{^1H\}$ chemical shifts are reported referenced to the external standard H_3PO_4 (85 %, 0.0 ppm). $^{19}F\{^1H\}$ chemical shifts are reported referenced to the external standard $CFCl_3$ (neat). Solution ^{15}N NMR spectra were recorded on a Bruker Advance-600 spectrometer operating at a resonance frequency of 60.84 MHz. ^{15}N NMR chemical shifts are reported referenced to external formamide-^{15}N ($H_2{}^{15}NC(O)H$, 55/45 v/v in DMSO); 113.0 ppm relative to liquid NH_3 (0.0 ppm).[151] Solution IR spectra were recorded on a Perkin-Elmer 1600 Series FTIR spectrometer. All spectra were recorded in C_6D_6 using a KBr plated solution cell. Solvent peaks were digitally subtracted from all spectra using an authentic spectrum obtained immediately prior to that of the sample. Combustion analyses were carried out by H. Kolbe Microanalytisches, Mülheim an der Ruhr, Germany.

5.2 One–Pot synthesis of Na(THF)[PNb(N[Np]Ar)$_3$] (Na(THF)[1a-P]).

To a THF solution of niobaziridine–hydride **1a**-H (3.00 g, 4.51 mmol, 7 mL) was added a THF solution of white phosphorus (P_4, 0.166 g, 1.35 mmol, 0.3 equiv, 5 mL) at room temperature. After addition and over a period of 5 min, the initially orange solution changed to the forest green color characteristic of bridging diphosphide (μ-P_2)[**1a**]$_2$. The reaction was allowed to stir an additional 30 min, whereupon 1.0% sodium amalgam (Na: 0.311 g, 13.53 mmol, 3.0 equiv/Nb, Hg: 31.1 g) was added. The mixture was vigorously stirred for 2.5 h while gradually becoming dark orange. Work–up and isolation of Na(THF)$_x$[**1a**-P] was performed as reported in Chapter 2. Yield: 75% based on **1a**-H.

5.3 Synthesis of (*t*-BuC(O)P)Nb(N[Np]Ar)$_3$ (2-*t*-Bu) and (1-AdC(O)P)Nb(N[Np]Ar)$_3$ (2-1-Ad).

Separately, a 7 mL THF solution of Na(THF)[**1a**-P] (0.500 g, 0.635 mmol) and a 2 mL THF solution containing 0.95 equiv of the corresponding acyl chloride (*t*-BuC(O)Cl – **2**-*t*-Bu, ^{1}AdC(O)Cl – **2**-1-Ad) were frozen in a glove box cold well (liquid N_2). Upon removal from the cold well, approximately 0.6 mL of the thawing solution containing the acyl chloride was added dropwise over 1 min to the thawing solution of Na(THF)[**1a**-P], eliciting a color change from dark yellow to red-orange. The reaction mixture was allowed to stir for an additional 3 min whereupon both solutions were placed back into the cold well. This procedure was repeated two more times until complete addition of the acyl chloride was achieved. The reaction mixture was then allowed to warm to room temperature and stirred for an additional 30 min before being evaporated to dryness *in vacuo*. The residue obtained was extracted with *n*-pentane (3-5 mL), filtered through Celite and the filtrate evaporated to dryness in vacuo. The resulting residue was then dissolved in a minimum of Et_2O and chilled at –35 °C for 1–2 d whereupon cherry-red crystals were obtained and collected. The synthesis of **2**-1-Ad-^{13}C was performed analogously employing ^{13}C–^{1}AdC(O)Cl.[147]

2-*t*-Bu: Cherry-red crystals, 70%. ^{1}H NMR (500 MHz, C_6D_6, 23 °C): δ 6.57 (s, 9H, p-Ar (3H) & o-Ar (6H)), 3.97 (s, 6H, NCH_2), 2.13 (s, 18H, Ar-CH_3), 1.58 (s, 9H, P=C(*t*-Bu)O), 0.91 (s, 27, *t*-Bu); ^{13}C{^{1}H} NMR (125.8 MHz, C_6D_6, 23 °C): δ 260.4 (d, P=*C*(*t*-Bu)O, $^1J_{CP}$ = 113.2 Hz), 151.9 (ipso-Ar), 138.1 (m-Ar), 126.7 (p-Ar), 122.3 (o-Ar), 66.2 (N*C*H$_2$), 36.6 (*C*(CH$_3$)$_3$), 30.0 (C(*C*H$_3$)$_3$), 29.1 (P=C(*C*(CH$_3$)O), 28.1 (P=C(C(*C*H$_3$)O), 21.8 (Ar-*C*H$_3$); ^{31}P{^{1}H} NMR (121.5 MHz, C_6D_6, 23 °C): δ 259.6 (s); FTIR (KBr windows, C_6D_6 solution): 2977, 2871, 1587, 1475, 1381, 1366, 1291, 1204, 1121 cm^{-1}. Anal. Calcd. for $C_{44}H_{69}N_3NbOP$: C, 67.76; H, 8.92; N, 5.39. Found C, 67.01; H, 8.78; N, 5.44.

2-1-Ad: Cherry-red crystals, 80%. ^{1}H NMR (500 MHz, C_6D_6, 23 °C): δ 6.58 (s, 6H, o-Ar), 6.57 (s, 3H, o-Ar), 4.00 (s, 6H, NCH_2), 2.39 (m, 6H, ^{1}Ad), 2.14 (s, 18H, Ar-CH_3), 2.10 (m, 3H, ^{1}Ad), 1.76 (m, 6H, ^{1}Ad), 0.942 (s, 27, *t*-Bu); ^{13}C{^{1}H} NMR (125.8 MHz, C_6D_6, 23 °C): 260.0 (d, P=*C*(^{1}Ad)O, $^1J_{CP}$ = 102.7 Hz), 152.1 (ipso-Ar), 138.1 (m-Ar), 126.7 (p-Ar), 122.3 (o-Ar), 66.2 (N*C*H$_2$), 40.3 (^{1}Ad), 37.8 (^{1}Ad), 36.7 ((*C*(CH$_3$)$_3$), 30.1 (C(*C*H$_3$)$_3$), 29.4 (^{1}Ad) , 21.8 (Ar-*C*H$_3$), 15.9 (^{1}Ad); ^{31}P{^{1}H} NMR (121.5 MHz, C_6D_6, 23 °C): δ 262.6 (s); FTIR (KBr windows, C_6D_6 solution): 2916, 2901, 1601, 1587, 1364, 1290, 928 cm^{-1}. Anal. Calcd. for $C_{50}H_{75}N_3NbOP$: C, 69.99; H, 8.81; N, 4.90. Found: C, 69.21; H, 8.44; N, 5.02.

5.4 Phosphaalkyne Ejection from Niobacycles 2-*t*-Bu and 2-1-Ad: Formation of *tert*-Butyl (*t*-BuC≡P, 3-*t*-Bu) and 1-Adamantyl (1-AdC≡P, 3-1-Ad) Phosphaalkyne.

Niobacycle **2**-*t*-Bu (0.100 g, 0.128 mmol) was dissolved in C_6D_6 (1.5 mL) and loaded into a NMR tube which was subsequently sealed under dinitrogen. A ^{1}H NMR spectrum was acquired at room temperature (Figure 3**A**) and the sample was then immersed in a 45 °C oil bath. After 45 min, the solution was observed to pale slightly in color and a ^{1}H NMR spectrum was obtained (Figure 3**B**). The resulting spectrum contained near-equimolar quantities of **2**-*t*-Bu, **3**-*t*-Bu and oxo **1a**-O. Phosphaalkyne, **3**-*t*-Bu, is assigned to the doublet located at 1.11 ppm ($^4J_{PH}$ = 0.9 Hz) in this mixture by similarity to reported values (1.15 ppm, $^4J_{PH}$ = 0.9 Hz).[34,45] The sample was then placed back in the heating bath for an additional 3.0 h, whereupon a golden yellow solution was obtained. ^{1}H NMR analysis of the solution at this point revealed resonances for **3**-*t*-Bu and

1a-O, with essentially complete consumption of **2**-*t*-Bu (Figure 3**C**). $^{31}P\{^{1}H\}$ NMR spectroscopy (128 MHz, 23°C, not shown) of this solution also indicated complete disappearance of the resonance for **4**-*t*-Bu (256.5 ppm) and appearance of a singlet located at -64.5 ppm assigned to phosphaalkyne **5**-*t*-Bu.

In a separate experiment, a 0.100 g sample of **2**-*t*-Bu was dissolved in C_6D_6 (1.0 mL) and heated at 80 °C for 45 min, after which, the volatile components of the reaction mixture were vacuum transferred to a sealable NMR tube. The ^{1}H NMR spectrum obtained, gave rise to a single resonance located at 1.09 ppm (doublet, $^{4}J_{PH}$ = 0.9 Hz , Figure 8) indicative of phosphaalkyne, **3**-*t*-Bu.[5] Analysis of the same solution by $^{31}P\{^{1}H\}$ NMR spectroscopy showed only one signal located at -67.6 ppm, also characteristic of phosphaalkyne, **3**-*t*-Bu (Lit = -69.2 ppm[34,45]). In a third experiment, the volatile components of the thermolysis mixture were vacuum transferred to an NMR tube containing a 1.0 molar equivalent sample of ferrocene. Analysis of the resulting C_6D_6 solution containing ferrocene and *t*-BuC≡P by ^{1}H NMR revealed a 90% yield based on **2**-*t*-Bu for the vacuum transfer procedure (single pulse integration). In all instances where the vacuum transfer of *t*-BuC≡P was performed, oxo **1a**-O was recovered in pure form (^{1}H NMR) from the reaction vessel.

Niobacycle **2**-1-Ad (0.100 g, 0.116 mmol) was dissolved in C_6D_6 (1 mL) and heated at 45 °C in a manner analogous to that described for complex **2**-*t*-Bu. Analysis by ^{1}H NMR (500 MHz, 23°C) indicated complete consumption of **2**-1-Ad, concomitant with resonances characteristic of oxo **1a**-O and phosphaalkyne **3**-1-Ad. The corresponding $^{31}P\{^{1}H\}$ NMR spectrum revealed only the characteristic signal for **3**-1-Ad (-66.5 ppm, Lit: -66.9 ppm[34]). Separation of phosphaalkyne **3**-1-Ad from oxo **1a** was not achieved.

5.5 Kinetic Measurements of *tert*-Butylphosphaalkyne Ejection.

All measurements were obtained by ^{1}H NMR on a Varian INOVA spectrometer operating at a resonance frequency of 500 MHz. Samples of niobacycle **2**-*t*-Bu were prepared in a glovebox as C_6D_6 solutions (0.015 g, 0.001 L, 19.2 mM) which contained 10 mg of Cp_2Fe (53.7 mM) as an internal standard. The solutions, once prepared, were loaded into a sealable NMR tube and immersed in a −78 °C bath for transfer to the spectrometer. Upon arrival the solution was removed from the cold bath, allowed to thaw and inserted into a pre-warmed spectrometer probe. Once inside the spectrometer, all samples were subjected to a 10 min. equilibration period prior to initial data collection. For the high-temperature studies (328 – 338 K), significant progress of the reaction had taken place during the equilibration period. The reaction progress during equilibration was much less at lower temperatures (308 – 318 K). Raw data for each kinetic run were obtained from integration of the resonances corresponding to the *tert*-butyl substituents for both **2**-*t*-Bu and **1a-O**. Rate data were fit to the logarithmic Eyring equation,

$$\ln\frac{k}{T} = -\frac{\Delta H^{\ddagger}}{R}\cdot\frac{1}{T} + \ln\frac{k_b}{h} + \frac{\Delta S^{\ddagger}}{R}$$

in order to obtain relevant activation parameters. All data were processed and fitted with the Mircoral Origin (v. 6.0) program suite.

5.6 Synthesis of $(TfO)_2Nb(N[Np]Ar)_3$ (1a-$(OTF)_2$, Tf = O_2SCF_3)

A cold (-35 °C) Et_2O solution of triflic anhydride (Tf_2O, 0.137 g, 0.485 mmol, 1.1 equiv, 3 mL) was added all at once to an equally cold Et_2O solution of oxo **1a** (0.300 g, 0.441 mmol, 5 mL). Upon addition, the resulting solution changed in color from golden yellow to bright orange, coincident with the formation of a considerable amount of orange precipitate. The reaction mixture was stirred for an additional 45 min at room temperature before all volatile materials were removed under reduced pressure. The light orange power obtained was found to be essentially pure bistriflate **1a**-$(OTF)_2$ as assayed by ^1H and ^{19}F spectroscopy. Bistriflate **1a**-$(OTF)_2$ is only sparingly soluble in cold (-35 °C) Et_2O and can be easily obtained in approximately 90% yield by filtration of a corresponding slurry. Orange, single–crystalline material was obtained by storing a THF/*n*-pentane (5:1) solution of **1a**-$(OTF)_2$ at -35 °C for 3 d. Yield 63 %, 0.267 g (single crystals). ^1H NMR (500 MHz, C_6D_6, 23 °C): δ 7.68 (s, 6H, o-Ar), 6.62 (s, 3H, p-Ar), 3.85 (s, 6H, NCH_2), 2.18 (s, 18H, Ar-CH_3), 0.46 (s, 27, *t*-Bu); $^{13}C\{^1H\}$ NMR (125.8 MHz, C_6D_6, 23 °C): δ 146.2 (ipso-Ar), 141.9 (m-Ar), 133.5 (p-Ar), 127.0 (o-Ar), 75.3 (NCH_2), 36.0 ($C(CH_3)_3$), 28.9 ($C(CH_3)_3$), 22.3 (Ar-CH_3); $^{19}F\{^1H\}$ NMR (282.3 MHz, C_6D_6, 23 °C): δ -76.9; Anal. Calcd. for $C_{41}H_{60}N_3NbO_6S_2F_6$: C, 51.10; H, 6.29; N, 4.37. Found: C, 50.92; H, 6.20; N, 4.27.

5.7 Synthesis of Nb(H)(*t*-Bu(H)C=NAr)(N[Np]Ar)$_2$ (1a-H) from $(TfO)_2Nb(N[Np]Ar)_3$ (1a-$(OTF)_2$, Tf = O_2SCF_3).

Substituting bistriflate **1a**-$(OTF)_2$ for bisiodide, $Nb(I)_2(N[Np]Ar)_3$, niobaziridine–hydride, **1a**-H was prepared analogously as reported in Chapter 1. The isolated yields of **1a**-H are identical for both starting materials.

5.8 Synthesis of 1,3-[(Ar[Np]N)$_3$Nb(P=C(O))]$_2$Ad (6)

Bisniobacycle **6** was prepared analogously to mononiobacycle **2**-1-Ad, employing 0.500 g of [Na(THF)][**1a**-P] (0.635 mmol) and 0.077 g of Adamantane-1,3-dicarbonyl chloride (0.289 mmol, 0.47 equiv). After removal of NaCl, **6** was isolated as an orange-red powder by precipitation from cold (-100 °C) *n*-pentane. Yield: 58 % . ^1H NMR (500 MHz, C_6D_6, 23 °C): δ 6.59 (s, 12H, o-Ar), 6.57 (s, 6H, p-Ar), 4.02 (s, 12H, N-CH_2), 2.85 (s, 2H, Ad), 2.53-2.39 (m, 8H, Ad), 2.35 (s, 2H, Ad), 2.15 (s, 36H, Ar-CH_3), 1.79 (s, 3H, Ad), 0.98 (s, 54H, *t*-Bu). $^{31}P\{^1H\}$ NMR (121.5 MHz, C_6D_6, 23 °C): δ 259.5 ppm (s); Anal. Calcd. for $C_{90}H_{134}N_6P_2O_2Nb$: C, 68.42; H, 8.55; N, 5.32. Found: C, 68.77; H, 8.40; N, 5.19.

Data for Bisphosphaalkyne **7**: ^1H NMR (500 MHz, C_6D_6, 23 °C): δ 1.93 (s, Ad), 1.57 (s, Ad), 1.13 (s, Ad); $^{31}P\{^1H\}$ NMR (121.5 MHz, C_6D_6, 23 °C): δ –64.4 ppm (s).

5.9 Synthesis of Bisphosphaalkyne Complex 1,3-((η^2–P≡C)Pt(PPh$_3$)$_2$)$_2$Ad (8)

To a C_6H_6 solution of bisphosphaalkyne **7** (0.040 g, 0.181 mmol, 5 mL) containing *ca.* 25 mol % oxo **1a**-O was added $(C_2H_4)Pt(PPh_3)_2$ (0.278 g, 0.3724 mmol, 2.5 mL, 2.05 equiv) as a C_6H_6 solution. No noticeable color change was observed upon addition. The reaction mixture was allowed to stir at room temperature for 1.5 h, afterwhich all volatile materials were removed under reduced pressure. The yellow-brown residue obtained was slurried in *n*-pentane (5 mL), filtered and washed twice (*n*-pentane, 2 x 2 mL) to provide complex **8** as a yellow solid. Yield 84% based on $(C_2H_4)Pt(PPh_3)_2$. ^1H NMR (300 MHz, C_6D_6, 23 °C): δ 7.59 (m, Ph), 6.93 (m, Ph),

2.31 (s, Ad), 1.64 (m, Ad), 1.61 (s, Ad), 1.19 (s, Ad); $^{31}P\{^{1}H\}$ NMR (121.3 MHz, C_6D_6, 23 °C): δ 83.0 (s, P_{alkyne}), 29.9 (t, P-trans, $^{1}J_{Pt\text{-}P}$ = 3562 Hz), 27.1 (t, P-cis, $^{1}J_{Pt\text{-}P}$ = 3215 Hz).

5.10 Synthesis and Silylation of Na[(MesNC(O)P)Nb(N[Np]Ar)$_3$] (Na[9])

To a THF solution of Na(THF)[**1a**-P] (0.500 g, 0.635 mmol 5 mL) was added a THF solution of MesNCO (0.112 g, 0.698 mmol, 1.1 equiv, 2 mL) at room temperature. The reaction mixture was allowed to stir for 2.5 h while gradually changing in color to dark red. Removal of THF, followed by slurring the resulting dark red residue in cold *n*-pentane (–35 °C, 5 mL), afforded Na[**9**] as a brick-red powder upon filtration. Silylation of Na[**9**] was achieved in a manner analogous to the synthesis of **2**-*t*-Bu, employing 0.300 g (0.341 mmol) of Na[**9**] and 0.035g (0.324 mmol) of $ClSiMe_3$. The resulting amino-substituted niobacycle, **10**, was obtained as cherry-red crystals upon work-up.

Na[**9**]: Brick red powder 88%. ^{1}H NMR (500 MHz, C_6D_6, 23 °C): δ 6.86 (s, 6H, o-Ar), 6.44 (bs, 2H, m-Mes), 4.18 (bs, 6H, N-CH_2), 2.45 (s, 6H, Mes-o-CH_3), 2.24 (s, 3H, Mes-p-CH_3), 2.19 (s, 18H, Ar-CH_3), 0.97 (s, 27H, *t*-Bu); $^{31}P\{^{1}H\}$ NMR (121.5 MHz, C_6D_6, 23 °C): δ 458.3 ppm (s).

10: Cherry-red crystals, 55%. ^{1}H NMR (500 MHz, C_6D_6, 23 °C): δ 7.08 (s, 6H, o-Ar), 6.71 (s, 2H, m-Mes), 6.43 (s, 3H, o-Ar), 4.17 (s, 6H, N-CH_2), 2.40 (s, 6H, Mes-o-CH_3), 2.18 (s, 18H, Ar-CH_3), 2.11 (s, 3H, Mes-o-CH_3), 0.94 (s, 27H, *t*-Bu), 0.58 (s, 9H, Si(CH_3)$_3$); $^{31}P\{^{1}H\}$ NMR (121.5 MHz, C_6D_6, 23 °C): δ 336.3 ppm (s).

5.11 Desilylation of (Me$_3$SiN$_2$)Mo(N[*t*-Bu]Ar)$_3$ (11a-N$_2$SiMe$_3$) with Sodium Methoxide: Optimized Synthesis of Na[(N$_2$)Mo(N[*t*-Bu]Ar)$_3$ (Na[11a-N$_2$]).

To a THF solution of **11a**-N_2SiMe_3[17] (3.00 g, 4.13 mmol, 20 mL), was added anhydrous NaOMe (1.11 g, 20.6 mmol, 5.0 equiv). The reaction mixture was allowed to stir for 24 h while gradually changing in color from orange to magenta. All volatile materials were then removed under reduced pressure and the excess NaOMe removed by extraction of the resulting purple residue with *n*-pentane (50 mL) followed by filtration through Celite. Concentration of the filtrate to 10 mL and cooling to -35 °C for 1-2 days provided Na[**11a**-N_2] as orange crystals in 70–80 % yield. Spectroscopic data for Na[**11a**-N_2] prepared by this method were identical to those previously reported.[17] For the ^{15}N-labled variant, Na[**11a**-$^{15}N_2$], NaOMe and **11a**-$^{15}N_2SiMe_3$ were allowed to react under static vacuum in order to prevent redox-catalyzed $^{14}N_2/^{15}N_2$ exchange.[17]

5.12 Synthesis of Mo(H)(*t*-Bu(H)C=NAr)(N[Np]Ar)$_2$ (11b-H).

To a thawing suspension of $MoCl_3(THF)_3$[149] (10.0 g, 23.8 mmol) in Et_2O (150 mL) was added solid (Et_2O)Li(N[Np]Ar) (13.6 g, 50.1 mmol). The head space of the reaction flask was evacuated and the reaction was allowed to stir for 6.0 h, while gradually changing in color to purple-brown. The mixture was then filtered through Celite to remove LiCl and unreacted $MoCl_3(THF)_3$, which was washed with Et_2O (30 mL). The filtrate was dried under vacuum and the resulting purple-brown residue extracted with *n*-pentane (100 mL) and filtered through Celite, where an intractable purple solid remained. The filtrate was dried again and the residue dissolved in Et_2O (75-100 mL). This solution was stored, under vacuum, at -35 °C for 1-2 days, whereupon purple-brown crystals of **11b**-H formed and were collected. The mother-liquor was reduced to approximately half the original volume and chilled again to produce a second crop of crystals. Yield 35 – 50 % based on multiple syntheses. ^{1}H NMR (500 MHz, C_6D_6, 20 °C): δ

2.00 (b), 1.50 (b) ppm. μ_{eff} (Evans Method) = 1.64 μ_B. Anal. Calcd. for $C_{39}H_{60}N_3Mo$: C, 70.24; H, 9.07; N, 6.30. Found: C, 71.01; H, 9.48; N, 6.01.

5.13 Synthesis of Na[(N_2)Mo(N[Np]Ar)$_3$] (Na[**11b**-N_2]).

In a dinitrogen-atmosphere glovebox, freshly prepared 1% sodium amalgam (Na; 0.350 g, approx. 10 equiv) was added to a THF solution of Mo(H)(*t*-Bu(H)C=NAr)(N[Np]Ar)$_2$ (**11b**) (1.00 g, 1.50 mmol, 50 mL). The reaction mixture was vigorously stirred for 20 h at room temperature while exposed to the atmosphere through an open gas-adapter port. The color of the solution was observed to gradually change from purple-brown to dark green. The mother liquor was decanted from the amalgam and evaporated to dryness under vacuum, resulting in a dark green residue. Addition of *n*-pentane (40 mL) resulted in a red-orange solution, which was filtered though Celite and dried under vacuum. Addition of *n*-pentane (15 mL) to resulting red-orange residue, followed by cooling to -35 °C for 30 min, precipitated essentially pure Na[**11b**-N_2] (^{1}H NMR, C_6D_6). Analytically pure, cherry-red single crystals of Na[**11b**-N_2] were obtained from a saturated, *n*-pentane solution stored at -35 °C for 2 d. Yield: 50–70% based on 3 separate syntheses. The ^{15}N-labled variant, Na[**11b**-$^{15}N_2$], was prepared identically under an atmosphere of 99.9% $^{15}N_2$. ^{1}H NMR (500 MHz, C_6D_6, 20 °C): δ 6.61 (bs, 6H, o-Ar), 6.49 (s, 3H, p-Ar), 4.32 (bs, 6H, N-CH_2), 2.19 (s, 18H, Ar-CH_3), 1.00 (bs, 27H, *t*-Bu); ^{113}C{^{1}H} NMR (125.8 MHz, C_6D_6, 20 °C): δ 159.3.8 (ipso-Ar), 138.9 (m-Ar), 122.4 (p-Ar), 119.9 (o-Ar), 84.9 (N-*C*H_2), 36.0 (*C*(CH$_3$)$_3$), 29.1 (C(*C*H$_3$)$_3$), 22.1 (Ar-*C*H$_3$); FTIR (KBr windows, C_6D_6 solution): (ν_{NN}) 1730 cm^{-1} also 2949, 2873, 1584, 1473, 1069, 681 cm^{-1}. For Na[**11b**-$^{15}N_2$], (ν_{NN}) 1784 and 1674 cm^{-1}. Anal. Calcd. for $C_{43}H_{68}N_5OMoNa$: C, 65.38; H, 8.68; N, 8.87. Found: C, 65.24; H, 8.80; N, 8.52.

5.14 Synthesis of Nb(I)(N[Np]Ar)$_3$ (1a-I).

To a thawing THF solution of **1a**-$(I)_2$ (4.500 g, 4.90 mmol, 75 mL) was added solid Mg(THF)$_3$(anthracene) (1.128 g, 2.690 mmol, 0.55 equiv). The reaction mixture was allowed to warm to room temperature and stirred for 1.5 h, while gradually changing in color from orange to purple. All volatile materials were removed in vacuo and the resulting purple-brown residue was extracted with *n*-pentane (40 mL) and filtered through Celite to remove the resultant MgI_2 and anthracene. The purple filtrate was then reduced to a volume of 20 mL and frozen. Upon thawing, the solution was quickly cold-filtered through Celite to remove residual anthracene and unreacted **1a**-$(I)_2$. The resulting purple filtrate was then reduced to a volume of 15 mL and stored at -35 °C for 2 d, whereupon a purple crystalline solid was obtained and collected. Yield: 1.220 g, 33.0 % in two crops. ^{1}H NMR (500 MHz, C_6D_6, 20 °C): δ 2.00 (bs) ppm; μ_{eff} (Evans Method) = 1.81 μ_B. Anal. Calcd. for $C_{39}H_{60}N_3INb$: C, 59.24; H, 7.65; N, 5.31. Found: C, 59.03; H, 7.60; N, 5.18. Unreacted, orange **1a**-$(I)_2$ (contaminated with approx. 25% anthracene) can be recovered by washing the Celite pad with Et_2O (25–30 mL) followed by evaporation, redissolution in cold *n*-pentane and filtration. Yield of recovered **1a**-I_2: 1.050 g.

5.15 Synthesis of Nb(OTf)(N[Np]Ar)$_3$ (1a-(OTF), Tf = O_2SCF_3).

Complex **1a**-(OTF) was prepared analogously to **1a**-I. The use of either Mg(THF)$_3$(anthracene) or cobaltocene (Cp_2Co) as a reducing agent gave identical results. Recrystallized **1a**-(OTf) was obtained from Et_2O as a purple-green crystalline solid. Yield: 1.220 g, 33.0 % in two crops. ^{1}H NMR (500 MHz, C_6D_6, 20 °C): δ 1.80 (bs) ppm;

5.16 Synthesis of Heterodinuclear N_2 Complexes (Ar[Np]N)$_3$Nb(μ-N_2)Mo(N[*t*-Bu]Ar)$_3$ (12b) and (Ar[Np]N)$_3$Nb(μ-N_2)Mo(N[Np]Ar)$_3$ (12c).

Separately, a 10 mL THF solution of **1a**-I (2.50 g, 3.16 mmol) and a 10 mL THF solution of the corresponding molybdenum dinitrogen anion salt (Na[**11**a-N_2] for **12b**, 2.13 g, 3.16 mmol; Na[**11b**-N_2] for **12c**, 2.25 g, 3.16 mmol) were frozen in a glove box cold well (liquid N_2). Upon removal from the cold well, approximately 4 mL of the thawing solution containing **1a**-I was added dropwise over 1 min to the thawing solution of the molybdenum salt, eliciting a color change from red-orange to green. The reaction mixture was allowed to stir for an additional 3 min whereupon both solutions were placed back into the cold well. This procedure was repeated two more times until complete addition of **1a**-I was achieved. The reaction mixture was then allowed to warm to room temperature and stirred for an additional 30 min before being evaporated to dryness. The residue obtained was extracted with *n*-pentane (10 mL), filtered through Celite to remove the NaI byproduct and the resulting filtrate evaporated to dryness. The resulting green powders obtained were sufficiently pure for subsequent synthetic applications. However, crystalline material could be obtained by storing Et_2O solutions of either **3b** or **3c** at –35 °C for several days. The monotriflato-Nb^{IV} complex, **1a**-OTf, can be readily substituted for **1a**-I in this procedure.

12b: Yield: 54%. μ_{eff} (Evans Method) = 2.36 μ_B. ^{1}H NMR (500 MHz, C_6D_6, 20 °C): δ 4.4 (b), 2.2 (b), 1.5 (b); FTIR (KBr windows, C_6D_6 solution): (ν_{NN}) 1564 cm^{-1}. For **3b**-$^{15}N_2$: (ν_{NN}) 1519 cm^{-1}. Anal. Calcd. for $C_{75}H_{114}N_8NbMo$: C, 68.95; H, 8.90; N, 8.25. Found: C, 69.15; H, 9.01; N, 8.49.

12c: Yield: 48%. μ_{eff} (Evans Method) = 2.58 μ_B. ^{1}H NMR (500 MHz, C_6D_6, 20 °C): δ 2.1 (b), 1.5 (b); FTIR (KBr windows, C_6D_6 solution): (ν_{NN}) 1576 cm^{-1}. For **3c**-$^{15}N_2$: (ν_{NN}) 1515 cm^{-1}. Anal. Calcd. for $C_{78}H_{120}N_8NbMo$: C, 68.95; H, 8.90; N, 8.25. Found: C, 68.33; H, 9.12; N, 8.44.

5.17 Reductive Cleavage of (Ar[Np]N)$_3$Nb(μ-N_2)Mo(N[Np]Ar)$_3$ (12c): Synthesis of Na[N≡Nb(N[Ar]Ar)$_3$)] (Na[1a-N]) and N≡Mo(N[Np]Ar)$_3$ (11b-N).

To a THF solution of **12c** (2.0 g, 1.47 mmol, 15 mL) was added an excess of freshly prepared 1% sodium amalgam (Na: 0.135 g, 4 equiv/Nb). The reaction mixture was allowed to stir at room temperature for 2 h, while gradually changing in color from green to orange-brown. The solution was then decanted from the amalgam and evaporated to dryness under reduced pressure. The resulting orange-brown residue was then extracted with *n*-pentane and filtered through Celite. The filtrate was then exposed to two additional cycles of *n*-pentane (~3 mL) addition and evaporation in order to completely desolvate Na[**1a**-N]. Additional exposure of the mixture to *n*-pentane (4 mL), cooling to –35 °C for 30 min followed by filtration, produced pure [Na][NNb(N[Np]Ar)$_3$)] as an off-white powder. Evaporation of the filtrate, dissolution in Et_2O and cooling to –35 °C produced orange single crystals of **11b**-N after 2 d. Complex **12b** can be substituted for **12c** in this procedure, providing the nitrido molybdenum complex **11a**-N[5] in 75-80% yield after crystallization from Et_2O.

Na[**1a**-N]: Yield: 80%. ^{1}H NMR (500 MHz, THF-d_8, 20 °C): δ 6.26 (s, 6H, o-Ar), 6.11 (s, 3H, p-Ar), 4.36 (s, 6H, N-CH_2), 1.90 (s, 18H, Ar-CH_3), 0.83 (s, 27H, *t*-Bu); ^{13}C{^{1}H} NMR (125.8 MHz, THF-d_8, 20 °C): δ 159.3 (ipso-Ar), 137.7 (m-Ar), 120.9 (p-Ar), 119.9 (o-Ar), 74.6 (N-*C*H$_2$), 36.4 (*C*(CH$_3$)$_3$), 29.9 (C(*C*H$_3$)$_3$), 21.8 (Ar-*C*H$_3$). ^{15}N NMR (60.84 MHz, THF-d_8, 20 °C): δ

754 ppm (s); Anal. Calcd. for $C_{39}H_{60}N_4NbNa$: C, 66.84; H, 8.63; N, 7.99. Found: C, 67.08; H, 8.94; N, 8.12. Single crystals of yellow [Na(THF)$_3$][**1a**-N] were obtained by allowing a saturated THF solution of Na[**1a**-N] to stand at –35 °C for several days.

11b-N: Yield: 72%. ^{1}H NMR (500 MHz, C_6D_6, 20 °C): δ 6.50 (s, 3H, p-Ar), 6.26 (s, 6H, o-Ar), 4.98 (s, 6H, N-CH_2), 1.94 (s, 18H, Ar-CH_3), 1.10 (s, 27H, *t*-Bu); ^{13}C{^{1}H} NMR (125.8 MHz, C_6D_6, 20 °C): δ 155.8 (ipso-Ar), 138.8 (m-Ar), 126.7 (p-Ar), 122.7 (o-Ar), 85.5 (N-*C*H$_2$), 36.0 (*C*(CH$_3$)$_3$), 29.3 (C(*C*H$_3$)$_3$), 21.7 (Ar-*C*H$_3$); ^{15}N NMR (60.84 MHz, THF-d_8, 20 °C): δ 870 ppm (s); Anal. Calcd. for $C_{39}H_{60}N_4Mo$: C, 68.80; H, 8.88; N, 8.23. Found: C, 68.60; H, 8.95; N, 8.11.

5.18 General Procedure for Niobium Mediated Nitrile Synthesis from Acyl Chloride Substrates (^{15}N–Labeled Variants).

To a THF-d_8 solution of Na[**1a**-N] (0.050 g, 0.071 mmol, 1.5 mL) was added to a THF-d_8 solution of the appropriate acyl chloride substrate (0.95 equiv in all cases, 0.5 mL) at room temperature. A rapid color change from pale brown to yellow orange accompanied the addition. For acyl chloride substrates resulting in a volatile organonitrile, the volatile components of the reaction mixture were vacuum transferred to a sealable NMR tube for analysis. The oxo-niobium byproduct, **1a**-O, was liberated from NaCl by extraction with *n*-pentane, followed by filtration and set aside for further use. For reactions which generated a non-volatile organonitrile, the addition of the appropriate acyl chloride to Na[**1a**-N] was carried out in THF and the resulting mixture was allowed to stir for 20 min. The reaction mixture was then evaporated to dryness, extracted with *n*-pentane and filtered. THF-d_8 was then introduced to the crude residue immediately prior to spectroscopic analysis. For the latter samples, **1a**-O was present in solution during analysis.

5.19 Synthesis of *t*-Bu(O)CN=Nb(N[*t*-Bu]Ar)$_3$ (1c-NC(O)*t*-Bu).

To a thawing THF solution of Na[**1c**-N][140] (0.200 g, 0.30 mmol, 3 mL) was added dropwise an equally cold THF solution of *t*-BuC(O)Cl (0.034 g, 0.28 mmol, 0.95 equiv, 2 mL). The resulting pale-yellow reaction mixture was allowed to stir for 45 min before all volatile components were removed under reduced pressure. Extraction of the residue with *n*-pentane, followed by filtration through Celite and evaporation, provided crude **1c**-NC(O)*t*-Bu as a pale-yellow powder. Near-colorless crystals of **1c**-NC(O)*t*-Bu were obtained by Et$_2$O re-crystallization at –35 °C (2 d). Yield: 60 %. ^{1}H NMR (500 MHz, C_6D_6, 20 °C): δ 6.71 (s, 3H, p-Ar), 6.02 (s, 6H, o-Ar), 2.12 (s, 18H, Ar-CH_3), 1.59 (s, 9H, *t*-Bu-acyl), 1.42 (s, 27H, *t*-Bu); ^{13}C{^{1}H} NMR (125.8 MHz, C_6D_6, 20 °C): δ 149.5 (ipso-Ar), 137.4 (m-Ar), 130.5 (o-Ar), 128.0 (p-Ar), 32.3 (*C*(CH$_3$)$_3$ - acyl), 32.2 (*C*(CH$_3$)$_3$), 29.1 (C(*C*H$_3$)$_3$), 21.8 (Ar-*C*H$_3$); FTIR (KBr windows, C_6D_6 solution): ν(C=O) 1640 cm^{-1}; Anal. Calcd. for $C_{41}H_{63}N_4NbO$: C, 68.31; H, 8.81; N, 7.77; Found: C, 68.44; H, 8.64; N, 7.93.

5.20 Computational Details.

All DFT calculations were carried out utilizing the Amsterdam Density Functional (ADF) program suite,[152,153] version 2004.01.[154] The all-electron, Slater-type orbital (STO) basis sets employed were of triple-ζ quality augmented with two polarization functions and incorporated relativistic effects using the zero-order regular approximation[155,156] (ADF basis ZORA/TZ2P). The local exchange-correlation potential of Vosko et al.[157] (VWN) was augmented self-consistently with gradient-corrected functionals for electron exchange according to Becke,[158] and

electron correlation according to Perdew.[159,160] This nonlocal density functional is termed BP86 in the literature and has been shown to give excellent results for the geometries and energetics of transition metal systems.[161] Crystallographically determined atomic coordinates were used as input where appropriate. Each optimized structure was subjected to a harmonic frequencies calculation to ensure representation as local minima on the potential energy surface. All enthalpic values reported were corrected for zero-point energy considerations.

5.21 Crystallographic Structure Determinations.

The X-ray crystallographic data collections were carried out on a Siemens Platform three-circle diffractometer mounted with a CCD or APEX-CCD detector and outfitted with a low-temperature, nitrogen-stream aperture. The structures were solved using direct methods, in conjunction with standard difference Fourier techniques and refined by full-matrix least-squares procedures. A summary of crystallographic data for all complexes is given in Tables 3 – 5. No symmetry higher than triclinic was indicated in the diffraction data for **2**-*t*-Bu and **10**. Complex $Na(THF)_3$[**1a**-N] was refined in the trigonal space group P-3. The systematic absences in the diffraction data are uniquely consistent with the assigned monoclinic space groups for all other complexes. These choices led to chemically sensible and computationally stable refinements. An empirical absorption correction (SADABS) was applied to the diffraction data for all structures. All non-hydrogen atoms were refined anisotropically. In most cases, hydrogen atoms were treated as idealized contributions and refined isotropically. The hydrido ligand in complex **11b**-H was located in the electron density difference map and refined isotropically.

Complex **2**-*t*-Bu was found to contain two-site, positional disorder for two methyl groups of the metallacyclic *t*-Bu substituent. This disorder was modeled and resulted in final occupancy ratio of 70:30 as indicated by the refinement statistics. Hydrogen atoms were not included as idealized riding groups for disordered carbon atoms. Complex **1a**-$(OTf)_2$ was found to possess three separate and non-crystallographically imposed sites of positional disorder. The methylene carbon of two anilido neopentyl residues were found to be disordered over two sites, which resulted in two tetrahedral conformations for the corresponding *t*-Bu substituent. Modeling of the disorder resulted in final occupancy ratios of 60:40 and 80:20 for the neopentyl residues corresponding to N(1) and N(2), respectively. Again, hydrogen atoms were not included as idealized riding groups for disordered carbon atoms. Additionally for complex **1a**-$(OTf)_2$, the triflato group corresponding to atom O(1) was disordered over two sites. A final occupancy ratio of 55:45 was suggested by the refinement statistics for the two triflato orientations fit to this model. Complex $Na(THF)_3$[**1a**-N] co-crystallized with several severely disordered molecules of THF, which could not be reasonably modeled as discrete entities. To account for this disorder, the crystallographic routine SQUEEZE[162,163] was employed and found a total of 119 electrons in a solvent-accessible void area of 713.5 $Å^3$ (22.5% of unit cell volume), corresponding to 2.94 molecules of THF per unit cell (~1.5 molecules of THF per molecule of $Na(THF)_3$[**1a**-N]). The final stages of refinement for complex $Na(THF)_3$[**1a**-N] were performed against the solvent-free reflection file obtained from SQUEEZE and resulted in significant improvements of the final residual values. The residual peak and hole electron density for $Na(THF)_3$[**1a**-N] were 0.590 and -0.173 $e^-·Å^{-3}$, respectively. All software used for diffraction data processing and crystal-structure solution and refinement are contained in the SAINT+ (v6.45) and SHELXTL (v6.14) program suites, respectively (G. Sheldrick, Bruker AXS, Madison, WI).

Table 3. Crystallographic Data for Complexes **2**-*t*-Bu, **2**-1-Ad, **1a**-$(OTf)_2$ and $Na(THF)_3$[**9**]

	2-*t*-Bu	**2**-1-Ad	**1a**-$(OTf)_2$	$Na(THF)_3$[**9**]
Formula	$C_{44}H_{63}N_3NbOP$	$C_{50}H_{75}N_3NbOP$	$C_{41}H_{47}F_6N_3NbO_6S_2$	$C_{61}H_{95}N_4O_4PNaNb$
Crystal System	Triclinic	Monoclinic	Monoclinic	Monoclinic
Space Group	*P*-1	$P2_1/c$	$P2_1/n$	$P2_1/c$
a, Å	11.9230(7)	12.5441(10)	12.7695(9)	12.4694(11)
b, Å	13.1067(8)	34.834(3)	16.2045(11)	34.420(3)
c, Å	16.6412(10)	12.2793(10)	22.6240(15)	18.2204(16)
α, deg	74.2510(10)	90	90	90
β, deg	105.9970(10)	115.9950(10)	91.8020(10)	108.749(2)
γ, deg	72.9650(10)	90	90	90
V, Å^3	2260.7(2)	4822.8(7)	4679.1(6)	7405.1(11)
Z	2	4	4	4
radiation		Mo-K_α (λ = 0.71073 Å)		
D(calcd), g/cm^3	1.137	1.182	1.347	1.144
μ (Mo Kα), mm^{-1}	0.334	0.320	0.415	0.240
temp, K	193(2)	193(2)	193(2)	193(2)
No. Reflections	9311	18407	24436	30956
No. Ind. Ref.(R_{int})	6426(0.0786)	6285(0.1356)	8246(0.0406)	10532(0.0487)
F(000)	824	1840	1956	2736
GoF (F^2)	1.014	1.102	1.071	1.341
$R(F)$, %[a]	0.0661	0.0906	0.0461	0.1194
$wR(F)$, %[a]	0.1540	0.1833	0.1381	0.2737

[a] Quantity minimized = $wR(F^2) = \sum[w(F_o^2 - F_c^2)^2]/\sum[(wF_o^2)^2]^{1/2}$; $R = \sum\Delta/\sum(F_o)$, $\Delta = |(F_o - F_c)|$, $w = 1/[\sigma 2(F_o^2) + (aP)^2 + bP]$, $P = [2F_c^2 + \text{Max}(F_o,0)]/3$.

Table 4. Crystallographic Data for Complexes **10**, **11b**-H, **1a**-I and $Na(THF)_3$[**1a**-N]

	10	**11b**-H	**1a**-I	$Na(THF)_3$[**1a**-N]
Formula	$C_{52}H_{80}N_4NbOPSi$	$C_{39}H_{60}N_3Mo$	$C_{39}H_{60}N_3NbI$	$C_{51}H_{84}N_4O_3NaNb$
Crystal System	Triclinic	Monoclinic	Monoclinic	Trigonal
Space Group	*P*-1	C_2/c	$P2_1/n$	*P*-3
a, Å	12.246(2)	38.035(3)	12.5745(19)	15.8927(8)
b, Å	12.819(2)	10.1353(9)	19.634(3)	15.8927(8)
c, Å	17.877(3)	20.3079(18)	17.226(3)	14.4775(15)
α, deg	90.038(4)	90	90	90
β, deg	95.270(4)	103.9130(10)	109.859(2)	120
γ, deg	107.914(4)	90	90	90
V, Å^3	2657.8(8)	7599.0(12)	4000.0(10)	3166.8(4)
Z	2	8	4	2
radiation		Mo-K_α (λ = 0.71073 Å)		
D(calcd), g/cm^3	1.161	1.166	1.313	0.962
μ (Mo Kα), mm^{-1}	0.317	0.373	1.100	0.231
temp, K	193(2)	183(2)	193(2)	183(2)
No. Reflections	34532	14990	22967	13348
No. Ind. Ref.(R_{int})	8159(0.0841)	5463(0.0644)	9229(0.0432)	3054(0.0299)
F(000)	996	2856	1636	988
GoF (F^2)	1.011	1.196	1.283	1.165
$R(F)$, %[a]	0.0440	0.0874	0.0899	0.0606
$wR(F)$, %[a]	0.0949	0.1739	0.1775	0.1612

[a] Quantity minimized = $wR(F^2) = \sum[w(F_o^2 - F_c^2)^2]/\sum[(wF_o^2)^2]^{1/2}$; $R = \sum\Delta/\sum(F_o)$, $\Delta = |(F_o - F_c)|$, $w = 1/[\sigma 2(F_o^2) + (aP)^2 + bP]$, $P = [2F_c^2 + \text{Max}(F_o,0)]/3$.

Table 5. Crystallographic Data for Complexes **1b**-N and **1c**-NC(O)*t*-Bu

	11b-N	**1c**-NC(O)*t*-Bu
Formula	$C_{39}H_{60}N_4Mo$	$C_{41}H_{63}N_4NbO$
Crystal System	Monoclinic	Monoclinic
Space Group	$P2_1/c$	$P2_1/n$
a, Å	10.085(2)	15.078(3)
b, Å	31.275(7)	13.465(2)
c, Å	12.676(3)	19.827(3)
α, deg	90	90
β, deg	102.704(4)	92.020(5)
γ, deg	90	90
V, Å^3	3900.4(14)	4022.9(11)
Z	4	4
radiation	Mo-K_α (λ = 0.71073 Å)	
D(calcd), g/cm^3	1.159	1.190
μ (Mo Kα), mm^{-1}	0.366	0.333
temp, K	193(2)	100(2)
No. Reflections	20153	80576
No. Ind. Ref.(R_{int})	6837(0.0378)	10378(0.0767)
F(000)	1456	1544
GoF (F^2)	1.058	1.238
$R(F)$, %[a]	0.0432	0.0844
$wR(F)$, %[a]	0.1144	0.2088

[a] Quantity minimized = $wR(F^2) = \sum[w(F_o^2 - F_c^2)^2]/\sum[(wF_o^2)^2]^{1/2}$; $R = \sum\Delta/\sum(F_o)$, $\Delta = |(F_o - F_c)|$, $w = 1/[\sigma 2(F_o^2) + (aP)^2 + bP]$, $P = [2F_c^2 + \text{Max}(F_o,0)]/3$.

6 References

1. Dehnicke, K.; Strähle, J. *Angew. Chem., Int. Ed. Engl.* **1992**, *31*, 955.
2. Eikey, R. A.; Abu-Omar, M. M. *Coord. Chem. Rev.* **2003**, *243*, 83.
3. Schrock, R. R.; Listemann, M. L.; Sturgeoff, L. G. *J. Am. Chem. Soc.* **1982**, *104*, 4291.
4. Chan, D. M.-T.; Chisholm, M. H.; Folting, K.; Huffman, J. C.; Marchant, N. S. *Inorg. Chem.* **1986**, *25*, 4170.
5. Herrmann, W. A.; Bogdanovic, S.; Poli, R.; Priermeier, T. *J. Am. Chem. Soc.* **1994**, *116*, 4989.
6. Caulton, K. G.; Chisholm, M. H.; Doherty, S.; Folting, K. *Organometallics* **1995**, *14*, 2585.
7. Ritter, S.; Abram, U. *Inorg. Chim. Acta.* **1995**, *231*, 245.
8. Crevier, T. J.; Meyer, J. M. *Angew. Chem. Int. Ed. Engl.* **1998**, *37*, 1891.
9. Laplaza, C. E.; Davis, W. M.; Cummins, C. C. *Angew. Chem. Int. Ed. Engl.* **1995**, *34*, 2042.
10. Zanetti, N. C.; Schrock, R. R.; Davis, W. M. *Angew. Chem. Int. Ed. Engl.* **1995**, *34*, 2044.
11. Scheer, M.; Schuster, K.; Budzichowski, T. A.; Chisholm, M. H.; Streib, W. E. *Chem. Commun.* **1995**, 1671.
12. Scheer, M.; Kramkowski, P.; Schuster, K. *Organometallics*, **1999**, *18*, 2874.
13. Stephens, F. H.; Figueroa, J. S.; Diaconescu, P. D.; Cummins, C. C. *J. Am. Chem. Soc.* **2003**, *125*, 9264.
14. Johnson, B. P.; Balazs, G.; Scheer, M. *Top. Curr. Chem.* **2004**, *232*, 1.
15. Laplaza, C. E.; Cummins, C. C. *Science* **1995**, *268*, 861.
16. Laplaza, C. E.; Johnson, M. J. A.; Peters, J. C.; Odom, A. L.; Kim, E.; Cummins, C. C.; George, G. N.; Pickering, I. J. *J. Am. Chem. Soc.* **1996**, *118*, 8623.
17. Peters, J. C.; Cherry, J. –P. F.; Thomas, J. C.; Baraldo, L.; Mindiola, D. J.; Davis, W. M.; Cummins, C. C. *J. Am. Chem. Soc.* **1999**, *121*, 10053.
18. Zanotti-Gerosa, A.; Solari, E.; Giannini, L.; Floriani, C.; Chiesi-Villa, A.; Rizzoli, C. *J. Am. Chem. Soc.* **1998**, *120*, 437.
19. Ferguson, R.; Solari, E.; Floriani, C.; Osella, D.; Ravera, M.; Re, N.; Chiesi-Villa, A.; Rizzoli, C. *J. Am. Chem .Soc.* **1997**, *119*, 10104-10115.
20. Clentsmith, G. K. B.; Bates, V. M. E.; Hitchcock, P. B.; Cloke, F. G. N. *J. Am. Chem. Soc.* **1999**, *121*, 10444.
21. Campazzi, E.; Solari, E.; Floriani, C.; Scopelliti, R. *Chem.Commun.* **1998**, 2603.
22. Ferguson, R.; Solari, E.; Floriani, C.; Chiesi-Villa, A.; Rizzoli, C. *Angew. Chem., Int. Ed. Engl.* **1993**, *32*, 396.
23. Fryzuk, M. D.; Love, J. B.; Rettig, S. J.; Young, V. G. *Science* **1997**, *275*, 1445.
24. Basch, H.; Musaev, D. G.; Morokuma, K.; Fryzuk, M. D.; Love, J. B.; Seidel, W. W.; Albainati, A.; Koetzle, T. F.; Klooster, W. T.; Mason, S. A.; Eckert, J. *J. Am. Chem. Soc.* **1999**, *121*, 523.
25. Johnson, M. J. A.; Lee, P. M.; Odom, A. L.; Davis, W. M.; Cummins, C. C. *Angew. Chem. Int. Ed. Engl.* **1997**, *36*, 87.
26. Scheer, M.; Muller, J.; Haser, M. *Angew. Chem. Int. Ed. Engl.* **1996**, *35*, 2492.
27. Scheer, M.; Muller, J.; Baum, G.; Haser, M. *Chem. Commun.* **1998**, 1051.
28. Chisholm, M. H.; Dlebridge, E. E.; Kidwell, A. R. Quinlan, K. B. *Chem. Commun.* **2003**, 126.
29. Schrock, R. R. *Chem. Rev.* **2002**, *102*, 145.
30. Cummins, C. C.; Schrock, R. R.; Davis, W. M. *Angew. Chem. Int. Ed. Engl.* **1993**, *32*, 756.

31. Regitz, M; Scherer, O. J.; Eds. *Multiple bonds and low coordination in Phosphorus chemistry*; Thieme Verlag, New York, 1990.

32. Hidai, M.; Mizobe, Y. *Pure. Appl. Chem.* **2001**, *73*, 261.

33. Gier, T. E. *J. Am. Chem. Soc.* 1961, *83*, 1769.

34. Regitz, M.; Binger, P. *Angew. Chem. Int. Ed. Engl.* **1988**, *27*, 1484.

35. Tyler, J. K. *J. Chem. Phys.* **1964**, *40*, 1170.

36. Hopkinson, H. W.; Kroto, H. W.; Nixon, J. F.; Simmons, N. P. C. Chem. Phys. Lett. **1976**, *42*, 460.

37. Kroto, H. W.; Nixon, J. F.; Simmons, N. P. C.; Westwood, N. P. C. *J. Am. Chem. Soc.* **1978**, 100, 446.

38. Burckett-St. Laurent, J. C. T. R.; Copper, T. A.; Kroto, H. W.; Nixon, J. F.; Ohashi, O.; Ohno, K. *J. Mol. Struct.* **1982**, *79*, 215.

39. Burckett-St. Laurent, J. C. T. R.; King, M. A. Kroto, H. W.; Nixon, J. F.; Suffolk, R. J. *J. Chem. Soc. Dalton. Trans.* **1983**, 755.

40. Märkl, G.; Seidl, E.; Trötsch, I. Angew. *Chem. Int. Ed. Engl.* **1983**, *22*, 879.

41. Loy, D. A.; Jamison, G. M.; McClain, M. D.; Alam, T. M. *J. Polym. Sci. A* **1999**, *37*, 129.

42. Becker, G.; Grosser, G.; Uhl, W. *Z. Naturforsch., Teil B.* **1981**, *36*, 16.

43. Nixon, J. F. *Chem. Rev.* **1988**, *88*, 1327.

44. Nixon, J. F. *Coord. Chem. Rev.* **1995**, *145*, 201.

45. Becker, G.; Schmidt, H.; Uhl, G.; Uhl, W. *Inorg. Synth.* **1990**, *27*, 249.

46. Jun, H.; Young Jr., V. G.; Angelici, R. J. *Organometallics*, **1994**, *13*, 2444.

47. Sugiyama, H.; Ito, S.; Yoshifuji, M. Angew. *Chem. Int. Ed. Engl.* **2003**, *42*, 3802.

48. Allspach, T.; Regitz, M.; Becker, G.; Becker, W. *Synthesis* **1986**, 31.

49. Burckett-St. Laurent, J. C. T. R.; Hitchcock, P. B.; Kroto, H. W.; Nixon, J. F. *Chem. Commun.* **1981**, 1141.

50. Yoshifuji, M.; Ito, S. *Top. Curr. Chem.* **2003**, *223*, 67.

51. For $(i\text{-Pr})_2$N-C≡P: Grobe, J.; Le Van, D.; Luth, B.; Hegemann, M. *Chem. Ber.* **1990**, *123*, 2317.

52. Grobe, J.; Le Van, D.; Luth, B.; Hegemann, M. Krebs, B.; Lage, M. *Chem. Ber.* **1993**, *126*, 63.

53. For $(i\text{-Pr})(Me_3Si)$N-C≡P: Appel, R.; Poppe, M. *Angew. Chem. Int. Ed. Engl.* **1989**, *28*. 53.

54. Bohle, D. S.; Clark, G. R.; Rickard, C. E. F.; Roper, W. R. *J. Organomet. Chem.* **1988**, *353*, 355.

55. Cowley, A. H. *Acc. Chem. Res.* **1997**, 30, 445.

56. Pauling, L. *The Nature of the Chemical Bond*, 3rd ed.; Cornell University Press, 1960, Ch. 11, p. 405.

57. For a review addressing the synthetic utility of Tf_2O, see: Baraznenok, I. L.; Nenajdenko, V. G.; Balenkova, E. S. *Tetrahedron* **2000**, *56*, 3077.

58. Howard, W. A.; Waters, M.; Parkin, G. *J. Am. Chem. Soc.* **1993**, *115*, 4917.

59. Hanna, T. A.; Baranger, A. M.; Bergman, R. G. *J. Org. Chem.* **1996** *61*, 4532.

60. Cheng, J. Y. K.; Cheung, K.-K.; Chan, M. C. W.; Wong, K.-Y.; Che, C.-H. *Inorg. Chim. Acta* **1998**, *272*, 176.

61. Mindiola, D. J. Ph.D. Thesis, Massachusetts Institute of Technology, 2000.

62. Figueroa, J. S.; Cummins, C. C. Unpublished Results.

63. Freeman, P. K.; Hutchinson, L. L. *J. Org. Chem.* **1983**, *48*, 879.

64. Kroto, H. W.; Nixon, J. F.; Simmons, N. P. C. *J. Mol. Spectrosc.* **1979**, *77*, 270.

65. Appel, R.; Maier, G.; Reisenauer, H.-P.; Westerhaus, A.; *Angew. Chem. Int. Ed. Engl.* **1981**, **20**, 197.

66. Guillemin, J.- C.; Janati, T.; Denis, J.- M. *J. Org. Chem.* **2001**, *66*, 7868.

67. Brym, M.; Jones, C. *J. Chem. Soc. Dalton. Trans.* **2003**, 3665.

68. Regitz, M.; Allspach, T. *Chem. Ber.* **1987**, *120*, 1269.

69. Cook, C. D.; Jauhal, G. S. *J. Am. Chem. Soc.* **1968**, *90*, 1464.

70. Hitchcock, P. B.; Jones, C.; Nixon, J. F. *Chem. Commun.* **1994**, 2061.

71. Chernega, A. N.; Koidan, G. N.; Marchenko, A. P.; Korkin, A. A. *Heteroatom. Chem.* **1993**, *4*, 365.

72. Lappert, M. F.; Power, P. P.; Sanger, A. R.; Srivastava, R. C. *Metal and Metalloid Amides*, Ellis Horwood, Chichester, 1980.

73. Becker, G.; Brombach, S. T.; Horner, S. T.; Niecke, E.; Schwartz, W.; Streubel, R.; Wurthwein, E.-U. *Inorg. Chem.* **2005**, *44*, 3080.

74. Yandulov, D. V.; Schrock, R. R. *Science* **2003**, *301*, 76.

75. Yandulov, D. V.; Schrock, R. R. *J. Am. Chem. Soc.* **2002**, *124*,6252.

76. Yandulov, D. V.; Schrock, R. R.; Rheingold, A. L.; Ceccarelli, C.; Davis, W. M. *Inorg. Chem.* **2003**, *42*, 796.

77. Pool, J. A.; Lobkovsky, E.; Chirik, P. J. *Nature* **2004**, *427*, 527.

78. Nishibayashi, Y.; Iwai, S.; Hidai, M. *Science* **1998**, *279*, 540.

79. Nishibayashi, Y.; Takemoto, S.; Iwai, S.; Hidai, M. *Inorg. Chem.* **2000**, *39*, 5946.

80. Ishino, H.; Nagano, T.; Kuwata, S.; Yokobayashi, Y.; Ishii, Y.; Hidai, M.; Mizobe, Y. *Organometallics* **2001**, *20*, 188.

81. Nishibayashi, Y.; Wakiji, I.; Hirata, K.; Du Bois, M. R.; Hidai, M. *Inorg. Chem.* **2001**, *40*, 578.

82. Hidai, M. *Coord. Chem. Rev.* **1999**, *185-186*, 99.

83. Mori, M. *J. Heterocycl. Chem.* **2000**, *37*, 623.

84. Hori, M.; Mori, M. *J. Org. Chem.* **1995**, *60*, 1480.

85. Mori, M.; Kawaguchi, M.; Hori, M.; Hamaoka, S. *Heterocycles* **1994**, *39*, 729.

86. Fryzuk, M. D. *Chem. Rec.* **2003**, *3*, 2.

87. Fryzuk, M. D.; Johnson, S. A. *Coord. Chem. Rev.* **2000**, *200-202*, 379.

88. Hidai, M.; Yasushi, M. *Top. Organomet. Chem.* **1999**, *3*, 227.

89. Hidai, M.; Mizobe, Y. *Chem. Rev.* **1995**, *95*, 1115.

90. Mizobe, Y.; Ishii, Y.; Hidai, M. *Coord. Chem. Rev.* **1995**, *139*, 281.

91. Goto, N. K.; Kay, L. E. *Curr. Opin. Struct. Biol.* **2000**, *10*, 585.

92. Mispelter, J.; Momenteau, M.; Lhoste, J.-M. *Biol. Magn. Reson.* **1993**, 299.

93. Kaess, H.; Bittersmann,-Weidlich, E. Andreasson, L.-E.; Boenigk, B.; Lubitz, W. *Chem. Phys.* **1995**, *194*, 419.

94. Fotadar, U.; Becu, C.; Borremans, F. A. M.; Anteunis, M. J. O. *Tetrahedron* **1978**, *49*, 3537.

95. Connell, R. D.; Tebbe, M.; Gangloff, A. R.; Heiquist, P. Aalermark, B. *Tetrahedron* **1993**, *49*, 5445.

96. Burkhart, D. J.; Mckenzie, A. R.; Nelson, J. K.; Myers, K. I.; Zhao, X.; Magnusson, K. R.; Natale, N. R.; *Org. Lett.* **2004**, *6*, 1285.

97. Royer, F.; Felpin, F.-X.; Doris, E. *J. Org. Chem.* **2001**, *66*, 6487.

98. Goldstein, B. M.; Kennedy, S. D.; Hennen, W. J. *J. Am. Chem. Soc.* **1990**, *112*, 8265.

99. Hennen, W. J.; Hinshaw, B. C.; Riley, T. A.; Wood, S. G.; Robins, R. K. *J. Org. Chem.* **1985**, *50*, 1741.

100. Riley, T. A.; Hennen, W. J.; Dalley, N. K.; Wilson, B. E.; Robins, R. K.; Larson, S. B. *J. Het. Chem.* **1987**, *24*, 955.

101. Hidai, M.; Mizobe, Y. *Pure. Appl. Chem.* **2001**, *73*, 261.

102. Berno, P.; Gamboratta, S. *Organometallics* **1995**, *14*, 2159.

103. Tsai, Y.-C.; Cummins, C. C. *Inorg. Chim. Acta* **2003**, *345*, 63.

104. The molybdenum N_2-complex, $(\eta^6\text{-}C_6H_5(PMePh))Mo(N_2)(PMePh_2)_2$, was employed in reactions with **1a** as a soluble form of N_2 gas. The reaction, $N_2 + (\eta^6\text{-}C_6H_5(PMePh))Mo(PMePh_2)_3 \rightarrow (\eta^6\text{-}C_6H_5(PMePh))Mo(N_2)\text{-}(PMePh_2)_2 + PMePh_2$ in C_7H_8, has an equilibrium constant of $K = 0.76 \pm 0.04$ at 35 °C, thus favoring formation of the N_2 complex in solution. (a) Luck, R.; Moris, R. J. *Inorg. Chem.* **1984**, *23*, 1489. (b) Luck, R.; Moris, R. J. Sawyer, J. F. *Organometallics*, **1984**, *3*, 247.

105. Mindiola, D. J.; Meyer, K.; Cherry, J.-P. F.; Baker, T. A.; Cummins, C. C. *Organometallics* **2000**, *19*, 1622.

106. Mindiola, D. J.; Cummins, C. C. *Organometallics* **2001**, *20*, 3626.

107. Schwindt, M.; Lejon, T.; Hegedus, L. *Organometallics* **1990**, *9*, 2814.

108. Tsai, Y.-C.; Johnson, M. J. A.; Mindiola, D. J.; Cummins, C. C.; Klooster, W. T.; Koetzle, T. F. *J. Am. Chem. Soc.* **1999**, *121*, 10426.

109. Cherry, J.-P. F.; Stephens, F. H.; Johnson, M. J. A.; Diaconescu, P. L.; Cummins, C. C. *Inorg. Chem.* **2001**, *40*, 6860.

110. Tsai, Y.-C.; Diaconescu, P. L.; Cummins, C. C. *Organometallics* **2000**, *19*, 5260.

111. Blackwell, J. M.; Figueroa, J. S.; Stephens, F. H.; Cummins, C. C. *Organometallics* **2003**, *22*, 3351.

112. Tsai, Y.-C.; Stephens, F. H.; Meyer, K.; Mendiratta, A.; Gheorghiu, M. D.; Cummins, C. C. *Organometallics* **2003**, *22*, 2902.

113. Stephens, F. H.; Figueroa, J. S.; Cummins, C. C.; Kryatova, O. P.; Kryatov, S. V.; Rybak-Akimova, E. V.; McDonough, J. E.; Hoff, C. D. *Organometallics* **2004**, *23*, 3126-3138.

114. Mercer, M.; Crabtree, R. H.; Richards, R. L. *J. Chem. Soc., Chem. Commum.* **1973**, 808.

115. Mercer, M. *J. Chem. Soc., Dalton Trans.* **1974**, 1637.

116. Cradwick, P. D.; Chatt, J.; Crabtree, R. H.; Richards, R. L. *J. Chem. Soc., Chem. Commun.* **1975**, 351.

117. Schrock, R. R.; Kolodziej, R. M.; Liu, A. H.; Davis, W. M.; Vale, M. G. *J. Am. Chem. Soc.* **1990**, *112*, 4338.

118. O'Donoghue, M. B.; Zanetti, N. C.; Davis, W. M.; Schrock, R. R. *J. Am. Chem. Soc.* **1997**, *119*, 2753.

119. O'Donoghue, M. B.; Davis, W. M.; Schrock, R. R. *Inorg. Chem* **1998**, *37*, 5149.

120. O'Donoghue, M. B.; Davis, W. M.; Schrock, R. R.; Reiff, W. M. *Inorg. Chem.* **1999**, *38*, 243.

121. O'Donoghue, M. B.; Zanetti, N. C.; Davis, W. M.; Schrock, R. R. *J. Am. Chem. Soc.* **1999**, *119*, 2753.

122. Odom, A. L.; Arnold, P. L.; Cummins, C. C. *J. Am. Chem. Soc.* **1998**, *120*, 5836.

123. Ishino, H.; Nagano, T.; Kuwata, S.; Yokobayashi, Y.; Ishii, Y.; Hidai, H.; Mizobe, Y. *Organometallics* **2001**, *20*, 188.

124. Laplaza, C. E.; Odom, A. L.; Davis, W. M.; Cummins, C. C.; Protasiewicz, J. D. *J. Am. Chem. Soc.* **1995**, *117*, 4999.

125. Odom, A. L.; Cummins, C. C.; Protasiewicz, J. D. *J. Am. Chem. Soc.* **1995**, *117*, 6613.

126. von Philipsborn, W.; Müller, R. *Angew. Chem., Int. Ed. Engl.* **1986**, *25*, 383.

127. Dilworth, J. R.; Donovan-Mtunzi, S.; Kan, C. T.; Richards, R. L.; Mason, J. *Inorg. Chim. Acta* **1981**, *53*, L161.

128. Donovan-Mtunzi, S.; Richards, R. L.; Mason, J. *J. Chem. Soc., Dalton Trans.* **1984**, 469.

129. For a discussion on the origin of highly downfield ^{15}N NMR chemical shifts in d^0 nitrido metal complexes, see: Sceats, E. L.; Figueroa, J. S.; Cummins, C. C.; Loening, N. M.,Van der Wel, P; Griffin, R. G. *Polyhedron,* **2004**, *23*, 2751. For the analogous phenomenon in triply-bound d^0 phosphido complexes, see: Wu, G.; Rovnyak, D.; Johnson, M. J. A.; Zanetti, N. C.; Musaev, D. G.; Morokuma, K.; Schrock, R. R.; Griffin, R. G.; Cummins, C. C. *J. Am. Chem. Soc.* **1996**, *118*, 10654.

130. Binsch, G.; Lambert. J. B.; Roberts, B. W.; Roberts, J. D. *J. Am. Chem. Soc.* **1964**, *86*, 5564.

131. Creary, X.; Sky, A. F.; Phillips, G.; Alonso, D. E. *J. Am. Chem. Soc.* **1993**, *115*, 7584.

132. Haupt, E. T. K.; Leibfritz, D. *Spectrochimica Acta A* **1989**, *45A*, 119.

133. Isotopically labled $^{13}CO_2$ was employed in the preparation of 1-adamantoyl chloride-^{13}C: Molle, G.; Bauer, P.; DuBois, J. E. *J. Org. Chem.* **1982**, *47*, 4120.

134. Clough, C. R. Greco, J. B.; Figueroa, J. S.; Diaconsecu, P. L.; Davis, W. M.; Cummins, C. C. *J. Am. Chem. Soc.* **2004**, *126*, 7742.

135. Leung, W.-H.; Chim, J. L. C.; Williams, I. D.; Wong, W.-T. *Inorg. Chem* **1999**, *38*, 3000.

136. Thomas, S.; Lim, P. J.; Gable, R. W.; Young, C. G. *Inorg. Chem.* **1998**, *37*, 590.

137. Tong, C.; Bottomley, L. A. *J. Porphyrins Phthalocyanines* **1998**, *2*, 261.

138. Nielson, A. J.; Hunt, P. A.; Rickard, C. E. F.; Schwerdtfeger, P. *J. Chem. Soc., Dalton Trans.* **1997**, 3311.

139. Brask, J. K.; Dura-Vila, V.; Diaconescu, P. L.; Cummins, C. C. *Chem. Commun.* **2002**, 902.

140. Ruck, R. T; Bergman, R. G. *Angew. Chem. Int. Ed. Engl.* **2004**, *43*, 5375.

141. Ruck, R. T.; Bergman, R. G *Organometallics* **2004**, *23*, 2231.

142. Fickes, M. G.; Odom, A. L.; Cummins, C. C. *Chem. Commun.* **1997**, 1994.

143. Fickes, G. M. Ph.D. Thesis, Massachusetts Institute of Technology, Cambridge, Ma, 1998.

144. The difference in covalent radii (Δr_{cov}) between Nb and V is 0.12 Å. See reference 56.

145. Wigley, D. E. *Prog. Inorg. Chem.* **1994**, *42*, 239.

146. Figueroa, J. S.; Cummins, C. C. *J. Am. Chem. Soc.* **2003**, *125*, 4020.

147. Mendiratta, A.; Cummins, C. C.; Kryatova, O. P.; Rybak-Akimova, E. V.; McDonough, J. E.; Hoff, C. D.*Inorg. Chem.* **2004**, *42*, 8621.

148. Caselli, A.; Solari, E; Scopelliti, R; Floriani, C.; Re, N.; Rizzioli, C.; Chiesi-Villa, A. *J. Am. Chem. Soc.* **2000**, *122*, 3652.

149. Kawaguchi, H.; Matsuo, T. Angew. *Chem. Int. Ed. Engl.* 2002, *41*, 2792.

150. Dilworth, J. R.; Zubieta, J. *Inorg. Synth.* **1986**, *24*, 193. (b) Stoffelbach, F.; Saurenz, D.; Poli, R. *Eur. J. Chem.* **2001**, 2699.

151. Ferris, T. D.; Lee, P. T.; Farrar, T. C. *Mag. Res. Chem.* **1997**, *35*, 571.

152. te Velde, G.; Bickelhaupt, F. M.; van Gisbergen, S. J. A.; Fonseca Guerra, C.; Baerends, E. J.; Snijders, J. G.; Ziegler, T. *J. Comput. Chem.* **2001**, *22*, 931.

153. Fonseca Guerra, C.; Snijders, J. G.; te Velde, G.; Baerends, E. J. *Theor. Chem. Acc.* **1998**, *99*, 391.

154. *ADF 2004.01*; SCM, Theoretical Chemistry, Vrije Universiteit, Amsterdam, The Netherlands, http://www.scm.com.

155. van Lenthe, E.; Baerends, E. J.; Snijders, J. G. *J. Chem. Phys.* **1993**, *99*, 4597.

156. van Lenthe, E. The ZORA Equation. Thesis, Vrije Universiteit Amsterdam, Netherlands, 1996.

157. Vosko, S. H.; Wilk, L.; Nusair, M. *Can. J. Phys.* **1980**, *58*, 1200.

158. Becke, A. *Phys. Rev.. A* **1988**, *38*, 3098.
159. Perdew, J. P. *Phys. Rev. B* **1986**, *34*, 7406.
160. Perdew, J. P. *Phys. Rev. B* **1986**, *33*, 8822.
161. See, for example: Deng, L.; Schmid, R.; Ziegler, T. *Organometallics* **2000**, *19*, 3069.
162. van der Sluis, P.; Spek, A. L. *Acta Crystallogr.* **1990**, *A46*, 194.
163. Spek, A. L. *Acta Crystallogr.* **1990**, *A46*, C34.

Joshua s. Figueroa

Department of Chemistry
Massachusetts Institute of Technology
77 Massachusetts Avenue, Room 6-332
Cambridge, Massachusetts 02139

Phone: (617) 452-2532
Fax: (617) 258-5700
E-mail: jsfig@mit.edu

Education

- Ph.D. Inorganic Chemistry, Massachusetts Institute of Technology, 2005
  Thesis: "Synthesis and Small Molecule Chemistry of the Niobaziridine-Hydride Functional Group"
  Advisor: Christopher C. Cummins

- B.S. with Honors, Major in Chemistry, University of Delaware, 2000
  Thesis: "Mechanistic Investigations of Pyrazole-Ring Rearrangement in Early Transition Metal Trispyrazolyl Borate Complexes"
  Advisor: Arnold L. Rheingold

Experience

- *Postdoctoral Research Fellow*, Columbia University, 2005 – 2007. Advisor: Gerard Parkin
- *Graduate Research Assistant*, Massachusetts Institute of Technology, 2000 – 2005.
- *Undergraduate Researcher*, University of Delaware, 1997 – 2000.
- *Teaching Assistant*, Massachusetts Institute of Technology, Fall 2000, Spring 2004
- *Teaching Assistant*, University of Delaware, Fall 1999 – Spring 2000.

Awards and Honors

- National Institutes of Health Postdoctoral Fellowship, Columbia University, 2005–2007.
- Presidential Predoctoral Fellowship, Massachusetts Institute of Technology, 2000.
- American Chemical Society Scholar, University of Delaware, 1998 – 2000.
- University of Delaware Science and Engineering Scholar, 1998 – 2000.
- University of Delaware Kelly Chemistry Scholar, 1998 – 1999.
- University of Delaware Scholastic Fellowship, 1996 – 2000.

Publications

1.) **Figueroa, J. S.**; Cummins, C. C, "Triatomic EP_2 Triangles (E = Ge, Sn, Pb) as μ_2:η^3,η^3 Bridging Ligands" *Angew. Chem. Int. Ed. Engl.* **2005** – *Accepted.*

2.) Murahashi, T.; Clough, C. R.; **Figueroa, J. S.**; Cummins, C. C. "A Ligand Comprised of Dinitrogen and Methyldiphenylphosphane in a Cationic Molybdenum Complex" *Angew. Chem. Int. Ed. Engl.* **2000**, *44*, 2560.

3.) Sceats, E. L.; **Figueroa, J. S.**; Cummins, C. C.; Loening, N. M.; Van der Wel, P.; Griffin, R. G. "Complexes Obtained by Electrophilic Attack on a Dinitrogen-Derived Terminal Molybdenum Nitride: Electronic Structure Analysis by Solid State CP/MAS ^{15}N NMR in Combination with DFT Calculations" *Polyhedron*, **2004**, *23*, 2751.

4.) Soo, H. S.; **Figueroa, J. S.**; Cummins, C. C. "A Homoleptic Molybdenum(IV) Enolate Complex: Synthesis, Molecular and Electronic Structure, and NCN Group Transfer to Form a Terminal Cyanoimide of Molybdenum(VI)" *J. Am. Chem. Soc.* **2004**, *126*, 11370.

5.) **Figueroa, J. S.**; Cummins, C. C. "Phosphaalkynes from Acid Chlorides via P for O(Cl) Metathesis: A Recyclable Niobium Phosphide (P^{3-}) Reagent that Effects C-P Triple-Bond Formation" *J. Am. Chem. Soc.* **2004**, *126*, 13916.

6.) Stephens, F. H.; **Figueroa, J. S.**; Cummins, C. C.; Kryatova, O. P.; Kryatov, S. V.; Rybak-Akimova, E. V.; Mcdonough, J. E.; Hoff, C. D. "Small Molecule Activation by Molybaziridine-Hydride Complexes: Mechanistic Sequence of the Small Molecule Binding and Molybaziridine-Ring Opening Steps. *Organometallics*, **2004**, *23*, 3126.

7.) Clough, C. R.; Greco, J. B.; **Figueroa, J. S.**; Diaconescu, P. L.; Davis, W. M.; Cummins, C. C. "Organic Nitriles from Acid Chlorides: An Isovalent N for (O)Cl Exchange Reaction Mediated by a Tungsten Nitride Complex" *J. Am. Chem. Soc.* **2004**, *126*, 7742.

8.) **Figueroa, J. S.**; Cummins, C. C. "Diorganophosphanylphosphinidenes as Complexed Ligands: Synthesis via an Anionic Terminal Phosphide of Niobium" *Angew. Chem. Int. Ed. Engl.* **2004**, *43,* 984.

9.) Stephens, F. H.; **Figueroa, J. S.**; Diaconescu, P. L.; Cummins, C. C. "Molybdenum-Phosphorus Triple Bond Stabilization by Ancillary Alkoxide Ligation: Synthesis and Structure of a Terminal Phosphide Tris-1-Methylcyclohexanoxide Complex" *J. Am. Chem. Soc.* **2003**, *125*, 9264.

10.) **Figueroa, J. S.**; Cummins, C. C. "The Niobaziridine-Hydride Functional Group: Synthesis and Divergent Reactivity" *J. Am. Chem. Soc.* **2003**, *125*, 4020.

11.) Blackwell, J. M.; **Figueroa, J. S.**; Stephens, F. H.; Cummins, C. C. "Enediynes via Sequential Acetylide Reductive Coupling and Alkyne Metathesis: Easy Access to Well-Defined Molybdenum Initiators for Alkyne Metathesis" *Organometallics* **2003**, *22*, 3351.

12.) Beckmann, P. A.; Burbank, K. S.; Clemo, K. M.; Slonaker, E. N.; Averill, K.; Dybowski, C.; **Figueroa, J. S.**; Glatfelter, A.; Koch, S.; Liable-Sands, L. M.; Rheingold, A. L. "^{1}H Nuclear Magnetic Resonance Spin-Lattice Relaxation, ^{13}C Magic-Angle-Spinning Nuclear Magnetic Resonance Spectroscopy, Differential Scanning Calorimetry, and X-ray Diffraction of Two Polymorphs of 2,6-Di-*tert*-Butylnaphthalene" *J. Chem. Phys.* **2000**, *113*, 1958.

13.) Rheingold, A. L.; **Figueroa, J. S.**; Dybowski, C.: Beckmann, P. A. "Superlattices, Polymorphs and Solid State NMR Spin-Lattice Relaxation (T_1) Measurements of 2,6-Di-*tert*-Butylnaphthalene" *Chem. Commun.* **2000** 651.

14.) Dollinger, L. M.; Ndakala, A. J.; Hashemzadeh, M.; Wang, G.; Wang, Y.; Martinez, I.; Arcari. J. T.; Galluzzo, D. J.; Howell, A. R.; Rheingold, A. L.; **Figueroa, J. S.** "Preparation and Properties of 2-Methyleneoxetanes" *J. Org. Chem* **1999**, *64*, 7074.

Acknowledgments

Many before me have claimed that the 'Acknowledgment Section' is the most difficult portion of the thesis. I just don't see this difficulty. I have been influenced and supported by some amazing people during my stay at MIT and it is an absolute pleasure for me to express my appreciation for them.

Firstly, let me thank Kit. I came to work with you in order to activate dinitrogen and feed the hungry. Most around the chemistry department wouldn't believe I have such altruistic motives, but - without making this a confessional - let me just say that I do. While I did some other cool things as well, I did split me some nitrogen baby! I can't fully express how grateful I am for the opportunity you provided to do this, if, at the very least, to simply say thank you. I am also grateful for the countless hours you invested in schooling me on subjects ranging from synthesis, computational techniques, writing, fine spirits and sailing. Furthermore, I have always been in awe of your creativity in and profound understanding of chemistry. I needed an advisor who would learn a new subject, talk to a student about it shortly after learning it and *expect* that student to know everything about it within an hour. This is exactly what I found in you and it drove/inspired me to the best and as intense I could be. I also want to express my appreciation to you for not only being an excellent advisor, but also a great friend. I don't think many students would express their relationship with their advisor as a partnership, but I do.

In addition to Kit, the entire inorganic faculty has had a profound influence on my graduate studies. I'd like to thank Dan Nocera for generously accepting me as his group's 'pet' and for graciously and tactfully pointing out several of life's 'subtle truths'. Dan has become a good friend and mentor as well, and I'd like to also thank him for allowing me to 'ride' the cluster for a year or two, making possible the electronic structure studies described in this thesis. My thesis committee members, Dick Schrock and Joseph Sadighi, have served as a tremendous support network and consistently provided insightful comments and suggestions about my research for which I am most appreciative. I'd also like to explicitly thank Dick for his unwavering interest in niobium chemistry. Steve Lippard has supported me as a scientist from the very beginning of my tenure at MIT and allowed me to use his use his APEX CCD for structural characterization of the bridging diphosphide complex described in chapter 2. Besides the niobaziridine-hydride, the diphosphide is the most pivotal result of this thesis. Lastly, I'd like to thank Alan Davison for reaching out to me during the tumultuous first two months of graduate school, especially with respect to research group selection.

No acknowledgment section would be complete without pointing out those who have been recipients of your neurotic episodes (O.K., my neurotic episodes). So let me just devote a few lines to the chemistry department staff Dave Bray, Mark Wall, Bill Davis, Peter Müller, Jeff Simpson and Li Li. Firstly, I'd like to say thanks for putting up with my incessant questioning and skepticism of the resultant answers. I am indebted to Dave and Mark for helping with kinetics measurements, multinuclear NMR studies and joke telling. Bill Davis (Bragg) taught me a ton of crystallography and what I think is possibly the true meaning of 'shake n' bake'. I'll be glad to visit you Bill, but please, never let the 'Curse of Bill Davis' return to New York City. In our brief time together, Peter Müller has proved to me that no structure is unsolvable.

No acknowledgment section would be complete without exalting those who have been the direct recipients of your full-blown insanity. Therefore, I have to thank Aetna Wun first and foremost for putting up with me and all my quirks for the past four years. Aetna radiates a penetrating beauty that has served as a source of inspiration in my work and in my life. Her love and caring, especially during bad times, was often all I had to keep me on my feet. I want to thank you from the deepest part of my heart for keeping me grounded, making me smile and being my best friend.

Next, I have to thank some of my labmates for i) simply dealing with me ii) providing an amazing atmosphere for chemistry and iii) being companions in many crusades of utter carnage. I need to express my sincere gratitude to James Blackwell (Death, Dr. Filth) for many reasons. James is without question one the most talented and creative chemists I have ever met and I would not have accomplished half the things I did in my graduate career had I not tried to emulate him in several ways. I also have to thank James for introducing me to rock music, co-founding the 6-332 sub-culture, providing the 'in' at the Miracle and for being a great friend. James will be the first recipient of the Goni Medal (cast in onyx and to be worn on the face) for proof-reading this thesis, especially in its fragmented and unintelligible forms.

Let me just say that I doubt I'll ever meet two people like Arjun Mendiratta (Sandy) and Christopher Clough (Manis) again. Luckily, I've befriended them both so that I can savor their unique qualities my whole life. Blessed with tremendous intellect and wit, Arjun can over-analyze and kill the intended point of any story. I'd like to say thank you for all the times I've had to say "that's a good point", countless hours talking shop, the MoX_3 gifts and being there (and being funny) the whole time. Manis (Little Bear) is a true warrior of the romantic who has the best auditory memory of anyone I know. Thanks for comforting me on the phone when I was in the cage, stories about Crystal Lake and your Old Man, fixing my box those two times and riding shotgun during the final months of 2004. Oh yeah, and thanks for covering Death's spot at the Britch all those summer nights.

Since joining the Cummins group in 2000, I have overlapped with several people who have taught me (mostly by example) many things to and *not to* do. For their respective contributions to each and their friendship, I'd like to acknowledge Paula Diaconescu, John-Paul Cherry, Fran Stephens and James Tsai. I must also explicitly credit James Tsai with showing me how to make and manipulate Cummins group compounds when I was a youngling. While the group has changed dramatically since I joined, one constant has been the enthusiasm and spunk of Allison Kelsey. Allison, thanks for being so cool, talking to me at times when I was freaking out and for coming through when I was freaking about lab ish. At this point I'd also like to say good luck to the newer members of the group AR Fox, Glen Alliger (Gleanis), Nick Piro and John Curley. Nick, good luck and all the best with niobium/phosphorus, Gleanis, watch out for them stegapotimi, AR Fox, I hope you aint wearing an eye-patch by the time you're done and Curley, I hope you figure it out. UROPs Kevin Yurkerwich, Erin Daida and Han Sen Soo are thanked for inexplicit statements, listening and magnesium anthracene, respectively.

I also wish to thank those who have strongly contributed to my MIT life over the years. Bart Bartlett and Dave Manke deserve special thanks for understanding 'you're bihe' and 'you have face' right away, 'keepin it real' and realizing the joke is really on everyone else. Thanks to

all the Organomets for making the summer (and the off-season) so enjoyable and the Nocera group past and present for always making me feel welcome. I'd like to especially acknowledge Steve Reece (Streece) for his friendship, Jullien Bachmann for his help with cluster-related problems and Gretchen Kappelmann for being Wonder Woman and saving the day many times. I have to say thanks to Adam Hock for always being down for conversations over coffee or beers since our Delaware days. Also, Phil Sheehy and Russ Driver are acknowledged for being accomplices on many crusades through Boston and Cambridge. I also need to acknowledge the contributions to my well-being made by my roommate Tom Malia. Tom will be the first recipient of the Jone Schwartz Award for Excellence (a pink shawl with accompanying tiara), because if anyone deserves an award for dealing with me (and is not named Aetna), it's Tom. Thanks Tom for so many nights of fun, dancing in the crib and for being a great friend.

I'd like to thank my many NYC and DE heads for providing reasons to leave Boston from time to time. Specifically, Dr. Jay (Mike Propon), A-Train, A-Greene, Greenbirch, Aint, Emily, Zon, Erica, Melissa, Manolo, Hip-Hop, Chaunce, Amy G., Dana and Danielle are all thanked for their friendship. Daniel Schiffer gets his own line because, being the closest thing I have to a brother, he deserves it.

I started studying chemistry because I was genuinely curious about the world around me. Fundamentally, I believe I am just a very curious person. Without some guidance when younger, I am doubtful I could have settled on a specific area of chemistry to focus my attention. Therefore, I must thank Professor Arnold L. Rheingold for taking me under his wing as a freshman at Delaware and steering my down the inorganic road. It was only later that I realized that inorganic chemistry actually embodied the types of questions I was seeking answers to and I could not have asked for a better and more supportive first mentor.

Lastly, I'd like to thank my entire family for their support, love and for always providing good times. I am blessed to be part of a diverse family with a fantastic sense of humor. Most importantly however, I wish to express my deepest gratitude to my parents, whose love, support and compassion is the driving force in my life. I am exceedingly thankful to have parents who have taught me that hard work and a love of life are the keys to happiness. I want you to know that I love you dearly and that this is all for you.